

https://dspace.org/

An assessment of temperature variability over South Africa

Lakhraj-Govender, Rakhee

2017

https://hdl.handle.net/10539/25018

Lakhraj-Govender, Rakhee (2017) An assessment of temperature variability over South Africa, University of the Witwatersrand, Johannesburg, <http://hdl.handle.net/10539/25018>

Downloaded from a DSpace repository. https://dspace.org/

AN ASSESSMENT OF TEMPERATURE VARIABILITY OVER SOUTH AFRICA

Rakhee Lakhraj-Govender

Supervisor: Prof. Stefan Grab

A thesis submitted to the Faculty of Science, University of the Witwatersrand, Johannesburg, in fulfilment of the requirements for the degree of Doctor of Philosophy.

November 2017, Johannesburg.

DECLARATION

I declare that this Thesis is my own work, unaided work. It is being submitted for the Degree of Doctor of Philosophy at the University of the Witwatersrand, Johannesburg. It has not been submitted before for any degree or examination at any other University.

……

Rakhee Lakhraj-Govender

(Signature of the Candidate)

November 2017, in Johannesburg.

ABSTRACT

The main aim of this PhD research is to use accurate, relatively long-temperature data sets (spanning 1851-2016) available in South Africa, to establish a more precise understanding of temporal temperature variability over this region. This is achieved through the use of robust methodology (i.e. data quality control and homogenization procedures, using a reference series) to produce high quality data sets for temperature trend analysis. Data quality and homogenization of data sets are conducted using RClimDex, ProClim and AnClim software. Long-term temperature trends are determined using a nonparametric statistic (i.e., Mann Kendall test). The core objectives are to provide a homogeneous dataset for the Western Cape region in South Africa and establish long-term (97 years) annual and seasonal instrumental temperature trends for this region. The second objective is to extend past work by examining temperature trends for KwaZulu-Natal (KZN) over a considerably longer period, with a specific focus on contrasting coastal and adjacent higher lying interior regions. The last objective is to assess the extent and timing of El Niño/La Niña impacts on maximum temperature (T_{max}) and minimum temperature (T_{min}) over selected South African stations for the period 1884-2016, and to establish any possible direct change in such temperature responses to ENSO over time.

Long-term temperature trends for the Western Cape Province indicate statistically significant increasing annual temperature trends for adjusted (homogenized) T_{max} and T_{min} data over the period 1916-2013, with the exception of an insignificant decreasing T_{max} trend at Cape St Blaize. For the common period (1937-2001), a statistically significant increasing trend (0.13°C/decade) is recorded for all stations in Western Cape Province, with a 0.04°C/decade stronger warming signal than before homogenization was applied. The seasonal trends also support significant increasing trends, with the exception of T_{max} trends for summer (-0.03°C/decade) and autumn (0°C/decade) at Kirstenbosch.

For KZN, cooler conditions are noted for the second half of the 19th century (i.e. 1851, 1858, 1860-1864) compared to more recent times. For the period 1930-2015, annual T_{min} records significant warming at all stations, with the rates of warming (°C/decade) over the interior being double that for the coast. T_{min} warming trends are 1.31 (summer), 2.75 (autumn), 3.33 (winter) and 1.25 (spring) times faster over the interior compared to the coast. Thus, higher

lying interior regions are warming considerably faster than adjacent coastal areas mainly due to T_{min} warming trends.

The impact of El Niño and La Niña events on T_{max} and T_{min} over South Africa is investigated using composite and Fourier series analysis (1884-2016). For 17 stations spread across South Africa, it is concluded that strong coherent relationships exist between El Niño/La Niña events and T_{max}/T_{min}. Contingency tables were constructed for each station during the austral summer season (December, January and February) and analysed using the Chi-squared statistic. The most notable finding is that El Niño events have had a stronger warming effect over many regions in South Africa after the late 1970s, the most prominent regions being the northern interior and southeast coast, where associated T_{max} record an average of 0.41°C and 0.45°C higher values over the period 1979-2016 compared to the earlier period (1940-1978) respectively. The Chi-squared statistic results indicate that ENSO phases exert a stronger influence over the interior of South Africa compared to that over the coast.

Keywords: homogeneity, temperature, trend analysis, Mann Kendall, historical climate, Western Cape, KwaZulu-Natal, South Africa, ENSO.

DEDICATION

To my husband, Kasavan and my son, Tahir.

ACKNOWLEDGEMENTS

Thank you to the South African Weather Services for providing the temperature data. I sincerely appreciate the Research Development Grant provided by the Tshwane University of Technology (TUT), South Africa, the Department of Higher Education and Training (DHET) and the Sabbatical grant from the National Research Foundation of South Africa (98258). Thank you to TUT for affording the time and opportunity to pursue this goal for growth and development. I am also grateful for the DHET/TUT funding to attend the International Time Series Conference in Granada, Spain in 2013. Thank you to my colleagues.

I would like to express my sincere gratitude to my supervisor, Professor Stefan Grab, for your encouragement, tireless guidance, patience, enthusiasm and motivation. I am indebted to you for the sacrifices you have made and the countless hours of commitment to fine tuning my writing and scientific research skills. I sincerely appreciate all the suggested reading material and all your support. Thank you to Mrs Nothabo Ndebele for your help during the first paper. Thank you, Ms Wendy Phillips for the maps.

Thank you my dear husband, Kasavan for your unconditional love, encouragement, time and patience. I am extremely grateful for your unwavering support and sacrifice. Thank you for being my pillar of strength. Not forgetting all the neat Excel tips! Thank you to my son, Tahir for the sacrifices made, for understanding at a young age and for being my inspiration. I am so proud of you! I am sorry for missing the wickets fall and missing your many cricket matches. Thank you to my mum and my late dad for working so hard in life to provide for us.

Thank you to the anonymous reviewers for the valuable inputs on drafts of Chapters three and four. Chapter three has been published in the "International Journal of Climatology."

Above all, my heartfelt thanks to God, Shri Hanumanji for the strength and courage to undertake this journey. Jai Shri Ram! Jai Shri Krishna! Thank you, Mother Saraswati for the knowledge and Shri Ganeshji for answering my prayers to remove obstacles. Aum Namah Shivaya!

TABLE OF CONTENTS

DECLARATION ii
ABSTRACT iii
DEDICATION v
ACKNOWLEDGEMENTS vi
LIST OF FIGURES xi
LIST OF TABLES xiv
LIST OF ACRONYMS xvi

CHAPTER ONE: INTRODUCTION 1
1.1. BACKGROUND 2
1.2. RATIONALE 5
1.3. AIM 6
1.4. OBJECTIVES 7
1.5. THESIS STRUCTURE 8
1.6. REFERENCES 8

CHAPTER TWO: LITERATURE REVIEW 16
2.1. INTRODUCTION 17
2.2. HISTORICAL DATA RECOVERY 19
2.3. DATA QUALITY CONTROL AND HOMOGENIZATION 23
2.4. GLOBAL TEMPERATURE TRENDS 27
2.4.1. Temperature trends in North America 29
2.4.2. Temperature trends in Europe 30
2.4.3. Temperature trends in Asia 32
2.4.4. Temperature trends in the Southern Hemisphere 34
2.4.5. Temperature trends in Africa 36
2.5. SOUTH AFRICAN TEMPERATURE TRENDS 37
2.6. COASTAL AND ADJACENT INLAND TEMPERATURE TRENDS 40

2.7. EL NIÑO-SOUTHERN OSCILLATION AND LAND TEMPERATURE 44

2.8. REFERENCES 49

CHAPTER THREE: A HOMOGENIZED LONG-TERM TEMPERATURE RECORD FOR THE WESTERN CAPE PROVINCE IN SOUTH AFRICA: 1916–2013 64

3.1. ABSTRACT 65

3.2. INTRODUCTION 65

3.3. METHODS 67

3.3.1. Study area 67

3.3.2. Establishing quality control 67

3.3.3. Homogenization process 69

3.3.4. Developing a composite reference series 70

3.3.5. Establishing trend analyses 70

3.4. RESULTS 72

3.4.1. Quality control 72

3.4.2. Homogeneity testing 73

3.4.3. Trend analysis 77

3.5. DISCUSSION 89

3.6. CONCLUSION 93

3.7. ACKNOWLEDGEMENTS 93

3.8. REFERENCES 94

CHAPTER FOUR: TEMPERATURE TRENDS FOR COASTAL AND ADJACENT HIGHER LYING INTERIOR REGIONS KWAZULU-NATAL 99

4.1. ABSTRACT 100

4.2. INTRODUCTION 100

4.3. METHODS 103

4.3.1. Regional context 103

4.3.2. Data sources 105

4.3.3. Analyses of temperature data 106

4.3.4. Methodological challenges 108

4.4. RESULTS

4.4.1. Earliest 19th century records 109

4.4.2. 19th-20th century transitional period 109

4.4.3. Temperature trends over the period 1930-2015 110

4.4.4. Temperature trends over the period 1985-2015 114

4.4.5. Decadal temperature variability 114

4.5. DISCUSSION 117

4.6. CONCLUSION 120

4.7. ACKNOWLEDGEMENTS 120

4.8. REFERENCES 121

CHAPTER FIVE: ASSESSING THE IMPACT OF ENSO ON SOUTH AFRICAN TEMPERATURE: 1884-2016 126

5.1. ABSTRACT 127

5.2. INTRODUCTION 128

5.3. METHODS 130

5.3.1. Study area and data 130

5.3.2. Composite and Fourier analysis 133

5.3.3. Season selection 134

5.3.4. Index Time Series and core regions 134

5.3.5. Assessing temperature response to El Niño and La Niña phases through time 135

5.3.6. Contingency table and Chi-square test 135

5.4. RESULTS 136

5.4.1. Northern interior region 137
5.4.2. Central interior 138
5.4.3. Western interior 139
5.4.4. Northeastern interior 140
5.4.5. Northeast coast 141
5.4.6. Southeast coast 141
5.4.7. Southwest coast 142
5.4.8. ENSO influence on temperature over time 143
5.4.9. Chi-square test results 144
5.5. DISCUSSION 163
5.6. CONCLUSION 167
5.7. ACKNOWLEDGEMENTS 168
5.8. REFERENCES 168

CHAPTER SIX: SYNTHESIS 175
6.1. INTRODUCTION 176
6.2. ACHIEVEMENTS OF STUDY OBJECTIVES 177
6.3. KEY FINDINGS 179
6.4. ADVANTAGES AND LIMITATIONS OF THIS STUDY 184
6.5. FUTURE WORK 187
6.6. SYNOPSIS 190
6.7. REFERENCES 191

APPENDICES 196

LIST OF FIGURES

Figure 3.1: Map showing location of Western Cape stations, South Africa, used in this study. 68

Figure 3.2: Percentage errors for T_{max} and T_{min} at eight stations (Cape Agulhas, SA Astronomical Observatory, Cape Columbine, Kirstenbosch, Jonkershoek, Cape St Blaize, Cape Point and Langgewens), Western Cape. T_{max} and T_{min} percentage errors for 1940–1949 at Langgewens were omitted from the graph as the high percentage (11%) masked the smaller percentage errors. 75

Figure 3.3: T_{max}, T_{min} and total number of change points per decade for the eight stations (Cape Agulhas, SA Astronomical Observatory, Cape Columbine, Kirstenbosch, Jonkershoek, Cape St Blaize, Cape Point and Langewens), Western Cape (see Table 3.2). 76

Figure 3.4: Annual T_{max} and T_{min} unadjusted (square dotted line) and adjusted (solid line) trends using ProClimDB software for eight Western Cape stations. The grey vertical lines indicate years of detected change points using SNHT and bivariate tests in AnClim (see also Table 3). The unadjusted linear trend lines (dashed lines) and adjusted linear trend lines (solid lines), with linear equations in the legends, represent temperature changes over the respective time periods (i.e. *x* (years) and *y* (T_{min}/T_{max})). 78

Figure 3.5: Scatter plot based on correlation and distance between the eight stations (Cape Agulhas, SA Astronomical Observatory, Cape Columbine, Kirstenbosch, Jonkershoek, Cape St Blaize, Cape Point and Langewens), Western Cape. T_{min} plot does not include the stations with low correlation coefficients (see Tables 3.4 and 3.5). 82

Figure 4.1: Map showing KwaZulu-Natal stations (black solid dots), South Africa. 104

Figure 4.2: Schematic representing the features that influence climate (from Tyson and Preston-Whyte, 2000). 104

Figure 4.3: Mean annual T_{mean}, T_{max} and T_{min} anomalies for the "Natal Observatory" (53 m a.s.l.) in Durban: 1884-1909, with 10-year Gaussian filter indicated by the black dotted line and the break indicated by the gray vertical line. 113

Figure 4.4: T_{max}, T_{min} and T_{mean} for different stations in Pietermaritzburg: a) Mental hospital (1896-1953), b) Purification Works (1970-1992) and c) Pietermaritzburg CBD (1994-2015). The vertical gray lines represent the breaks in the time series. 115

Figure 4.5: Annual T_{mean}, $T_{max,}$ and T_{min} anomalies, with respect to the long-term mean (1961-1990) for KZN stations, with the 10 year Gaussian filter. 116

Figure 5.1: Map showing location of South African temperature stations. 131

Figure 5.2: El Niño T_{max} (a) and T_{min} (c) and La Niña T_{max} (e) and T_{min} (g) aggregate composite, with the dashed box denoting the possible signal period. The index time series for El Niño T_{max} (b); El Niño T_{min} (d); La Niña T_{max} (f) and La Niña T_{min} (h) for the signal season detected from the aggregate composite over the northern interior region. White bars indicate ENSO years, black bars are the neutral years and the boxes represent the months of the year before the ENSO event (-), the year of the ENSO event (0) and the months of the year after the ENSO event (+), respectively. 146

Figure 5.3: El Niño T_{max} (a) and T_{min} (c) and La Niña T_{max} (e) and T_{min} (g) aggregate composite, with the dashed box denoting the possible signal period. The index time series for El Niño T_{max} (b); El Niño T_{min} (d); La Niña T_{max} (f) and La Niña T_{min} (h) for the signal season detected from the aggregate composite over the central interior region. White bars indicate ENSO years, black bars are the normal years and the boxes represent the months of the year before the ENSO event (-), the year of the ENSO event (0) and the months of the year after the ENSO event (+), respectively. 148

Figure 5.4: El Niño T_{max} (a) and T_{min} (c) and La Niña T_{max} (e) and T_{min} (g) aggregate composite, with the dashed box denoting the possible signal period. The index time series for El Niño T_{max} (b); El Niño T_{min} (d); La Niña T_{max} (f) and La Niña T_{min} (h) for the signal season detected from the aggregate composite for the western interior region. White bars indicate ENSO years, black bars are the neutral years and the boxes represent the months of the year before the ENSO event (-), the year of the ENSO event (0) and the months of the year after the ENSO event (+), respectively. 150

Figure 5.5: El Niño T_{max} (a) and T_{min} (c) and La Niña T_{max} (e) and T_{min} (g) aggregate composite, with the dashed box denoting the possible signal period. The index time series for El Niño T_{max} (b); El Niño T_{min} (d); La Niña T_{max} (f) and La Niña T_{min} (h) for the signal season detected from the aggregate composite over the northeastern interior region. White bars indicate ENSO years, black bars are the neutral years and the boxes represent the months of the year before the ENSO event (-), the year of the ENSO event (0) and the months of the year after the ENSO event (+), respectively. 152

Figure 5.6: El Niño T_{max} (a) and T_{min} (c) and La Niña T_{max} (e) and T_{min} (g) aggregate composite, with the dashed box denoting the possible signal period. The index time series El Niño T_{max} (b); El Niño T_{min} (d); La Niña T_{max} (f) and La Niña T_{min} (h) for the signal season detected from the aggregate composite over the northeast coast region. White bars indicate ENSO years, black bars are the neutral years and the boxes represent the months of the year before the ENSO event (-), the year of the ENSO event (0) and the months of the year after the ENSO event (+), respectively. 154

Figure 5.7: El Niño T_{max} (a) and T_{min} (c) and La Niña T_{max} (e) and T_{min} (g) aggregate composite, with the dashed box denoting the possible signal period. The index time series El Niño T_{max} (b); El Niño T_{min} (d); La Niña T_{max} (f) and La Niña T_{min} (h) for the signal season detected from the aggregate composite over the southeast coast region. White bars indicate ENSO years and black bars are the neutral years and the boxes represent the months of the year before the ENSO event (-), the year of the ENSO event (0) and the months of the year after the ENSO event (+), respectively. 156

Figure 5.8: El Niño T_{max} (a) and T_{min} (c) and La Niña T_{max} (e) and T_{min} (g) aggregate composite, with the dashed box denoting the possible signal period. The index time series El Niño T_{max} (b); El Niño T_{min} (d); La Niña T_{max} (f) and La Niña T_{min} (h) for the signal season detected from the aggregate composite over the southwest coast. White bars indicate ENSO years, black bars are the neutral years and the boxes represent the months of the year before the ENSO event (-), the year of the ENSO event (0) and the months of the year after the ENSO event (+), respectively. 158

Figure 6.1: Graphical summary of major findings (gray shaded boxes), chapter numbers and major themes (bold). 183

LIST OF TABLES

Table 2.1: A selection of annual temperature trends from around the globe. 31

Table 3.1: Western Cape stations used in the study, detailing the GPS coordinates and start/end dates for each station. 69

Table 3.2: Change points detected using standard normal homogeneity test (SNHT) and bivariate tests in AnClim software for T_{max} and T_{min}, Western Cape. 74

Table 3.3: T_{max} correlation coefficients and distances between neighbour stations, Western Cape. 83

Table 3.4: T_{min} correlation coefficients and distances between neighbour stations, Western Cape. 85

Table 3.5: Mann Kendall statistics and Sen's slope estimate (Q; °C/decade) for annual T_{max} at all stations in the Western Cape region before and after adjustment. 86

Table 3.6: Mann Kendall statistics and Sen's slope estimate (Q; °C/decade) for annual T_{min} at all stations in the Western Cape region before and after adjustment. 87

Table 3.7: Sen's slope estimate (Q; °C/decade) for annual T_{max} and T_{min} at all stations in the Western Cape region, for the common period 1937–2001 after adjustment. 87

Table 3.8: Seasonal Mann Kendall statistics and Sen's slope estimates (Q; °C /decade) for adjusted T_{max} and T_{min} values for the Western Cape region. 88

Table 3.9: Comparison of annual temperature trends (°C/decade) between the Kruger and Shongwe (2004) and the current study for the period 1960–2003. 91

Table 3.10: Summer and winter temperature trends (°C/decade) for the period

1960–2010; for comparison with the MacKellar *et al.* (2014) study. 92

Table 4.1: KwaZulu-Natal station details with start/end dates for temperature recording. 107

Table 4.2: Mean temperature (°C) for Briercliffe near DBN (taken at sunrise, noon and night) in 1851 (data calculated from Holden, 1855); PMB and DBN in 1858 (data calculated from Mann, 1859); and PMB (taken at 9am, 3pm and 9pm) for 1860-1865 (calculated from Mann 1878). 111

Table 4.3: Annual and seasonal T_{mean}, T_{max} and T_{min} Mann Kendall statistics and Sen's slope estimate (Q) (°C/decade) at KZN stations. 112

Table 5.1: South African stations, detailing GPS coordinates and start/end dates for each station. 132

Table 5.2: List of ENSO episode years (Year 1) included in this study. 132

Table 5.3: Temporal consistency rates and coherence rates for each region. 138

Table 5.4: Probability of random occurrence based on the hypergeometric distribution for El Niño and La Niña events. 140

Table 5.5: Strengthening/weakening of the ENSO influence on temperature through time. 145

Table 5.6: Regional chi-square statistics for traditional summer T_{max}/T_{min} anomalies (average of December, January and February), rate of occurrence and strengthening/ weakening influence of El Niño phases on T_{max}/T_{min}. Chi-square critical value = 9.48, degree of freedom = 4 and p-values in bold are significant. 160

LIST OF ACRONYMS

ACMANT: Adapted Caussinus Mestre Algorithm for homogenizing networks of monthly temperature data

ACORN-SAT: Australian Climate Observations Reference Network-Surface Air temperature

ALT: Altitude

AR5: Fifth Assessment Report

CRU: Climate Research Unit

CRUTEM4: Climate Research Unit land station temperature dataset

DEA: Department of Environmental Affairs

DTR: Diurnal Temperature Range

ENSO: El Niño Southern Oscillation

ETCCDI: Expert Team on Climate Change Detection and Indices

GCM: General Circulation Model

GHCNv3: Global Historical Climatology Network version 3

GISS: Goddard Institute of Space Studies

HOMER: Homogenization in R

IPCC: Intergovernmental Panel on Climate Change

IPSL: Institute Pierre Simon Laplace

KZN: KwaZulu-Natal

LTAS: Long-Term Adaptation Scenarios Flagship Research Programme

MIROC: Model for Interdisciplinary Research on Climate

MK: Mann Kendall

MASH: Multiple Analysis of Series for Homogenisation

NOAA: National Oceanic and Atmospheric Administration

PMB: Pietermaritzburg

PMF: Penalized Maximal F-test

PMT: Penalized Maximal t-test

QM: Quantile Matching

SAWS: South African Weather Services

SOI: Southern Oscillation Index

SNHT: Standard Normal Homogeneity Test

SSTs: Sea surface temperatures

T_{max}: Maximum temperature

T_{mean}: Mean temperature

T_{min}: Minimum temperature

USHCN: United States Historical Climatology Network

CHAPTER ONE

INTRODUCTION

1.1. BACKGROUND

Climate is the average weather conditions of a particular area over an extended duration, ranging from decades to centuries (Miller and Spoolman, 2012; Cubasch *et al*., 2013). Schulze (2003) highlighted an important difference between climate variability and climate change, where climate variability is reversible and non-permanent. Climate change on the other hand is irreversible and permanent, and refers to a "statistically significant change in the mean state of the climate or in its variability, persisting for an extended time" (Schulze, 2003, p1). Climate change is characterised by a variation in the mean as well as extreme climatic variables (Santos, 2011). Scientific evidence suggests that the earth's atmosphere is warming due to a combination of natural effects and human activities (Miller and Spoolman, 2012). According to the Intergovernmental Panel on Climate Change (IPCC) Fifth Assessment Report (AR5), the global average land and ocean surface temperature linear trend displayed a warming of 0.85°C during the period 1880-2012 (IPCC, 2013). Long-term climate model simulations also corresponded to the observed trend for the period 1951-2012, but differences were noted for short periods (i.e. 10 to 15 years) (IPCC, 2013). The IPCC released the second assessment report in 1996, in which it concluded that there is evidence to suggest that human activity influences global climate change. The Global Coalition (energy industry lobby group) discredited the aforementioned report, indicating that the IPCC altered the report for political reason (Edwards and Schneider, 2001: 219). This led to widespread debate and motivation for critical investigations and publications. More recent IPCC (2013) reports indicate that it is "extremely likely" that human activity is the dominant cause of global warming since the mid-20th century, as evidence for this has grown and become more conclusive since previous IPCC reports.

Increasing evidence for climate change (e.g. rising temperatures globally and higher frequency of natural disasters such as floods and droughts) suggests that global climate change is threatening sustainable development, especially in developing countries (DEA, 2013). Developing countries are considered more vulnerable to climate change compared to developed countries due to their more limited capacity to cope with the consequences of climate change (IPCC, 2013). Africa is one of the most vulnerable continents to climate change and its adaptive capacity is weakened by developmental challenges such as poverty, limited access to capital, ecosystem degradation and complex disasters and conflicts (Niang

et al., 2014). South Africa is highly vulnerable to climate change and climate variability (Akoon *et al.*, 2010; Thornton *et al*., 2014). The South African health sector, agriculture, plant and animal biodiversity, water resources and rangelands, have all been identified as highly vulnerable to climate change (Akoon *et al.*, 2010). According to South Africa's National Climate Change Response White Paper, South Africa is vulnerable to climate change as a result of greenhouse gas emission levels, and a consequence of its energy intensive fossil fuel powered economy (DEA, 2011). However, South Africa is making progress in understanding the impacts of climate change as well as implementing and evaluating adaptation responses (Ziervogel *et al*., 2014).

Observed global mean surface temperature trends display robust multi-decadal warming, and substantial decadal and interannual variability, with a total increase of 0.78°C from the 1850-1900 average to the 2003-2012 average (IPCC, 2013). In Africa, decadal analyses of temperature over the past 50 to 100 years strongly support increasing warming trends (Niang *et al*., 2014). For the period 1961-2010, observed trends of 0.32°C/decade are recorded over subtropical Africa, subtropical North Africa and parts of central tropical Africa (Engelbrecht *et al*., 2015). In addition, significantly higher surface temperature anomalies are observed over the period 1995-2010 compared to 1979-1994 across the African continent (Collins, 2011). Maximum temperatures (T_{max}) and minimum temperatures (T_{min}) over South Africa have displayed significant increases annually as well as for almost all seasons. Annual mean temperature (T_{mean}) increased by at least 1.5 times the observed global average for the past five decades (DEA, 2013). Temperature trends at different locations in South Africa, record a statistically insignificant rate of increase for the period 1960-1990 (Hughes and Balling, 1995). However, in a widely cited South African study, Kruger and Shongwe (2004) recorded an increase in T_{mean} for 23 of 26 stations, with 13 showing a significant trend for the period 1960-2003. In a more recent study of South African temperature trends, mean annual T_{max} recorded an increase of 0.19°C/decade, while mean annual T_{min} warming rates of 0.33°C/decade were observed over South Africa for the period 1960-2010 (MacKellar *et al*., 2014). Notably, the aforementioned studies for South Africa investigate periods after 1960 up to the year prior to publication. The most recent study by Kruger and Nxumalo (2017) coinciding with the work of this PhD includes a start date of 1931. Therefore, this PhD study focuses on long-term temperature trends based on available data dating as far back as possible (e.g. 97 years for the Western Cape Province - see Chapter three; 85 years for KwaZulu-Natal - see Chapter four) in South Africa.

Climate model simulations performed under the Coupled Model Intercomparison Project Phase 5 (CMIP5) using the new set of scenarios in AR5 (i.e. Representative Concentration Pathway (RCP)), project global surface temperature warming of 0.3°C to 0.7°C for the period 2016-2035, relative to the 1986-2005 average (IPCC, 2013). For Southern Africa, projected increases of 3.4°C to 4.2°C above the 1981-2000 average are reported under the A2 (high emissions) scenario of the Special Report on Emissions Scenarios (SRES) developed in AR4 (Niang *et al.*, 2014). Also under the A2 emissions scenario, Engelbrecht *et al*. (2015) report increases of 4°C to 6°C for the subtropics of Africa and 3°C to 5°C for the tropics of Africa by the end of the 21st century. These regional downscalings indicate annual-average temperature increases at 1.5 times that of the global temperature increase (Engelbrecht *et al*., 2015). The Conformal-Cubic Atmospheric Model (CCAM), under the A2 emission scenario, projects annual surface temperature increases of 1°C for the period 2015-2035 (near-future) (DEA, 2013). For the period 2040-2060 (mid-future), increases of 2.5°C to 3.5°C, relative to the baseline period (1971-2005) are projected over the interior of South Africa (DEA, 2013). Temperature increases of 4°C are projected over the central and northern interior regions of South Africa for the period 2080-2100, relative to the baseline period 1971-2005 (DEA, 2013). The temperature projections over the interior of South Africa, under very high greenhouse gas emission scenario (RCP 8.5), indicate significant warming of 5°C to 8°C by the end of this century (DEA, 2013). The rapid increases in temperature projected for Southern Africa are expected to impact a variety of sectors, including agriculture, water resources, biodiversity and human health.

Temperature projections over southern Africa indicate warming greater than +0.4°C/decade in Model for Interdisciplinary Research on Climate (MIROC) and Institute Pierre Simon Laplace (IPSL) model simulations, based on A1B emission scenario (medium-high emissions scenario; assumes a linear increase to a doubled CO_2 by 2100) over the period 1979-2010 (Jury, 2013). For the same period, observed temperature trends vary between 0.3°C/decade (for National Climate Data Center data) and 0.14°C/decade (for Global Historical Climate Network data) (Jury, 2013). Observed rainfall trends (-0.003 mm/day per year) were found to be consistently lower than model projections (IPSL (-0.013 mm/day per year) and MIROC) for the 20th century (Jury, 2013). Clearly, the results of Jury (2013) demonstrate that the model outputs for temperature data more closely reflect the observed trends while there are larger differences between model and observed trends for rainfall. In addition, a comparison of observed South African trends and multiple General Circulation Model

simulations also report closer agreement with temperature indices compared to precipitation indices for the period 1960-2010 (DEA, 2013), a result supported by the IPCC Fifth Assessment Report. Similarly, MacKellar *et al*. (2014) compared observed trends to simulated trends using 11 downscaled Global Circulation Models (GCMs) and found that models do not accurately represent observed rainfall changes or the cooling trend of T_{min} over the central interior of South Africa. This study, however, does not explicitly provide the outputs of the models. In addition, the Long Term Adaptation Scenario technical report indicates that observed trends over South Africa have not risen as steeply since 2000 as indicated by multiple GCMs (DEA, 2013). Given these discrepancies between observed trends and model output, as well as the knowledge that a model will only perform optimally if the input is accurate, high quality of data is essential. Discrepancies between observed historical trends and model projections are possibly due to the inability of models to represent key climatic processes at regional or local level or due to uncertainties in observational records (DEA, 2013; MacKellar *et al*., 2014). It is also important to note that a model cannot completely represent the complexity of the Earth's system. However, to improve the inadequacies of models, scientists have integrated different emission scenarios because the rate of future greenhouse emissions is uncertain (Engelbrecht *et al*., 2015). Model simulations are verified according to their ability to represent observed temperature trends (Engelbrecht *et al*., 2015). This emphasizes the need for accurate analysis of temperature trends to produce reliable future projections, which is essential for future disaster planning and mitigation measures.

Long-term, high quality data sets are required for robust and consistent trend analyses to detect and understand climate variability and change (Brunet and Jones, 2011). To achieve these high quality datasets, data must be subjected to robust quality control and homogenization processes in order to remove erroneous data and non-climatic biases in the time series (Štěpánek *et al*., 2013). These non climatic biases may be caused by instrument changes, station relocation or observing practices which are characteristic of weather stations operating over a long period (Freitas *et al*., 2013). Therefore, homogenization techniques are applied to ensure that the variability in climate time series is only a result of changes in weather and climate (Aguilar *et al*., 2003). Homogenization techniques (discussed in detail in Chapter two) include absolute or relative methods. Absolute methods apply statistical tests directly to the time series to detect non-climatic biases while relative homogenization methods use neighbour stations as reference series (Venema *et al*., 2012). The

homogenization process is complex in nature, and therefore requires a study of metadata records (Vincent *et al.*, 2012). Metadata records detail major movements, inadequate exposure and maintenance problems (Kruger and Sekele, 2013). The examination of these records consumes a great deal of time and thus scientists often limit studies to the identification of only the major problems and proceed to perform trend analyses (Vincent *et al.*, 2012; Kenawy, 2013). Thus, available metadata and station histories must be examined (in terms of instrumentation or location change) to determine their contributing influence on data bias (Aguilar *et al.*, 2003). Metadata indicate how, where, when and by whom the information was collected. A complete metadata should record all the changes a station has undergone during the station's lifetime (i.e. the station history) (Aguilar *et al.*, 2003), which seems an omission in previous southern African studies. Although homogenization techniques have advanced over time, developing homogeneous long-term time series remains a challenge due to the inherent limitations when accounting for non-climatic factors (Hartmann *et al*., 2013). These techniques are, however, essential for removing some of the bias in time series and have therefore been applied in this PhD study. This PhD study thus subjects temperature data sets to robust quality control (i.e. RClimDex) and a homogenization process (i.e. ProClimDB and AnClim software) to produce high quality datasets.

Initiatives to improve the quantity and quality of temperature datasets have also been undertaken at a global scale (Jones, 2012). The IPCC AR5 has cited four global monthly land surface temperature datasets and a new set (i.e. China Meteorological Administration global Land Surface Air Temperature (CMA-LSAT)) have been released this year (Xu *et al*., 2017). The Climate Research Unit (CRU) land station temperature database is a grid - box data set of 5° latitude by 5° longitude called CRUTEM4, with 5583 station records (Jones *et al.*, 2012). Other examples of global datasets which include improved or homogenized station data are the Global Historical Climatology Network version 3 (GHCNv3), the Goddard Institute of Space Studies (GISS) and Berkeley Earth Surface Temperature (BEST) (Hartmann *et al*., 2013). While global datasets are automatically quality controlled and use very different methods to homogenize data records compared to national and regional datasets, it is important to note that high-quality national and regional temperature records can help verify, improve and extend global datasets. The release of the most recent global dataset (i.e. CMA-LSAT) demonstrates the continued efforts of scientist to improve the quality of temperature data and increase the number of stations included in the global datasets, required for accurate estimates of global warming. This further illustrates the

importance of homogenizing the station records for South Africa in this PhD study. Filling knowledge gaps with findings of this investigation has significant implications for ongoing debates on the extent of recent climate warming in South Africa and beyond.

1.2. RATIONALE

Understanding and predicting temperature trends is important because of the impact that temperature has on human comfort, agricultural production and the spread of pests and diseases (Grab and Nash, 2010), just to name a few reasons. Efforts made by climate scientists around the world are noted through the wealth of literature on climate change, particularly highlighted by the IPCC assessment reports. Human activities are increasing the concentration of greenhouse gases and land use which in turn is changing the Earth's energy budget (Cubasch *et al*., 2013). IPCC AR5 reports emphasize increasing scientific evidence for human-induced climate change (especially rising temperatures at global and regional scales) (Cubasch *et al*., 2013). However, regional scale long-term temperature trends based on high quality homogenized South African data have been a knowledge gap. Long-term temperature time series often contain abrupt changes, called changepoints or inhomogeneities, which result from changes in instrumentation or exposure, station relocation, urbanization or land cover changes (Peterson *et al*., 1998). Therefore, a technique called homogenization is used to detect and remove these inhomogeneities to produce a homogeneous time series (Aguilar *et al*., 2003). A homogeneous time series is defined as a time series whose variations are only caused by weather and climate (Venema *et al*., 2012).

To ensure the homogeneity of data, previous temperature trend studies conducted for South Africa used stations which had not undergone any major relocations or changes in exposure (Kruger and Shongwe, 2004). The Kruger and Nxumalo (2017) study, coinciding with the work of this thesis applied absolute homogenization methods on South African temperature data for the period 1931-2015. This PhD study ensures that temperature data undergo robust quality control and relative homogenization procedures (with ProClimDB and AnClim software, using a reference series), considered more reliable than the absolute homogenization methods (Venema *et al*., 2012).

Previous temperature trend studies over South Africa (e.g. Muhlenbruch-Tegen, 1992; Hughes and Balling, 1996, Kruger and Shongwe, 2004; MacKellar *et al*., 2014) have investigated relatively short periods. While the most recent study on temperature trends over South Africa (Kruger and Nxumalo, 2017) covers the period 1931-2015, this new study uses linear regression analysis to determine trends. Yet, the majority of studies (e.g. Turkes and Sumer, 2004; Li *et al.*, 2011; Gocic and Trajkovic, 2013; Kousari *et al.*, 2013; Sonali and Kumar, 2013; Viola *et al*., 2014) suggest that nonparametric statistics are superior methods compared to parametric analysis for environmental trend analysis. The majority of temperature trend analyses across the globe use the nonparametric Mann Kendall statistic (see Chapter two) because this method does not require the data to be normally distributed (Kousari *et al*., 2013). Parametric statistics (such as Least square linear regression) require the data to be normally distributed, whereas climatic data are skewed (Sonali and Kumar, 2013). This PhD study thus determines temperature trends using the Mann Kendall nonparametric statistic.

To further understand temperature variability over South Africa, this PhD study assesses the impact of El Niño Southern Oscillation (ENSO) on high quality temperature data because ENSO is known as the leading mode of inter-annual temperature variability at global and regional scales. The majority of the studies conducted in South Africa have examined the relationship between ENSO phases and rainfall. Previous studies related to the impacts of ENSO on southern Africa temperature have been limited to those by Halpert and Ropeleski (1992), Kruger and Shongwe (2004) and Manatsa and Reason (2016), which do not provide a comprehensive account of the impacts that El Niño/La Niña have on T_{max} and T_{min}. This PhD study therefore examines El Niño/La Niña impacts on T_{max} and T_{min} over South Africa over the common period 1940-2016.

1.3. AIM

The main aim of this PhD project is to use accurate, relatively long data sets of temperature (spanning 1851-2016) available in South Africa, to establish a more precise understanding of temporal temperature variability over this region. This is achieved through the use of robust methodology (i.e. data quality control and homogenization procedures, using reference series) to produce high quality data sets for temperature trend analysis: Chapter three, as well

as an analysis of temperature trends over coastal and higher lying adjacent inland areas: Chapter four and an examination of climatic control on temperatures in Chapter five (i.e. the El Niño-Southern Oscillation (ENSO) mechanism influencing temperature through the last several decades).

1.4. OBJECTIVES

In order to establish a deeper understanding of temporal temperature variability over South Africa, this research is guided by three core objectives:

- To provide a homogeneous dataset for the Western Cape region in South Africa and establish the first long-term (1916-2013) annual and seasonal instrumental temperature trends for this region (see Chapter three). This objective is achieved through robust quality control and homogenization procedures, which is further applied to the KwaZulu-Natal (KZN) region (in Chapter four), which also requires accurate data sets and temperature trends to achieve objective two.

- To extend past work by examining temperature trends and cyclical patterns for KZN over a considerably longer period (1851-2015), with a specific focus on contrasting coastal and adjacent higher lying interior regions (see Chapter four). In combination with temperature trend analyses (in Chapters three and four), the assessment of climatic control mechanisms (such as ENSO in Chapter five) is essential to better understand temporal temperature variability over South Africa.

- To assess the extent and timing of El Niño/La Niña impacts on T_{max} and T_{min} over selected South African stations for the period 1884-2016, and to establish any possible direct change in such temperature responses to ENSO over time (see Chapter five).

The study of long-term temperature trends over South Africa's west and east coasts as well as the assessment of the leading mode of interannual variability (ENSO) on temperature over different regions (i.e. northern interior, central interior, western interior, northeastern interior,

northeast coast, southeast coast and southwest coast) of South Africa will enable the achievement of the overarching aim to further understand seasonal, annual and decadal temperature variability across South Africa during the recent past. In addition, exploring the role of oceanic and atmospheric drivers of regional temperature variability in South Africa is expected to add to our current knowledge and understanding of such temperature variability.

1.5. THESIS STRUCTURE

This introductory chapter provides the background, including the motivation for this PhD study to advance some aspects of our understanding of temperature variability in South Africa, followed by the aims and objectives of the study. Chapter two outlines the literature review pertaining to long-term temporal temperature variability, both globally and regionally. The three core objectives are addressed through separate chapters written up as research papers for journal publication. The homogenized long-term temperature trends for the Western Cape Province (South Africa) for the period 1916-2013 is presented in Chapter three and has been published in the *International Journal of Climatology*. Chapter four discusses historical temperature records for coastal and adjacent higher lying interior regions of KwaZulu-Natal (South Africa) over the period 1851-2015. Chapter five examines the extent and timing of El Niño and La Niña impacts on T_{max}/T_{min} over parts of South Africa. The synthesis discussion and conclusion contained in Chapter six reflects on the key findings made in Chapters three to five, and provides an overarching conclusion for the PhD project. In addition, Chapter six discusses the extent to which the objectives of this PhD study have been achieved, and makes recommendations for future research on temperature trends in southern Africa.

1.6. REFERENCES

Aguilar E, Auer I, Brunet M, Peterson TC, Wieringa J. 2003. Guidelines on Climate Metadata and Homogenisation. WCDMP-No. 53, WMO-TD No. 1186. World Meteorological Organization, Geneve.

Akoon I, Archer E, Engelbrecht F, Landman W, Le Roux A, Van Huyssteen E, Fatti C, Vogel C, Maserumule R, Colvin C, Le Maitre D, Lotter D, Olwoch J, Wright C, Meyer AA, Theron A, Diedericks G, Maherry A, Rossouw M, Midgley G, Davis C, Stevens N, Sinden LA, Warburton M, Nkambule C. 2010. South African risk and vulnerability atlas. Department of Science and Technology, Pretoria, pp.62.

Brunet M, Jones P. 2011. Data rescue initiatives: bringing historical climate data into the 21st century. *Climate Research* **47**: 29-40.

Collins JM. 2011. Temperature Variability over Africa. *Journal of Climate* **24**: 3649-3666.

Cubasch UD, Wuebbles D, Chen MC, Facchini D, Frame N, Mahowald, Winther J-G. 2013. Introduction. In: Climate Change 2013: The Physical Science Basis. Contribution of Working Group I to the Fifth Assessment Report of the Intergovernmental Panel on Climate Change (Stocker TF, Qin D, Plattner G-K, Tignor M, Allen SK, Boschung J, Nauels A, Xia Y, Bex V, Midgley PM (eds.)). Cambridge University Press, Cambridge, United Kingdom and New York, NY, USA, pp.119-158.

Department of Environmental Affairs (DEA). 2011. National Climate Change Response Plan White Paper. Pretoria: Department of Environmental Affairs. Available online: https://www.environment.gov.za/sites/default/files/legislations/national_climatechange_response_whitepaper.pdf (Accessed 7 January 2017).

Department of Environmental Affairs (DEA). 2013. Long-Term Adaptation Scenarios Flagship Research Programme (LTAS) for South Africa. Climate Trends and Scenarios for South Africa. Pretoria, South Africa, pp.1-132.

Edwards PN, Schneider SH. 2001. Self-Governance and Peer Review in Science for Policy: The Case of the IPCC Second Assessment report. In Changing the atmosphere: Expert knowledge and environmental governance. Miller CA, Edwards PN (eds.). MIT Press, Cambridge. pp. 219-246.

Engelbrecht F, Adegoke J, Bopape MM, Naidoo M, Garland R, Thatcher M, McGregor J, Katzfey J, Werner M, Ichoku C, Gatebe C. 2015. Projections of rapidly rising surface temperatures over Africa under low mitigation. *Environmental Research Letters* **10**: 085004, doi: 10.1088/1748-9326/10/8/085004.

Freitas L, Pereira MG, Caramelo L, Mendes M, Nunes LF. 2013. Homogeneity of monthly air temperature in Portugal with HOMER and MASH. *Quarterly Journal of the Hungarian Meteorological Service* **117**:69-90.

Gocic M, Trajkovic S. 2013. Analysis of changes in meteorological variables using Mann-Kendall and Sen's slope estimator statistical tests in Serbia. *Global and Planetary Change* **100**: 172-182.

Grab SW, Nash DJ. 2010. Documentary evidence of climate variability during cold seasons in Lesotho, southern Africa, 1833-1900. *Climate Dynamics* **34**: 473-499.

Halpert MS, Ropelewski CF. 1992. Surface temperature pattern associated with Southern Oscillation. *Journal of Climate* **5**: 577-593.

Hartmann DL, Klein Tank AMG, Rusticucci M, Alexander LV, Brönnimann S, Charabi Y, Dentener F, Dlugokencky EJ, Easterling DR, Kaplan A, Soden BJ, Thorne PW, Wild M, Zhai PM. 2013: Observations: Atmosphere and Surface. In: Climate Change 2013: The Physical Science Basis. Contribution of Working Group I to the Fifth Assessment Report of the Intergovernmental Panel on Climate Change (Stocker TF, Qin D, Plattner G-K, Tignor M, Allen SK, Boschung J, Nauels A, Xia Y, Bex V, Midgley PM (eds.)). Cambridge University Press, Cambridge, United Kingdom and New York, NY, USA. pp. 159-254.

Hughes WS, Balling RC. 1996. Urban Influences on South African Temperature Trends. *International Journal of Climatology* **16**: 935-940.

IPCC. 2013. Summary for Policymakers. In: Climate Change 2013: The Physical Science Basis. Contribution of Working Group I to the Fifth Assessment Report of the Intergovernmental Panel on Climate Change (Stocker, TF, Qin D, Plattner G-K, Tignor M, Allen SK, Boschung J, Nauels A, Xia Y, Bex V, Midgley PM (eds.)). Cambridge University Press, Cambridge, United Kingdom and New York, NY, USA. pp. 29.

Jones PD, Lister DH, Osborn TJ, Harpham C, Salmon M, Morice CP. 2012. Hemispheric and large-scale land-surface air temperature variations: An extensive revision and an update to 2010. *Journal of Geophysical Research* **117**: D05127, doi:10.1029/2011JD017139.

Jury MR. 2013. Climate trends in southern Africa. *South African Journal of Science* **109**: 1-11 . http://dx.doi.org/10.1590/ sajs.2013/980.

Kenawy AE, Lopez-Moreno JI, Štěpánek P, Vicente-Serrano SM. 2013. An assessment of the role of homogenisation protocol in the performance of daily temperature series and trends: application to northeastern Spain. *International Journal of Climatology* **33**: 87–108.

Kousari MR, Ahani H, Hendi-zadeh R. 2013. Temporal and spatial trend detection of maximum air temperature in Iran during 1960–2005. *Global and Planetary Change* **111**: 97–110.

Kruger AC, Shongwe S. 2004. Temperature trends in South Africa: 1960–2003. *International Journal of Climatology* **24**: 1929–1945.

Kruger AC, Sekele SS. 2013. Trends in extreme temperature indices in South Africa: 1962-2009. *International Journal of Climatology* **33**: 661-676.

Kruger AC, Nxumalo M. 2017. Surface temperature trends from homogenized time series in South Africa: 1931-2015. *International Journal of Climatology* **37**: 2364-2377.

Li Z, He Y, Wang C, Wang X, Xin H, Zhang W, Cao W. 2011. Spatial and temporal trends of temperature and precipitation during 1960 and 2008 at the Hengduan Mountains, China. *Quaternary International* **236**: 127-142.

MacKellar N, New M, Jack C. 2014. Observed and modeled trends in rainfall and temperature for South Africa: 1960–2010. *South African Journal of Science* **110:** 1-13, http://dx.doi.org/10.1590/sajs.2014/20130353.

Manatsa D, Reason C. 2016. ENSO-Kalahari Desert linkages on southern Africa summer surface air temperature. *International Journal of Climatology* **37**: 1728-1745.

Miller, GT, Spoolman, SE. 2012. Living in the Environment. 17th ed. Brooks/Cole, Cengage Learning. Canada. pp. 482.

Niang I, Ruppel OC, Abdrabo MA, Essel A, Lennard C, Padgham J, Urquhart P. 2014. Africa. In: *Climate Change 2014: Impacts, Adaptation, and Vulnerability. Part B: Regional Aspects. Contribution of Working Group II to the Fifth Assessment Report of the Intergovernmental Panel on Climate Change* (Barros VR, Field CB, Dokken DJ, Mastrandrea, MD, Mach, KJ, Bilir TE, Chatterjee M, Ebi KL, Estrada YO, Genova, RC, Girma B, Kissel ES, Levy AN, MacCracken S, Mastrandrea PR, White LL (eds.)).

Cambridge University Press, Cambridge, United Kingdom and New York, NY, USA, pp. 1199-1265.

Peterson TC, Easterling DR, Karl TR, Groisman P, Auer I, Bohm R, Plummer N, Nicholis N, Torok S, Vincent L, Tuomenvirta H, Salinger J, Førland EJ, Hanssen-Bauer I, Alexandersson H, Jones P, Parker D. 1998. Homogeneity adjustments of in situ climate data: a review. *International Journal of Climatology* **18**: 1493–1517.

Santos, CACD. 2011. Trends in indices for Extremes in daily air temperature over UTAH, USA. *Revista Brasileira de Meteorologia* **26**: 19 - 28.

Schulze RE. 2003. Dialogue on Water and Climate Training Package. Managing Climate Variability and Climate Change in Water Resources. University of Natal, Pietermaritzburg, RSA, School of Bioresources Engineering and Environmental Hydrology. ACRUcons Report no. 45. pp. 92.

Sonali P, Kumar DN. 2013. Review of trend detection methods and their application to detect temperature changes in India. *Journal of Hydrology* **476**: 212- 227.

Thornton PK, Ericksen PJ, Herrero M, Challinor AJ. 2014. Climate variability and vulnerability to climate change: a review. *Global Change Biology* **20**:3313-3328.

Trenberth KE, Caron JM, Stepaniak DP, Worley S. 2002. Evolution of El Niño-Southern-oscillation and global atmospheric surface temperature. *Journal of Geophysical Research* **107**: 5-12.

Turkes M, Sumer UM. 2004. Spatial and temporal patterns of trends and variability in diurnal temperature ranges of Turkey. *Theoretical Applied Climatology* **77**: 195–227.

Vincent LA, Wang XL, Milewska EJ, Wan H, Feng Y, Swail V. 2012. A second generation of homogenized Canadian monthly surface air temperature for climate trend analysis. *Journal of Geophysical Research* **117**: D18110, doi:10.1029/2012JD017859.

Viola F, Liuzzo L, Noto LV, Lo Conti F, La Loggia G. 2014. Spatial distribution of temperature trends in Sicily. *International Journal of Climatology* **34**: 1-17.

Xu W, Li Q, Jones PD, Wang XL, Trewin B, Yang S, Zhu C, Zhai P, Wang J, Vincent L, Dai A, Gao Y, Ding Y. 2017. A new integrated and homogenized global monthly land surface air

temperature dataset for the period since 1900. *Climate Dynamics,* doi: 10.1007/s00382-017-3755-1.

Ziervogel G, New M, van Garderen EA, Midgley G, Taylor A, Hamann R, Stuart-Hill S, Myers J, Warburton M. 2014. Climate change impacts and adaptation in South Africa. *WIREs Climate Change* **5**: 605–620.

CHAPTER TWO

LITERATURE REVIEW

2.1. **INTRODUCTION**

The temperature of the Earth's atmosphere is controlled naturally by the greenhouse effect, whereby one third of incoming solar radiation is reflected back into space and the remainder is absorbed by land and the oceans (Miller and Spoolman, 2012). Greenhouse gases (GHGs) such as water vapour, methane, nitrous oxide, carbon dioxide and ozone, trap solar radiation and maintain temperature to sustain life on Earth. Human activities such as the burning of fossil fuels, forestry, agricultural practices and land clearing, increase greenhouse gases in the atmosphere (Miller and Spoolman, 2012). According to the IPCC's AR5, the concentration of carbon dioxide, methane and nitrous oxide have increased since 1750 as a result of human activity (Cubasch *et al*., 2013). This increase in greenhouse gas concentration will trap more heat and further increase the temperature on Earth (Creamer and Goa, 2015). Although much scientific evidence exists to support human-induced climate change, and which has resulted in scientific consensus amongst the majority of scientists, ongoing debates still continue (Hartman *et al*., 2013). The average global land and ocean surface temperature has warmed by 0.85°C for the period 1880 to 2012 (IPCC, 2013).

The Earth's climate is a complex system influenced by internal and external forcing. Natural climate variability in the Earth's system is caused by interactions between the atmosphere, ocean, land as well as solar and volcanic forcings (Cubasch *et al*., 2013). The interplay of large-scale climate modes such as El Niño-Southern Oscillation (ENSO), Indian Ocean Dipole (IOD) and Southern Annular Mode (SAM), influence climate variability in the Southern Hemisphere (Neukom *et al*., 2014). Southern Africa is also influenced by several atmospheric and oceanic systems (such as shifts in the Inter-Tropical Convergence Zone (ITCZ), the midlatitude westerlies, sea surface temperatures and the continental and oceanic cyclones) as a result of its position at the interface of temperate, subtropical and tropical climate zones and the Indian, Atlantic and southern oceans (Hannaford *et al*., 2015). Madden-Julian Oscillation (MJO), the eastward propagation of large-scale convective clusters in the tropics, strongly affects convection over South African during the El Niño phase, whereby intraseasonal convection variability is high while the convection itself is less active (Pohl *et al*., 2007; MacKellar *et al*., 2014).

The increasing observations, theoretical analyses and modelling studies over time, have strengthened the evidence to support links between human activities and climate change (Cubasch *et al*., 2013). The main anthropogenic drivers of climate change are population growth, deforestation, industrialisation, land use changes and the increase in GHGs, with the most important influences being greenhouse gas emissions and changes in land use, such as for urbanisation and agriculture (Odindi *et al.,* 2012). Population growth and urbanisation have frequently been held solely responsible for the increase in greenhouse gases, and hence climate change (Satterwaite, 2009). The various factors responsible for driving climate change are complex in nature. The effects of urbanisation on the Earth-climate system are not fully understood (Lamptey *et al.*, 2005). Urbanisation affects microclimatic variables such as vegetation cover, surface moisture availability and radiant surface temperature (Carlson and Arthur, 2000). The replacement of vegetation with impervious surfaces results in a change of physical characteristics of the area, such as thermal capacity and heat conductivity (Arathyram and Venugopala Raoa, 2012). The effect of urbanisation is important for climate change and attribution studies because urbanisation induces a warming trend in air temperature trends, similar to that of the increasing concentration of greenhouse gases (Jun and Zhong-Wei, 2016). Although the effect of urbanisation on global temperature trends is negligible, its influence on local or regional temperature trends is more considerable (Jun and Zhong-Wei, 2016). This is further discussed in the Synthesis chapter of this thesis (Chapter six).

The aforementioned synergistically operating climate mechanisms are not fully understood (Kane 2009), therefore a better understanding of all the factors that play a role in climate variability and climate change is important for establishing effective adaptation and mitigation strategies. In addition, reliable estimates of historical temperature changes will assist with accurate determination of future projections (Miller and Spoolman, 2012). This chapter reviews the literature on historical data recovery, data quality control, homogenization and temperature trends at global and regional (South African) scales. This is followed by the comparison of coastal and adjacent inland temperature trends, and finally reviews the effects of ENSO in various countries.

2.2. **HISTORICAL CLIMATE DATA RECOVERY**

Historical climate data broadly refers to past climate data from instrumental or documentary sources (Bradzil *et al*., 2005). Historical temperature data provide an important context for climate change projections and attribution studies (Brohan *et al*., 2012). Instrumental temperature records largely date back to 1850, with longer time scales based on proxies (e.g. tree rings and ice-cores) (Brohan *et al*., 2012). The quality of long-term digital temperature records is questioned as the exercise of collecting, digitising, processing, transfering, storing and transmitting instrumental data, all introduce errors (Brunet and Jones, 2011). The recovery of datasets as well as increasing geographical coverage of data is necessary for advancing the understanding of how climate is changing in space and time (Boko *et al*., 2007; Collins, 2011).

Palaeotemperature indicators have been used to determine temperature variations in the absence of instrumental records (Nicholson *et al*., 2013), however this review focuses on the recent recovery of documentary and instrumental historical records, specifically for the Southern Hemisphere. Compared to the Northern Hemisphere, Southern Hemisphere temperature data are scarce (Jones *et al*., 2016). This is clearly evident by the dense station coverage and long datasets (>200 years) available for Europe, North America and parts of Asia, while that for South America and Africa are more limited (Jones *et al*., 2016). Instrumental temperature records are available for large parts of the Northern Hemisphere, in some cases dating back to the mid-17th century (Bodri and Cermak, 1999). In contrast, surface air temperature records for the Southern Hemisphere only become more widely available from ca. 1858 (Jones *et al*., 1986), with only a few studies having scritinized the earliest instrumental records (e.g. Ashcroft *et al*., 2014 discussed below). The lack of historical data for the Southern Hemisphere hampers the understanding of climate variability in this region (Ashcroft *et al*., 2014). The infilling of data gaps, especially for early years (before the 1950s), will improve coverage (Jones and Wigley, 2010) and assist in the reconstruction and temporal extension of climatological time series (Valero *et al*., 1996). The scarcity of temperature records for the Southern Hemisphere further supports the importance of the current PhD work, which includes the recovery of 19th century data for the KwaZulu-Natal region of South Africa.

Recent literature (e.g. Prieto and Herrera, 2009; Ashcroft *et al*., 2014; Hannaford and Nash, 2016; Nash *et al*., 2016) on qualitative and quantitative historical climate data recovery efforts in the Southern Hemisphere, reflects the importance of this initiative. For South America, regional archives, magazines and newspaper libraries from Equador, Peru, Bolivia, Chile and Argentina were recovered to reconstruct climatic variations for past centuries (Prieto and Herrera, 2009). Although Spanish colonization led to documents being scattered across diverse archives, temperature and precipitation records for the 16th, 17th and 18th centuries were constructed using content analysis (Prieto and Herrera, 2009). Although a large number of climate reconstructions across South America were mostly for precipitation, a long temperature record spanning the period 1754-1856 was recovered for Lima (Prieto and Herrera, 2009). However, such records require cautious interpretation given that metadata were not available for quality assurance.

For southeastern Australia, Fenby and Gergis (2013) consolidate twelve documentary-based rainfall chronologies based on secondary sources such as newspapers, government records, almanacs and local histories. By classifying months as either wet/dry from qualitative data collected by European settlers, 27 drought periods for the period 1788-1860 and 14 years of high rainfall in New South Wales for the period 1788-1840 were identified (Fenby and Gergis, 2013). The historical data recovered by the aforementioned study is restricted to the geographic regions where Europeans settled, a limitation which cannot be overcome. In a departure from secondary sources, historical instrumental climate data (i.e., temperature, atmospheric pressure, rainfall and rain days) were recovered for southeastern Australia from 39 archival sources for the period 1788-1859 (Ashcroft *et al*., 2014). The rescued data were continuous for the period 1826-1859, with short observations for the periods 1788-1791, 1803-1805 and 1821-1824 (Ashcroft *et al*., 2014). The data recovery process involved the location of sources, digitization of data and the conversion to modern units. However, due to the biases detected in these early records, data were subjected to quality control and homogenization procedures (discussed in section 2 of this literature review) for accurate determination of trends and climate variability (Ashcroft *et al*., 2014). The historical instrumental data display high correlations between neighbouring records and also agree with documentary climate records (Ashcroft *et al*., 2014).

For southern Africa, efforts have been made using documentary based approaches to reconstruct 19th century climate, which mainly focussed on rainfall patterns and also included cold season severity analysis (e.g. Grab and Nash, 2010). Unpublished material by missionary societies (e.g. London Missionary Society, Wesleyan Methodist Missionary Society) and published material by hunters and explorers were used to derive a 19th century (1815-1900) climate chronology for the Kalahari region of central Africa (Nash and Endfield, 2002). Six drought periods (1820-1827, 1831-1835, 1844-1851, 1857-1865, 1877-1886, 1894-1899) and seven periods of above average rainfall (1816-1817, 1829-1830, 1851-1852, 1863-1864, 1874-1875, 1889-1891 and 1899-1900) were identified (Nash and Endfield, 2002). Published and unpublished documentary sources were also used to determine the relationship between ENSO events and rainfall variability for the Kalahari Desert and the adjacent regions of central southern Africa for the period 1840-1900 (Nash and Endfield, 2008). The results suggest that the warm phase of ENSO events were preceded by wet conditions during austral summer and succeeded with drought during the following summer (Nash and Endfield, 2008).

The historical rainfall records for southern Africa were extended to the semi-arid area of Namaqualand in the Northern Cape province of South Africa by conducting extensive archival research, making use of historical documentary sources such as missionary journals and letters, traveller's writings and government reports and letters (Kelso and Vogel, 2007). The data uncover drought periods affecting the southern and Eastern Cape, Namaqualand and the Kalahari for the periods 1820–1821; 1825–1827; 1834; 1861–1862; 1874–1875; 1880–1883 and 1894–1896 (Kelso and Vogel, 2007). The first cold season climate chronology based on documentary sources (including letters, diaries, monographs and newspapers articles from southern Africa and British archives) for the 19th century (1833-1900) over Lesotho, classified the mid-1880s as severely cold and suggested an important association with volcanic eruptions (1883 Krakatau eruption) (Grab and Nash, 2010). Historical documentary sources (including letters, journals, missionary reports, newspapaers and diaries archived in Lesotho and the United Kingdom) were used to also uncover drought episodes and floods in Lesotho for the semi-continuous period 1824-1900 (Nash and Grab, 2010). The most severe drought years being 1850-1851 and 1862-1863, while floods were recorded for the periods 1835-1836, 1838, 1847-1848, 1854-1856, 1863-1865, 1880-1881, 1885-1886 and 1890-1894 (Nash and Grab, 2010). Only the latter period (1886-1900) of the records could be checked for accuracy against instrumental precipitation records from Maseru (Nash and

Grab, 2010). The first statistical rainfall reconstruction for southern Africa covering the last two centuries used historical documentary records from some of the aforementioned studies (i.e. Kelso and Vogel, 2007; Nash and Endfield, 2008; Nash and Grab, 2010) as well as coral and tree ring records (Neukom *et al*., 2014). This study used an ensemble-based nested principal component reconstruction method and results recorded a decrease in the amount of precipitation over time in the summer rainfall zone while no significant change occurred for the winter rainfall zone (Neukom *et al*., 2014).

Wind information from ship logbooks used to statistically reconstruct summer and winter season precipitation at four stations in southern Africa over the period 1796-1854 indicate that the decade beginning in 1810 was the wettest period and the 1820s were the driest at Mthatha and Royal National Park (Hannaford *et al*., 2015). However, the 1820s was reported as the wettest decade while the 1830s was dry at the Cape Town station (Hannaford *et al*., 2015). As recently as last year (2016), the first documentary based annual and seasonal 19th century rainfall chronology for southeast Africa (focussing on KwaZulu-Natal, South Africa) was published (Nash *et al*., 2016). Using a variety of documentary sources, eight severe drought periods (1836–1838, 1861–1863, 1865–1866, 1868–1870, 1876-1879, 1883-1885, 1886-1890 and 1892-1894) and six severe wet periods (1847–1849, 1854–1857, 1863–1865, 1879–1881, 1890–1891 and 1892–1894) were identified (Nash *et al*., 2016). Together with the recovered historical Australian data, a continued recovery of such climate records for South Africa and South America would extend the length of records and advance our understanding of climate variability over the Southern Hemisphere during recent historical times. It is clear from the existing literature that the majority of research efforts to recover historical climate data for southern Africa have been for rainfall rather than temperature. In addition, instrumental historical temperature records for the 19th century are severely lacking, emphasizing the need for the recovery of such records. The station network for South Africa is relatively sparse and robust long-term data with minimal gaps are rather few. Data recovery and digitization are therefore essential for extending records in order to increase our understanding of temporal and spatial temperature variability in South Africa.

2.3. **DATA QUALITY CONTROL AND HOMOGENIZATION**

Data quality tests are key components of data quality assessment, which are also required to avoid potential errors that compromise the homogeneity test calculations (Brunet *et al.*, 2008). Therefore, gross error checks such as checking for consistency of calendar dates (i.e. number of days per year and number of days per month) and internal consistency involving the inspection of data for coherency between associated elements within each record (e.g. $T_{max} < T_{min}$) are essential to detect erroneous values. The inclusion of incorrect data complicates the statistical detection of inhomogeneities (Aguilar *et al.*, 2003).

Homogenization is a complex process consisting of a comparison of time series, change point detection and an adjustment of the time series for the detected bias (Domonkos, 2013). Time series data are considered homogeneous only when the variation is due to weather and climate (Peterson *et al*., 1998). Homogeneity testing or homogenization are used to free climate time series of sudden shifts or artificial bias (called change points) which may be caused by non-climatic factors such as instrumentation changes, relocation of a station, environmental changes surrounding the weather station (such as urbanization) or the introduction of different observing practices (Brunet and Jones, 2011). Increasing urbanization surrounding weather stations is likely to affect temperature measurements, whereby temperature at the urban stations are warmer than that recorded at nearby rural stations (Jones, 2016). White-louvered screens were developed in 1870 by Stevenson to reduce the impact of sunlight on thermometer exposure (Jones, 2016). Therefore, any data recorded prior to this time would have a warmer summer bias because the thermometer would have been exposed to direct sunlight (Jones, 2016). Data are also influenced by factors that act at the meso-scale (1 km to 30 km; e.g. proximity to water bodies), local-scale (300 m to 2 km; e.g. nearby trees) (Aguilar *et al.*, 2003) and micro-scale (few centimetres to 1 km; e.g. frost hollows) (Tyson and Preston-Whyte, 2000). The detection of inhomogeneities is particularly difficult when parallel changes in observing practices (e.g. a change in observation time) are made because this would affect the entire network at the same time, thereby influencing data at neighbouring stations which could be used as a reference series (Trewin, 2010). These factors that influence the accuracy of weather records must be taken into account before determining temperature trends (Vincent *et al*., 2012). The complex nature of a temperature trend study, and the importance of conducting studies at a

fine spatio-temporal scale, is emphasized (Aguilar *et al.*, 2003). Improved techniques and available literature (e.g. Menne *et al*., 2009; Wang *et al*., 2010; Venema *et al*., 2012; Vincent *et al*., 2012; Kenawy *et al*., 2013) demonstrate the efforts made around the world to improve the accuracy of temperature trends by subjecting data to quality control and homogenization procedures.

A great deal of effort has been made to develop procedures to identify and remove non climatic inhomogeneities, which include absolute and relative homogeneity tests. Relative methods assume that neighbour stations are exposed to the same climate signal so the differences between two neighbour stations may be used to detect inhomogeneities (Venema *et al*., 2012). This method uses data from neighbouring stations as a reference series to identify inhomogeneities and change points. The challenge associated with the relative homogenization method is the construction of a homogeneous reference series. Absolute methods on the other hand, apply statistical tests directly to the station data without the consideration of neighbouring data. This can be problematic because the detected changes or lack of changes cannot be attributed to climatic or non-climatic influences (Peterson *et al*., 1998). It is for this reason that metadata and station history are important for evaluating detected breaks in the time series (Costa and Soares, 2009). To improve the reliability of homogeneity tests, the use of multiple tests to detect change points is recommended (Štěpánek *et al.*, 2011). Several widely used statistical techniques, either parametric (e.g. Buishand range) or nonparametric (e.g. Kruskal-Wallis, Pettit test, Von Neumann and Wald-Wolfowitz Runs test) are available for the detection of change points (Costa and Soares, 2009). The Standard Normal Homogeneity Test (SNHT) is the most widely used test, usually performed with a composite reference series (Costa and Soares, 2009). SNHT is a *location-specific* test (i.e., gives information about the year of the test) which easily detects breaks close to the beginning and the end of the series (Wijngaard *et al*., 2003). The application of SNHT for homogeneity testing is demonstrated in a study to create a dataset referred to as the "Spanish daily temperature record" using twenty two of the longest Spanish daily (T_{max} and T_{min}) data for the period 1850-2003 (Brunet *et al*., 2006). SNHT relative homogeneity was used to detect and correct inhomogeneities on a monthly scale and temperature records were linearly interpolated to a daily scale (Brunet *et al*. (2006). The article refers the reader to the Aguliar *et al*. (2002) reference for the SNHT "guided application" scheme used, but unfortunately the latter reference is not in English.

Various homogenization algorithms to eliminate inhomogeneities are continuously being developed and improved with time, some of which are outlined below. The Rhtest V4 software, based on the Penalized Maximal t (PMT) test utilises a reference series (Wang *et al*., 2007) and assumes a zero trend and Gaussian errors in the base series. The software detects change points that could be significant at the nominal level (i.e., p=0.95), even without metadata support (i.e. Type 1 change points) (Wang and Feng, 2013). Careful consideration must be taken to determine which detected change points would be adjusted. The Quantile Matching (QM) adjustment adjusts the empirical distribution of all segments of the base series to match each other (Wang *et al*., 2010). The advantage of using QM is that the adjustments differ according to where the monthly temperature value is situated in the probability distribution (Vincent *et al*., 2012). The Rhtest also contains the Penalized Maximal F (PMF) test, which detects undocumented mean shifts without a reference series and allows the base series to have a linear trend (Wang, 2008). Wang and Feng (2013) emphasized the need for caution when using the Rhtest V4 without a reference series. In addition, one of the outcomes of the COST (European Cooperation in Science and Technology) Action ES0601 project: *advances in homogenization methods of climate series: an integrated approach (HOME)*, is that these absolute homogenizations typically decrease the homogeneity of the data for monthly and annual means (Venema *et al*., 2012). In addition, absolute homogenization was found to make the station data more inhomogeneous in a study using a benchmark dataset, with known change points (Venema *et al*., 2012). The Rhtest V3 software (an earlier version), however, has been used by recent studies, such as by Aschcroft *et al*. (2012), where both PMF and PMT are used to detect change points in temperature data over southeastern Australia for the period 1860-2011. The absolute homogenization technique is used in the aforementioned study due to a lack of reliable neighbouring stations for use as reference series.

The HOME project, evaluated the performance of homogenization methods during 2007 to 2011. The main objective of the HOME project was to review and improve common homogenization methods (Venema *et al*., 2012). The best aspects of the most efficient methods were used to produce HOMER (HOMogenization in R) namely PRODIGE (Caussinus and Mestre, 2004), adapted caussinus mestre algorithm for homogenizing networks of monthly temperature data (ACMANT, Domonkos, 2011), CLIMATOL and comparative genomic hybridization (*cghseg*). PRODIGE depends on a pairwise strategy to detect change points and *chseg* is a joint segmentation method. ACMANT (Domonkos 2011)

is fully automatic and applies reference series built from composites (Mestre *et al*., 2013). HOMER is an interactive homogenization software for homogenizing temperature and precipitation data at monthly and annual scales (Mestre *et al*., 2013). HOMER was not considered for use in this PhD work as the software homogenizes data at monthly and annual scale (Mestre *et al*., 2013). The procedure for adjusting temperature time series on a daily scale is the spline daily homogenization method (SLIPDHOM). The detection of change points and the adjustment of time series data at a daily scale are important for computing extreme indices. SPLIDHOM is an indirect nonlinear, nonparametric regression method, which uses cubic smoothing spline (Mestre *et al*., 2011). The use of the PRODIGE and SPLIDHOM techniques for change point detection were used for an analysis of daily extreme T_{max} and T_{min} over Austria for the period 1948-2009 (Nemec *et al*., 2013).

This PhD study initially used Rhtest V4 software for the homogenization of the Western Cape temperature data, without the use of reference series. The undesirable consequences of absolute homogenization were realised and improved methods were thus sought. The use of Rhtest V4 software using a reference series was considered, however the software does not allow the creation of a homogeneous reference series. The software requires the user to create the homogeneous reference series and only allows the homogeneity of the reference series to be checked (Wang and Feng, 2013). While Rhtest V4 is a user friendly software with a comprehensive manual, finding neighbouring stations with homogeneous time series for use as reference series is a challenge. Therefore, ProClimDB was used, as the software provided many options for creating a reference series with the limited number of available neighbouring stations (discussed in detail in Chapter three). The software tools, ProClimDB and AnClim, allow the automation of data quality control, homogenization and filling in missing data. ProClimDB is a powerful database tool, which can be used at daily or monthly scale (Štěpánek *et al*., 2011, 2013). This PhD study used the daily mode for quality control (i.e. identifying outliers using interquartile range and pairwise comparison by analysing differences between candidate and neighbouring stations) because possible errors can be masked in average values. ProClimDB also automatically converted the quality controlled daily data to a monthly timescale for the homogenization procedures. Statistical homogeneity tests produce results with a degree of uncertainty as a result of noise in time series (Štěpánek *et al*., 2009). Therefore, multiple statistical tests were employed (using AnClim) to increase the reliability of the inhomogeneities detected. AnClim is a user friendly tool that allows the calculation of basic statistics, quality control and multiple

homogenization methods such as SNHT and Bivariate tests. The Bivariate test developed by Maronna and Yohai (1978) is also known as Potter's method because it was first used on precipitation data by Potter (1981). The Bivariate test, designed to detect single inhomogeneities, is capable of detecting multiple change points and produces the magnitude of a change point at the time of the shift (Potter, 1981; Kirono and Jones, 2007). The SNHT test was also first applied on precipitation data, however this test determines a change in ratio between a candidate series and a reference series (Alexandersson, 1986).

The general steps during the homogenization process in ProClimDB include the creation of a reference series for comparison with the test series. Various parameter settings are available such as methods of weights, number of stations used, individual statistics tests applied and method of correlation calculation for selection of neighbour stations. In order to create a reliable composite reference series, this PhD study used a weighted average of neighbour stations with a correlation coefficient greater than 0.6, a maximum distance of 300 km between stations, an altitudinal range less than 500 m and a minimum overlap of 10 years between stations as constructed by Kenawy *et al*. (2013). The distance function is used to ensure that the candidate and neighbour stations experience similar climate fluctuations (Peterson and Easterling, 1994). The correction or adjustment method employed by the software is an adaptation of a method used in climate model outputs by Déqué (2007). This method compares percentiles (empirical distribution) of differences (ratios) between the candidate and reference series before and after a change point (Štěpánek *et al*., 2013). A final correction factor (adjustement value) is determined by proceesing percentiles for each month individually and taking into account adjacent months before and after a change point, by smoothing with a low pass filter (Štěpánek *et al*., 2013). The ProClim software allows for several iterations of homogeneity testing, evaluation and the adjustment of time series for detected change points in order to obtain more precise results (Štěpánek *et al*., 2013).

2.4. **GLOBAL TEMPERATURE TRENDS**

The minimum time required for measuring ‘climate’ is three decades, according to the World Meteorological Organization, but preferably 60 or more years of data are required to establish climate change (Cubasch *et al*., 2013). Trends based on short records do not reflect long-

term trends and are sensitive to beginning and end dates due to natural variability (IPCC, 2013). Temperature is the most important climatic variable used to detect climate change, with the most common climatic variables being T_{max}, T_{min} and T_{mean} (Kousari *et al.*, 2013). A major concern of climate change is the possible rise in temperature extremes (Mestre *et al*., 2011). Global temperature extreme trends were comprehensively analysed for the 20th century, using high quality daily data (Alexander *et al.*, 2006). Using RClimDex software, results showed widespread significant changes in temperature extremes associated with warming. A significant decrease in cold nights and a significant increase in warm nights were observed over 70% of the world for the period 1951-2003 (Alexander *et al.*, 2006).

For the period 1880-2012, the global average land and ocean surface temperature recorded an average increase of 0.85°C, varying between 0.65°C and 1.06°C (IPCC, 2013). This equates to an average warming rate of 0.06°C/decade for the period 1880-2012 (IPCC, 2013). For the more recent period 1991-2012, a faster rate of increase (0.14°C/decade) is recorded (Fyfe *et al*., 2013). This is reflected by many regional temperature trend studies that follow in this review. For only land based temperature (CRUTEM4 data), the Northern Hemisphere warmed to a greater extent (by 1.12°C) compared to the Southern Hemisphere (0.84°C) over the period 1901-2010 (Jones *et al*., 2012). Warming is statistically significant over most of the earth's surface, with the exception of southern Greenland, three small regions over southeastern United States and parts of Bolivia and the Congo basin (Trenberth *et al*., 2007). A large body of literature has examined surface air temperature variability over the past 160 years, both globally and regionally (Ji *et al*., 2014). In a deviation from the considerable literature which determines temperature trends with nonparametric analysis, Ji *et al*. (2014) used the multidimensional ensemble empirical mode decomposition (MEEMD) method to demonstrate how global land surface air temperature has evolved for the period 1901-2009. Prior to 1950, only moderate warming and weak cooling were observed globally. By the 1990s warming regions expanded across almost all of the northern mid-latitudes. The fastest warming rates occurred in the arid and semiarid regions of the mid-latitude Northern Hemisphere (Ji *et al*., 2014). Notably, the majority of recent regional temperature studies (e.g. Turkes and Sumer, 2004; Li *et al.*, 2011; Gocic and Trajkovic, 2013; Kousari *et al.*, 2013; Sonali and Kumar, 2013; Viola *et al*., 2014) use the nonparametric Mann Kendall (MK) statistic test to determine trends. The purpose of reviewing relevant published literature (across the globe) similar to that undertaken in this PhD, is to place the current results in the context of previous temperature trend analyses and most importantly to

demonstrate the spatial distribution and magnitude of temperature changes across the globe. In addition, the review of temperature trend analyses across the globe is conducted to gain insight into the challenges experienced by other researchers as well as identify uncertainties and knowledge gaps that arise out of these investigations. This section of the literature review on regional temperature trends is restricted to articles published after the year 2000 and starts with North America, located in the western Northern Hemisphere, then moves across to Europe, Asia, Australia and eventually Africa.

2.4.1. Temperature trends in North America

Annual T_{mean} significantly increased over most regions of Canada, with faster warming rates for the more recent period 1948-2012 (varying from 0.15°C/decade to 0.64°C/decade) compared to long-term warming (0.11°C/decade to 0.18°C/decade) for the period 1900-2012 (Table 2.1) (Vincent *et al*., 2015). For a similar period (1900-2013), Tyler *et al*. (2015) also report an average T_{mean} warming rate of 0.14°C/decade and an annual T_{max} warming rate of 0.7°C/decade over the British Columbia, Canada. Both studies attribute annual warming primarily to faster winter warming rates. In British Columbia, an increase of 0.22°C/decade is noted during winter for the period 1900-2013 (Tyler *et al*., 2015), while for the more recent period (1948-2012) across Canada, mean winter warming rates compute to 0.5°C/decade (Vincent *et al*., 2015), again reflecting an increased warming for the more recent period. Across Canada, for the period 1948-2012, average T_{mean} anomalies are 3.3°C for winter, 1.8°C for spring, 1.4°C for summer and 1.5°C for autumn, with strongest warming observed during winter and spring. Winter trends are predominant in the western region, varying from 4-6°C for the period 1948-2012 (Vincent *et al*., 2015). The Vincent *et al*. (2015) study used homogenized data, specifically adjusted to account for a change in observation time and to address station relocation for the evaluation of temperature trends. However, the Tyler *et al*. (2015) study, conducted for the Ministry of Environment, does not indicate whether the data were homogenized.

In the USA, annual T_{min} record faster warming rates (0.27°C/decade) compared to T_{max} (0.04°C/decade) and a decrease in diurnal temperature range (0.15°C/decade) at 253 California National Weather Services (NWS) Cooperative Observer Programme (COOP) sites over the period 1950-2005 (Lebassi *et al.*, 2009). However, Kalnay and McCai (2003)

report T_{max} warming over the eastern and western USA and a cooling trend for the midwest region, resulting in an overall cooling T_{max} trend (-0.017°C/decade) and an increasing T_{min} trend (0.19°C/decade) for the period 1950-1999. The 2007 IPCC report indicated that the southeastern United States is one of few places in the world reporting an overall cooling trend through the 20th century. However, other studies report this cooling region in central United States (Portmann *et al*., 2009). Cooling is most prominent in early summer in the southeastern USA, while cooling in the north-central USA occurs in late summer (Portmann *et al*., 2009). Although multiple global climate model studies have tried to explain this cooling, no consensus yet exists (Portmann *et al*., 2009).

2.4.2. Temperature trends in Europe

Statistically significant increases in air temperatures are recorded for all regions of the United Kingdom, with rates of change increasing from north (west) to south (east) for the period 1910-2011, and with a particularly marked warming for the last 30 years (Prior and Perry, 2014). Trend analyses were undertaken using linear regression, and the significance of trends was determined using the Mann Kendall test. Realising that trends are not always linear, the authors also assessed the degree of change by comparing the 30 year (1981-2010) record with the 1910-1981 base period. The change in T_{mean} between the periods 1910-1980 and 1981-2010 is 0.34°C in northern Scotland, 0.45°C in northern Ireland and 0.65°C in south-eastern England (Prior and Perry, 2014). This study did not test station data for inhomogeneities, indicating that the effect of biases on the results were minimal due to the adherence to standard observing practice and the methods used for gridding and trend analysis.

In Switzerland the average T_{mean} increased by 0.01°C/decade and 0.57°C/decade for 12 homogenized time series over the periods 1901-2000 and 1975-2004, respectively (Rebetez and Reinhard, 2008). While this study does not explicitly state the method used for determining trends, the table captions refer to linear trends. The assumption that trends are linear can be problematic when dealing with climatic variables such as temperature. While Ceppi *et al*. (2012) use linear regression for determining the magnitude of temperature trends in Switzerland, the significance of the trends are determined using the non parametric Mann Kendall statistic. The analyses of homogenized data at 91 stations across Switzerland over the period 1959-2008 record a mean annual increase of 0.35°C/decade (Ceppi *et al*., 2012).

Table 2.1: A selection of annual temperature trends from around the globe, arranged by continents.

Source	Country/place	Duration	Rates of warming/cooling for different temperature variables		
			T_{mean} (°C/decade)	T_{max} (°C/decade)	T_{min} (°C/decade)
Vincent *et al*. (2015)	Canada	1900-2012	0.14	-	-
Vincent *et al*. (2015)	Canada	1948-2012	0.26	-	-
Lebassi *et al.* (2009)	California	1950-2005	-	0.04	0.27
Rebetez and Reinhard (2008)	Switzerland	1901-2000	0.01	-	-
Rebetez and Reinhard, 2008	Switzerland	1901-2000	0.01		
Rebetez and Reinhard, 2008	Switzerland	1975-2004	0.19	-	-
Viola et al. (2014)	Italy	1924-2006	0.19	0.34	-
Mamara *et al.* (2016)	Greece	1977-2004	0.2-0.6	-	-
Kousari *et al.* (2013)	Iran	1960-2005	-	0.09	-
Gunawardhana and Al-Rawas (2014)	Oman	1986-2011		-0.42	-0.61
Sonali and Kumar (2013)	India	1901-2003	-	0.03	0.02
Sonali and Kumar (2013)	India	1948-2003	-	0.06	0.05
Sonali and Kumar (2013)	India	1970-2003	-	0.16	0.21
Li *et al*. (2011)	China	1960-2008	0.15	-	-
Fujibe (2009)	Japan	1979-2006	0.3-0.4		
Peralta-Hernandez (2009)	Southern Mexico	1960-2004	0.09	0.17	0.007
Marengo and Camargo (2008)	Southern Brazil	1960-2002	-	0.4	0.5-0.8
Barros *et al*. (2015)	Argentina	1901-2012	0.5	-	-
Ashcroft *et al*. (2012)	Southeast Australia	1860-1909	-	0.01	-0.02
Ashcroft *et al*. (2012)	Southeast Australia	1910-1959	-	-0.06	0.00
Ashcroft *et al*. (2012)	Southeast Australia	1960-2011	-	0.22	0.18
Ashcroft *et al*. (2012)	Southeast Australia	1860-2011	-	0.04	0.07
CSIRO (2016)	Australia	1910-2016	0.09	-	-
Safari, 2012	Rwanda, Africa	1958-2010	0.56	-	-
Safari, 2012	Rwanda, Africa	1958-1977	-0.24	-	-
Ageena *et al*. (2014)	Libya	1945-2009	0.21	0.17	-
Hughes and Balling (1995)	South Africa	1960-1990	-	0.11	0.12
Kruger and Shongwe (2004)	South Africa	1960-2003	-	0.12	0.14
MacKellar *et al*. (2010)	South Africa	1960-2010	-	0.19	0.33

- = study did not include an analysis of the temperature variable.

In a more recent study over Switzerland, significant warming rates are recorded for the period 1959-2011 based on radiosonde data, with the shorter period (1959-1980) recording slightly insignificant cooling, followed by a strong warming for the period 1981-2000 and a more constant state for the period 2001-2011 (Brocard *et al*., 2013).

In Sicily (Italy), annual, seasonal and monthly temperature trends at 80 stations were investigated using the Mann Kendall analysis for the period 1924-2006 (Viola *et al*., 2014). Annual T_{mean} significantly increase by 0.19°C/decade, while annual T_{max} warmed by 0.34°C/decade. An impressive 210 year temperature record for a single station (over the period 1793-2003) in Sicily reported an increase of 0.05°C/decade (Viola *et al*., 2014). For the last 50 and 100 years of the record, temperature increased by a similar rate of 0.18°C/decade while the warming rate was 0.4°C/decade for the last 25 years of the record (Viola *et al*., 2014), again reflecting the faster warming rates for the more recent period. In Greece, statistically significant decreasing T_{mean} trends were observed for the period 1960-1976, varying between -0.4°C/decade and -0.9°C/decade (Mamara *et al*., 2016). Increasing T_{mean} trends of 0.2°C/decade to 0.6°C/decade were recorded for the period 1977-2004 using homogenized data at 52 stations spread across the seven climatic regions (Mamara *et al*., 2016). Long-term trends over the period 1960-2004 display statistically significant annual warming in northern and central Greece. In addition, all stations show strong warming during summer (44 being statistically significant), with stations in northern and eastern Greece recording the greatest warming (0.3-0.4°C/decade) (Mamara *et al*., 2016). Viola *et al*. (2014) and Mamara *et al*. (2016) use the Mann Kendall statistic to determine temperature trends and display warming rates for the more recent period. However, Viola *et al*. (2014) homogenized temperature data with the Kruskal–Wallis test while Mamara *et al*. (2016) used HOMER.

2.4.3. Temperature trends in Asia

In western Asia, at 70 stations in Turkey, T_{max} record mostly weak insignificant warming and cooling compared to the significant T_{min} warming over the period 1929-1999 (Turkes and Sumner, 2004). Weak warming of annual T_{max} is recorded over the western and eastern regions and cooling trends are observed over Central Anatolia and the Black Sea regions (Turkes and Sumner, 2004). Annual, seasonal and monthly T_{max} trends over Iran were investigated using the non-parametric Mann Kendall test, Sen's slope estimator and a 10 year

moving average for the period 1960-2005 (Kousari *et al.,* 2013). The different trends at 32 stations at various elevations and climate zones were mapped to show spatial distribution patterns. Non parametric tests were used on non-normally distributed and censored data, including missing values. Significant positive T_{max} trends were recorded for the warmer months (April, June, July, August and September) while the colder months (January, February, March, October, November, and December) did not display outstanding significant trends over Iran (Kousari *et al.,* 2013). Annual T_{max} record increases of 0.09°C/decade across Iran, with approximately 47% of the stations displaying warming. The majority of these stations with significant positive trends were mainly located in the western, north-east, south-east and central parts of Iran (Kousari *et al.,* 2013). A more recent study on temperature trends in Iran uses discrete wavelet transform and Mann Kendall for the period 1956-2010, and also records significant positive trends at monthly, seasonal and annual scales (Araghi *et al*., 2015).

Also in Asia, statistical spatial and temporal analyses of annual, monthly and seasonal T_{max} and T_{min} over India for the periods 1903-2003, 1948-2003 and 1970-2003 were conducted, using rank based tests (i.e. Mann Kendall and Spearman Rank correlation) for trend detection and the Sen's robust slope test for estimating the magnitude of the trend (Sonali and Kumar, 2013). Increasing trends were observed for T_{min} for most regions of India during the last three decades. The study also reports that T_{min} trends were more intense compared to T_{max}, indicating that the difference between daily T_{max} and nocturnal T_{min} is decreasing (Sonali and Kumar, 2013). An attempt was made to use least square regression (LR) for the slope based test, but the data were not normally distributed. LR being a parametric statistical analysis must satisfy both distributional and independent assumptions, while nonparametric methods must only satisfy independent assumptions (Sonali and Kumar, 2013). In China, the temporal and spatial climatic differences for the Hengduan Mountains were studied over the period 1960-2008 (Li *et al.,* 2011). Linear trends of 27 stations were calculated using nonparametric Kendall's t-based Sen's slope estimator. Significant increasing trends were observed for spring (0.15° C/decade), summer (0.59°C/decade), autumn (0.17°C/decade) and winter (0.35° C/decade) (Li *et al.,* 2011). The spline method was used because it is suitable for mountainous regions and it is best for varying surfaces such as elevation (Li *et al.,* 2011). A significant increase in temperature of 0.12°C/decade was observed during the monsoon summer and 0.25°C/decade increase during the winter monsoon months (Li *et al.,* 2011). Annual T_{mean} record significant increasing trends of 0.18°C/decade, 0.16°C/decade and

0.11°C/decade in the northern, central and southern Hengduan Mountains respectively (Li *et al.*, 2011). Similarly, in Japan, warming trends of 0.3-0.4°C/decade were recorded for low population density regions over the period 1979-2006 (Fujibe, 2009).

2.4.4. Temperature trends in the Southern Hemisphere

In the Southern Hemisphere, statistically significant warming trends of 0.05°C/decade (T_{max}) and 0.1°C/decade (T_{min}) were recorded at 224 stations in Australia over the period 1910-1993 (Torok and Nicholls, 1996). For the adjustment of time series using a reference series, these authors used neighbouring stations which did not experience discontinuities, or have few missing data, or experienced similar climatological conditions to the candidate station (Torok and Nicholls, 1996). They adjusted the time series for inhomogeneities caused by station relocation, changes in exposure and other discontinuities (Torok and Nicholls, 1996). Subsequently, Della-Marta *et al*. (2004) updated and improved the Torok and Nicholls (1996) Australian dataset, reassessing the quality based on metadata records. In addition, two methods of creating reference series were used (i.e. the median reference series and distance weighted mean of highly correlated neighbour stations). This study resulted in the rejection of some datasets, producing 133 good quality datasets. Slightly increased warming rates are recorded for T_{max} (0.06°C/decade) and T_{min} (0.11°C/decade) at 133 stations in Australia for the period 1910-2002 (Della-Marta *et al.*, 2004), notably T_{min} displaying steeper increases compared to T_{max}. For a longer period (1860-2011), T_{max} and T_{min} record increasing trends of 0.04°C/decade and 0.07°C/decade respectively over southeast Australia (Ashcroft *et al.*, 2012). Notably, a comparison of Della-Marta *et al*. (2004) and Ashcroft *et al*. (2012), reflects a reduced T_{min} warming trend, which is due to the cooling observed for the earlier period (i.e. -0.02°C/decade for the period 1860-1909). Similarly, a reduced T_{max} trend is also observed and may be due to the cooling for the period 1910-1959 (i.e. -0.06°C/decade) (Ashcroft *et al.*, 2012). In a more recent study, Trewin (2013) produced the Australian Climate Observations Reference Network-Surface Air temperature (ACORN-SAT) data set, consisting of 112 locations, with 60 stations containing the complete temperature record since 1910. This work used a combination of multiple reference stations and percentile matching algorithm to correct inhomogeneities. According the State of Climate report 2016 for Australia, the observed T_{mean} has increased by 1°C since 1910 (CSIRO, 2016).

These trends are not dissimilar to those reported from 27 stations in southern Brazil, where annual T_{max} record increases of 0.4°C/decade while annual T_{min} record steeper warming rates of 0.5°C/decade to 0.8°C/decade for the period 1960-2002 (Marengo and Camargo, 2008). While Marengo and Camargo (2008) used data quality procedure to check for missing values, outliers and correct sequence of days, the study does not mention any homogenization procedures that may have been employed, thereby providing room for further studies to improve the accuracy of temperature trends. Similarly, T_{mean} increases of 0.5°C/decade, were reported across most of Argentina for the period 1901-2012, derived from the IPCC (2013) (Barros *et al*., 2015).

For South Pacific islands, statistically significant warming trends of 0.1°C/decade (Apia, Somoa, Alofi, Niue, and Aitutaki, Cook Islands) to 0.3°C/decade (Papeete, French Polynesia) are recorded over the period 1954-1998 (Folland *et al*., 2003). This 45-year period was selected to maximise the number of islands included in the study. Temperature trends were analysed using linear methods, even though the authors recognise that the trends are often nonlinear. While efforts have been made to homogenize the temperature data for the South Pacific Islands, the articles have not been included in this review as only articles published after the year 2000 have been reviewed for this section.

Annual T_{mean} for New Zealand demonstrates an increasing trend of 0.1°C/decade over the period 1941-2010 (Sturman and Quenol, 2013). However, significant differences were observed between regions, with annual T_{mean} and T_{min} in Marlborough (at airport) decreasing (-0.005°C/decade and -0.01°C/decade, respectively) over the same period (Sturman and Quenol, 2013). Whilst linear regression was used to fill in missing data, it is unclear as to what methods were used to determine temperature trends. However, the study used the Bayesian method of Lee and Heghinian (1977) and the Pettitt (1979) method to test the homogeneity of temperature records. No changepoints were detected for the T_{mean} and the time series were assumed to be homogeneous. When change points were detected in the T_{max} and T_{min} time series by the aforementioned older homogenization techniques, the study employed a more recent suite of techniques and did not detect change points. At this point the authors conclude that time series is homogeneous due to the inconsistent detection of major change points by different homogenization techniques and there is no mention of an examination of metadata records.

2.4.5. Temperature trends in Africa

For Africa, near-surface air temperatures investigated using remote sensing systems record significant increasing trends for the entire continent of Africa for the period 1979-2010 (Collins, 2011). In support of these increasing trends, mean annual T_{max} and T_{mean} in Libya also record warming rates of 0.17°C/decade and 0.21°C/decade respectively for the period 1945-2009 (Ageena *et al*., 2014). Similarly, annual T_{mean} record increasing trends (0.56°C/decade) at five stations in Rwanda over the period 1958-2010, however cooling trends were observed at 4 of the stations (-0.24°C/decade) for the earlier period (1958-1977) (Safari, 2012), again emphasizing the faster warming rates for the more recent period. The effect of urbanisation on annual surface temperatures was tested for the period 1970-2005 at an urban station (Mejametalana) and several rural stations (Mafeteng, Moshoeshoe and Teyateyaneng) in the Maseru district of Lesotho (Maletjane, 2006). The study records warming trends at the urban station in the early 1990s, recording a greater change in T_{min} (Maletjane, 2006). In a another southern African study investigating climate trends, observed climate data for surface air temperature, rainfall, air pressure, wind and ocean currents were investigated (Jury, 2013). Using Global Historical Climate Network data, Jury (2013) established surface air temperature trends and recorded increasing trends of 0.14°C/decade for the period 1979-2010. For GCM simulations over southern Africa, the Institute Pierre Simon Laplace (IPSL) and Model for Interdisciplinary Research on Climate (MIROC)) were used (Jury, 2013). Increasing temperature trends were also reported for IPSL 20C (0.39°C/decade), IPSL A1B (0.45°C/decade); MIROC A1B (0.46°C/decade) and MIROC 20C (0.42°C/decade) for the period 1979-2010 (Jury, 2013).

The comparison of results across the globe is challenging due to different timescales at which studies are conducted, however, the key concepts of warming, especially for more recent decades, as well as differences between various temperature variables are highlighted by the literature presented. Most studies perform trend analysis to include the year prior to the date of publications and generally start around 1960 when instrumental data become more reliable (Kruger and Nxumalo, 2017). However, more recent studies have examined longer periods due to the advancement of quality control and homogenization methods.

2.5. **SOUTH AFRICAN TEMPERATURE TRENDS**

Previous studies (e.g. Muhlenbruch-Tegen, 1992; Kruger and Shongwe, 2004; MacKellar *et al*., 2014) on South African temperature trends investigated relatively short periods due to the unavailability of high quality data prior to 1960. In addition, studies were confined to using only the stations which did not undergo major moves or changes in exposure to ensure homogeneity (Kruger and Shongwe, 2004). The most recent study by Kruger and Nxumalo (2017), coinciding with the work of this thesis, examined longer temperature trends for South Africa over the period 1931-2015, following absolute homogenization. In addition, the work by Hughes and Balling (1996) examined temperature trends for the period 1885-1993 over South Africa, reporting that warming in the three most recent decades was influenced by urbanisation and due to an increase in regional temperature. For the period 1960-1990, T_{max} record increases of 0.11°C/decade at small towns and 0.12°C/decade at larger cities (Hughes and Balling, 1996). T_{min} also increased at a rate of 0.07°C/decade at non-urban stations, with only statistically significant increasing trends recorded at large towns (0.34°C/decade) (Hughes and Balling, 1996). Non-urban areas were concentrated in the eastern part of South Africa and an adjustment was made to allow one station in the west to weigh more (Hughes and Balling, 1996).

In a more comprehensive study of South African temperature trends, the t-test was used to analyse the annual, monthly, seasonal T_{mean}, $T_{max,}$ T_{min} and diurnal temperature range (DTR) trends at 26 stations for the period 1960-2003 (Kruger and Shongwe, 2004). Average annual T_{mean} record significant increasing trends of 0.13°C/decade for the period 1960-2003, with insignificant increases of 0.04°C/decade and 0.01°C/decade for the periods 1960-1982 and 1983-2003 respectively (Kruger and Shongwe, 2004). Average temperatures for the period 1991-2003 (18.48°C) were significantly warmer than those for preceding decades (18.18°C) (Kruger and Shongwe, 2004). Annual T_{max} indicate significant increasing trends at 13 stations, mostly situated close to the coast, 10 stations with insignificant positive trends and 3 stations with negative trends (Kruger and Shongwe, 2004). Annual T_{min} record significant increasing trends at 18 stations and insignificant decreasing trends at 4 stations, the latter mostly situated in the central interior (Kruger and Shongwe, 2004). Kruger and Shongwe (2004) also examined the effect of urbanisation on temperature data, and it was concluded that stations classified as urban stations did not differ from their rural counterparts (Kruger

and Shongwe, 2004). Warming trends of 0.21°C/decade for autumn, 0.13°C/decade for winter, 0.08°C/decade for spring and 0.12°C/decade for summer are recorded at 26 stations across South Africa for the period 1960-2003 (Kruger and Shongwe, 2004). A very brief update of temperature trends based on 27 stations in South Africa, report an annual T_{mean} of 0.8°C above the 1961-1990 long-term average, and indicated the year 2010 as the warmest year since 1961 (Kruger *et al*., 2011). This however, has changed as the warmest year on record since 1880 is now 2016 (Potter *et al*., 2017), as also mentioned in Chapter five of this PhD thesis.

In a separate South African study by MacKellar *et al*. (2014), temperature trends were investigated using the Mann Kendall trend test for the period 1960-2010. Daily T_{max} and T_{min} significantly increased for all seasons, with the exception of a significant T_{min} decrease over the central interior (MacKellar *et al*., 2014). The strongest regionally averaged T_{max} increase was 0.34°C/decade over the central interior of the country in autumn, with the weakest (0.07°C/decade) occurring in the same region in summer (MacKellar *et al*., 2014). MacKellar *et al*. (2014) record stronger mean annual T_{min} warming rates (0.33°C/decade) over South Africa compared to that of T_{max} (0.19°C/decade) for the period 1960-2010 (Table 2.1). The Western Cape Province results of the aforementioned study have been discussed and compared to the results of this PhD study in greater detail in Chapter three. However, MacKellar *et al*. (2014) did not provide details on the specific stations used for each region, which could potentially be useful for comparative purposes in further research for South Africa.

The most recent study on temperature trends over South Africa uses least square linear regression to determine trends over the period 1930-2015 (Kruger and Nxumalo, 2017). Although annual T_{mean} record significant positive trends at 24 out of 27 stations, the magnitude of trends for each station are not easily obtainable from the included map, given that the map (in the article) provides a range of the trend magnitudes for each station in the form of a triangle. Significant increases are noted for warm spell duration over most of the western and northern interior, while significant decreases in cold spell duration are observed over the eastern half of the country and the coast (Kruger and Nxumalo, 2017). Significant negative trends in cold nights are observed at 25 out of the 27 stations while warm nights show the opposite trend. DTR display 14 decreasing trends (12 statistically significant) and 13 increasing trends (10 statistically significant) for the 27 stations across the country

(Kruger and Nxumalo, 2017). Seasonal warming rates vary considerably across sub-regions, with the strongest average warming of 0.018°C/decade for austral (DJF) summer, 0.007°C/decade for autumn (MAM), −0.004°C/decade for winter (JJA) and −0.016°C/decade for spring (SON) (Kruger and Nxumalo, 2017).

On a regional scale, annual, seasonal $T_{mean,}$ T_{max}, T_{min} and DTR were investigated in 30 catchments in the Limpopo province, South Africa, using the Mann Kendall analysis (Tshila *et al.*, 2011). Mean annual T_{mean} trends record an overall increase of 0.12°C/decade over the period 1950-1999 (Tshila *et al.*, 2011). Positive trends are recorded at 70% of the catchments for annual T_{max} while 63% of the catchments experience positive trends for annual T_{min} (Tshila *et al.*, 2011). T_{mean} significantly increased by 0.18°C/decade and 0.09°C/decade for winter and summer respectively, for approximately 87% of the catchments (Tshila *et al.*, 2011). Regional increases/decreases are, however, not clearly discussed in detail for the various temperature variables. In a regional study of Namaqualand, high resolution data (CRU TS 3.1) indicate a faster annual T_{min} warming rate of 0.14°C/decade compared to the annual T_{max} increase of 0.11°C/decade for the period 1901-2009 (Davis *et al*., 2016). The greatest T_{max} warming was noted for the southeastern region while the greatest T_{min} occurs over the northeastern region of Namaqualand. Inconsistent trends were noted across seasons, with slightly more warming during spring and autumn (Davis *et al*., 2016).

Studies on temperature extremes in South Africa also report consistent warming trends. Daily T_{max} and T_{min} extremes were investigated using RClimDex software over southern and west Africa for the period 1961-2000 (New *et al*., 2006). The results record a decrease in extreme cold days and nights and an increase in extreme hot days and nights, with the average duration of warm (cold) increasing (decreasing) by 2.4 (0.5) days/decade. A large proportion of the stations show statistically significant trends, with the statistical significance increasing from subtropics to tropics (New *et al*., 2006). In a more recent study, specifically for South Africa, daily T_{max} and T_{min} extreme trends were investigated for 28 stations over the common period 1962-2009 (Kruger and Sekele, 2013). Using 10 core indices of the 27 developed by the Expert Team on Climate Change Detection and Indices (ETCCDI), with RClimDex software, the study showed an increase in warm extremes and a decrease in cold extremes, with the western half, parts of the northeast and east of the country displaying a stronger increase in warm extremes and decrease in cold extremes compared to other parts of South Africa (Kruger and Sekele, 2013). A general warming trend is observed, with a

tendency toward stronger increases for T_{max} indices compared to T_{min} (Kruger and Sekele, 2013). Similarly, for the regional study of Namaqualand, warm extremes increased and cold extremes decreased, demonstrated by the increase in the number of hot days and the decrease in the number of cold days, using the RClimDex (Davis *et al*., 2016). In addition, the warm spell duration also increased at five stations, being significant at two of the stations (Davis *et al*., 2016).

2.6. **COASTAL AND ADJACENT INLAND TEMPERATURE TRENDS**

Geographical factors (such as latitude, elevation and distance from the sea) influence climate. Therefore, this PhD study examines the importance of the geographical location of stations (i.e. coastal stations located in close proximity to the sea compared to interior station situated further away). Interaction between the ocean and atmosphere influences climate variability and climate change (Tyson and Preston-Whyte, 2000). The following review of temperature trends between coastal and inland locations across the globe demonstrates the relatively limited work undertaken to determine the influence of the coast on land temperature. Oceans strongly influence temperatures recorded at coastal stations (Tyson and Preston-Whyte, 2000). Coastal stations within 15 km of the sea, generally report an increase in annual T_{mean} range, with a decrease in distance from the sea over the north of Tokyo (Japan) over the period 1994-1998 (Sakakibara and Owa, 2005). In addition, summer is generally hotter and winter colder at inland regions compared to coastal areas (Sakakibara and Owa, 2005). This study classified stations as either coastal or interior based on the distance from the sea, however the article lacks an indepth discussion of the influence of the coast on temperature. For a significantly longer period (27 years) over Japan, Fujibe (2009) report slightly larger annual T_{mean} values at inland sites compared to the coast over the period 1979-2006, with the difference being insignificant. The main focus of this study was to investigate the warming trends at rural and urban stations. In the coastal city of Muscat (Oman) annual T_{max} decreased by 1°C (0.42°C/decade) while annual T_{min} decreased by nearly 1.50°C at a rate of 0.61°C/decade over the period 1986-2011 (Gunawardhana and Al-Rawas, 2014). Although the aforementioned study does not compare warming rates between coastal and inland regions, the latter study emphasizes the coastal cooling observed in certain regions of the globe. Conversely, at four stations along the Israeli Mediterranean coast, average annual

T_{mean} record a significant increase of 0.34°C/decade, while inland stations record faster warming rates of 0.36°C/decade over the period 1970–2002 (Kafle and Bruins, 2009).

Also in the Northern Hemisphere, early studies reported a decrease in temperature at coastal stations around the periphery of the North Atlantic for the period 1950-1990, which is opposite to the warming observed inland of Canada (Morgan *et al.*, 1993). However, Tyler *et al*. (2015) report a more rapid warming over the interior of the British Columbia (Canada) compared to the coast for the period 1900-2013, with southern coastal regions reporting rates of 0.08°C/decade, western coast warming at 0.1°C/decade and interior warming rates of 0.1°C/decade to 0.18°C/decade. During autumn, the coastal regions warmed by 0.06°C/decade to 0.08°C/decade while the sub-boreal interior regions increased at a slightly faster rate of 0.1°C/decade, with all other interior regions displaying insignificant trends (rates not supplied) (Tyler *et al*., 2015). During spring, both coastal and southern interior regions increase at a rate of 0.11°C/decade, while temperature increased by 0.08°C/decade over the central interior of British Columbia (Tyler *et al*., 2015). Annual T_{min} record increasing trends (0.12 to 0.15°C/decade) at the coast while that for the interior of British Columbia (Canada) varied between 0.18 to 0.28°C/decade over the period 1900-2013 (Tyler *et al*., 2015). However, annual T_{max} do not record significant increasing trends at the coast as well as over the central interior of British Columbia (Canada) (Tyler *et al*., 2015).

A complex pattern is observed for boreal summer mean monthly (June-August) temperatures over two basins in California (South Coast Air Basin and San Francisco Bay Area) for the period 1950-2005, where cooling was noted in low-elevation coastal regions and warming observed at both inland and higher-elevation coastal areas (Lebassi *et al.*, 2009). Summer T_{max} record a coastal cooling of 0.3°C/decade, while inland warming was 0.32°C/decade. Similarly, summer T_{mean} record a cooling rate of 0.01°C/decade and an interior warming of 0.24°C/decade is observed. However, T_{min} record increasing trends at both inland (0.16°C/decade) and coastal (0.28°C/decade) sites (Lebassi *et al.*, 2009). In addition, averaged 1950-1999 summer T_{mean} values from 11 GCMs show summer T_{mean} warming rates that decrease from inland California (0.13°C/decade) to the coastal area north of SoCAB. The authors suggest that the coastal cooling observed in California results from global warming of inland areas resulting in increased sea breeze flow, which is supported by a GCM (Lebassi *et al.*, 2009). Other authors, however, suggest that the observed summer coastal

cooling along California's coast is due to the urban heat island, increased irrigation, coastal upwelling and cloud cover (Abatzoglou *et al*., 2009; Lebassi *et al.*, 2009).

The characterisation of the spatial distribution of global warming along the west coast of South America (central and northern Chile) over the period 1979-2006, reported an annual T_{mean} surface cooling (-0.2°C per decade) at three coastal stations (Falvey and Garreaud, 2009). The authors suggest that coastal cooling is a part of a larger scale La Niña-like pattern, extending below the ocean mixed layers reaching a minimum depth of 500m. In strong contrast, warming (annual T_{mean}: +0.25°C/decade) was observed only 100km - 200km inland (Falvey and Garreaud, 2009). Due to the change in elevation (1000-1500m) from the coast to the Andes, the contrast is due to a change in temperature trends with altitude. The oceanic and continental variability may modulate Chile's climate, given its location along the coast of a large continental landmass (Falvey and Garreaud, 2009). Furthermore, the authors note a stronger decreasing trend for T_{max} compared to T_{min} and suggest that the trends at the coastal stations are strongly modulated by the cooling effect of the ocean since the low level atmospheric flow is onshore during the day (bringing the oceanic air to land) and weakly offshore during the night (Falvey and Garreaud, 2009).

In southern Africa, temperature trends over the Mozambique Channel regions were investigated using graphical and statistical methods for the period 1939-1992 (King'uyu *et al.*, 2000). Daytime warming and night time cooling were observed at coastal and lake areas, which was the reverse of trends experienced in East African regions. The study also showed large geographical and temporal variation, with decreasing trends in temperature at stations located close to the coast and major inland lakes (King'uyu *et al.*, 2000). Similarly, Hulme *et al*. (2001) report cooling over the coastal regions of Senegal and South Africa and a strong warming over the central interior of southern Africa over the period 1901-1995. In a separate study of southern Africa, Jury (2013) suggests warming will be faster over the coastal plains compared to the Kalahari plateau. In addition, stations further inland recorded higher rates of warming compared to temperature along the coastline of Namaqualand for all seasons over the period 1901-2009 (Davis *et al*., 2016). Annual average temperatures along the Namaqualand coast are mild due to the cold Benguela current, hence temperatures recorded inland are typically considerably higher (Davis *et al*., 2016).

In South Africa, Kruger and Shongwe (2004) reported that stations with significant trends in mean annual T_{max} were mainly close to the coast for the period 1960-2003, but no comparison was made to trends at inland stations. In a study of South African temperature extremes, Kruger and Sekele (2013) use cluster analysis which defines regions with similar climatological analysis. Cluster A represented the western and southern coastal region with a mild Mediterranean climate while cluster B represents the southeast and eastern coast (subtropical climate). Results indicate no trends for warm spell duration index as the number of cases when T_{max} is greater than the 90th percentile for six or more consecutive days was too few (Kruger and Sekele, 2013). The east coast was identified as one of the regions in South Africa which are more prone to hot daily extremes. The strongest T_{max} trends were observed along the southern coastline (mean of 2.97% per decade), with strong positive trends also recorded over the Northern Cape province (2.26% per decade) and parts of the central and northern interior (1.87% per decade) of the country. Strong positive T_{min} (90th percentile) trends were reported for western and southern coastal regions while negative trends were observed for Northwest Province, the central interior and southeastern regions (Eastern Cape) of the country (Kruger and Sekele, 2013). In the most recent study of temperature trends over South Africa, Kruger and Nxumalo (2017) report that consecutive 30 year trends (e.g. 1951-1980; 1952-1981; 1953-1982) for annual T_{mean} over the interior are positive in the south (0.04°C/decade) and far north (0.07°C/decade), negative in the central parts (-0.05°C/decade) and insignificant over the south-western Cape. An average annual T_{mean} of 0.3°C/decade at five coastal stations (Cape Agulhas, Cape St Blaize, Port Elizabeth, Mount Edgecombe and Cape St Lucia) is recorded for the period 1964-1993 and a gradual decline of 0.1°C/decade for the period 1975-2015 (Kruger and Nxumalo, 2017). However, insignificant and significant cooling trends are observed over the central interior of South Africa (Kruger and Nxumalo, 2017). This differs from trends observed by aforementioned studies (i.e. Falvey and Garreaud, 2009; Kafle and Bruins, 2009; Tyler *et al*., 2015) across the globe. Previous studies of temperature trends over South Africa do not contrast inland and coastal trends over KwaZulu-Natal for the period 1930-2015, hence this is investigated in Chapter four of this PhD study.

2.7. EL NIÑO-SOUTHERN OSCILLATION AND LAND TEMPERATURE

Important drivers of climate variability over southern Africa include El Niño-Southern Oscillation (ENSO), Antarctic Oscillation (AAO) and Indian Ocean Dipole (IOD) (Tadross and Johnston, 2012). Both ENSO and IOD are coupled ocean-atmosphere phenomenon, however the former originates in the Pacific ocean while the latter originates in the Indian Ocean (Sankar *et al*., 2011). AAO, also called the southern annular mode (SAM), is a mode of atmospheric variability in the Southern Hemisphere, whereby the positive phase is associated with enhanced rainfall over South Africa (stronger during the La Niña phase) and the negative phase enhances rainfall over the southwestern Cape during winter (Pohl *et al*., 2010). The fluctuations of AAO are related to Madden-Julian Oscillation (MJO) and impacts South African convection and rainfall at an intraseasonal scale (Pohl *et al*., 2007; Pohl *et al*., 2010). One of the most important sources of natural climate variability is ENSO, therefore this PhD study assesses the impact of ENSO phases on South African temperatures. This section of the review therefore examines studies related to ENSO phases and temperature across the globe, including the mechanisms responsible for the responses.

The ENSO cycle is the main source of inter-annual variability in global weather and climate and is driven by in sea-surface temperatures (SSTs) in the equatorial Pacific Ocean and air-pressure called Southern Oscillation (WMO, 2014). ENSO is important for maintaining long-term global climate stability by transporting heat from the Tropics to higher latitudes (WMO, 2014). ENSO affects many parts of the globe, specifically in the tropics, where the varying ENSO phases result in rainfall and temperature changes (Scaife, 2010). ENSO is an important driver of atmospheric teleconnections that alter surface air temperature, humidity, wind and cloud distribution (Alexander *et al*., 2002). The ocean loses heat to the atmosphere through evaporation, resulting in latent heat in the atmosphere which drives teleconnections (Trenberth *et al*., 2002). The mechanisms responsible for Southern-Oscillation (SO) temperature covariability are a result of short wave radiative and surface latent heat fluxes, which are driven by cloud cover and rainfall (Jones and Trewin, 2000). Positive Southern Oscillation Index (SOI) values are associated with cloudy conditions and a decrease of incoming short-wave radiation, resulting in decreased temperatures, while negative SOI

values are associated with decreased cloudiness and increased temperatures (Jones and Trewin, 2000).

ENSO's influence is evident over North America, South America, Asia, Africa and Australia (Scaife, 2010). Different methods of analyses have also reported different strengths of ENSO-related climatic response (surface air pressure, temperature, and precipitation) over Europe (Scaife, 2010). ENSO also influences extreme weather events such as floods, drought and tropical cyclones across the Earth. This is particularly important for agricultural regions such as Australia, Africa and America (Gergis and Fowler, 2008). The understanding of ENSO and its effects has expanded since earliest studies, and it is now accepted that ENSO is a dominant cause for atmospheric variability at decadal and sub decadal scales (Welhouse *et al*., 2016).

Possibly the best known analysis of ENSO impacts on regional and global temperature was conducted in the 1990s by Halpert and Ropelewski (1992) (cited by Davey *et al*., 2014), which reported consistent Southern Oscillation-temperature relationships. The relationship between ENSO and the entire Northern Hemisphere atmospheric temperature has been explored (Li and Chen, 2014). Teleconnections between El Niño and temperature anomalies in the Northern Hemisphere have been established, with most studies focussing on ENSO impacts for boreal winter because ENSO peaks coincide during this time (Laken and Stordal, 2016). The impact of El Niño on Europe is related to conditions in the North Pacific (Brönnimann, 2007). During El Niño events, low sea surface temperatures (SSTs) are recorded in the central North Pacific and high surface air temperatures in western Canada and Alaska that sometimes stretch across the entire continent (Brönnimann, 2007). The ENSO signal in Europe varies with season but is mostly consistent in late winter. The ENSO signal is weak on average, however, some events such as the 1940-1942 El Niño event had a particularly strong effect, resulting in three of the coldest winters of the 20th century (Brönnimann, 2007). A strong association between ENSO and European temperature has also been established for boreal summer, using composite analysis (Laken and Stordal, 2016).

The intra-seasonal relationship between Southern Oscillation Index (SOI) and T_{mean} at 138 stations across the Pacific Northwest of the United States report a pronounced ENSO influence along the coast and in northern Idaho (McAfee and Wise, 2016). El Niño winters are warmer compared to La Niña, with statistically significant correlation noted for El Niño

events during February to March (late boreal winter) (McAfee and Wise, 2016). However, in the southeastern USA, the ENSO impact causes a pattern of cooling, specifically in winter (McAfee and Wise, 2016). The response of ENSO in summer (May-October) is minimal in the southeastern USA, even when considering lag responses in the response to ENSO (Portman *et al*., 2009).

In western Asia, significant correlation between SOI and temperature for July and August are recorded at six sites across Iran for the period 1966-1995 (Soltani and Gholipoor, 2006). In East Asia, the relationship between winter mean surface temperature (DJF) and ENSO was established using empirical orthogonal function (EOF) over the period 1957-2012 (Jia *et al*., 2015). In India, major patterns of seasonal inter-annual air temperature variability were investigated for the period 1900-2005 (Chowdary *et al*., 2014). Results concluded that air temperature is remotely influenced by ENSO and locally influenced by Indian Ocean warming and cooling (Chowdary *et al*., 2014). Other studies in Asia (e.g. Li and Chen, 2014; Lee and Julien, 2016) also support teleconnections between ENSO events and temperature, specifically across South Korea, where 76 temperature stations confirm teleconnections with the Southern Oscillation (SO) for the period 1904-2014, based on composite and harmonic analysis (Lee and Julien, 2016). El Niño years are associated with below normal temperature anomalies for summer through to autumn and above normal for winter through to spring of the following year (Lee and Julien, 2016). However, in South China, results differ between temperature variables at 20 stations for the period 1960-2005 (Li and Chen, 2014). ENSO is not significantly correlated to T_{max} while significant effects are recorded for T_{min}, with a delay time of 4 months. The influence of ENSO on T_{min} is stronger along the southern coast of China (Li and Chen, 2014).

In the Southern Hemisphere, the relationship between ENSO and the Antarctic seasons was examined with composite analysis for the period 1973-2013 (Welhouse *et al*., 2016). El Niño events were found to warm western Antarctica and cool the Antarctic Peninsula (Welhouse *et al*., 2016). For La Niña, a statistically significant signal exists in the East Antarctic coastal region (negative temperature anomalies) (Welhouse *et al*., 2016). In addition, negative temperature anomalies are noted throughout the Ross Sea and Amundsen and Bellingshausen Seas (ABS) region and a slight warming of the Antarctic Peninsula and a small region of cooling in the East Antarctic plateau (Welhouse *et al*., 2016). Similarly, teleconnections have been established with Australian data. In an analysis of Australian surface temperature (at 97

stations), Jones and Trewin (2000) demonstrated that the SOI is significantly related to seasonal T_{max}, T_{min}, T_{mean} and diurnal temperature range (DTR) for the period 1950-1994, particularly across the northern and eastern regions of Australia. The strongest correlation between T_{max} and the SOI occurred over eastern Australia during summer (-0.6) (Jones and Trewin, 2000). The Australian climate is sensitive to ENSO, generally associated with warm, dry conditions for El Niño events and cool and wet weather for La Niña events (Ashcroft *et al*., 2016). The relationship is strongest in the inland eastern region and more complex in southeastern Australia, due to topography and the influence of remote large scale atmospheric and oceanic circulation (Ashcroft *et al*., 2016). Annual and seasonal correlations were investigated between SOI/ Niño 3.4 and T_{max}, T_{min} and DTR for the period 1876-2011 (Ashcroft *et al*., 2012). Significant correlations are reported between annual (May-April) ENSO and T_{max}/DTR, while a non-significant positive correlation is observed between annual ENSO and T_{min} (Ashcroft *et al*., 2012). In a more recent study, Ashcroft *et al*. (2016) report that the influence of ENSO events are not stationary over time, with weak ENSO-southeast Australian rainfall teleconnections for the period 1920-1950 (Ashcroft *et al*., 2016). In addition, low ENSO-southeast Australian rainfall correlations coincide with reduced La Niña events for the period 1835-1850 (Ashcroft *et al*., 2016). The recovery of historical data in South Africa, such as those in the aforementioned Australian study, is vital for the confirmation of ENSO relationships during the 19th century for the Southern Hemisphere.

ENSO is the most dominant perturbation responsible for inter-annual climate variability over eastern and southern Africa (Hulme *et al*., 2001). Global studies (Ropelewski and Halpert, 1986; Halpert and Ropelewski, 1992) have linked ENSO events to inter-annual climate variability over southern Africa. This influence occurs during the October-November rain period in eastern equatorial Africa and in southeastern Africa during November-February (Ropelewski and Halpert, 1986; Hulme *et al*., 2001). The relationship between ENSO and South African rainfall is well-known, where El Niño events are associated with below average summer rainfall and La Niña are linked to above average rainfall over South Africa by several studies (e.g., Lindesay, 1988; Kruger, 1999; Reason and Rouault, 2002; Landman and Beraki, 2012; Philippon *et al*., 2012; Weldon and Reason, 2014). The influence of El Niño on southern African rainfall is due to the weakening of the tropical convection over the subcontinent (Kane, 2009). Before the 1970s, warm events in the tropical Indian Ocean occurred more frequently in association with ENSO warm events, both associated with dry conditions over South Africa (Kane, 2009). The ENSO signal has weakened in Indian Ocean

sea surface temperatures since the late 1970s, with sea surface temperature variability in the tropical western Indian Ocean less dependent on ENSO (Kane, 2009). In addition, the warm (cold) events in the tropical western Indian Ocean have become linked to wet (dry) conditions over the northeastern half of South Africa (Kane, 2009).

Studies investigating the relationship between ENSO events and temperature over South Africa are more limited. The impact of ENSO events on T_{mean} over southeast Africa for the period 1880-1991 was investigated using composite and harmonic analysis and a link was established (Halpert and Ropelewski, 1992). Subsequent to this, in a minor section of the Kruger and Shongwe (2004) study, the authors examine ENSO influence over eight stations in South Africa and concluded that El Niño and La Niña events *do not* play a significant role in increasing temperatures observed for austral summer over the period 1960 to 2003 (Kruger and Shongwe, 2004). The current PhD study provides an updated investigation of the impacts of ENSO phases on both T_{max} and T_{min}, using long-term high quality datasets. This study is also expected to determine whether the influence El Niño and La Niña phases have strenghthened /weakened over time.

The purpose of the literature review was to demonstrate the importance of this PhD study in the context of similar work undertaken globally, regionally and in South Africa. Historical climate data recovered for the Southern Hemisphere have mainly focussed on 18th and 19th century rainfall, possibly because it is easier to extract information about droughts and rainfall from historical documents. Thus, this PhD study makes an effort to increase the recovery of historical temperature data for South Africa. A wide variety of homogenization techniques are available, each with their own advantages and limitations. Clearly, a great deal of effort has been made by scientists around the world to establish regional temperature trends over the past 17 years. With the exception of decreasing temperature trends (0.42 and 0.61C/decade) experienced in Oman over the period 1986-2011, the remaining regional studies reviewed in this chapter demonstrate increasing temperature trends (Table 2.1). Scientific studies contrasting coastal and inland temperature trends have also been limited, especially over South Africa. Studies related to ENSO teleconnections with South African climate have focussed mainly on precipitation while that for temperature over South Africa have been limited. This literature review identified gaps in knowledge, thereby paving the way for the research as reflected in this PhD thesis.

2.8. **REFERENCES**

Abatzoglou, JT, Redmond KT, Edwards LE. 2009. Classification of regional climate variability in the state of California. *Journal of Applied Meteorology and Climatology* **48**: 1527-1541.

Ageena I, Macdonald N, Morse AP. 2014. Variability of maximum and mean average temperature across Libya (1945–2009). *Theoretical and Applied Climatology* **117**: 549-563.

Aguilar E, Auer I, Brunet M, Peterson TC, Wieringa J. 2003. Guidelines on Climate Metadata and Homogenisation. WCDMP-No. 53, WMO-TD No. 1186. World Meteorological Organization, Geneve.

Alexander LV, Zhang X, Peterson TC, Caesar J, Gleason B, Klein Tank AMG, Haylock M, Collins D, Trewin B, Rahimzadeh F, Tagipour, A, Kumar KR, Revadekar J, Griffiths G, Vincent L, Stephenson DB, Burn J, Aguilar E, Brunet M, Taylor M, New M, Zhai P, Rusticucci M, Vazquez-Aguirre JL. 2006. Global observed changes in daily climate extremes of temperature and precipitation. *Journal of Geophysical Research* **111**: D05109. doi:10.1029/2005JD006290.

Alexandersson H. 1986. A homogeneity test applied to precipitation data. *Journal of Climatolology* **6***:* 661-75.

Araghi A, Baygi MM, Adamowski J, Malard J, Nalley D, Hasheminia SM. 2015. Using wavelet transforms to estimate surface temperature trends and dominant periodicities in Iran based on gridded reanalysis data. *Atmospheric Research* **155**: 52-72.

Arathyram RS, Venugopala Raoa K. 2012. Characterisation of Urban Heat Islands in one of the most urbanised Corridors of India from Space Based Multi-sensor, Spatio-Temporal data. *Applied Geoinformatics for Society and Environment* **20**: 17-23.

Ashcroft L, Karoly DJ, Gergis J. 2012. Temperature variations of southeastern Australia, 1860-2011. *Australian Meteorological and Oceanographic Journal* **62**: 27-245.

Ashcroft L, Gergis J, Karoly DJ. 2014. A historical climate dataset for southeastern Australia, 1788–1859. *Geoscience Data Journal* **1**: 158-178.

Ashcroft L, Gergis J, Karoly DJ. 2016. Long-term stationarity of El Niño–Southern Oscillation teleconnections in southeastern Australia. *Climate Dynamics* **46**: 2991-3006.

Barros VR, Boninsegna JA, Camilloni AI, Chidiak M, Magrin GO, Rusticucci M. 2015. Climate change in Argentina: trends, projections, impacts and adaptation. *Advanced Review* **6**: 151-169.

Bodri L, Cermak V. 1999. Climate change of the last millennium inferred from borehole temperatures: regional patterns of climatic changes in the Czech Republic—Part III. *Global Planet Change* **21**: 225–235. doi:10.1016/S0921-8181(99)00044-2.

Boko M, Niang I, Nyong A, Vogel C, Githeko A, Medany M, Osman-Elasha B, Tabo R, Yanda P. 2007. Africa. Climate Change 2007: Impacts, Adaptation and Vulnerability. Contribution of Working Group II to the Fourth Assessment Report of the Intergovernmental Panel on Climate Change. Parry, ML, Canziani OF, Palutikof JP, van der Linden PJ, Hanson CE (Eds.), Cambridge University Press, Cambridge UK, pp. 433-467.

Bradzil R, Pfister C, Wanner H, von Storch H, Luterbacheer J. 2005. Historical Climatology In Europe – The State Of The Art. *Climatic change* **70**:363-430.

Brocard E, Jeannet P, Begert M, Levrat G, Philipona R, Romanens G, Scherrer SC. 2013. Upper air temperature trends above Switzerland 1959-2011. *Journal of Geophysical Research: Atmospheres* **118**:4303-4317.

Brohan P, Allan R, Freeman E, Wheeler D, Wilkinson C, Williamson F. 2012. Constraining the temperature history of the past millennium using early instrumental observations. *Climate of the Past* **8:** 1551-1563.

Brönnimann S. 2007. El Nino-Southern Oscillation on European climate. *Reviews of Geophysics* **45**: 1-28.

Brunet M and Jones P. 2011. Data rescue initiatives: bringing historical climate data into the 21st century. *Climate Research* **47**: 29-40.

Brunet M, Saladie O, Jones P, Sigro J, Aguilar E, Moberg A, Lister D, Walther A, Lopez D, Almarza C. 2006. The development of a new dataset of Spanish daily adjusted temperature Series (SDATS) (1850–2003). *International Journal of Climatology* **26**: 1777-1802.

Brunet M, Saladie O, Jones, P, Sigro, J, Anguilar E, Moberg A, Lister, D, Walther A, Almarz C. 2008. A case-study/guidance on the development of long-term daily adjusted temperature datasets: Climate Data and Monitoring WCDMP-No. 66. World Meteorological Organization, Geneva, Switzerland. pp.1-43.

Caussinus H, Mestre O. 2004: Detection and correction of artificial shifts in climate series. *Journal of the Royal Statistical Society Series: Applied Statistic* **53**: 405–425.

Carlson TN, Arthur ST. 2000. The impact of land use-land cover changes due to urbanisation on surface microclimate and hydrology: a satellite perspective. *Global and Planetary Change* **25**: 49-65.

Chowdary JS, John N, Gnanaseelan C. 2014. Interannual variability of surface sir-temperature over India: impact of ENSO and Indian Ocean Sea surface temperature. *International Journal of Climatology* **34**: 416-429.

Collins JM. 2011. Temperature Variability over Africa. *Journal of Climate* **24**: 3649-3666.

Costa AC, Soares A. 2009. Homogenisation of Climate data: review and new perspective using Geostatistics. *Mathematical Geosci*ences **49**: 291-305.

Creamer AE, Goa B. 2015. Carbon Dioxide capture: an effective way to combat global warming. Springer International Publishing. pp.1-15. doi: 10.1007/978-3-319-17010-7.

CSIRO. 2016. State of the Climate Report 2016. Australian Government: Bureau Meteorology. Available online http://www.bom.gov.au/state-of-the-climate/ (accessed 25 January 2017).

Cubasch UD, Wuebbles D, Chen MC, Facchini D, Frame N, Mahowald, Winther J-G. 2013. Introduction. In: Climate Change 2013: The Physical Science Basis. Contribution of Working Group I to the Fifth Assessment Report of the Intergovernmental Panel on Climate Change (Stocker TF, Qin D, Plattner G-K, Tignor M, Allen SK, Boschung J, Nauels A, Xia Y, Bex V, Midgley PM (eds.)). Cambridge University Press, Cambridge, United Kingdom and New York, NY, USA, pp.119-158.

Davey MK, Brookshaw A, Ineson S. 2014. The probability of the impact of ENSO on precipitation and near-surface temperature. *Climate Risk Management* **1**: 5-24.

Davis CL, Hoffman MT, Roberts W. 2016. Recent trends in the climate of Namaqualand, a megadiverse arid region of South Africa. *South African Journal of Science* **112:** 1-9.

Della-Marta P, Collins D, Braganza K. 2004. Updating Australia's high quality annual temperature dataset. *Australian Meteorological Magazine* **53**: 75-93.

Department of Environmental Affairs and Tourism. 2004. A National Climate Change Response Strategy for South Africa. Department of Environmental Affairs, Republic of South Africa, Pretoria.

Déqué M. 2007. Frequency of precipitation and temperature extremes over France in an anthropogenic scenario: model results and statistical correction according to observed values. *Global and Planetary Change* **57**: 16–26.

Domokos P. 2011. Adapted Caussinus Mestre Algorithm for homogenizing Networks of monthly Temperature series (ACMANT). *International Journal of Geoscience* **2**: 293-309.

Engelbrecht FA, Landman WA, Engelbrecht CJ, Landman **S**, Bopape MM, Roux B, McGregor JL**,** Thatcher M. 2011. Multi-scale climate modelling over Southern Africa using a variable-resolution global model. *Water SA* **37**: 647-658.

Falvey M, Garreaud RD. 2009. Regional cooling in a warming world: Recent temperature trends in the southeast Pacific and along the west coast of subtropical South America (1979–2006). *Journal of Geophysical Research* **114**: 1-16. doi:10.1029/2008JD010519.

Fenby C, Gergis J. 2013. Rainfall variations in south-eastern Australia part 1: consolidating evidence from pre-instrumental documentary sources, 1788–1860. *International Journal of Climatology* **33**: 2956-2972.

Folland CK, Salinger MJ, Jiang N, Rayner NA. 2003. Trends and Variations in South Pacific Island and Ocean Surface Temperatures. *Journal of Climate* **16**: 2859-2874.

Fujibe F. 2009. Detection of urban warming in recent temperature trends in Japan. *International Journal of Climate Change* **29**: 1811-1822.

Fyfe JC, Gillett NP, Zwiers FW. 2013. Overestimated global warming over the past 20 years. *Nature Climatic Change* **3**: 767-769.

Gergis JL, Fowler AM. 2008. A history of ENSO events since A.D. 1525: implications for future climate change. *Climatic Change* **92**: 343-387.

Gocic M, Trajkovic S. 2013. Analysis of changes in meteorological variables using Mann-Kendall and Sen's slope estimator statistical tests in Serbia. *Global and Planetary Change* **100**: 172-182.

Grab SW, Nash DJ. 2010. Documentary evidence of climate variability during cold seasons in Lesotho, southern Africa, 1833-1900. *Climate Dynamics* **34**: 473-499.

Gunawardhana LN, Al-Rawas GA. 2014. Trends in extreme temperature and precipitation in Muscat, Oman. *Evolving Water Resources Systems: Understanding, Predicting and Managing Water–Society Interactions* Proceedings of ICWRS2014, Bologna, Italy, June 2014 (IAHS Publ. 364, 2014). pp. 57-63.

Halpert MS, Ropelewski CF. 1992. Surface temperature pattern associated with Southern Oscillation. *Journal of Climate* **5**: 577-593.

Hannaford MJ, Jones JM, Bigg GR. 2015. Early nineteenth century southern African precipitation reconstructions from ship logbooks. *The Holocene* **25**: 379-390.

Hannaford MJ, Nash DJ. 2016. Climate, history, society over the last millennium in southeast Africa. *WIRES: Climate Change* **7**: 370-393.

Hartmann DL, Klein Tank AMG, Rusticucci M, Alexander LV, Brönnimann S, Charabi Y, Dentener F, Dlugokencky EJ, Easterling DR, Kaplan A, Soden BJ, Thorne PW, Wild M, Zhai PM. 2013: Observations: Atmosphere and Surface. In: Climate Change 2013: The Physical Science Basis. Contribution of Working Group I to the Fifth Assessment Report of the Intergovernmental Panel on Climate Change (Stocker TF, Qin D, Plattner G-K, Tignor M, Allen SK, Boschung J, Nauels A, Xia Y, Bex V, Midgley PM (eds.)). Cambridge University Press, Cambridge, United Kingdom and New York, NY, USA. pp. 159-254.

Hughes WS, Balling RC. 1996. Urban Influences on South African Temperature Trends. *International Journal of Climatology* **16**: 935-940.

Hulme M, Doherty R, Ngara T, New M, Lister D. 2001. African climate change: 1900-2100. *Climate Research* **17**: 145-168.

IPCC. 2013. Summary for Policymakers. In: Climate Change 2013: The Physical Science Basis. Contribution of Working Group I to the Fifth Assessment Report of the Intergovernmental Panel on Climate Change (Stocker, TF, Qin D, Plattner G-K, Tignor M, Allen SK, Boschung J, Nauels A, Xia Y, Bex V, Midgley PM (eds.)). Cambridge University Press, Cambridge, United Kingdom and New York, NY, USA. pp. 3- 29.

Pohl B, Richard Y. 2007. Influence of the Madden–Julian Oscillation on Southern African summer rainfall. *Journal of Climate* **20**: 4227-4242.

Pohl B, Fauchereau N, Reason CJC, Rouault M. 2010. Relationships between the Antarctic Oscillation, the Madden–Julian Oscillation, and ENSO, and consequences for rainfall analysis. *Journal of Climate* **23**: 238-254.

Ji F, Huang ZW Chassignet EP. 2014. Evolution of land surface air temperature trend. *Nature Climate Change* **4**: 462-466.

Jia X., Lin H, Ge J. 2015. The interdecadal change of ENSO impact on wintertime East Asian climate. *Journal of Geophysical Research Atmospheres* **120**, doi:10.1002/2015JD023583.

Jones P. 2016. The Reliability of Global and Hemispheric Surface Temperature Records. *Advances in Atmospheric Sciences* **33**:1-14.

Jones DA, Trewin BC. 2000. On the relationship between the El Niño-Southern Oscillation and Australian land surface temperature. *International Journal of Climatology* **20**: 697-719.

Jones PD, Wigley TML. 2010. Estimation of global temperatures: what's important and what isn't. *Climatic Change* **100**:59-69.

Jones PD, Lister DH, Osborn TJ, Harpham C, Salmon M, Morice CP. 2012. Hemispheric and large-scale land-surface air temperature variations: An extensive revision and an update to 2010. *Journal of Geophysical Research* **117**: D05127, doi:10.1029/2011JD017139.

Jones PD, Parker DE, Osborn TJ, Briffa KR. 2016. Global and hemispheric temperature anomalies—land and marine instrumental records. In *Trends: A Compendium of Data on Global Change*. Carbon Dioxide Information Analysis Center, Oak Ridge National Laboratory, U.S. Department of Energy, Oak Ridge, Tenn., U.S.A. Available online: http://cdiac.esd.ornl.gov/trends/temp/jonescru/jones.html (accessed 2 January 2017).

Jun W, Zhong-Wei Y. 2016. Urbanization-related warming in local temperature records: a review. *Atmospheric and Oceanic Science Letters* **9:** 129-138.

Jury MR. 2013. Climate trends in southern Africa. *South African Journal of Science* **109**: 1-11. http://dx.doi.org/10.1590/sajs.2013/980.

Kafle HK, Bruins HJ. 2009. Climatic trends in Israel 1970-2002: warmer and increasing aridity inland. *Climatic Change* **96**: 63-77.

Kalnay E, Cai M. 2003. Impact of urbanization and land use on climate. *Nature* **423**: 528-531.

Kane RP. 2009. Periodicities, ENSO effects and trends of some South African rainfall series: an update. *South African Journal of Science* **105**: 199-207.

Kelso C, Vogel C. 2007. The climate of Namaqualand in the nineteenth century. *Climatic Change* **83**: 357-380.

Kenawy AE, Lopez-Moreno JI, Štěpánek P, Vicente-Serrano SM. 2013. An assessment of the role of homogenisation protocol in the performance of daily temperature series and trends: application to northeastern Spain. *International Journal of Climatology* **33**: 87–108.

King'uyu SM, Ogallo, LA, Anyamba, EK. 2000. Recent trends of minimum and maximum over Eastern Africa. *Journal of Climate* **13**: 2876-2886.

Kirono DGC, Jones RN. 2007. A bivariate test for detecting inhomogeneities in pan evaporation time series. *Australian Meteorological Magazine* **56**: 93-103.

Kousari MR, Ahani H, Hendi-zadeh R. 2013. Temporal and spatial trend detection of maximum air temperature in Iran during 1960–2005. *Global and Planetary Change* **111**: 97–110.

Kruger AC. 1999. The influence of the decadal-scale variability of summer rainfall on the impact of El Niño phase and La Niña events in South Africa. *International Journal of Climatology* **19***:* 59–68.

Kruger AC, Shongwe, S. 2004. Temperature trends in South Africa: 1960–2003. *International Journal of Climatology* **24**: 1929–1945.

Kruger AC, McBride C, Thiaw WM. 2011. Southern Africa Regional Climate in "State of the Climate 2010". *Bulletin of the American Meteorological Society* **92**: S161–S163.

Kruger AC, Sekele SS. 2013. Trends in extreme temperature indices in South Africa: 1962-2009. *International Journal of Climatology* **33**: 661-676.

Kruger AC, Nxumalo M. 2017. Surface temperature trends from homogenized time series in South Africa: 1931-2015. *International Journal of Climatology* **37:** 2364-2377.

Laken BA, Stordal F. 2016. Are there statistical links between the direction of European weather systems and ENSO, the solar cycle or stratospheric aerosols? *Royal Society Open Science* **3**:1-25. http://dx.doi.org/10.1098/rsos.150320

Lamptey BL, Barron EJ, Pollard D. 2005. Impacts of agriculture and urbanisation on the climate of the North-eastern United States. *Global and Planetary Change* **49**: 203-221.

Landman WA, Beraki A. 2012. Multi-model forecast skill for mid-summer rainfall over southern Africa. *International Journal of Climatology* **32**: 303–314.

Lebassi B, Gonzalez J, Fabris D, Maurer E, Miller N, Milesi, C, Bornstein, R. 2009. Observed 1970-2005 Cooling of Summer Daytime Temperatures in Coastal California. *Journal of Climate* **22**: 3558-3573.

Lee JH, Julien PY. 2016. ENSO impacts on temperature over South Korea. *International Journal of Climatology* **36**: 3651-3663.

Li Z, He Y, Wang C, Wang X, Xin H, Zhang W, Cao W. 2011. Spatial and temporal trends of temperature and precipitation during 1960 and 2008 at the Hengduan Mountains, China. *Quaternary International* **236**: 127-142.

Li Q, Chen J. 2014. Teleconnection between ENSO and climate in South China. *Stochastic Environmental Research Risk Assessment* **28**: 927-941.

Lindesay JA. 1988. South African rainfall, the Southern Oscillation and a Southern Hemisphere semi-annual cycle. *Journal of Climatology* **8**: 17–30.

MacKellar N, New M, Jack C. 2014. Observed and modeled trends in rainfall and temperature for South Africa: 1960–2010. *South African Journal of Science* **110:** 1-13. http://dx.doi.org/10.1590/sajs.2014/20130353

Maletjane, M. 2006. An investigation of the effect of urbanisation on the climate of Maseru, Lesotho. MSc dissertation. University of Nairobi. http://erepository.uonbi.ac.ke:8080/handle/11295/20762

Mamara A, Argiriou AA, Anadranistakis M. 2016. Recent trend analysis of mean air temperature in Greece based on homogenized data. *Theoretical and Applied Climatology* **126**: 543-573.

Marengo JA, Camargo CC. 2008. Surface air temperature trends in Southern Brazil 1960-2002. *International Journal of Climatology* **28**: 893- 904.

Maronna R, Yohai VJ. 1978. A bivariate test for the detection of a systematic change in mean. *Journal of the American Statistical Association* **73**: 640-645.

Mason SJ. 2001. El Niño, climate change, and southern African climate. *Environmetrics* **12**: 327–345.

McAfee SA, Wise EK. 2016. Intra-seasonal and inter-decadal variability in ENSO impacts on the Pacific Northwest. *International Journal of Climatology* **36:** 508-516.

Menne MJ, Williams CN. 2009. Homogenisation of temperature series via pairwise comparisons. *Journal of Climate* **22:** 1700-1717.

Mestre O, Gruber C, Prieur C, Caussinus H, Jourdain S. 2011. SPLIDHOM: A method for homogenization of daily temperature observations. *Journal of Applied Meteorology and Climatology* **50**: 2343-2358.

Mestre O, Domonkos P, Picard F, Auer I, Robon S, Lebarbier E, Bohm R, Aguilar E, Guijarro J, Vertachnik G, L Klancar M, Dubuisson B, Stepanek P. 2013. HOMER: a homogenization software- methods and applications. *Quarterly Journal of the Hungarian Meteorological Service* **117**: 47-67.

Miller, GT, Spoolman, SE. 2012. Living in the Environment. 17th ed. Brooks/Cole, Cengage Learning. Canada. pp. 482.

Morgan, MR, Drinkwater KF, Pocklington, R. 1993. Temperature trends at coastal stations in Eastern Canada. *Climatological Bulletin* **27**:135-153.

Muhlenbruch-Tegen A. 1992. Long-term surface temperature variations in South Africa. *South African Journal of Science* **88**: 197-205.

Nash DJ, Endfield GH. 2002. A 19th century climate chronology for the Kalahari region of central southern Africa derived from missionary correspondence. *International Journal of Climatology* **22**:821–841.

Nash DJ, Endfield GH. 2008. 'Splendid rains have fallen': links between El Niño and rainfall variability in the Kalahari, 1840–1900. *Climatic Change* **86**: 257-290.

Nash DJ, Grab SW. 2010. "A sky of brass and burning winds": documentary evidence of rainfall variability in the Kingdom of Lesotho, Southern Africa, 1824–1900. *Climatic Change* **101**:617-653.

Nash DJ, Pribyl K, Klein J, Neukom R, Endfield, GH, Adamson GCD, Kniveton DR. 2016. Seasonal rainfall variability in southeast Africa during the nineteenth century reconstructed from documentary sources. *Climatic Change* **134**: 605-619.

Nemec J, Gruber C, Chimani B, Auer I. 2013. Trends in extreme temperature indices in Austria based on new homogenized dataset. *International Journal of Climatology* **33:** 1538-1550.

Neukom R, Nash DJ, Endfield GH, Grab SW, Grove CA, Kelso C, Vogel C, Zinke J. 2014. Multi-proxy summer and winter precipitation reconstruction for southern Africa over the last 200 years. *Climate Dynamics* **42**: 2713-2726.

New M, Hewitson B, Stephenson DB, Tsiga A, Kruger A, Manhique A, Gomez B, Coelho CAS, Masisi DN, Kululanga E, Mbambalala, Adesina F, Saleh H, Kanyanga J, Adosi J, Bulane L, Fortunata L, Mdoka ML, Lajoie R. 2006. Evidence of trends in daily climate extremes over southern and west Africa. *Journal of Geophysical Research* **111**: D14102. doi:10.1029/2005JD006289.

Nicholson SE, Nash DJ, Chase BM, Grab SW, Shanahan TM, Verschuren D, Asrat A, Lezine AM, Umer M. 2013. Temperature variability over Africa during the last 2000 years. *The Holocene* **23**: 1085–1094.

NOAA National Centers for Environmental Information, State of the Climate: Global Analysis for Annual 2015, published online January 2016, http://www.ncdc.noaa.gov/sotc/global/201513 (accessed 1 September 2016).

Odindi J, Mhangara P, Kakembo V. 2012. Remote Sensing Land Cover Change during South Africa's democratic transition. *South African Journal of Science* **108**: 1-7, http:// dx.doi.org/10.4102/sajs. v108i5/6.886

Parker A. 2015. The ACORN adjustments of Australian temperatures are in the wrong direction. *Physical Science International Journal* **6**: 245-252.

Peralta-Hernandez AR, Balling RC, Barba-Martinez LRB. 2009. Analysis of near-surface diurnal temperature variations and trends in southern Mexico. *International Journal of Climatology* **29**: 205-209.

Peterson TC, Easterling DR. 1994. Creation of homogeneous composite climatological reference series. *International Journal of Climatology* **14**: 671–679.

Peterson TC, Easterling DR, Karl TR, Groisman P, Auer I, Bohm R, Plummer N, Nicholis N, Torok S, Vincent L, Tuomenvirta H, Salinger J, Førland EJ, Hanssen-Bauer I, Alexandersson H, Jones P, Parker D. 1998. Homogeneity adjustments of in situ climate data: a review. *International Journal of Climatology* **18**: 1493–1517.

Peterson TC, Zhang X, Brunet-India M, Vazquez-Aguirre JL. 2008. Changes in North American extremes derived from daily weather data. *Journal of Geophysical Research* **113:** D07113, doi:10.1029/2007JD009453.

Philippon N, Rouault M, Richard Y, Favre A. 2012. The influence of ENSO on winter rainfall in South Africa. *International Journal of Climatology* **32**: 2333-2347.

Potter, K. 1981. Illustration of a new test for detecting a shift in mean in precipitation series. *Monthly Weather Review* **109**: 2040-2045.

Potter S, Cabbage M, McCarthy L. 2017. NASA, NOAA Data Show 2016 Warmest Year on Record Globally. Available online: https://www.nasa.gov/press-release/nasa-noaa-data-show-2016-warmest-year-on-record-globally (accessed 22 January 2017).

Portmann RW, Solomon S, Heger GC. 2009. Spatial and seasonal patterns in climate change, temperatures, and precipitation across the United States. *PNAS Early edition*. **106**: 7324-7329.

Prieto MR, Herrera RG. 2009. Documentary sources from South America: Potential for climate reconstruction. *Palaeogeography, Palaeoclimatology, Palaeoecology* **281**:196–209.

Prior MJ, Perry MC. 2014. Analyses of trends in air temperature in the United Kingdom using gridded data series from 1910 to 2011. *International Journal of Climatology* **34**: 3766-3779.

Rebetez M, Reinhard M. 2008. Monthly air temperature trends in Switzerland 1901-2000 and 1975-2004. *Theoretical and Applied Climatology* **91**: 27-34.

Reason CJC, Rouault M. 2002. ENSO-like decadal variability and South African rainfall. *Geophysical Research Letters* **29**: 1638-1641.

Ropelewski CF, Halpert MS. 1986. North American Precipitation and temperature pattern associated with El Niño/Southern oscillation (ENSO). *Monthly Weather Review* **114**: 2352-2362.

Safari B. 2012. Trend analysis of the mean annual temperature in Rwanda during the last fifty years. *Journal of Environmental Protection* **3**: 538-551.

Sakakibara Y, Owa K. 2005. Urban-rural temperature differences in coastal cities: influence of rural sites. *International Journal of Climatology* **25**: 811-820.

Sankar S, Kumar MRR, Reason C. 2011. On the relative roles of El Niño and Indian Ocean Dipole Events on the Monsoon Onset over Kerala. *Theoretical and Applied Climatology* **103***:*359-374.

Satterthwaite D. 2009. The implications population growth and urbanisation for climate change. *Environment and Urbanisation* **21**: 545-567.

Scaife AA. 2010. Impact of ENSO on European climate. ECMWF Seminar on Predictability in the European and Atlantic regions, 6 to 9 September 2010. Met. Office Hadley Centre.

Soltani A, Gholipoor M. 2006. Teleconnections between El Niño/Southern Oscillation and rainfall and temperature in Iran. *International Journal of Agricultural Research* **1**: 603-608.

Sonali P, Kumar DN. 2013. Review of trend detection methods and their application to detect temperature changes in India. *Journal of Hydrology* **476**: 212- 227.

Štěpánek P, Zahradníček P, Skalák P. 2009. Data quality control and homogenization of air temperature and precipitation in the area of the Czech Republic in the period 1961-2007. *Advances in Science and Research* **3**: 23-26.

Štěpánek P, Zahradníček P, Huth R. 2011. Interpolation techniques used for data quality control and calculation of technical series: an example of Central European daily time series. *Idöjárás* **115**: 87–98.

Štěpánek P, Zahradníček P, Farda A. 2013. Experiences with data quality control and homogenisation of daily records of various meteorological elements in the Czech Republic in the period 1961-2010. *Quarterly Journal of the Hungarian Meteorological Service* **117**: 123-141.

Sturman A, Quenol H. 2013. Changes in atmospheric circulation and temperature trends in major vineyard regions of New Zealand. *International Journal of Climatology* **33:**2609-2621.

Tadross M, Johnston P. 2012. Climate Systems Regional Report: Southern Africa. ICLE Local Governments for Sustainability – Africa. Cape Town, South Africa. pp38.

Torok SJ, Nicholls N. 1996. A historical annual temperature dataset for Australia. *Australian Meteorological Magazine* **45**: 251-260.

Trenberth KE, Jones PD, Ambenje P, Bojariu R, Easterling D, Klein Tank A, Parker D, Rahimzadeh F, Renwick JA, Rusticucci M, Soden B, Zhai P. 2007. Observations: surface and atmospheric climate change. In *Climate Change 2007: The Physical Science Basis. Contribution of Working Group I to the Fourth Assessment Report of the Intergovernmental Panel on Climate Change*, Solomon S, Qin D, Manning M, Chen Z, Marquis M, Averyt KB, Tignor M, Miller HL (eds). Cambridge University Press: Cambridge; New York. pp. 235-336.

Trewin B. 2013. A daily homogenized temperature dataset for Australia. *International Journal of Climatology* **33**: 1510-1529.

Tshiala MF, Olwoch JM, Engelbrecht FA. 2011. Analysis of temperature trends over Limpopo Province, South Africa. *Journal of Geography* **3**: 13-21.

Turkes M, Sumer UM. 2004. Spatial and temporal patterns of trends and variability in diurnal temperature ranges of Turkey. *Theoretical and Applied Climatology* **77**: 195–227.

Tyler K, White T, Anslow F. 2015. Indicators of climate change for British Columbia 2015 Update. Ministry of Environment, Victoria, Canada. pp. 50

Tyson PD, Preston-Whyte RA. 2000. *The Weather and Climate of Southern Africa*. Oxford University Press Southern Africa, Cape Town. pp. 396.

Valero F, Gonzalaez JF, Doblas FJ, Garcia-Miguel JA. 1996. A method for the recomstruction and temporal extension of climatological time series. *International Journal of Climatology* **16**: 213-227.

Venema VKC, Mestre O, Aguilar E, Auer I, Guijarro JA, Domonkos P, Vertacnik G, Szentimrey T, Štěpánek P, Zahradnicek P, Viarre J, Muller-Westermeier G, Lakatos M, Williams CN, Menne MJ, Lindau R, Rasol D, Rustemeier E, Kolokythas K, Marinova T, Andresen L, Acquaotta F, Fratianni S, Cheval S, Klancar M, Brunetti M, Gruber C, Prohom Duran M, Likso T, Esteban P, Brandsma T. 2012. Benchmarking monthly homogenisation algorithms. *Climate of the Past Discussions* **7**: 2655–2718.

Vincent LA, Wang XL, Milewska EJ, Wan H, Feng Y, Swail V. 2012. A Second Generation of Homogenized Canadian Monthly Surface Air Temperature for Climate Trend Analysis, *Journal of Geophysical Research* **117**: D18110, doi:10.1029/2012JD017859.

Vincent LA, Zhang X, Brown RD, Feng Y, Mekis E, Milewska EJ, Wan H, Wang XL. 2015. Observed Trends in Canada's Climate and Influence of Low-Frequency Variability Modes. *Journal of Climate* **28**: 4545-4560.

Viola F, Liuzzo L, Noto LV, Lo Conti F, La Loggia G. 2014. Spatial distribution of temperature trends in Sicily. *International Journal of Climatology* **34**: 1-17.

Wang XL, Wen QH, Wu Y. 2007. Penalized maximal *t* test for detecting undocumented mean change in climate data series. *Journal of Applied Meteorology and Climatology* **46***:* 916-931.

Wang XL. 2008. Penalized maximal F-test for detecting undocumented mean-shifts without trend-change. *Journal of Atmospheric Oceanic Technology* **25***:* 368-384.

Wang XL, Chen H, Wu Y, Feng Y, Pu Q. 2010. New techniques for detection and adjustment of shifts in daily precipitation data series. *Journal of Applied Meteorology and Climatology* **49***:* 2416-2436.

Wang, XL, Feng Y. 2013. RHtestsV4 User Manual. Climate Research Division, Atmospheric Science and Technology Directorate, Science and Technology Branch, Environment Canada. p28. (published online July 2013). Available online at http://etccdi.pacificclimate.org/software.shtml.

Weldon D, Reason CJC. 2014. Variability of rainfall characteristics over the South Coast region of South Africa. *Theoretical and Applied Climatology* **115**: 177-185.

Welhouse LJ, Lazzara MA, Keller LM, Tripoli GJ, Hitchman MH. 2016. Composite analysis of the effects of ENSO on Antarctica. *Journal of Climate* **29**: 1797-1808.

Wijngaard JB, Tank AMGK, Konnen GP. 2003. Homogeneity of 20th century European daily temperature and precipitation series. *International Journal of Climatology* **23**: 679-692.

WMO. 2014. El Niño/Southern Oscillation. WMO No. 1145, Geneva, Switzerland, 2–4. Available online http://www.wmo.int/pages/prog/wcp/wcasp/documents/JN142122_WMO1145_EN_web.pdf (accessed 27 June 2016).

CHAPTER THREE

A HOMOGENIZED LONG-TERM TEMPERATURE RECORD FOR THE WESTERN CAPE PROVINCE IN SOUTH AFRICA: 1916-2013

This chapter has been published:

Lakhraj-Govender R, Grab S, Ndbele NE. 2016. A homogenized long-term temperature record for the Western Cape Province in South Africa: 1916-2013. ***International Journal of Climatology*** **37: 2337-2353.**

3.1. ABSTRACT

To establish precise climate trend analyses, highly reliable and accurate homogeneous historical climate data are required. To this end, this work undertakes a robust quality control and homogenization process of daily maximum temperature (T_{max}) and minimum temperature (T_{min}) data (1916-2013) for the Western Cape Province, South Africa, using RClimDex, ProClimDB and Anclim software. Inhomogeneities were detected using the pairwise method in AnClim, suggesting possible artificial biases in the time series, as a result of non-climatic factors. The adjustment of time series utilised ProClimDB software to create reference series using highly correlated or nearest neighbour stations. Given few available long-term data sets, the study is limited to eight suitable stations. The modified Mann Kendall test in XLSTAT 2015 software identified annual and seasonal trends in the newly homogenized monthly T_{max} and T_{min} data. Annual T_{max} and T_{min} adjusted data over the Western Cape region indicate statistically significant increasing temperature trends over the period 1916 to 2013, with the exception of an insignificant decreasing T_{max} trend at Cape St Blaize. A statistically significant increasing trend (0.13°C/decade) for all stations used in this study is recorded for the common period 1937-2001. The seasonal trends also support significant increasing annual trends, with the exception of T_{max} trends for summer (-0.03°C/decade) and autumn (0°C/decade) at Kirstenbosch.

Keywords: homogeneity, temperature, trend analysis, Mann Kendall, Western Cape.

3.2. INTRODUCTION

Climate change is one of the most significant global concerns and environmental problems of today. To quantify and understand such climate variability and change, long-term, high quality homogeneous data sets are essential. Time series data are only considered homogeneous when identified variations are due to weather and climate. Inhomogeneities of long-term temperature data may result from instrumentation changes/failures and calibration issues, station relocation, urbanization and land cover changes (i.e. albedo/evapotranspiration effects), or changes in observing practices (see Peterson *et al.*, 1998). Technological changes over time, such as a shift from manual recordings to automatic stations, are also a cause for

artificial shifts in time series data (Wang *et al*., 2010). Thus, detection and adjustment of such artificial shifts is essential for reliable assessments of longer-term climate trends. Given the relatively common situation of inaccurate and/or incomplete metadata in many developing regions, it is imperative that statistical tests be performed on available data sets, so as to detect and assess the potential for any undocumented shifts (Wang, 2008). Undocumented shifts are artificial shifts in climatic series (e.g. temperature, rainfall) where the time and cause of the shifts are not recorded in the metadata (an example of which may be found in the study by Menne *et al*., 2009). Several techniques have been employed to detect and correct such inhomogeneities – these are briefly reviewed below.

Homogeneity testing techniques are essential for the removal of the aforementioned artificial biases before employing trend analysis (Williams *et al*., 2012). Homogeneity testing techniques include absolute and relative methods, each with their own advantages and drawbacks. An absolute method uses data from a single station while the relative method employs a reference series from neighbouring stations to detect inhomogeneities. The latter is based on the assumption that the reference series will maintain the climate signal of the candidate series (Kenawy *et al*., 2013), but presents the challenge of finding well correlated homogeneous neighbour stations (Mitchell and Jones, 2005). Although the relative homogeneity test is considered a superior test compared to absolute tests, trend analyses are dependent on the quality of the reference series (Yozgatligil and Yacisi, 2016). Relative homogeneity techniques, such as the Standard Normal Homogeneity Test (SNHT), use one composite reference series, assumed to be homogeneous, while Multiple Analysis of Series for Homogenization (MASH) uses multiple reference series, which are not assumed to be homogeneous. Further techniques, such as that used to develop the United States Historical Climatology Network (USHCN), use pairwise comparison (Venema *et al.*, 2012). Absolute methods are challenging because separating the climate change signal and the inhomogeneity signal is impracticable (Szentimrey, 2008). A particular challenge is working with African data given their highly variable availability and quality, both in space and time (Christy *et al.*, 2009). Building temporally flexible reference series from the most suitable stations available for each year may be a solution (e.g. Peterson and Easterling, 1994), yet the challenge often remains in finding well correlated homogeneous neighbour stations.

Despite previously established temperature trends in South Africa (e.g. Muhlenbruch-Tegen, 1992; Kruger and Shongwe, 2004; MacKellar *et al*., 2014), these cover relatively short (49,

43, 50 years, respectively) periods. Although Hughes and Balling (1996) examined a longer period (1885-1993), only mean temperature trends for relatively large cities of South Africa were investigated, and the remaining T_{max} and T_{min} trends only covered the period 1960-1990. The work by Kruger and Shongwe (2004) established that significant increasing trends had occurred in annual T_{mean} over South Africa for the period 1960-2003, yet when the periods were subdivided, trends were statistically insignificant for the periods 1960-1982 and 1983-2003, indicating the importance of using longer temporal data sets. The aim is to provide a homogeneous dataset for the Western Cape region in South Africa and establish long-term annual and seasonal instrumental temperature record for this region. This should make a valuable contribution towards ongoing debates on the extent of recent (decadal to centennial) climate warming in southern Africa. In addition, the results are important for precise future downscaled climate projections and modeling for sectors such as agriculture in the Western Cape region of South Africa.

3.3. METHODS

3.3.1. Study area

Raw daily T_{max} and T_{min} data for the Western Cape region (Figure 3.1) in South Africa were obtained from the South African Weather Services (SAWS). Stations were selected based on the availability of long-term temperature time series and those which did not exceed 5% missing daily records in the series. For a robust quality control and homogenization process, RClimDex, ProClimDB and Anclim software (available online http://www.climahom.eu) were used to process daily temperature data for the period 1916-2013 (Table 3.1). ProClimDB and AnClim software were selected for use as these offer the creation of homogeneous reference series as well as multiple statistical tests, thereby increasing the reliability of homogeneity results (Štěpánek *et al.,* 2009).

3.3.2. Establishing quality control

Data quality control was undertaken at the daily scale to avoid potential errors that compromise homogeneity test calculations (Brunet *et al.*, 2008). These errors are mainly the result of archiving, transcription and digitisation (Kenawy *et al*., 2013). The consistency of calendar dates (i.e. number of days per year and number of days per month) (Aguilar *et al*., 2003) were checked and corrected. The RClimDex software (Zhang and Yang, 2004), a

graphical user interface based on the statistical package R (run on Microsoft Windows) was used for simple quality control. To run this software, the input data file must be in the form of ASCII text file, with specific columns (i.e. Year, Month, Day, Precipitation, T_{max}, T_{min} with elements separated by one space) and missing data coded as -99.9 (Zhang and Yang, 2004). This software identified manual keying errors and unreasonable values, such as minimum values equal to or greater than maximum temperature values (Alexander *et al*., 2006).

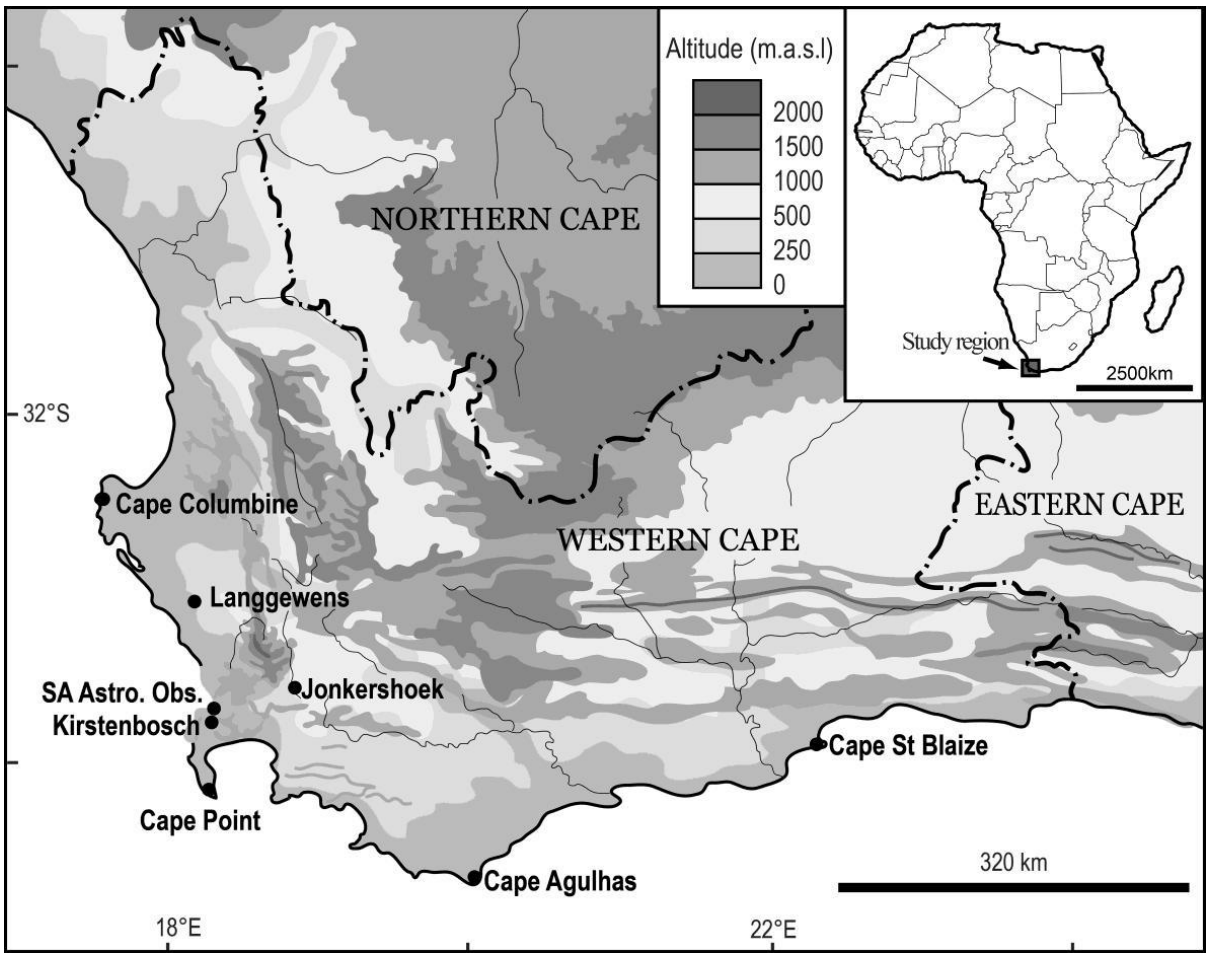

Figure 3.1: Map showing location of Western Cape stations, South Africa, used in this study.

This internal consistency test performed by the RClimDex software involves automated checking of data for coherency between associated elements within each record (e.g. maximum temperature < minimum temperature) (Aguilar *et al*., 2003; Estevez, *et al.,* 2011; Kenawy *et al.*, 2013). Where the cause for anomalous values could not be established and corrected, values were set to missing (i.e. -999). Automated searches for outliers in daily T_{max} and T_{min} were also identified using the ProClimDB interquartile range. Outliers were

checked manually and obvious errors were further investigated to determine whether digits were reversed or missing. Outlier values were verified using temperature data from altitudinally standardized neighbour stations. Where values could not be verified, the datum for the specific day was set to a missing value. The quality controlled and homogenized Western Cape data sets will be collated and sent back to the SAWS for the benefit of future users.

Table 3.1: Western Cape stations used in the study, detailing the GPS coordinates and start/end dates for each station.

Climate No.	Station name	Latitude (deg. S)	Longitude (deg. E)	Altitude (m a.s.l.)	Start year	End year	Total years
0003020 4	Cape Agulhas	-34.49	20.01	11	1916	2013	97
0060620 9	Cape Columbine	-32.49	17.51	62	1937	2013	76
0004891 9	Cape Point[a]	-34.20	18.28	228	1918	2013	94
0012251 7	Cape St Blaize	-34.18	22.15	60	1920	2001	81
0020866 9	SA Astron. Observ.	-33.56	18.28	15	1933	2013	80
0021778 8	Jonkershoek	-33.58	19.00	239	1936	2009	73
0020779 3	Kirstenbosch	-33.98	18.25	156	1916	2013	97
0041347 X	Langgewens	-33.27	18.25	179	1931	2013	82

a: Cape Point station closed from 1961/12/31 to 1963/01/01, thus no data for 1962 were used in the study. The start years began on 1 January and end years ended on 31 December for all stations.

3.3.3. Homogenization process

Change points were detected at a monthly resolution given the high variability and noise identified in daily scaled data (Table 3.2) (Kenawy *et al*., 2013). Target stations were paired with the most highly correlated or the nearest neighbour stations (Tables 3.4 and 3.5), using the pairwise method offered by ProClimDB software (Freely available at http://www.climahom.eu/download). In addition, detailed documentation on how to run the software is available at http://www.climahom.eu/software-solution/proclimdb/documentation. The pairwise method employs the difference in the mean of the candidate station's time series and the neighbour's time series to estimate the magnitude of the change (Menne *et al*., 2009). Using pairwise comparison avoids problems related to the development of a composite reference series, such as ensuring homogeneity of the reference series and mixed record

lengths of time series (Menne and Williams, 2009). Utilizing several statistical tests in the AnClim software (Štěpánek, 2008) helps assess homogeneity more reliably than from a single test (Štěpánek *et al.*, 2013), thus SNHT and Bivariate tests (using the AnClim software) were used to detect change points.

Careful consideration was given to establish which detected change points required adjustment. Department of Transport and South African Weather Bureau Meteorological Office reports, available through the online NOAA Central Library (2013), and station history information from the SAWS, were consulted during the homogenization process. This helped establish whether any of the dates of change recorded corresponded with a change point detected by the software. Careful application of homogenization procedures is essential because the removal of falsely detected inhomogeneities or the acceptance of inhomogeneous series may significantly affect subsequent trend analyses (Toreti *et al*., 2011).

3.3.4. Developing a composite reference series

Establishing a homogeneous reference series is important to relatively homogenize time series (Peterson and Easterling, 1994; Kenawy *et al.*, 2013); therefore ProClimDB software (Štěpánek *et al*., 2011) is used to develop feasible composite reference series. Composite reference series are computed as a weighted average of data from highly correlated neighbour stations (i.e. Pearson Correlation Coefficients >0.6) (Tables 3.4 and 3.5). To avoid additional inhomogeneities from the reference series, Pearson correlation analysis was performed on the first difference series as per the Peterson *et al.* (2008) method. Developing a reliable composite series takes several factors into account. These factors include the correlation coefficient must be >0.6; the maximum distance and altitudinal range between stations does not exceed 300km and 500m respectively; and a minimum overlap of 10 years is required between stations (Peterson and Easterling, 1994; Kenawy *et al*., 2013).

3.3.5. Establishing trend analyses

Mean annual and seasonal T_{max} and T_{min} values for the Western Cape region were established. Seasonal means were determined from monthly data, defined as austral summer (December, January, and February), autumn (March, April, May), winter (June, July, August) and spring (September, October, November). The modified Mann Kendall test was used to detect significant annual and seasonal temperature trends during the period 1916-2013, using

XLSTAT 2015 software. XLSTAT 2015 is an add-on software tool for Microsoft Excel, which is used for data analyses and statistical applications. Upon launching Excel, select the XLSTAT icon and the Mann Kendall test is available under the Time-series option tab. The Mann Kendall (MK) statistic (Mann, 1945; Kendall, 1975) is a rank based non-parametric test that has high power for non-normally distributed data (Novotny and Stefan, 2007). Non parametric statistics are commonly used, particularly for trend analyses, given that they are capable of tolerating outliers and do not require normally distributed data (Kousari *et al*., 2013). Given that the Mann Kendall test requires data to be serially independent, the modified version was used to eliminate the effects of serial autocorrelation (Yue and Wang, 2004). The sign of the Mann Kendall test statistic (S) indicates whether the trend is increasing or decreasing, and the value reflects the strength of the temperature trend. When the p value is lower than the chosen significance level, alpha=0.05, the null hypothesis (H_0, i.e. no trend in the series) is rejected and the alternative hypothesis (Ha, i.e. there is a trend) is accepted (XLStat, 2015). The Z test statistic which indicates the statistical significance of the trend is determined as follows:

$$S = \sum_{i=1}^{n-1} \sum_{j=i+1}^{n} sign(x_i - x_j) \quad (1)$$

Where n is the number of data points and x_j are sequential data points

$$sign(x_i - x_j) = \begin{cases} +1, if\ (x_i - x_j) > 0 \\ 0, if\ (x_i - x_j) = 0 \\ -1, if\ (x_i - x_j) < 0 \end{cases} \quad (2)$$

$$Var(S) = \frac{n(n-1)(2n+5) - \sum_{i=1}^{m} t_i(t_i-1)(2t_i+5)}{18} \quad (3)$$

Where t_i denotes number of ties with i tied values and m is the number of tied groups of values.

Then

$$Z = \begin{cases} \frac{S-1}{\sqrt{Var(S)}} & S > 0 \\ 0 & S = 0 \\ \frac{S+1}{\sqrt{Var(S)}} & S < 0 \end{cases} \quad (4)$$

(Gocic and Trajkovic, 2013).

The null hypothesis of no trend is rejected if $Z > Z_{1-\alpha/2}$, at the chosen 5% significance level (α=0.05); where Z_S >1.96 (Gocic and Trajkovic, 2013) the trend is deemed significant.

Sen's nonparametric slope estimator (Sen, 1968) was used to determine the magnitude of the trend. The trend is assumed to be linear, thus:

$$f(t) = Qt + B, \quad (5)$$

where t is the time index, Q is the slope and B is the constant.

The slopes of the data pairs are calculated with:

$$Q_i = \frac{(x_j - x_k)}{j-k} \quad (6)$$

for $i = 1,2, \ldots, N: j > k$

Where x_j and x_k are the data points at times j and k respectively. With n values in a time series, there will be $N = n(n-1)/2$ slope estimates. The Q_i values are ranked from smallest to largest and Sens slope estimator is the median of the N values and is calculated as:

$Q = Q_{\left[\frac{N+1}{2}\right]}$ if N is odd (7)

$Q = 1/2\ (Q_{\left[\frac{N}{2}\right]} + Q_{\left[\frac{N+2}{2}\right]-})$ if N is even. (8)

3.4. RESULTS

3.4.1. Quality control

Quality control is important to eliminate data that could erroneously influence trends. For instance, the 1941 T_{max} data for Langgewens were set to missing values in response to quality control revealing that the records were unusually low for the entire year. This would not have been categorised as an 'extreme' value as similarly low values were observed throughout all seasons of 1941 and could thus possibly be due to a new inexperienced observer misreading the temperature by using the wrong end of the instrument's recording pin, as has been previously raised for other regions (e.g. El Fadli *et al.*, 2013).

Equally important was to compare the detected outliers (using the interquartile range) with neighbour station data using the ProClimDB software. For instance, the interquartile range

detected a T_{max} of 42°C as an outlier at the SA Astronomical Observatory on 19th January 2000. Compared to neighbour stations, this is a reasonable value and was thus not removed or amended. In addition, the comparison of outliers to temperatures at neighbour stations revealed that digits were sometimes reversed (e.g. '21' should be '12') or a digit missing for a double digit temperature (e.g. '5' should be '15') (see Figure 3.2 for percentage of errors per station). Errors detected in this study follow the SAWS quality control, hence the zero percentage errors recorded for the majority of stations. The few errors found could be a consequence of the SAWS offices having moved and some data possibly having been lost from their original databases, hence the necessity to recapture some data.

Jonkershoek (239m a.s.l.) and Cape Point (238m a.s.l.) are at higher altitudes compared to their neighbour stations, thus making the comparison of temperature data for quality control more challenging. Similar concerns have been documented in previous studies, such as by Štěpánek *et al.* (2011) who encountered problems with stations in Churanov, central Europe, where altitudes were as much as 877m higher than that of neighbour stations. In addition, using distant and less correlated stations may result in the reference series not reflecting the true climatic signal of the candidate station (Costa and Soares, 2009). This is a specific concern to South African climate data given the scarcity of stations with long temporal data sets.

3.4.2. Homogeneity testing

Relative homogenization (i.e. change point detected with a composite homogeneous reference series) was performed by AnClim and ProClimDB software (Štěpánek *et al.*, 2011, 2013) (Table 3.2 and Figure 3.3). According to the station history, the SA Astronomical Observatory changed from a second to third order station on 1st January 1940 (i.e. a change in reporting of T_{max} and T_{min} at 8 am and 2 pm to only 8 am). Although the change in station order does not indicate a change in the time of observation (which could result in a change point in the time series), it is possible that a change in data recording may have resulted in the 1941 change point, detected by the relative homogeneity tests (Table 3.2). Notably, the statistical detection of change points does not always correspond to the exact change period when the bias occurred.

Table 3.2: Change points detected using both Standard Normal Homogeneity Test (SNHT) and Bivariate tests in AnClim software for mean monthly T_{max} and T_{min}, Western Cape.

Station name		**T_{max}**		**T_{min}**	
	Date of conversion to Automatic weather station	**Month and year of change point**	**Average change (°C)[a]**	**Month year of change point**	**Average change (°C)[a]**
Cape Agulhas	01/10/2006	04/1932	0.6	06/1988	0.4
		01/1957	0.8	08/1993	0.3
		01/1972	0.4	10/2004	0.7
		07/1985	0.5		
		02/1997	0.7		
		08/2008	-0.7		
SA Astron. Observ.	01/12/2009		-1.0	**05/1959**	0.5
		10/1941			
		12/1970	1.2		
		02/2004	-0.3		
Cape Point	01/11/2013	08/1927	-1.0	08/1926	0.9
		04/1971	0.3	**02/1950**	-1.0
		10/2006	-1.0	01/1971	0.4
Cape Columbine	01/10/2007	02/1948	0.3	01/1951	0.5
		05/1962	0.7	01/1964	0.5
		01/1972	0.7	08/1982	0.7
		09/1992	0.7	02/1988	0.8
				08/1996	0.9
				09/2007	0.8
Jonkershoek	Not available	01/1959	1.4	07/1963	-0.9
		07/1964	0.6		
		02/1971	0.5		
		02/2004	1.4		
Kirstenbosch	Not available	11/1949	0.7	04/1927	-0.5
		05/1972	0.7	05/1948	0.2
		01/1982	0.4	03/1957	0.5
		07/1998	0.4	10/1970	0.3
				07/1998	0.5
Langgewens	01/08/2008	03/1964	-1.0	03/1965	0.6
		02/1991	0.5	04/1970	0.8
				05/1997	0.8
Cape St Blaize	Not available	02/1935	-0.2	**06/1934**	0.4
		03/1944	-0.7	10/1956	-0.6
		03/1953	-0.2	10/1967	-0.4
		02/1971	0.3	06/1988	-0.4
		08/1997	0.3	09/1994	-0.4

a: The average temperature adjustment per month in the given year.

Bold values denote change point confirmed with station history.

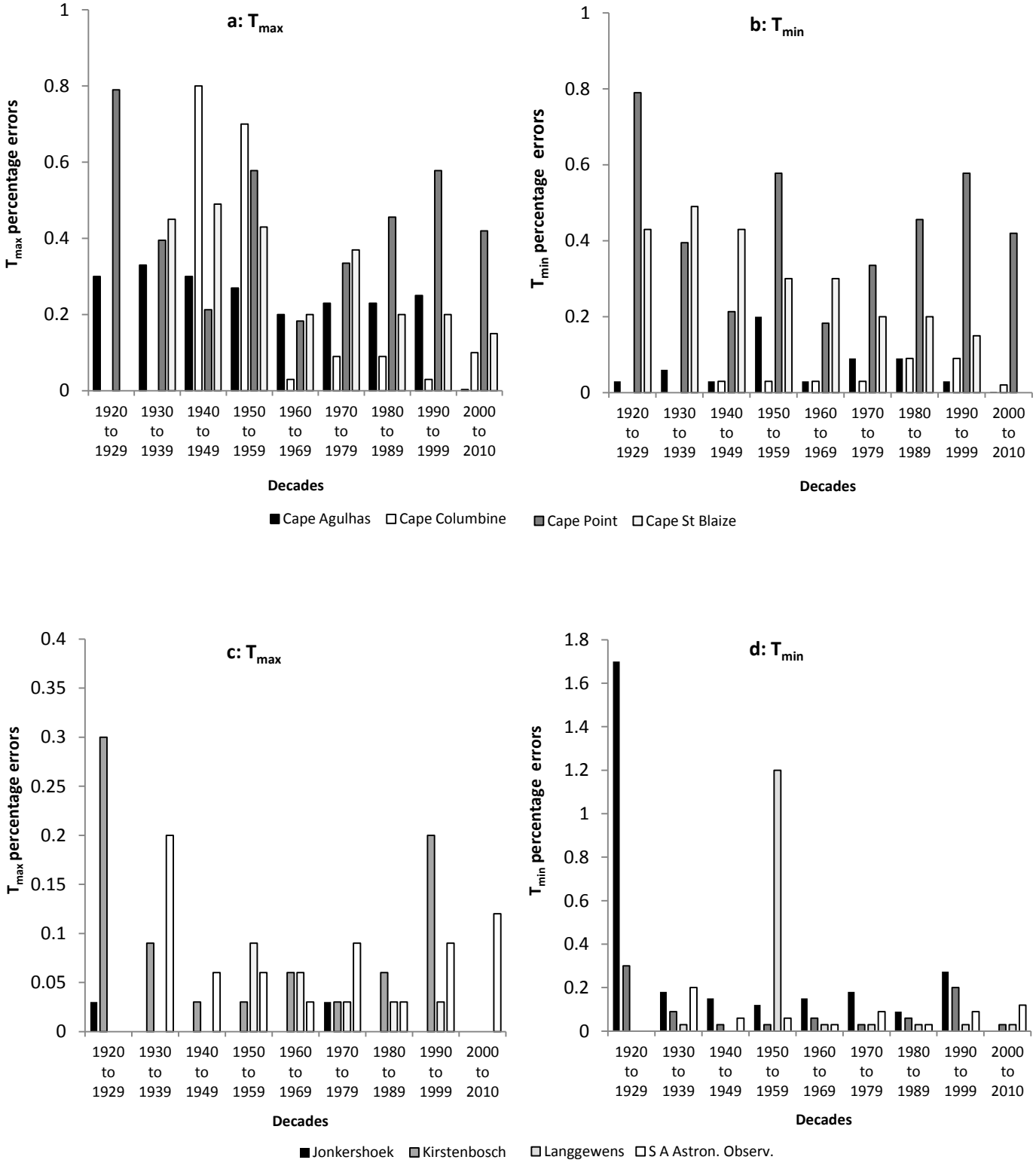

Figure 3.2: Percentage errors for T_{max} and T_{min} at eight stations (Cape Agulhas, SA Astronomical Observatory, Cape Columbine, Kirstenbosch, Jonkershoek, Cape St Blaize, Cape Point and Langgewens), Western Cape. * T_{max} and T_{min} percentage errors for 1940-1949 at Langgewens were omitted from the graph as the high percentage (11%) masked the smaller percentage errors.

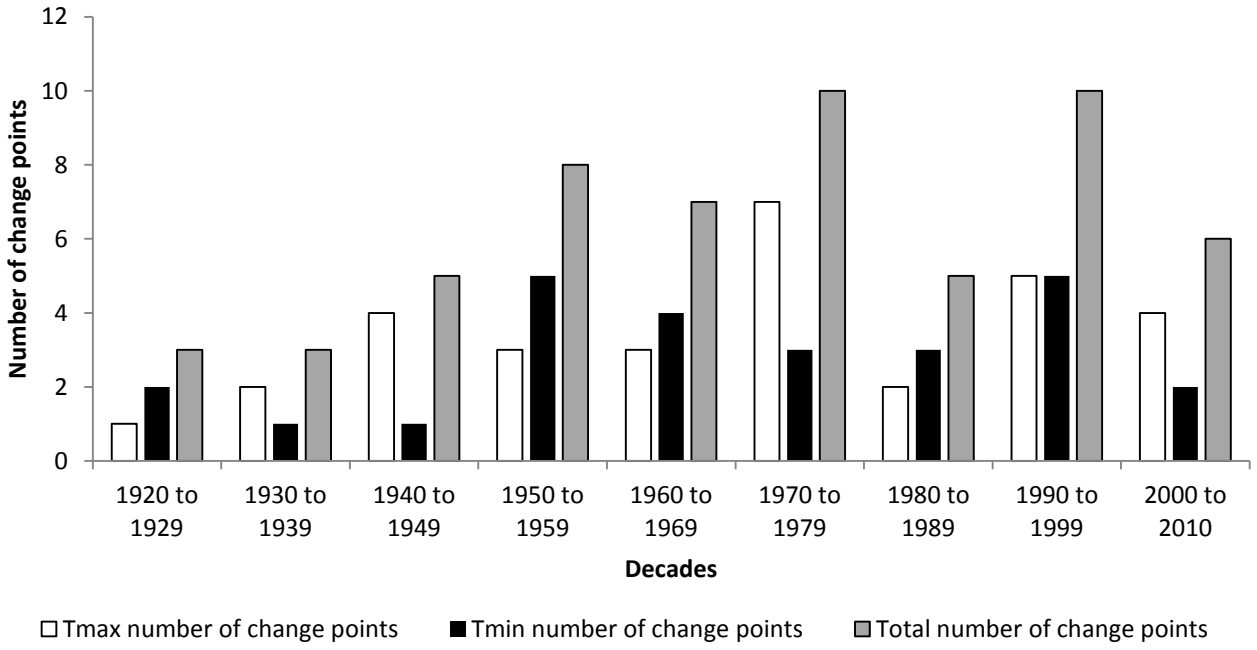

Figure 3.3: T_{max}, T_{min} and total number of change points per decade for the eight stations (Cape Agulhas, SA Astronomical Observatory, Cape Columbine, Kirstenbosch, Jonkershoek, Cape St Blaize, Cape Point and Langgewens), Western Cape (see Table 3.2).

Changes in temperature measurement can lead to bias in individual station records (Williams *et al*., 2012). The Department of Transport and South African Weather Bureau Meteorological Office reports indicate that in 1948, South African observations changed from 8:30 am and 3:00 pm to 8 am and 2:00 pm respectively, in accordance with the International Meteorological Organization (Department of Transport, South Africa Weather Bureau, 1948, pp iii). This was taken into account when selecting the change points for adjustment. According to the Department of Transport, South Africa Weather Bureau, South African observers did not always strictly keep to the observation times, thus causing further bias in the records over time. The Department of Transport and South African Weather Bureau Meteorological Office Reports reveal that Cape St Blaize, Cape Point and Cape Agulhas became 1st order stations in March 1959, April 1959 and 1 January 1956 respectively. In addition, the Cape Agulhas station was moved 18.3 m and 6 m higher from its former locality in January 1956. In South Africa, when stations became automatic, the frequency of observations changed to hourly. With Langgewens being a 3rd order station before having changed to an automatic station, T_{max} and T_{min} readings were taken at 8 am only. These

biases are not always detected by statistical tests at the exact time of occurrence, possibly due to poor correlation coefficients between neighbour stations. In addition, there is much uncertainty associated with the sole use of statistical homogeneity detection (Štěpánek *et al*., 2013). The average correlation calculated from all stations is 0.68 in the case of T_{max} and 0.64 in the case of T_{min}, indicating that T_{max} has a stronger spatial relationship (Tables 3.4 and 3.5).

3.4.3. Trend analysis

The adjusted and unadjusted annual temperature data were plotted to visualise the impact of homogenization on long-term trends (Figure 3.4). When the dotted line appears above the solid line, the original temperature data have been adjusted to lower values, thus establishing the adjusted time series. Monthly adjustments were applied to the period before the detected change point so as to correspond with the most recent homogeneous period of the time series. Adjustments were made utilizing a reference series (using ProClim software), thus the poor correlation between the base station and the reference series mainly contributed toward the inconsistent offsets visible in the graphs. In addition, some of the stations have a greater number of missing daily temperature data for the period 1930-1960. For example, T_{max} at Cape Agulhas has 30 days of missing data for 1925. With the assumption that the reference series contains a greater number of days for the specific year, the resultant adjusted data point will not exactly match the Cape Agulhas annual unadjusted T_{max}. The T_{max} scatter plot indicates decreasing correlation coefficients with increasing distance between stations (Figure 3.5a and Table 3.3), however, T_{min} does not display such a pattern (Figure 3.5b and Table 3.4). Removing the less correlated neighbour stations has subsequently helped with the production of a more accurate series. Annual T_{max} and T_{min} trends (Tables 3.6 and 3.7) do not change in direction after adjustment, with the exception of T_{min} at Jonkershoek (Figure 3.4(h)). This result is in agreement with that by Kenawy *et al*. (2013) from northeastern Spain, where only a small percentage of trends changed from an increasing (or decreasing) to a decreasing (or increasing) trend after homogenization. Temperature trends in our study change from a gentle to steeper increasing tendency. For instance, T_{max} adjusted annual data for Langgewens display a steeper temperature increase with time (0.16°C/decade), compared to that using unadjusted data (0.06°C/decade), yet the climate signal is retained (Figure 3.4(m)). This study also examined temperature trends for the period 1937-2001 in order to compare trends between stations for a common period (see Table 3.7).

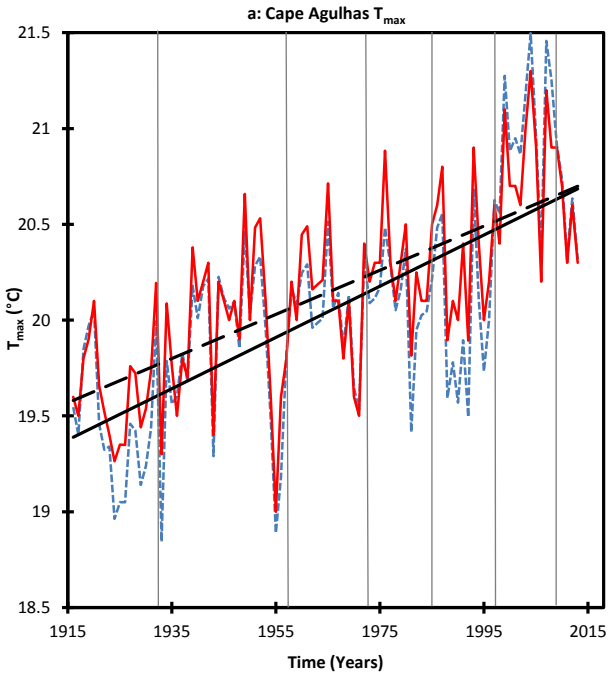

Unadjusted y = 0.0115x - 2.5152 Adjusted y = 0.0134x - 6.2358

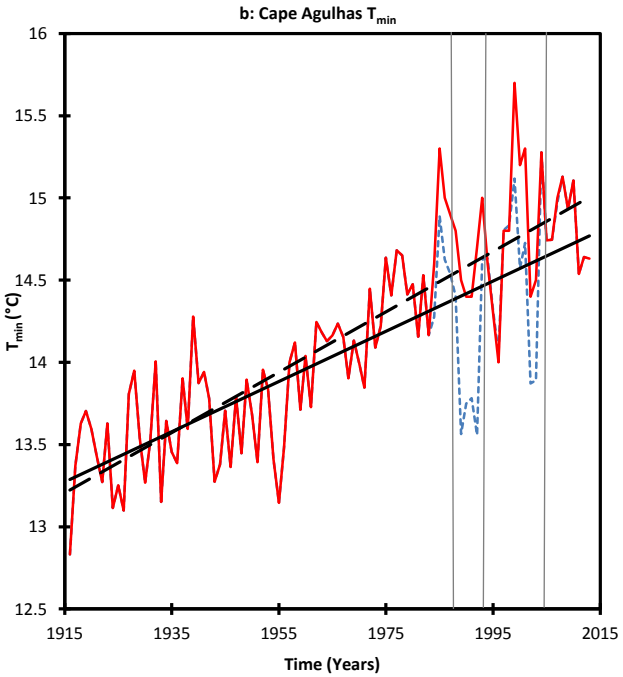

Unadjusted y = 0.0184x - 21.982 Adjusted y = 0.0153x - 16.014

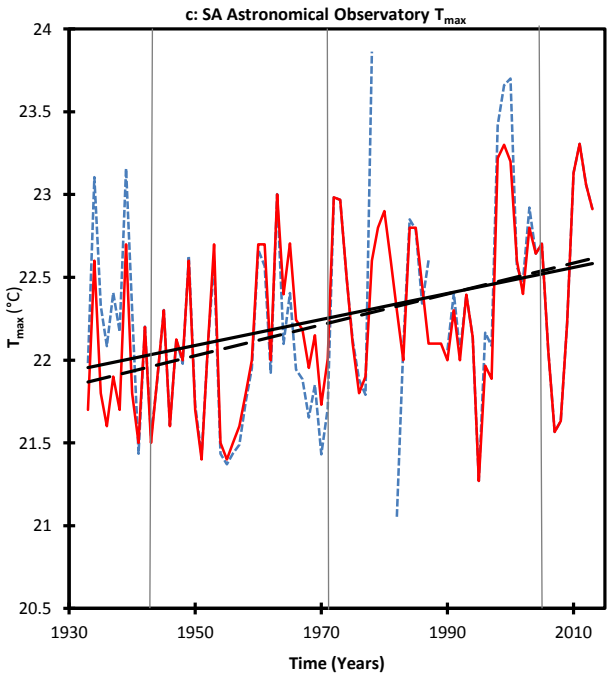

Unadjusted y = 0.0079x + 6.7589 Adjusted y = 0.0093x + 3.8675

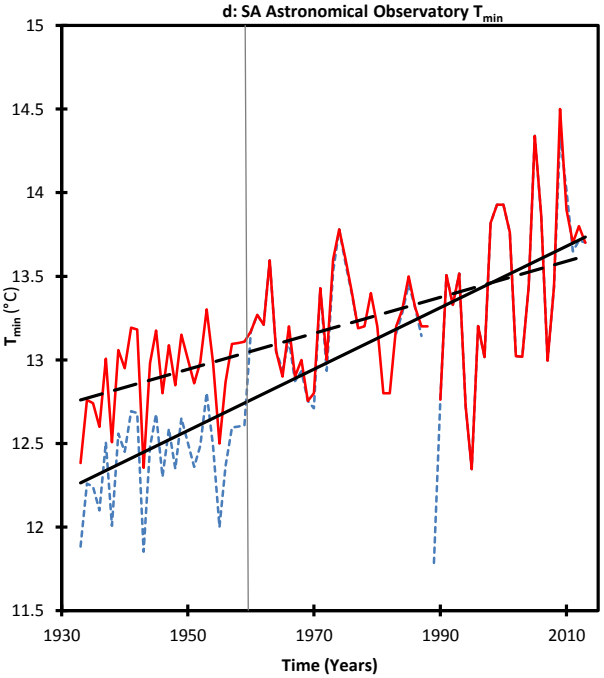

Unadjusted y = 0.0184x - 23.233 Adjusted y = 0.0108x - 8.0737

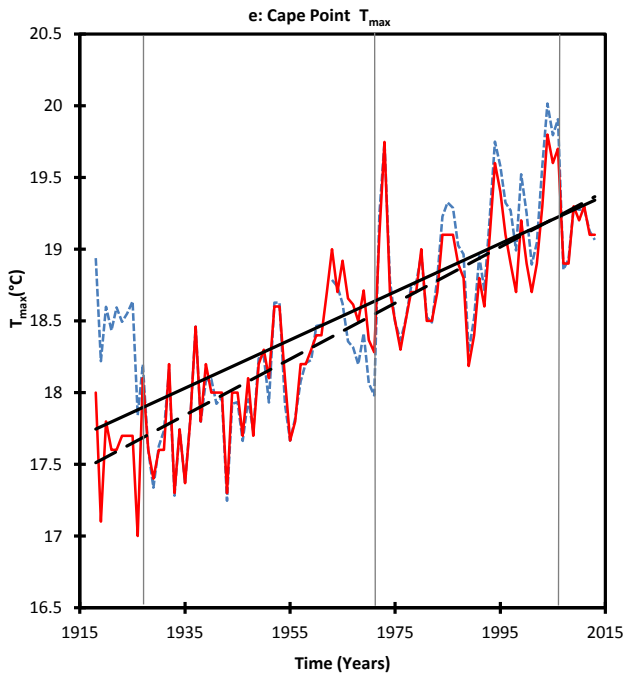

Unadjusted y = 0.0168x - 14.449 Adjusted y = 0.0195x - 19.931

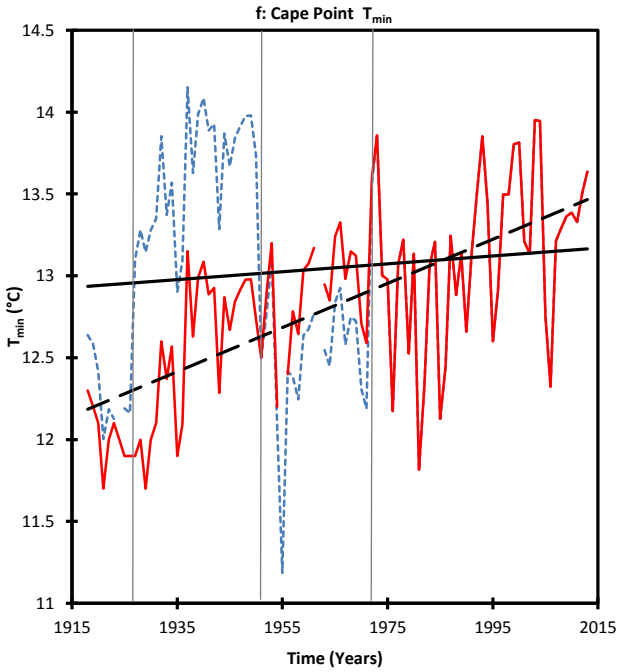

Unadjusted y = 0.0024x + 8.3311 Adjusted y = 0.0135x - 13.638

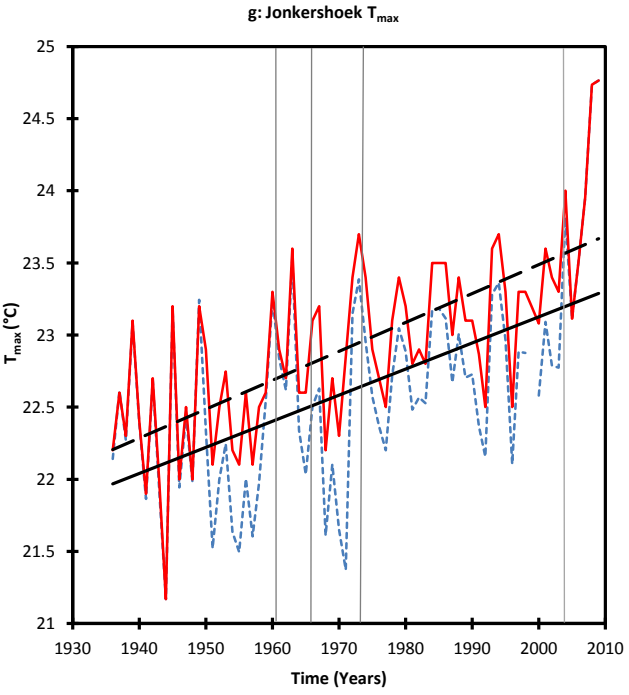

Unadjusted: y = 0.0181x - 13.018 Adjusted y = 0.0201x - 16.62

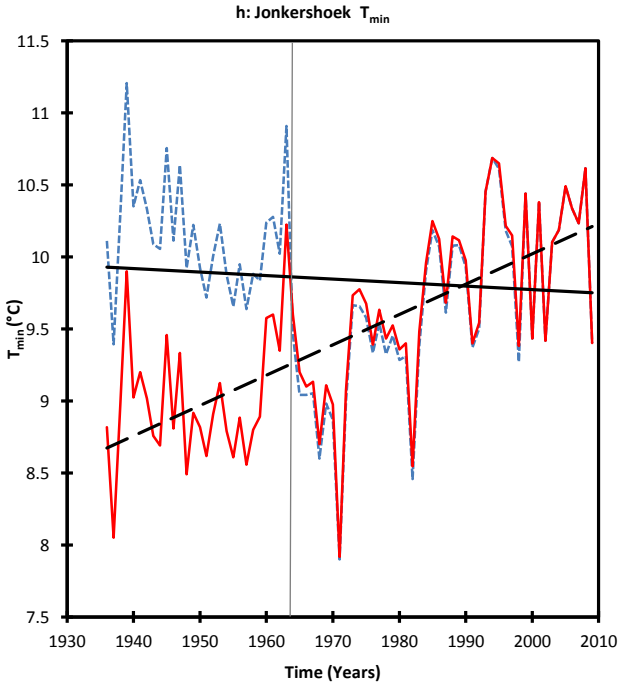

Unadjusted y = -0.03x + 14.662 Adjusted y = 0.241x - 38.154

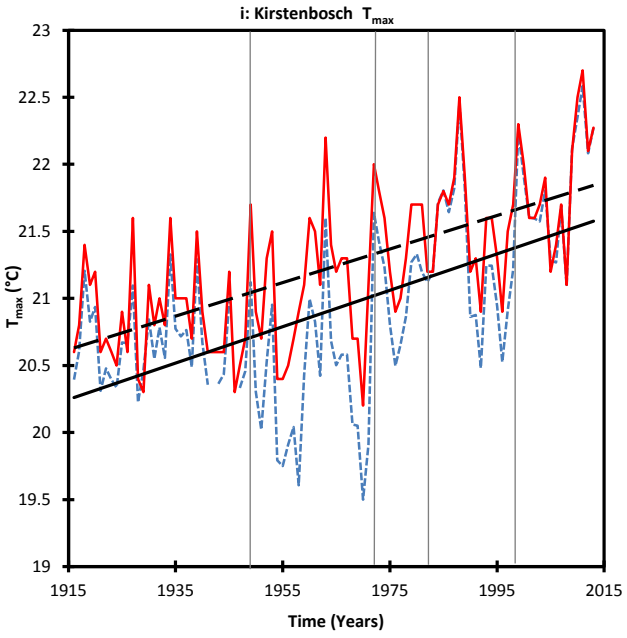

Unadjusted y = 0.0136x - 5.7197 Adjusted y = 0.0125x - 3.3378

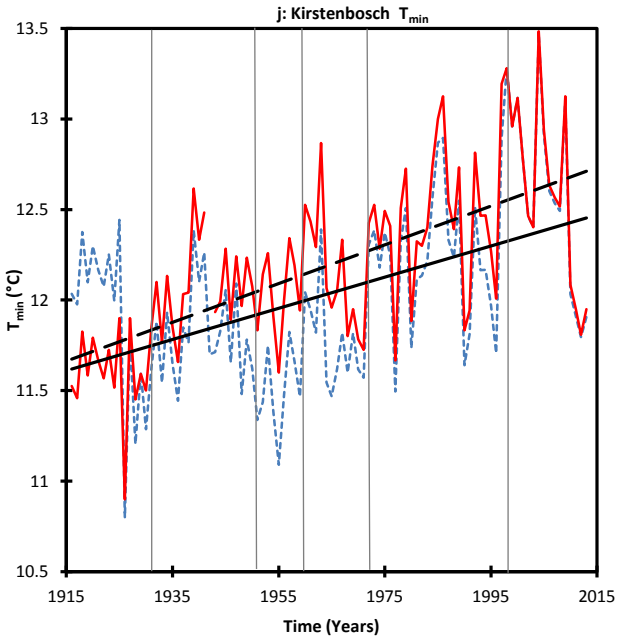

Unadjusted y = 0.0086x - 4.8338 Adjusted y = 0.0107x - 8.8275

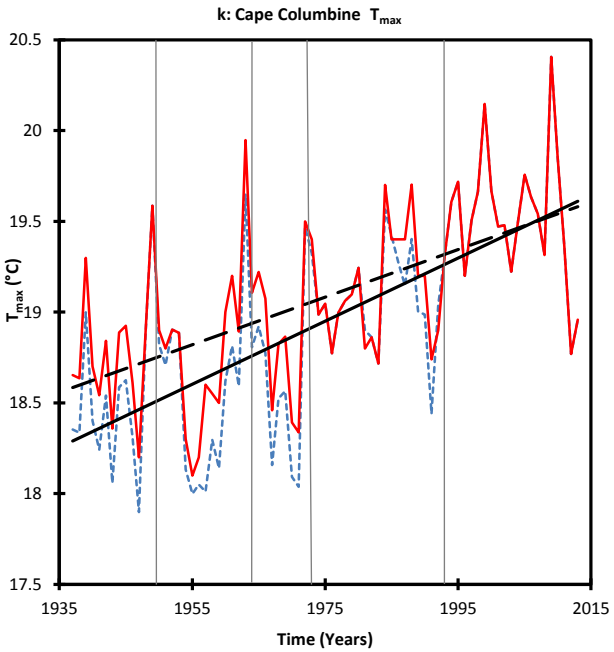

Unadjusted y = 0.0174x - 15.369 Adjusted y = 0.0131x - 6.8144

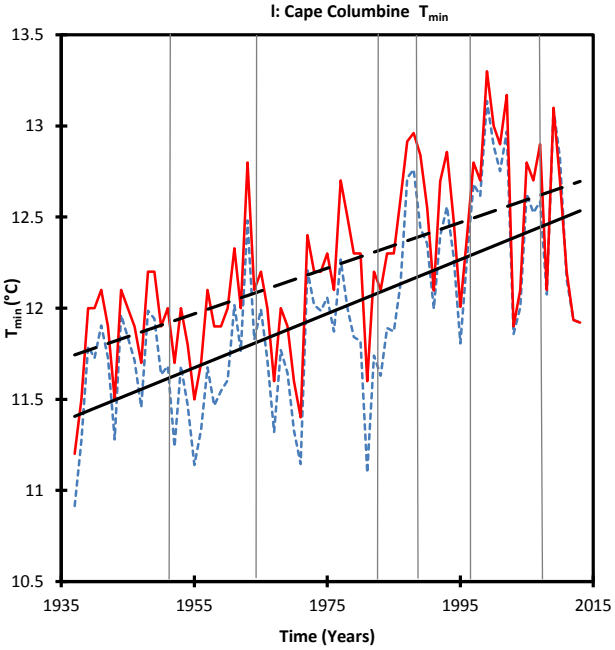

Unadjusted y = 0.0148x - 17.323 Adjusted y = 0.0125x - 12.524

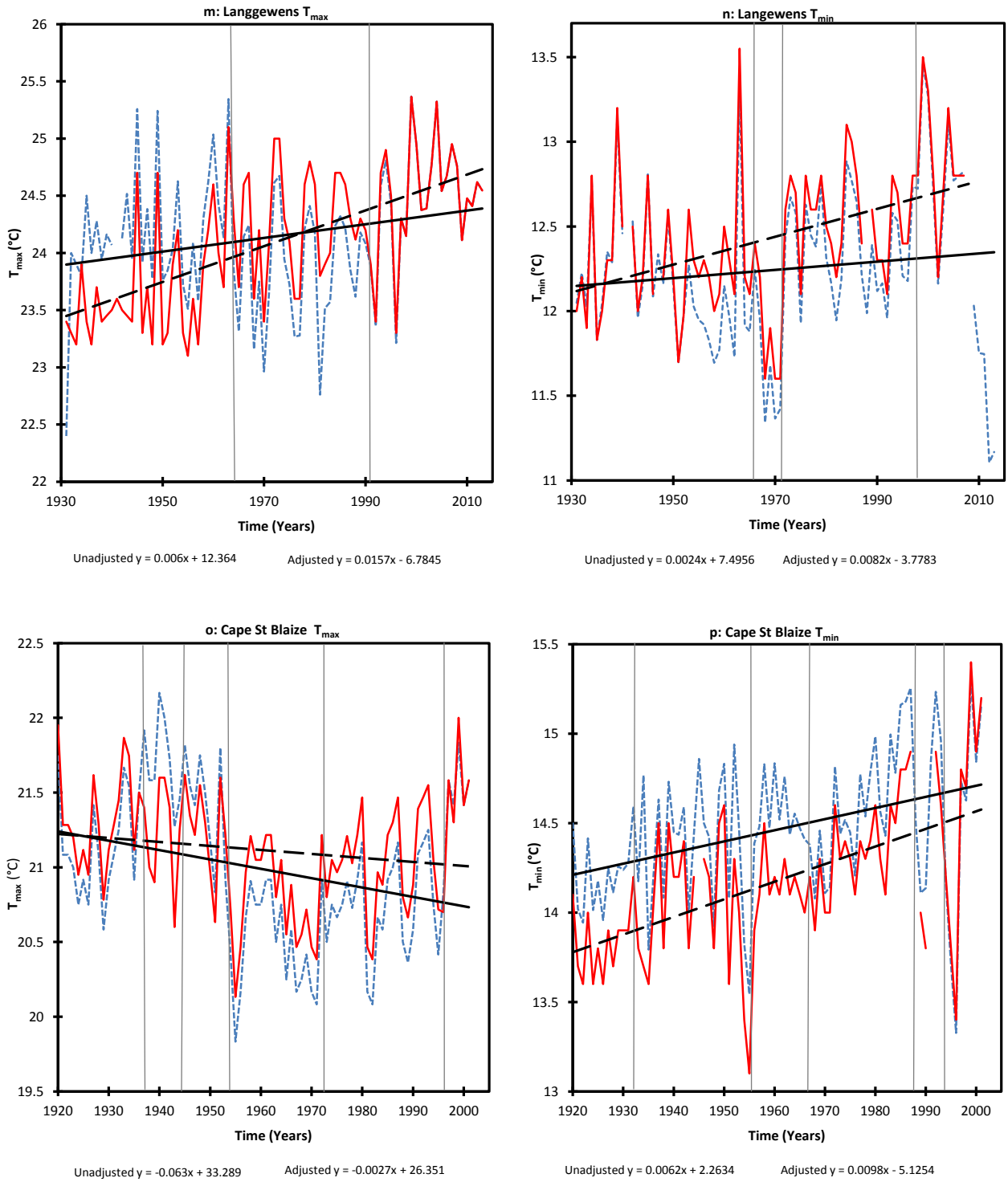

Figure 3.4: Annual T_{max} and T_{min} unadjusted (square dotted line) and adjusted (solid line) trends using ProClimDB software for eight Western Cape stations. The gray vertical lines indicate years of detected change points using SNHT and Bivariate tests in AnClim (see also Table 3.3). The unadjusted linear trend lines (dashed lines) and adjusted linear trend lines (solid lines), with linear equations in the legends, represent temperature changes over the respective time periods (i.e., x (years) and y (T_{min}/T_{max})).

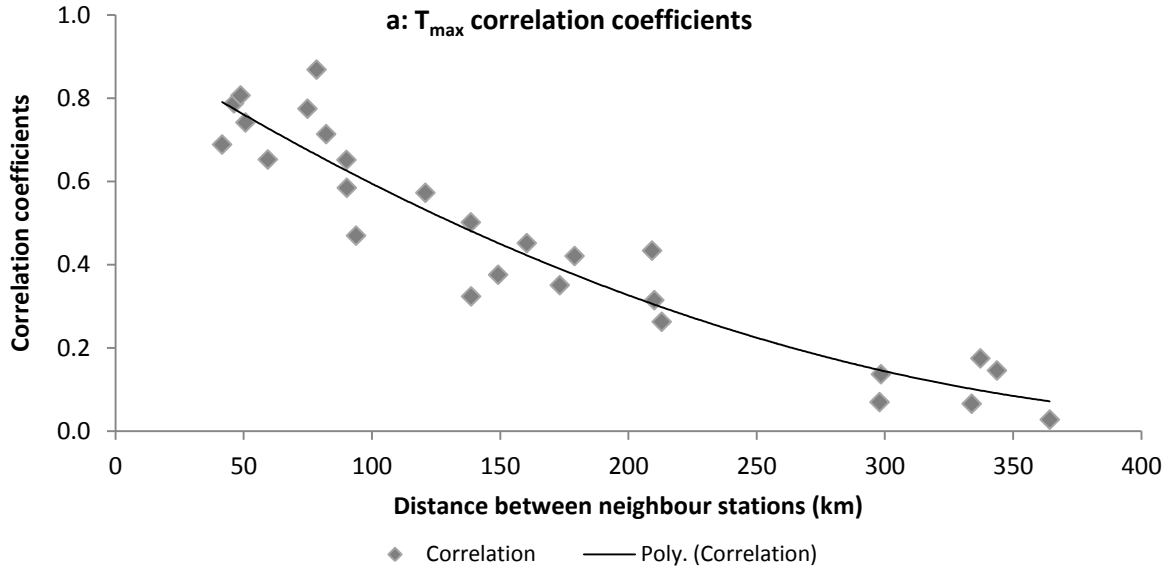

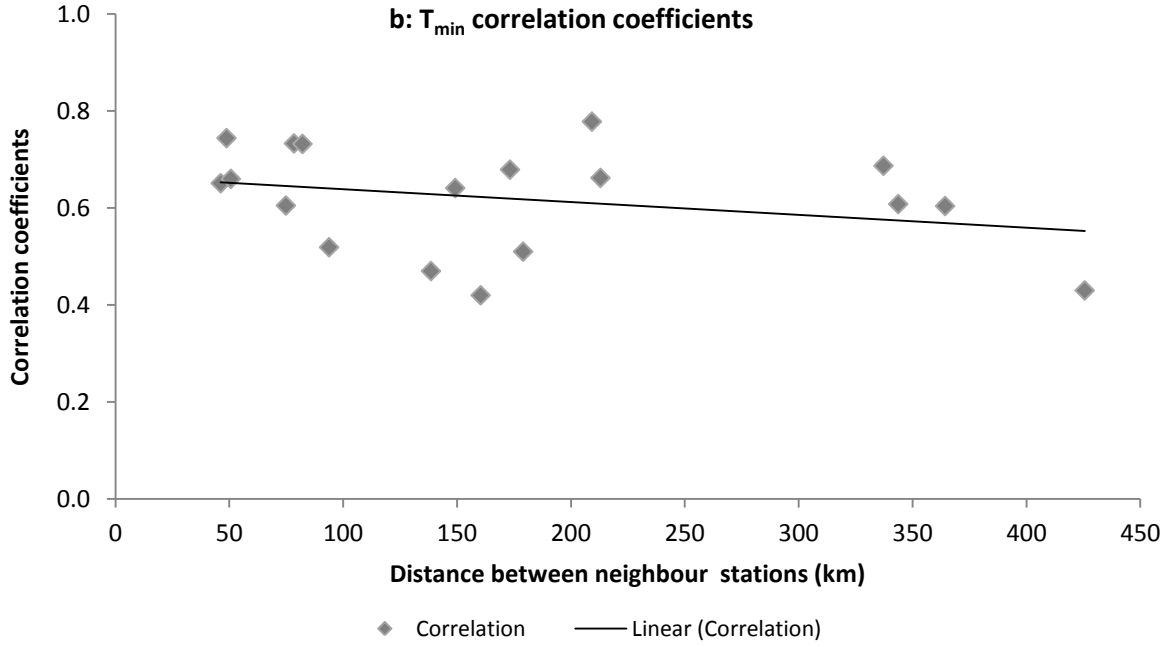

Figure 3.5: Scatter plot based on correlation and distance between the eight stations (Cape Agulhas, SA Astronomical Observatory, Cape Columbine, Kirstenbosch, Jonkershoek, Cape St Blaize, Cape Point and Langgewens), Western Cape. T_{min} plot does not include the stations with low correlation coefficients (see Tables 3.4 and 3.5).

Table 3.3: T_{max} correlation coefficients and distances between neighbour stations, Western Cape. Stations in gray shading were excluded due to low correlation coefficients (being <0.6) with the base station. Alt_1 = altitude of the base station (meters above sea level (m a.s.l.)); Alt_2 = altitude of the neighbour station (meters above sea level); Dist=Distance (km); Correl.=Pearson correlation coefficient.

Base station	Neighbour station	Begin	End	Dist. (km)	Alt_1 (m a.s.l.)	Alt_2 (m a.s.l.)	Correl.
SA Astron. Observ.	SA Astron. Observ.	1933/01/02	2013/12/31		15		
	Kirstenbosch	1916/01/01	2013/12/31	48.77	15	89	0.807
	Jonkershoek	1936/01/01	2009/12/31	74.84	15	239	0.775
	Langgewens	1931/01/01	2013/12/31	50.67	15	179	0.742
	Cape Point	1918/01/01	2013/12/31	90.05	15	228	0.652
	Cape Columbine	1937/01/01	2013/12/31	90.19	15	62	0.585
	Cape Agulhas	1916/01/01	2013/12/31	212.97	15	11	0.263
	Cape St Blaize	1920/01/01	2001/12/30	364.27	15	60	0.028
Cape Agulhas	Cape Agulhas	1916/01/01	2013/12/31		11		
	Cape St Blaize	1920/01/01	2001/12/30	209.21	11	60	0.434
	Cape Point	1918/01/01	2013/12/31	149.19	11	228	0.376
	Kirstenbosch	1916/01/01	2013/12/31	173.23	11	89	0.351
	Jonkershoek	1936/01/01	2009/12/31	138.64	11	239	0.324
	Langgewens	1931/01/01	2013/12/31	210.10	11	179	0.315
	SA Astron. Obs.	1933/01/02	2013/12/31	212.97	11	15	0.263
	Cape Columbine	1937/01/01	2013/12/31	298.46	11	62	0.137
Cape Columbine	Cape Columbine	1937/01/01	2013/12/31		62		
	SA Astron. Obs.	1933/01/02	2013/12/31	90.19	62	15	0.585
	Kirstenbosch	1916/01/01	2013/12/31	138.54	62	89	0.502
	Langgewens	1931/01/01	2013/12/31	93.80	62	179	0.470
	Jonkershoek	1936/01/01	2009/12/31	160.35	62	239	0.452
	Cape Point	1918/01/01	2013/12/31	179.00	62	228	0.421
	Cape Agulhas	1916/01/01	2013/12/31	298.46	62	11	0.137
Jonkershoek	Jonkershoek	1936/01/01	2009/12/31		239		
	Langgewens	1931/01/01	2013/12/31	78.39	239	179	0.869
	Kirstenbosch	1916/01/01	2013/12/31	46.21	239	89	0.788
	SA Astron. Obs.	1933/01/02	2013/12/31	74.84	239	15	0.775
	Cape Point	1918/01/01	2013/12/31	59.39	239	228	0.653
	Cape Columbine	1937/01/01	2013/12/31	160.35	239	62	0.452
	Cape Agulhas	1916/01/01	2013/12/31	138.64	239	11	0.324
	Cape St Blaize	1920/01/01	2001/12/30	297.91	239	60	0.070
Kirstenbosch	Kirstenbosch	1916/01/01	2013/12/31		89		
	SA Astron. Obs.	1933/01/02	2013/12/31	48.77	89	15	0.807
	Jonkershoek	1936/01/01	2009/12/31	46.21	89	239	0.788
	Langgewens	1931/01/01	2013/12/31	82.13	89	179	0.714
	Cape Point	1918/01/01	2013/12/31	41.56	89	228	0.689
	Cape Columbine	1937/01/01	2013/12/31	138.54	89	62	0.502

	Cape Agulhas	1916/01/01	2013/12/31	173.23	89	11	0.351
	Cape St Blaize	1920/01/01	2001/12/30	343.68	89	60	0.146
Langgewens	Langgewens	1931/01/01	2013/12/31		179		
	Jonkershoek	1936/01/01	2009/12/31	78.39	179	239	0.869
	SA Astron. Obs.	1933/01/02	2013/12/31	50.67	179	15	0.742
	Kirstenbosch	1916/01/01	2013/12/31	82.13	179	89	0.714
	Cape Point	1918/01/01	2013/12/31	120.83	179	228	0.573
	Cape Columbine	1937/01/01	2013/12/31	93.80	179	62	0.470
	Cape Agulhas	1916/01/01	2013/12/31	210.10	179	11	0.315
	Cape St Blaize	1920/01/01	2001/12/30	333.83	179	60	0.066
Cape Point	Cape Point	1918/01/01	2013/12/31		228		
	Kirstenbosch	1916/01/01	2013/12/31	41.56	228	89	0.689
	Jonkershoek	1936/01/01	2009/12/31	59.39	228	239	0.653
	SA Astron. Obs.	1933/01/02	2013/12/31	90.05	228	15	0.652
	Langgewens	1931/01/01	2013/12/31	120.83	228	179	0.573
	Cape Columbine	1937/01/01	2013/12/31	179.00	228	62	0.421
	Cape Agulhas	1916/01/01	2013/12/31	149.19	228	11	0.376
	Cape St Blaize	1920/01/01	2001/12/30	337.22	228	60	0.175
Cape St Blaize	Cape St Blaize	1920/01/01	2001/12/30		60		
	Cape Agulhas	1916/01/01	2013/12/31	209.21	60	11	0.434
	Cape Point	1918/01/01	2013/12/31	337.22	60	228	0.175
	Kirstenbosch	1916/01/01	2013/12/31	343.68	60	89	0.146
	Jonkershoek	1936/01/01	2009/12/31	297.91	60	239	0.070
	Langgewens	1931/01/01	2013/12/31	333.83	60	179	0.066
	SA Astron. Obs.	1933/01/02	2013/12/31	364.27	60	15	0.028

T_{min} at Langgewens decreases from 2008 to the end of the time series (Figure 3.4(n)), possibly associated with the change to automatic data recording. The time series could not be adjusted for this inhomogeneity, as it is too close to the end of the recording period. However, T_{max} at Langgewens station does not indicate cooling after 2008 (Figure 3.4(m)). Conversion to automatic data recording may produce variable temperature responses, depending on site-specific parameters and conditions; for instance across the USA, T_{max} and T_{min} records yielded lower values in response to such a conversion (Williams *et al*., 2012).

Table 3.4: T_{min} correlation coefficients and distances between neighbour stations, Western Cape. Alt_1 = altitude of the base station (meters above sea level (m a.s.l.)); Alt_2 = altitude of the neighbour station (m a.s.l.); Correl.= Pearson correlation coefficient (threshold value for correlation coefficient >0.6); Dist=Distance (km).

Base station	Neighbour station	Begin	End	Dist. (km)	Alt_1 (m a.s.l.)	Alt_2 (m a.s.l.)	Correl. T_{min}
Cape Agulhas	Cape Agulhas_1_c	1916	2013		11		
	Cape St Blaize	1920	2001	209.21	11	60	0.778
	Kirstenbosch	1916	2013	173.23	11	89	0.679
	SA Astron. Obs.	1933	2013	212.97	11	15	0.662
	Cape Point	1918	2013	149.19	11	228	0.641
SA Astron. Obs.	SA Astron. Obs._1_c	1933	2013		15		
	Kirstenbosch	1916	2013	48.77	15	89	0.744
	Cape Agulhas	1916	2013	212.97	15	11	0.662
	Langgewens	1931	2013	50.67	15	179	0.660
	Jonkershoek	1936	2009	74.84	15	239	0.605
	Cape St Blaize	1920	2001	364.27	15	60	0.604
Cape Columbine	Cape Columbine_1_c	1937	2013		62		
	Langgewens	1931	2013	93.80	62	179	0.519
	Kirstenbosch	1916	2013	138.54	62	89	0.470
	Jonkershoek	1936	2009	160.35	62	239	0.420
	Cape Point	1918	2013	179.00	62	228	0.510
Jonkershoek	Jonkershoek_1_c	1936	2009		239		
	Langgewens	1931	2013	78.39	239	179	0.733
	Kirstenbosch	1916	2013	46.21	239	89	0.651
	SA Astron. Obs.	1933	2013	74.84	239	15	0.605
Kirstenbosch	Kirstenbosch_1_c	1916	2013		89		
	SA Astron. Obs.	1933	2013	48.77	89	15	0.744
	Langgewens	1931	2013	82.13	89	179	0.732
	Cape Agulhas	1916	2013	173.23	89	11	0.679
	Jonkershoek	1936	2009	46.21	89	239	0.651
	Cape St Blaize	1920	2001	343.68	89	60	0.608
Langgewens	Langgewens_1_c	1931	2013		179		
	Jonkershoek	1936	2009	78.39	179	239	0.733
	Kirstenbosch	1916	2013	82.13	179	89	0.732
	SA Astron. Obs.	1933	2013	50.67	179	15	0.660
Cape Point	Cape Point_1_c	1918	2013		228		
	Cape St Blaize	1920	2001	337.22	228	60	0.687
	Cape Agulhas	1916	2013	149.19	228	11	0.641
Cape St Blaize	Cape St Blaize_1_c	1920	2001		60		
	Cape Agulhas	1916	2013	209.21	60	11	0.778
	Cape Point	1918	2013	337.22	60	228	0.687
	Kirstenbosch	1916	2013	343.68	60	89	0.608
	SA Astron. Obs.	1933	2013	364.27	60	15	0.604

Table 3.5: Mann Kendall statistics and Sen's slope estimate (Q) (°C/decade) for annual T_{max} at all stations in the Western Cape region before and after adjustment. The Mann Kendall test statistic (S) = the strength of the temperature trend and the sign indicates whether the trend is increasing or decreasing. The Z test statistic = statistical significance of the trend, calculated from the variance of S (Var(S)). When the p value is lower than the chosen significance level, alpha=0.05, the null hypothesis (H_0, i.e. no trend in the series) is rejected and the alternative hypothesis (Ha, i.e. there is a trend) is accepted (XLStat, 2015).

Station	**Unadjusted data**				**Adjusted data**			
	S	**Var(S)**	**Z[a]**	**Q**	**S**	**Var(S)**	**Z[a]**	**Q**
Cape Agulhas 1916-2013	2259	42685	**10.94**	**0.13**	2725	25890	**16.92**	**0.14**
Cape Point 1918-2013	2433	80948	**8.55**	**0.18**	3225	13975	**27.27**	**0.20**
Cape Columb. 1937-2013	1476	10798	**14.19**	**0.17**	1560	7793	**18.58**	**0.15**
Cape St Blaize 1920-2001	-591	77249	**-2.13**	**-0.06**	-343	55404	-1.46	-0.02
SA Astron. Obs. 1933-2013	535	9734	**5.41**	**0.08**	1303	7309	**15.23**	**0.13**
Jonkershoek 1936-2009	1004	17323	**7.62**	**0.17**	1334	7844	**15.05**	**0.18**
Kirstenbosch 1916-2013	1820	127514	0.13	0.07	2109	29133	**12.30**	**0.13**
Langgewens 1931-2013	506	40124	**2.52**	**0.01**	1448	9687	**14.70**	**0.16**

a. If $Z>Z_{1-\alpha/2}$, at the chosen level of significance alpha=0.05%, where Z greater than 1.96, the trend is significant. All Z values were rounded off to 2 decimal places.

Bold values show significant trends.

Table 3.6: Mann Kendall statistics and Sen's slope estimate (Q) (°C/decade) for annual T_{min} at all stations in the Western Cape region before and after adjustment. The Mann Kendall test statistic (S) = the strength of the temperature trend and the sign indicates whether the trend is increasing or decreasing. Var(S) = variance of S. When the p value is lower than the chosen significance level, alpha=0.05, the null hypothesis (H_0, i.e. no trend in the series) is rejected and the alternative hypothesis (Ha, i.e. there is a trend) is accepted (XLStat, 2015).

Station	**Unadjusted data**				**Adjusted data**			
	S	**Var(S)**	**Z**	**Q**	**S**	**Var(S)**	**Z**	**Q**
Cape Agulhas 1937-2013	4784	209042	**10.40**	**0.12**	1759	27299	**10.64**	**0.16**
Cape Point 1918-2013	445	99190	1.42	0.04	2810	15087	**22.90**	**0.17**
Cape Colum. 1937-2013	1396	17396	**10.57**	**0.15**	1249	6246	**15.79**	**0.11**
SA Astron. Obs. 1933-2013	1608	10403	**15.76**	**0.20**	845	73060	**15.75**	**0.07**
Jonkershoek 1936-2009	-163	66722	-0.03	-0.03	1451	16606	1.01	0.23
Langgewens 1931-2013	269	25908	0.02	0.02	837	20996	**5.77**	**0.07**
Kirstenbosch 1916-2013	1390	107003	**4.25**	**0.08**	2591	8480	**3.21**	**0.28**
Cape St Blaize 1920-2001	967	13420	**8.34**	**0.08**	1268	11181	**12.00**	**0.04**

a. If $Z>Z_{1-\alpha/2}$, at the chosen level of significance alpha=0.05%, where Z greater than 1.96, the trend is significant. All Z values were rounded off to 2 decimal places.

Table 3.7: Sen's slope estimate (Q) (°C/decade) for annual T_{max} and T_{min} at all stations in the Western Cape region, for the common period 1937-2001 after adjustment.

Station	**T_{max}**	**T_{min}**
Cape Agulhas	**0.10**	**0.09**
Cape Point	**0.18**	**0.14**
Cape Columbine	**0.17**	**0.13**
SA Astronomical Obs.	**0.12**	**0.11**
Jonkershoek	**0.15**	**0.23**
Langgewens	**0.16**	**0.07**
Kirstenbosch	**0.16**	**0.08**
Cape St Blaize	0.00	**0.09**
Mean	0.13	0.12

Bold values are significant trends.

Table 3.8: Seasonal Mann Kendall statistics and Sen's slope estimates (Q) (°C /decade) for adjusted T_{max} and T_{min} values for the Western Cape region.

Station	Maximum temperature				Minimum temperature			
	Summer	**Autumn**	**Winter**	**Spring**	**Summer**	**Autumn**	**Winter**	**Spring**
Cape Agulhas 1916-2013								
S	1893	1461	1257	1732	1277	1360	1266	1461
Var(S)	23532	24187	40481.2	46722	25637	31625	24858	6648
Q[a]	**0.13**	**0.10**	**0.07**	**0.11**	**0.07**	**0.07**	**0.09**	**0.09**
Z	**6.7**	**9.4**	**6.3**	**8.0**	**8.0**	**7.7**	**8.0**	**17.9**
Cape Point 1918-2013								
S	1519	1046	1218	1086	2118	2281	2002	2077
Var(S)	94671	85254	16766	80516	6640	11994	12929	16248
Q[a]	**0.14**	**0.09**	**0.11**	**0.07**	**0.18**	**0.19**	**0.16**	**0.16**
Z	**4.9**	**3.6**	**9.4**	**3.8**	**26**	**20.8**	**17.6**	**16.3**
Kirstenbosch 1916-2013								
S	-346.0	-104.0	482	671.0	1740	1513	1335	1493
Var(S)	26094.3	38797.4	10219.9	9337	15960	30958	26225	10867.5
Q	**-0.03**	0.00	**0.04**	**0.06**	**0.10**	**0.10**	**0.11**	**0.10**
Z	**-2.2**	-0.5	**3.4**	**7.0**	**13.8**	**8.6**	**8.2**	**14.3**
Jonkershoek 1936-2009								
S	882	965	193	720.00	1074	1209	680	1111
Var(S)	3315	9086	6753	3279	34411	199446	23779	4389
Q[a]	**0.24**	**0.22**	**0.04**	**0.19**	**0.29**	**0.24**	**0.13**	**0.27**
Z	**15.3**	**10.1**	**10.1**	**12.6**	**5.8**	**8.7**	**4.4**	**16.8**
Langgewens 1931 -2013								
S	864	1465	538	812	787	1035	535	623
Var(S)	35421	8088	11468	3804	18810	11894	11090	5519
Q[a]	**0.20**	**0.29**	**0.11**	**0.16**	**0.11**	**0.13**	**0.07**	**0.08**
Z	**4.6**	**17.4**	**5.0**	**13.2**	**5.7**	**9.5**	**5.1**	**7.2**
Cape Columbine 1937-2013								
S	1600	1529	976	1348	1336	1254	938	1105
Var(S)	7636	9745.9	9343.7	11406.9	4630.8	15028.6	15081	18496
Q[a]	**0.23**	**0.20**	**0.17**	**0.17**	**0.17**	**0.16**	**0.13**	**0.15**
Z	**18.3**	**15.5**	**10.1**	**12.6**	**19.6**	**10.2**	**7.6**	**8.1**
SA Astronomical Observatory 1933-2013								
S	698	1250	1196	1076	749	721	481	1003
Var(S)	26029	14333	20327	20373	12623.5	15042	9373.8	9747.8
Q[a]	**0.11**	**0.23**	**0.50**	**0.22**	**0.06**	**0.07**	**0.05**	**0.11**
Z	**4.3**	**10.4**	**8.4**	**7.5**	**6.7**	**5.9**	**4.9**	**10.2**
Cape St Blaize 1920-2001								
S	1315	933	1069	1386	947	1004	903	873
Var(S)	13542	11093	18376	18235	7491.6	18512	12741	16832
Q[a]	**0.19**	**0.11**	**0.14**	**0.16**	**0.10**	**0.12**	**0.12**	**0.10**
Z	**11.3**	**8.8**	**7.9**	**10.3**	**11.0**	**7.3**	**8.0**	**6.7**

a: sign indicated trend direction (i.e. "-" = decreasing trend).
Bold values reflect significant trends.

3.5. DISCUSSION

Our paper emphasizes the importance of data quality control and homogenization when ascertaining long-term temperature trends. This has important implications for the analysis of regional temperature trends (i.e. the inclusion of erroneous data would subsequently influence the accuracy of temperature trends). However, the possibility that inhomogeneities still remain, cannot be ruled out due to the uncertainties of homogenization techniques. A major challenge for homogeneity testing of South African temperature data is an insufficiently dense station network containing robust long-term data with minimal gaps. Therefore, as suggested by Peterson *et al*. (2008), it is more feasible to homogenize available data rather than discard stations with large step changes and long periods of missing data. In addition, the absence of a dense station network and highly correlated stations to create homogeneous reference series, weakens the methods used to improve the quality and homogenization of South African temperature data. Pairwise comparison is considered more effective when a large number of neighbour stations are available for comparison with the target series (Menne and Williams, 2009). As there is much uncertainty associated with homogenizing time series, the use of multiple tests to detect change points will improve the reliability of eventual results (Štěpánek, 2011; Venema *et al*., 2012), hence the use of the SNHT and Bivariate tests in AnClim to detect change points. Notably, when identifying the timing of undocumented change points, the detected change point in a group of neighbour station temperature series will cluster around the true date (Williams *et al*., 2012).

Mean annual T_{max} and T_{min} data for the Western Cape region of South Africa indicate temperature trends that maintain the same direction (either increasing/decreasing trends) before and after homogenization over their respective recording periods (1916 to 2013), with the exception of T_{min} at Jonkershoek (Figure 3.4(h)), which changed from a decreasing trend before homogenization to an increasing trend after homogenization. Similarly, temperature trends in northeastern Spain do not indicate considerable differences in their direction before and after homogenization, with 13% and 35% of trends changing from increasing (or decreasing) to decreasing (or increasing) after homogenization of T_{max} and T_{min} respectively (Kenawy *et al*., 2013). Although not statistically significant, the directional change for mean annual T_{min} at Jonkershoek changed from marginally decreasing (-0.03°C/decade) to

increasing (0.23°C/decade) for the period 1936-2009, according to the Sen's slope estimate (Figure 3.4(h) and Table 3.6).

Increasing annual temperature trends have been recorded for the majority of stations in South Africa for the period 1960-2003 (Kruger and Shongwe, 2004), which represents a shorter period than our study. To ensure homogeneity was not influenced, Kruger and Shongwe (2004) utilized stations that had not moved and had no changes to exposure of instrumentation. Their study demonstrated that mean annual T_{max} trends had increased significantly at 50% of stations investigated (n = 26 stations), while annual T_{min} trends had increased significantly at 86% of stations (n = 21 stations). Yet, for the five stations investigated (i.e., Cape Columbine, Cape Agulhas, Langgewens, Cape Point and Jonkershoek), some notable differences in temperature trends are recorded after homogenization (Table 3.9). For instance, the current study calculates significant increasing trends of 0.11°C/decade and 0.19°C/decade for mean T_{max} at Cape Columbine and at Cape Agulhas respectively, for the period 1960-2003, while Kruger and Shongwe (2004) record significant increasing trends of 0.21°C/decade and 0.16°C/decade, respectively for these stations over the same period. As cautioned by Kenawy *et al*. (2013), short or fragmented temperature series may significantly alter the magnitude and direction of calculated trends, thus longer homogenized series are preferable. The warming rate recorded for Cape Columbine for the shorter period (determined by Kruger and Shongwe (2004)) is twice the rate determined by this study, indicating that the homogenization process and the length of the record play an important role in the magnitude of the trend. However, for Cape Agulhas, the rate of warming has increased with an increase in the length of the record and the homogenization techniques employed.

This study is based on the meteorological definition of a season, whereby a year is subdivided into four seasons of three months each because an official designation of starting dates for a season does not exist and the timing of a season is dependent on the location on the planet (Trenberth, 1983). While the limitation of the assumption is acknowledged, seasons needed to be calculated using similar methodologies employed by other South African studies in order to compare the seasonal temperature trends. The majority of Western Cape stations record statistically significant positive trends for mean seasonal T_{max} and T_{min} variables, with the exception of T_{max} trends for summer (-0.03°C/decade) and autumn (0°C/decade) at Kirstenbosch (Table 3.8). Previous South African studies have indicated significant T_{max}

increases for all seasons for the period 1960-2010, varying from 0.19°C/decade for summer to 0.15°C/decade for winter over the Western Cape region (MacKellar *et al*., 2014). During the same period, the current data indicate mean warming trends of 0.19°C/decade for summer to 0.17°C/decade for winter, using only homogenized records from Cape Agulhas, Cape Columbine, Cape Point, the SA Astronomical Observatory and Langgewens (Table 3.10). Both studies indicate substantially faster warming rates during summer over the Western Cape region for the period 1960-2010. However, if expanded over a longer period from 1937 to 2013 (the common period for the four stations), such a longer-term change equates to 0.14°C/decade during summer and 0.16°C/decade during winter, thus indicating substantially faster warming trends in winter than summer over this part of South Africa. MacKellar *et al*. (2014) calculated a significant mean T_{min} increase of 0.15°C/decade in summer but an insignificant increase of 0.11°C/decade in winter over the Western Cape for the period 1960-2010. During the same period, our homogenized series indicates a mean T_{min} increase of 0.16°C/decade in summer and 0.14°C/decade in winter (Table 3.10). Such differences could possibly be a function of different stations having been selected between the two studies, which itself has implications for calculating regional climate trends (MacKellar *et al*., 2014) do not reveal the identity of their five stations used in calculating mean trends).

Table 3.9: Comparison of annual temperature trends (°C/decade) between the Kruger and Shongwe (2004) and the current study for the period 1960-2003.

Station name	**This study-annual trends: 1960-2003**		**Kruger & Shongwe (2004): annual trends: 1960-2003**	
	T_{max}	**T_{min}**	**T_{max}**	**T_{min}**
Cape Agulhas	0.19*	0.07*	0.16*	0.09*
Cape Columbine	0.11*	0.15*	0.21*	0.22*
Cape Point	0.13*	0.20*	0.22*	0.20*
Jonkershoek	0.10*	0.23*	0.15	0.15*
Langgewens	0.06*	0.13*	0.09	0.17*
Mean	0.13	0.16	0.17	0.17

* indicates the trend is significant.

Trends from the Kruger and Shongwe (2004) study are estimates from the graphs provided in that paper.

Table 3.10: Summer and winter temperature trends (°C/decade) for the period 1960-2010; for comparison with the MacKellar *et al*. (2014) study.

Station name	**T_{max}**		**T_{min}**	
	Summer	**Winter**	**Summer**	**Winter**
Cape Agulhas	0.17*	0.17*	0.14*	0.16*
Cape Columbine	0.26*	0.30*	0.19*	0.23*
Cape Point	0.26*	0.16*	0.16*	0.13*
S A Astronom. Obs.	0.13*	0.12*	0.05*	0.06
Kirstenbosch	-0.06*	0.03	0.17*	0.12*
Langgewens	0.36*	0.21*	0.23*	0.14*
Mean	0.19	0.17	0.16	0.14
MacKellar *et al.*[a]	0.19*	0.15*	0.15*	0.11

* indicates the trend is significant.

a: MacKellar *et al*. (2014) did not provide statistics for individual stations. Only regional averages were provided.

The combined mean annual T_{max}/T_{min} increase over the Western Cape region of South Africa for the period 1916-2013 is 0.13°C/decade. For the common period 1937-2001, the mean temperature increase for Western Cape stations, as calculated by Sen's slope estimate, is 0.12°C/decade and 0.13°C/decade for T_{min} and T_{max} respectively (Table 3.7). However, despite such a similar regional trend for $T_{max/min}$, this is not unanimous across all stations. At Cape Point, annual T_{min} increased more substantially (by 0.17°C/decade) than T_{max} (by 0.02°C/decade) during the period 1918-2013.

The importance of data quality control and homogenization has been emphasized for establishing temperature trends in South Africa. The combined use of statistical methods and metadata are important for detecting inhomogeneities in historical time series. However, metadata are not sufficient because changes are not always recorded, and all changes found in metadata do not always have a significant impact on observations (Caussinus and Mestre, 2004; Vincent *et al*., 2012; Williams *et al*., 2012). An additional challenge includes the inability to construct a reliable composite reference series where the common period between the candidate and neighbour station is too short (Costa and Soares, 2009).

3.6. CONCLUSION

This work demonstrates the importance of critically assessing and preparing temperature datasets when establishing temperature trends in South Africa and elsewhere. Adjusted (homogenized) T_{max} and T_{min} data over the Western Cape region indicate statistically significant increasing annual temperature trends, with the exception of an insignificant decreasing T_{max} trend at Cape St Blaize. A statistically significant mean increasing trend (0.13°C/decade) for all stations used is recorded for the common period (1937-2001), with a 0.04°C/decade stronger warming signal than before homogenization was applied. This has important implications for the determination of accurate regional temperature trends, particularly if used for future climate projections and for linkages made with other bio-environmental changes. Future work on climate trends, in regions such as southern Africa where data sets are potentially problematic, should include the confirmation of all detected change points in metadata, thus hopefully providing for more accurate scientific outcomes. Unfortunately, detailed metadata records are private property housed at the SAWS and are also not available electronically. However, undocumented change points are often detected by statistical methods using software because metadata records are often incomplete, with many changes not documented over the lifetime of the station. In addition, future work contributing to the challenges of developing composite homogeneous references will increase the accuracy of temperature trends.

3.7. ACKNOWLEDGEMENTS

Thank you to the South African Weather Services for providing temperature data. RL-G appreciates the Research Development Grant provided by the Tshwane University of Technology (TUT), South Africa, the Department of Higher Education and Training and the National Research Foundation of South Africa (98258). Thank you to the anonymous reviewers who provided valuable inputs on an earlier draft of this paper.

3.8. REFERENCES

Aguilar E, Auer I, Brunet M, Peterson TC, Wieringa J. 2003. *Guidelines on Climate Metadata and Homogenization*. WCDMP-No. 53, WMO-TD No. 1186. World Meteorological Organization, Geneve, Switzerland.

Alexander LV, Zhang X, Peterson TC, Caesar J, Gleason B, Klein Tank AMG, Haylock M, Collins D, Trewin B, Rahimzadeh F, Tagipour A, Kumar KR, Revadekar J, Griffiths G, Vincent L, Stephenson DB, Burn J, Aguilar E, Brunet M, Taylor M, New M, Zhai P, Rusticucci M, Vazquez-Aguirre JL. 2006. Global observed changes in daily climate extremes of temperature and precipitation. *Journal of Geophysical Research* **111**: D05109. doi:10.1029/2005JD006290

Brunet M, Saladie O, Jones P, Sigro J, Anguilar E, Moberg A, Lister D, Walther A, Almarz C. 2008. *A case-study/guidance on the development of long-term daily adjusted temperature datasets: Climate Data and Monitoring.* WCDMP-No. 66. World Meteorological Organization, Geneva, Switzerland. pp. 1-43.

Caussinus H, Mestre O. 2004. Detection and correction of artificial shifts in climate series *Applied Statistics* **53**: 405-425.

Christy JR, Norris WB, McNider RT. 2009. Surface temperature variations in East Africa and possible causes. *Journal of Climate* **22**: 3342-3356.

Costa AC, Soares A. 2009. Homogenization of Climate data: review and new perspective using Geostatistics. *Mathematical Geosciences* **49**: 291-305.

Department of Transport, South Africa Weather Bureau. Meteorological Office reports. 1920-1977. The Government Printer, Pretoria. NOAA Central Library. Available online at: http://www.lib.noaa.gov/collections/foreign_climate_data_pages/foreign_climate_data_south_africa.html (Accessed 01 June 2015).

El Fadli K, Cerveny RS, Burt CC, Eden P, Parker D, Brunet M, Peterson TC, Mordacchini G, Pelino V, Bessemoulin P, Stella JL, Driouech F, Abdel wahab MM, Pace MB. 2013. World Meteorological Organization Assessment of the Purported World Record 58ºC Temperature Extreme at El Azizia, Libya (13 September 1922). *Bulletin of the American Meteorological Society* **94**: 199-204.

Estevez J, Gavilán P, Giráldez JV. 2011. Guidelines on validation procedures for meteorological data from automatic weather stations. *Journal of Hydrology* **402**: 144–154.

Gocic M, Trajkovic S. 2013. Analysis of changes in meteorological variables using Mann-Kendall and Sen's slope estimator statistical tests in Serbia. *Global and Planetary Change* **100**: 172-182.

Hughes WS, Balling RC. 1996. Urban Influences on South African Temperature Trends. *International Journal of Climatology* **16**: 935-940.

Kenawy AE, Lopez-Moreno JI, Štěpánek P, Vicente-Serrano SM. 2013. An assessment of the role of homogenization protocol in the performance of daily temperature series and trends: application to northeastern Spain. *International Journal of Climatology* **33**: 87–108.

Kendall MG. 1975. Rank Correlation Methods, Griffin, London.

Kousari M R, Ahani H, Hendi-zadeh R. 2013. Temporal and spatial trend detection of maximum air temperature in Iran during 1960–2005. *Global and Planetary Change* **111**: 97–110.

Kruger AC, Shongwe S. 2004. Temperature trends in South Africa: 1960–2003. *International Journal of Climatology* **24**: 1929–1945.

MacKellar N, New M, Jack C. 2014. Observed and modeled trends in rainfall and temperature for South Africa: 1960–2010. *South African Journal of Science* **110:** 1-13. http://dx.doi.org/10.1590/sajs.2014/20130353.

Mann HB. 1945. Nonparametric tests against trend. *Econometrica* **13**: 245–259.

Menne MJ, Williams CN. 2009. Homogenization of temperature series via pairwise comparisons. *Journal of Climate* **22**: 1700-1717.

Menne MJ, Williams Jr., CN, Vose RS. 2009. The U.S historical climatology network monthly temperature data, Version 2. *Bulletin American of the Meteorological Society* **90:** 993–1007.

Mitchell TD, Jones PD. 2005. An Improved Method of Constructing a Database of Monthly Climate Observations and Associated High-resolution grids. *International Journal of Climatology* **25**: 693–712.

Muhlenbruch-Tegen A. 1992. Long-term surface temperature variations in South Africa. *South African Journal of Science* **88**: 197-205.

NOAA Central Library. 2013. Department of Transport, South Africa Weather Bureau. Meteorological Office reports. 1920-1977. The Government Printer, Pretoria. Available online at: http://www.lib.noaa.gov/collections/foreign_climate_data_pages/foreign_climate_data_south_africa.html (Accessed 01 June 2015).

Novotny EV, Stefan HG. 2007. Stream flow in Minnesota: Indicator of climate change. *Journal of Hydrology* **334**: 319-333.

Peterson TC, Easterling DR. 1994. Creation of homogeneous composite climatological reference series. *International Journal of Climatology* **14**: 671–679.

Peterson TC, Easterling DR, Karl TR, Groisman P, Auer I, Bohm R, Plummer N, Nicholis N, Torok S, Vincent L, Tuomenvirta H, Salinger J, Førland EJ, Hanssen-Bauer I, Alexandersson H, Jones P, Parker D. 1998. Homogeneity adjustments of in situ climate data: a review. *International Journal of Climatology* **18**: 1493–1517.

Peterson TC, Zhang X, Brunet-India M, Va´zquez-Aguirre JL. 2008. Changes in North American extremes derived from daily weather data. *Journal of Geophysical Research* **113**: D07113. doi:10.1029/2007JD009453.

Sen PK. 1968. Estimates of the regression coefficient based on Kendall's Tau. *Journal of the American Statistical Association* **63**: 1379–1389.

Štěpánek P. 2008. AnClim - software for time series analysis. Dept. of Geography, Faculty of Natural Sciences, MU, Brno. http://www.climahom.eu/AnClim.html

Štěpánek P, Zahradníček P, Huth R. 2011. Interpolation techniques used for data quality control and calculation of technical series: an example of Central European daily time series. *Idöjárás* **115**: 87–98.

Štěpánek P, Zahradníček P, Farda A. 2013. Experiences with data quality control and homogenization of daily records of various meteorological elements in the Czech republic in the period 1961-2010. *Quarterly Journal of the Hungarian Meteorological Service* **117**: 123-141.

Szentimrey T. 2008. *Methodological Questions of Series Comparison*. In Proceedings of the Sixth Seminar for Homogenization and Quality Control in Climatological Databases. WMO-TD No. 1576. WMO, Geneva: 1-7.

Toreti A, Kuglitsch FG, Xoplaki P, Della-Marta M, Aguilar E, Prohom M, Luterbacher J. 2011. A note on the use of the standard normal homogeneity test to detect inhomogeneities in climatic time series. *International Journal of Climatology* **31**: 630–632.

Trenberth KE. 1983. What are the seasons? *Bulletin American Meteorological Society* **64**: 1276-1282.

Venema VKC, Mestre O, Aguilar E, Auer I, Guijarro JA, Domonkos P, Vertacnik G, Szentimrey T, Štěpánek P, Zahradnicek P, Viarre J, M¨uller-Westermeier G, Lakatos M, Williams CN, Menne MJ, Lindau R, Rasol D, Rustemeier E, Kolokythas K, Marinova T, Andresen L, Acquaotta F, Fratianni S, Cheval S, Klancar M, Brunetti M, Gruber C, Prohom Duran M, Likso T, Esteban P, Brandsma T. 2012. Benchmarking monthly homogenization algorithms. *Climate of the Past Discussions* **7**: 2655–2718.

Vincent LA, Wang XL, Milewska EJ, Wan H, Feng Y, Swail V. 2012. A second generation of homogenized Canadian monthly surface air temperature for climate trend analysis. *Journal of Geophysical Research* **117**: D18110. doi:10.1029/2012JD017859.

Wang XL, Chen H, Wu Y, Feng Y, Pu Q. 2010. New techniques for detection and adjustment of shifts in daily precipitation data series. *Journal Applied Meteorology and Climatology* **49**: 2416-2436.

Wang XL. 2008. Penalized maximal F-test for detecting undocumented mean-shifts without trend-change. *Journal Atmospheric Oceanic Technology* **25**: 368-384.

Williams CN, Menne MJ, Thorne PW. 2012. Benchmarking the performance of pairwise homogenization of surface temperatures in the United States. *Journal of Geophysical Research* **117**: D05116. doi:10.1029/2011JD016761.

XLSTAT. 2015. Available online: https://www.xlstat.com/en/order (Accessed 10 January 2014).

Yue S, Wang C. 2004. The Mann-Kendall Test Modified by Effective Sample Size to Detect Trend in Serially Correlated Hydrological Series. *Water Resources Management* **18**: 201–218.

Yozgatligil C, Yazici C. 2016. Comparison of homogeneity tests for temperature using a simulation study. *International Journal of Climatology* **36**: 62-81.

Zhang X, Yang FE. 2004. RClimDex (1.0) Climate Research Branch Environment Canada Downsview, Ontario, Canada. Available online at: http://etccdi.pacificclimate.org/software.shtml (accessed 20/05/2014).

CHAPTER FOUR

TEMPERATURE TRENDS FOR COASTAL AND ADJACENT HIGHER LYING INTERIOR REGIONS OF KWAZULU-NATAL, SOUTH AFRICA

4.1. ABSTRACT

Temperature trends for KwaZulu-Natal (KZN), South Africa, are investigated over the period 1851-2015, with a focus on comparing coastal and higher lying adjacent (within ~100 km) interior regions. This is achieved through analyzing instrumental temperature records from the coastal stations of Durban and Mount Edgecombe, and adjacent interior stations of Pietermaritzburg, Cedara and Emerald Dale. Comparisons of temperature for the second half of the 19th century (i.e. 1851, 1858, 1860-1864) with more recent times in KZN indicate cooler conditions for the earlier period. The modified Mann Kendall test is used to determine annual and seasonal mean temperature (T_{mean}), maximum temperature (T_{max}) and minimum temperature (T_{min}) trends over the period 1930-2015, and for the most recent few decades. For annual T_{max}, a significant increasing trend (0.07°C/decade) is recorded at the coast, whereas adjacent interior stations record no trend. Annual T_{min} record significant warming at all stations, with warming rates over the interior being double that for the coast over the period 1930-2015. Rates of T_{min} warming are 1.31 (summer), 2.75 (autumn), 3.33 (winter) and 1.25 (spring) times faster over the interior compared to the coast. Thus, higher lying interior regions are warming considerably faster than adjacent coastal areas mainly due to T_{min} warming trends. Over the period 1930-2015, record positive annual T_{max} departures are recorded for 2015 at Mount Edgecombe (mean departure = 1.6°C), Cedara (mean departure = 1.7°C) and Emerald Dale (mean departure = 2.0°C), in part due to the strong El Niño event in that year.

Keywords: Temperature, trends, historical climate, KwaZulu-Natal, coastal.

4.2. INTRODUCTION

Globally, there has been much focus on recent decadal trends in continental and sea surface temperatures (SSTs) (Santos *et al*., 2012), yet relatively few studies have investigated trends for the geographic boundary between these major global regions (i.e. coastal and adjacent interior zones), with consequent knowledge gaps remaining (Baumann and Doherty, 2013). Although coastal regions (located in close proximity to the sea) only represent ~2% of global land area, these host ~10% of the world's population and ~13% of urban population

(McGranahan *et al*., 2007). Coastal zones are recognized as vulnerable to global warming given their exposure to consequent sea-level rise (McGranahan *et al*., 2007), but perhaps less widely mentioned is that warming in coastal regions may have a variety of other consequences, such as enhanced eutrophication of coastal waters (Rabalais *et al*., 2009). To this end, establishing recent past climate-thermal trends in coastal and adjacent higher lying interior regions is important for associated adaptive planning and risk preparedness.

Notably, some studies have measured mean annual cooling trends during recent decades along several coastlines (e.g. some portions of the North- and South-American west coast; east coast of Canada), while higher elevation adjacent interior regions recorded strongly diverging warming trends (e.g. Morgan *et al*., 1993; Falvey and Garreaud, 2009; Lebassi *et al*., 2009). In contrast, very strong warming is recorded along the west coast of Greenland, particularly during the last 10-20 years, while weaker warming has occurred on the east Greenland coast for the period 1881-2012 (Hanna *et al*., 2012). Similarly, significant increasing annual mean temperature (T_{mean}) have been observed at coastal stations along the Mediterranean coast (0.22-0.46°C/decade) and inland (0.27-0.42°C/decade) stations in Israel for the period 1970–2002 (Kafle and Bruins, 2009). The aforementioned studies thus demonstrate inconsistent global temperature trends for coastal and adjacent inland regions.

In the African context, the mean annual maximum temperature (T_{max}) in Libya recorded increasing trends at five of the nine coastal stations (0.18°C/decade - 0.21°C/decade) and four of the six inland stations (0.14°C/decade - 0.24°C/decade) over the period 1945-2009. For the same period, annual T_{mean} increases were observed at all (nine) coastal stations (0.13°C/decade - 0.29°C/decade) and at all six inland stations (0.03°C/decade - 0.43°C/decade). Strong T_{mean} seasonal warming trends are recorded at inland stations (autumn: 0.27°C/decade; winter: 0.14°C/decade; spring: 0.23°C/decade and summer: 0.30°C/decade) and at the coast (autumn: 0.25°C/decade; winter: 0.14°C/decade; spring: 0.17°C/decade and summer: 0.19°C/decade) (Ageena *et al*., 2014). In southern Africa, temperature trends for coastal and lake areas along the Mozambique channel regions for the period 1939-1992, indicate daytime warming and night time cooling trends, while the northern part of eastern Africa inversely recorded nighttime warming and daytime cooling during the same time (King'uyu *et al.,* 2000). Although some work has focused on recent decadal temperature changes in South Africa (e.g. Kruger and Shongwe, 2004; MacKellar *et al*., 2014), there has not been a specific focus investigating trends along coastal regions. The

only exception is an earlier study (Jury, 1998) which demonstrated quasi cyclical temperature trends for the period 1960-1997 at four coastal stations (Port Shepstone, Durban, Mount Edgecombe and St Lucia) in KwaZulu-Natal (KZN). Although Kruger and Shongwe (2004) established that stations with significant mean annual T_{max} positive trends are mainly located in coastal regions, such findings have not been directly contrasted with those for adjacent inland regions. In addition, previous South African work establishing temperature trends has focused mainly on the last half century (e.g. Kruger and Shongwe, 2004; MacKellar *et al*., 2014). However, most recently, Lakhraj-Govender *et al*. (2017) established significant increasing temperature trends over the Western Cape Province for the period 1916-2013. While Kruger and Nxumalo (2017) also recently established long-term temperature trends for the period 1931-2015 across parts of South Africa, the study used absolute homogenization procedures. These methods typically decrease the homogeneity of data for monthly and annual means (Venema *et al*., 2012). The risk of using absolute homogenization is acknowledged by Kruger and Nxumalo (2017), who confirm that dubious results were obtained after homogenization of datasets with a large number of inhomogeneities, which prior to homogenization produced strong trends.

To adequately establish such aforementioned temperature trends, long-term meteorological station data with sufficient coverage are required, yet these are not always available (MacKellar *et al.*, 2014). Regions such as Europe, North America and parts of Asia have dense and long (>200 years) station coverage, while much of South America and Africa has more limited coverage (Jones *et al*., 2016). In part, the problem for some regions has been that older records have been lost, or still require data rescue and digitization. To address such data scarcity in the Southern Hemisphere in particular, the recovery of historical instrumental data has become an important recent initiative (Hannaford and Nash, 2016), and one which forms part of the work presented here. The aim of this study is to extend past work by examining temperature trends for KZN over a considerably longer period, with a specific focus on comparing coastal and adjacent (within ~100 km) higher lying interior regions. This is expected to increase our understanding of factors (such as the location, specifically the regional gradient from coastal to interior) that influence annual, seasonal and decadal temperature trends.

4.3. METHODS

4.3.1. Regional context

KZN is a province situated along the southeast coast of South Africa. It has a varied topography with relatively flat coastal plain in the east, rising gradually westwards toward the so called 'midlands' and more substantially ca 200 km inland on reaching the Drakensberg (Main Escarpment) (Figure 4.1) (Eeley *et al*., 1999). KZN's climate is strongly influenced by the Indian Ocean, and particularly the warm Agulhas current (Reason, 2001; Green *et al*., 2012), hence accounting for high humidity, temperatures and summer rainfall. Tropical temperate troughs, east coast low pressure systems and southeast coast ridging high pressure systems dominate during summer and spring (Figure 4.2; Tyson and Preston-Whyte, 2000). The anticyclone belt weakens and shifts southward, allowing the tropical easterly flow to influence weather during summer. Near surface low pressure systems dominate during summer, when moisture from the tropics is transported to the region (Landman *et al*., 2009). During winter, moisture from the tropics is reduced by the northward migration of the Inter-tropical Convergence Zone (ITCZ) and the intensification of the anticyclonic circulation, hence limiting precipitation. However, perturbations in the westerly circulation, in the form of anticyclones, as well as ridging high pressure systems behind cold fronts, dominate during winter (Tyson and Preston-Whyte, 2000).

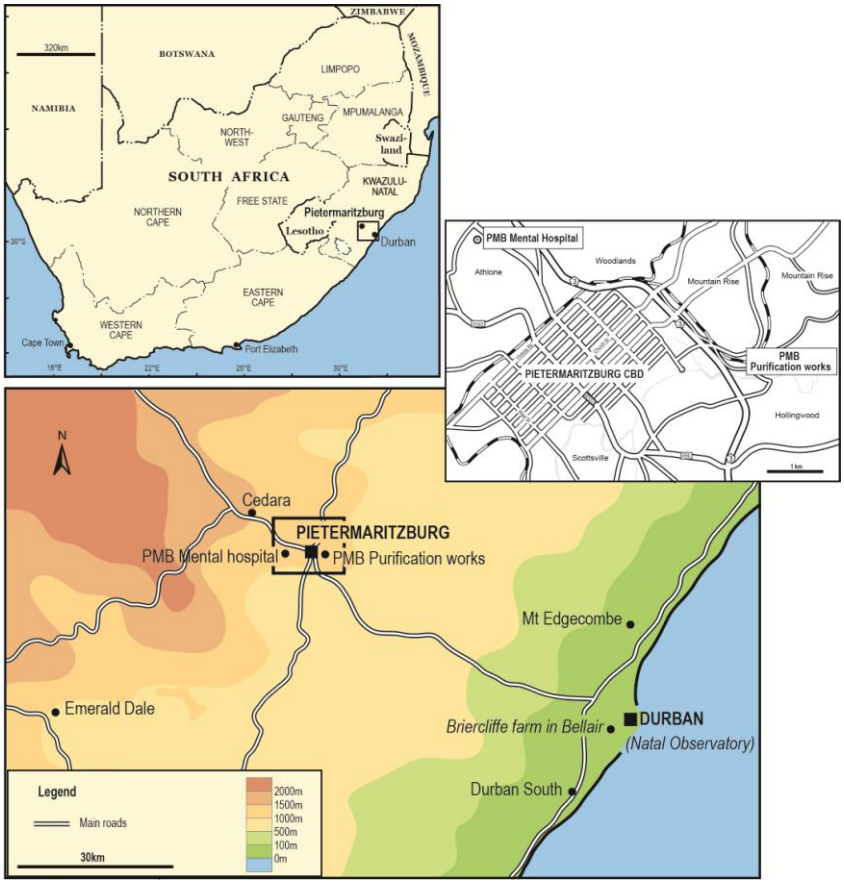

Figure 4.1: Map showing KwaZulu-Natal stations (black solid dots), South Africa.

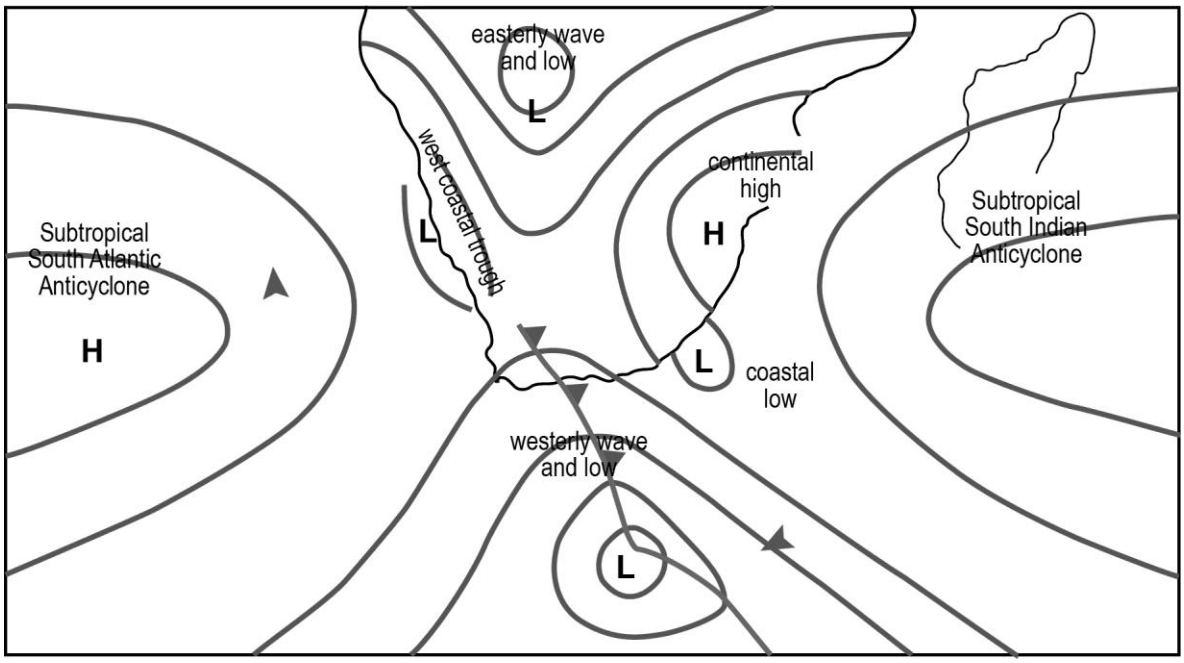

Figure 4.2: Schematic representing the features that influence climate (from Tyson and Preston-Whyte, 2000).

4.3.2. Data sources

In an attempt to avoid latitudinal climatic influence in our assessment, we only focus on stations located within a narrow latitudinal band (29.5-29.9S) in KZN. This is achieved through an analysis of instrumental temperature records available for the coastal stations of Durban and Mount Edgecombe, and inland stations of Pietermaritzburg, Cedara and Emerald Dale (Figure 4.1). A variety of historical documentary sources was obtained through the South African Weather Service (SAWS), National Oceanic and Atmospheric Administration (NOAA) Central Library, Atmospheric Circulation Reconstruction over the Earth Initiative, and publications available online, providing temperature data at various temporal resolutions (daily to monthly) and dating back to 1851 (Table 4.1). The earliest temperature recordings were relatively brief in duration, such as that in Briecliffe near Durban between November 1850 and February 1852 (Appendices, Table A1; Holden, 1855), and a set of records for both Pietermaritzburg and Durban in 1858 (Appendices, Table A2), provided by Dr R.J. Mann (1859). The observatory in Pietermaritzburg moved by 8 km in March 1859 and subsequently yielded temperature data from 1860-1865, but consequently the data are not easily comparable with those from 1858/1859. The monthly temperature records for Pietermaritzburg (1860-1865) were published in the *Quarterly Journal of the Royal Meteorological Society* (Mann, 1878), but original records have yet to be found, should they still exist.

Raw daily T_{max} and T_{min} values for various KZN stations were selected based on available long-term temperature data and quality/completeness of the dataset. Early (1896-1939) daily T_{max} and T_{min} data for Pietermaritzburg were digitized from original hard copy weather records (see Appendices, Figure A1) held by the SAWS. Mean monthly T_{max} and T_{min} data for Pietermaritzburg (1940-1953), Cedara (1957) and Mt Edgecombe (September 1947-December 1947, 1959) were digitized from the Department of Transport Meteorological Data Reports, sourced from the NOAA Central Library (2013). Historical temperature data were converted from degrees Fahrenheit to degrees Celsius. Daily T_{max} and T_{min} for the remaining stations (i.e. Cedara, Emerald Dale and Mount Edgecombe) were obtained electronically from the SAWS (Table 4.1). While the 19th century records provided T_{mean} data, the remaining T_{mean} values used in this study were calculated by averaging T_{max} and T_{min} values.

Department of Transport Meteorological Data Reports indicate that the Cedara station was relocated on 4 November 1969 (by 274.3m horizontally and losing 9m altitudinally) and the Emerald Dale station became a 3rd order station (i.e. records only T_{max} and T_{min} at 08:00) on 1st August 1969. Station history reports that the Mount Edgecombe station changed to an automatic station on 1st October 1992 and Cedara was converted to an automatic station on the 1st September 2005. However, no change points were detected at these stations.

4.3.3. Analyses of temperature data

Daily temperature data were quality controlled and homogenized as per methods outlined in Lakhraj-Govender *et al*. (2016). Notably, T_{mean}, T_{max} and T_{min} time series were adjusted for detected inhomogeneities separately. The correlation coefficients and distances between the candidate station and the neighbour stations (used for the construction of the reference series) are reflected in Table A3 in the Appendices and the detected changepoints appear in Table A4 of the Appendices. Ashcroft *et al*. (2014) suggest that records with more than 3 years of data can be subjected to homogenization procedures. For the period 1930-2015, monthly $T_{mean,}$ T_{max} and T_{min} anomalies were calculated, relative to the 1961-1990 mean. It was not feasible to remove the seasonal cycle of some historical sources given the short length (<5 years) of some records (cf. Ashcroft *et al*., 2014). Seasonal means are defined as austral summer (December, January and February), autumn (March, April and May), winter (June, July and August) and spring (September, October and November).

The modified Mann Kendall (MK) test was used to identify possible annual and seasonal T_{mean}, $T_{max,}$ and T_{min} trends at Mount Edgecombe, Cedara and Emerald Dale for the full period (1930-2015), as well as the most recent 30-year (1985-2015) period. To remove serial autocorrelation expected in the data, the modified version of the MK test was used (Yue and Wang, 2004). The MK test statistic (S) is initially assumed to be 0 (i.e. no trend). S is incremented (decremented) by 1 if a later datum is higher (lower) than the datum from the earlier time. The net result of the increments and decrements yields the final S (Shahid *et al*., 2008) which indicates the magnitude of temperature trends, while the sign denotes whether the trend is increasing or decreasing. Statistical significance of the trend is based on the MK Z test statistic, calculated from the variance of S. Positive Z values indicate increasing trends while negative values are decreasing trends (Gocic and Trajkovic, 2013). At the 5% significance level, if Z >1.96 or Z <-1.96, the trend is significant.

Table 4.1: KwaZulu-Natal station details with start/end dates for temperature recording.

Source of data and timescale	Station name	Latitude (deg. S)	Longitude (deg. E)	Altitude (m a.s.l.)	Dist. from the coast (km)	Start date	End date
Digitized from Holden (1851) (Monthly)	Briercliffe farm near D'Urban, Port Natal	-29.88	30.96	a	8.8	1850/11/01	1852/02/28
Digitized from Mann (1859) (Monthly)	Durban	-29.90	31.00	27	1.5	1858/01/01	1858/12/31
ACRE[c] (Daily)	Natal Observatory in Durban	-29.90	31.00	43	3.2	1884/01/01	1906/12/31
SAWS (Monthly)	Durban South	-29.97	30.95	14	2.2	1994/01/01	2013/12/31
Digitized from Mann (1859) (Monthly)	Pietermaritzburg	-29.5[b]	31.0[b]	657	Approx. 65-72	1858/01/01	1858/12/31
Digitized from Mann (1878)	Pietermaritzburg	a	a	a	a	1859/01/01	1866/12/31
Digitized from Mann (1870) (Monthly)	Pietermaritzburg	-29.5[b]	30.0[b]	639	Approx. 65-72	1860/01/01	1865/12/31
Digitized from hard copies at SAWS (Daily)	Pietermaritzburg (Mental Hospital)	-29.58	30.37	684	72	1896/01/01	1939/12/31
Digitized from Meteorological Reports on NOAA web site (Monthly)	Pietermaritzburg (Mental Hospital)	-29.58	30.37	684	72	1940/01/01	1953/12/31
SAWS (Daily)	Pietermaritzburg Purification	-29.60	30.43	613	65.46	1970/01/01	1992/12/31
SAWS (Daily)	Pietermaritzburg (CBD)	-29.63	30.40	673	69.6	1994/01/01	2015/12/31
SAWS (Daily)	Cedara	-29.54	30.27	1071	83.3	1930/01/01	2015/12/31
SAWS (Daily)	Mount Edgecombe	-29.70	31.05	103	5.6	1930/01/01	2015/12/31

SAWS (Daily)	Emerald Dale	-29.94	29.96	1189	86.5	1930/01/01	2015/12/31

a: Information is not available.

b: The accuracy of coordinates during this early period is questionable (likely to be central Pietermaritzburg).

c: Atmospheric Circulation Reconstruction over the Earth Initiative.

Magnitudes of the trends were determined using Sen's nonparametric slope estimator (Q) (Sen, 1968). P values less than the chosen significance level (alpha (α) = 0.05) indicate the null hypothesis (H_0, i.e. no trend in the series) must be rejected and the alternative hypothesis (Ha, i.e. there is a trend) is accepted (XLStat, 2015). The slope is statistically different from zero for the selected confidence interval (95%) if the upper (Q_{max}) and lower (Q_{min}) limits have similar signs (Gocic and Trajkovic, 2013). AnClim software (Štěpánek, 2008) was used to produce a 10-year Gaussian low pass filter, which smooths annual average temperature and exhibits decadal temperature variability.

4.3.4. Methodological challenges

A limitation to this study is the absence of suitable neighbour stations for use as reference series, required for the adjustment of time series. Therefore, all subsets of data, such as the Natal Observatory (1884-1909) and Pietermaritzburg Mental hospital data (1896-1953), were subjected to the detection of change points with AnClim software (Štěpánek, 2008). Consequently, the time series were subjected to a technique called scalpel, whereby a record was split into portions at points before and after the apparent discontinuities (Rohde *et al*., 2013). Change points are abrupt changes in the time series, often caused by instrumentation changes or urbanization and land cover changes (Wang *et al*., 2010). Change points were detected in 1917 (T_{max}), 1912 (T_{min}) and 1901 (T_{mean}) at the Pietermaritzburg Mental hospital, and in 1893 (T_{max}) and 1888 (T_{min} and T_{mean}) at the Natal Observatory. No change points were detected for the Pietermaritzburg stations over the periods 1860-1865, 1970-1992 and 1994-2015.

Pietermaritzburg meteorological observations started in 1896 at the Mental hospital, but the station was moved several times. Given that the data could not be integrated or homogenized due to differences in location and temporal gaps, data subsets for Pietermaritzburg are presented as discontinuous records (1896-1916; 1917-1953; 1970-1992; 1994-2015) (Figure 4.4). Temperatures recorded at the Pietermaritzburg Municipality during the years 1960-

1968 were omitted given too many data gaps. Similarly, data were discarded for the period 2004-2006 at Mount Edgecombe, because of too many data errors.

4.4. RESULTS

4.4.1. Earliest 19th century records

The earliest complete year of temperature values for Durban are those collected by Mr J. Ecroyd in 1851 and values for central Durban are first available in 1858. To place the seasonal values in context, 1851 and 1858 are compared with the full range and average of mean seasonal temperatures for Durban for the period 1994-2012 (Table 4.2). The first year for which monthly temperatures are available for both Durban (coastal) and Pietermaritzburg (65-72km inland; exact location of meteorological station is uncertain) is 1858. Annual T_{mean} in Pietermaritzburg varied little (17.17 to 17.38°C) over the period 1860-1864, yet 1865 stands out as substantially warmer (mean = 17.38°C). This is largely owing to a considerably higher departure from the 1860-1865 average of T_{max} (+0.80°C) rather than T_{min} (+0.40°C) in 1865. To place the 1860-1865 mean temperatures for Pietermaritzburg in context, these are compared with those for the periods 1896-1953, 1970-1992 and 1994-2015 (see Table 4.2).

4.4.2. 19th-20th century transitional period

At the Natal Observatory in Durban, annual T_{mean} averaged 21.62°C and 21.10°C for the periods 1884 to 1900 and 1901-1909, respectively. Annual T_{max} averaged 27.26°C and 26.16°C for the periods 1884-1892 and 1893-1909, respectively, with the warmest T_{max} year being 1896 and the coolest years occurring over the period 1905-1909. Cool annual T_{max} years are 1908 and 1909 (both have a departure of -0.78°C from the 1893-1909 mean), while particularly warm years are 1896 and 1900 (departure from 1893-1909 mean = 1.10 and 1.04°C, respectively). Annual T_{min} averaged 16.69°C, with warmest T_{min} years being 1896 and 1900 (departure from 1884-1909 mean = 0.70 and 0.60°C, respectively) and the coolest year being 1898 (departure from 1888-1909 mean = -0.78°C). For the common homogeneous period (1893-1900), annual $T_{mean,}$ T_{max} and T_{min} averaged 21.50°C, 26.49°C and 16.52°C, respectively (Figure 4.3).

For the period 1901-1953, annual T_{mean} record an average of 18.57°C at the Mental hospital in Pietermaritzburg, with the warmest year being 1899 and the coolest year being 1917. Annual T_{max} record an average of 24.70°C for the period 1917-1953 with the warmest year

being 1945 and the coolest year being 1918. Annual T_{min} record an average for the period 1913-1953, with the warmest year being 1942 and the coolest year being 1916 (Figure 4.4).

4.4.3. Temperature trends over the period 1930-2015

The results of the Mann Kendall test and Sen's slope estimate corresponded. For the period 1930-2015, annual T_{mean} marginally increases at Mount Edgecombe (0.07°C/decade) and Cedara (0.08°C/decade), while no trend is recorded for Emerald Dale. With regard to Emerald Dale, although the S value indicates increasing increments and the Q is 0.01, the trend cannot be regarded as increasing because the p value is greater than 0.05 and the Z value is less than 1.96. Annual T_{max} slightly increases at Mount Edgecombe (0.07°C/decade) while inland stations record no trend at Cedara and at Emerald Dale. Highly significant annual T_{min} warming rates occur at inland stations (i.e. Cedara = 0.24°C/decade; Emerald Dale = 0.15°C/decade), while that for the coastal station of Mount Edgecombe is somewhat lower (0.10°C/decade) (Table 4.3).

For the period 1930-2015, T_{mean} record significant increasing trends during all seasons at Mount Edgecombe. No trend is observed at Emerald Dale and Cedara during winter, while significant increasing trends are recorded for summer at Cedara (0.14°C/decade) and Emerald Dale (0.09°C/decade). T_{max} record weakly significant warming during autumn and winter (0.09°C/decade and 0.1°C/decade, respectively) at Mount Edgecombe and decreasing trends during all seasons at Emerald Dale, but significant during only spring. At Cedara, T_{max} also records a weakly significant decreasing trend (-0.08°C/decade) during spring, while the remaining seasons record warming trends. For the period 1930-2015, T_{min} record significant warming trends (0.05-0.34°C/decade) during all seasons at all three stations, with the strongest warming during autumn (0.26°C/decade) and winter (0.34°C/decade) at Cedara (Table 4.3).

Table 4.2: Mean temperature (°C) for Briercliffe near Durban (taken at sunrise, noon and night) in 1851 (data calculated from Holden, 1855); Pietermaritzburg and Durban in 1858 (data calculated from Mann, 1859); and Pietermaritzburg (taken at 9am, 3pm and 9pm) for 1860-1865 (calculated from Mann 1878).

Year	**T_{mean}**	**T_{max}**	**T_{min}**	**T_{mean}**			
				Summer	**Autumn**	**Winter**	**Spring**
Durban							
1851	19.8	24.5	14.6	23.0	20.2	15.9	19.6
1858	20.9	-	-	24.2	21.8	17.6	20.2
1884-1900*	21.6	-	-	-	-	-	-
1901-1909*	21.1	-	-	-	-	-	-
1884-1892*	-	27.3	-	-	-	-	-
1893-1909*	-	26.2	-	-	-	-	-
1884-1887*	-	-	15.7	-	-	-	-
1888-1909*	-	-	16.5	-	-	-	-
1994-2012*	21.0	25.4	16.7	-	-	-	-
Pietermaritzburg							
1858	18.4	23.9	12.8	21.7	18.2	15.2	18.6
1860	17.2	23.2	12.9	21.8	17.7	12.7	17.1
1861	17.2	23.1	12.8	19.9	17.2	12.8	18.5
1862	17.3	23.1	13.1	20.9	17.3	12.5	18.0
1863	17.4	22.8	13.4	21.4	17.5	13.3	17.4
1864	17.4	22.7	13.6	21.5	16.7	12.6	18.5
1865	17.9	23.9	13.7	21.6	18.2	13.6	18.6
1860-1865*	17.4	23.1	13.2	-	-	-	-
1901-1953*	18.6	-	-	-	-	-	-
1918-1953	-	24.8	-	-	-	-	-
1913-1953	-	-	12.3	-	-	-	-
1970-1992*	18.3	25.5	11.2	-	-	-	-
1994-2015*	19.5	25.8	13.2	-	-	-	-

*Averages included for comparative purpose.

Table 4.3: Annual and seasonal T_{mean}, T_{max} and T_{min} Mann Kendall statistics and Sen's slope estimate (Q) (°C/decade) at KZN stations.

	T_{mean}			T_{max}			T_{min}		
Annual	**S**	**Q**	**Z**	**S**	**Q**	**Z**	**S**	**Q**	**Z**
1930-2015									
Mount Edgecombe	1141	**0.09**	**3.66**	658	0.07	2.10	754	**0.10**	**6.20**
Cedara	1467	**0.13**	**7.89**	98	0.01	0.40	2483	**0.24**	**19.80**
Emerald Dale	341	0.03	1.13	-446	-0.08	-1.40	1690	**0.15**	**17.70**
1985-2015									
Mount Edgecombe	154	**0.20**	**5.68**	152	**0.32**	**8.00**	84	**0.14**	**2.50**
Cedara	135	**0.23**	**6.2**	123	**0.32**	**5.40**	143	**0.19**	**5.10**
Emerald Dale	129	**0.30**	**4.40**	117	**0.40**	**3.10**	109	**0.21**	**3.90**
PMB 1896-1953	-167	**-0.05**	**-2.02**	-671	-0.35	-5.00	572	**0.23**	**5.30**
PMB 1970-1992	51	**0.13**	**3.50**	27	**0.15**	**2.30**	93	**0.30**	**5.50**
PMB 1994-2015	-11	-0.05	-0.63	25	0.21	1.50	-47	**-0.20**	**-2.50**
Seasonal									
Mount Edgecombe									
Summer	1271	**0.14**	**6.10**	759	0.1	3.1	1449	**0.16**	**9.7**
Autumn	836	**0.09**	**3.70**	695	0.09	2.4	634	**0.08**	**5.3**
Winter	671	**0.09**	**2.50**	583	0.10	2.3	583	**0.06**	**2.3**
Spring	783	**0.08**	**3.14**	240	0.03	1.0	1283	**0.12**	**7.7**
Emerald Dale									
Summer	661	**0.07**	**2.91**	-423	-0.08	-1.4	1844	**0.22**	**12.7**
Autumn	499	**0.07**	**2.32**	-338	-0.08	-1.1	1436	**0.17**	**10.0**
Winter	197	0.02	0.89	-160	-0.03	-0.7	601	**0.05**	**3.8**
Spring	-352	**0.02**	**-0.55**	-630	-0.15	-2.2	998	**0.12**	**12.5**
Cedara									
Summer	1242	**0.12**	**8.77**	336	**0.04**	**2.1**	1967	**0.19**	**22.9**
Autumn	1273	0.**14**	**9.34**	212	0.03	1.2	1882	**0.26**	**16.5**
Winter	1658	**0.22**	18.90	603	**0.09**	**4.6**	2171	**0.34**	**20.0**
Spring	369	0.04	1.96	-488	-0.08	-2.2	1610	**0.17**	**18.6**

Mann Kendall test statistic (S) = the strength of the temperature trend; sign indicates increasing or decreasing trend. Z test statistic = statistical significance of the trend, calculated from the variance of S. If $Z > Z_{1-\alpha/2}$, at the chosen level of significance α =0.05%, where Z greater than 1.96, the trend is significant (bold). (Gocic and Trajkovic, 2013). When the p value is lower than the chosen significance level, alpha=0.05, the null hypothesis (no trend in the series) is rejected and the alternative hypothesis (there is a trend) is accepted (XLStat, 2015).

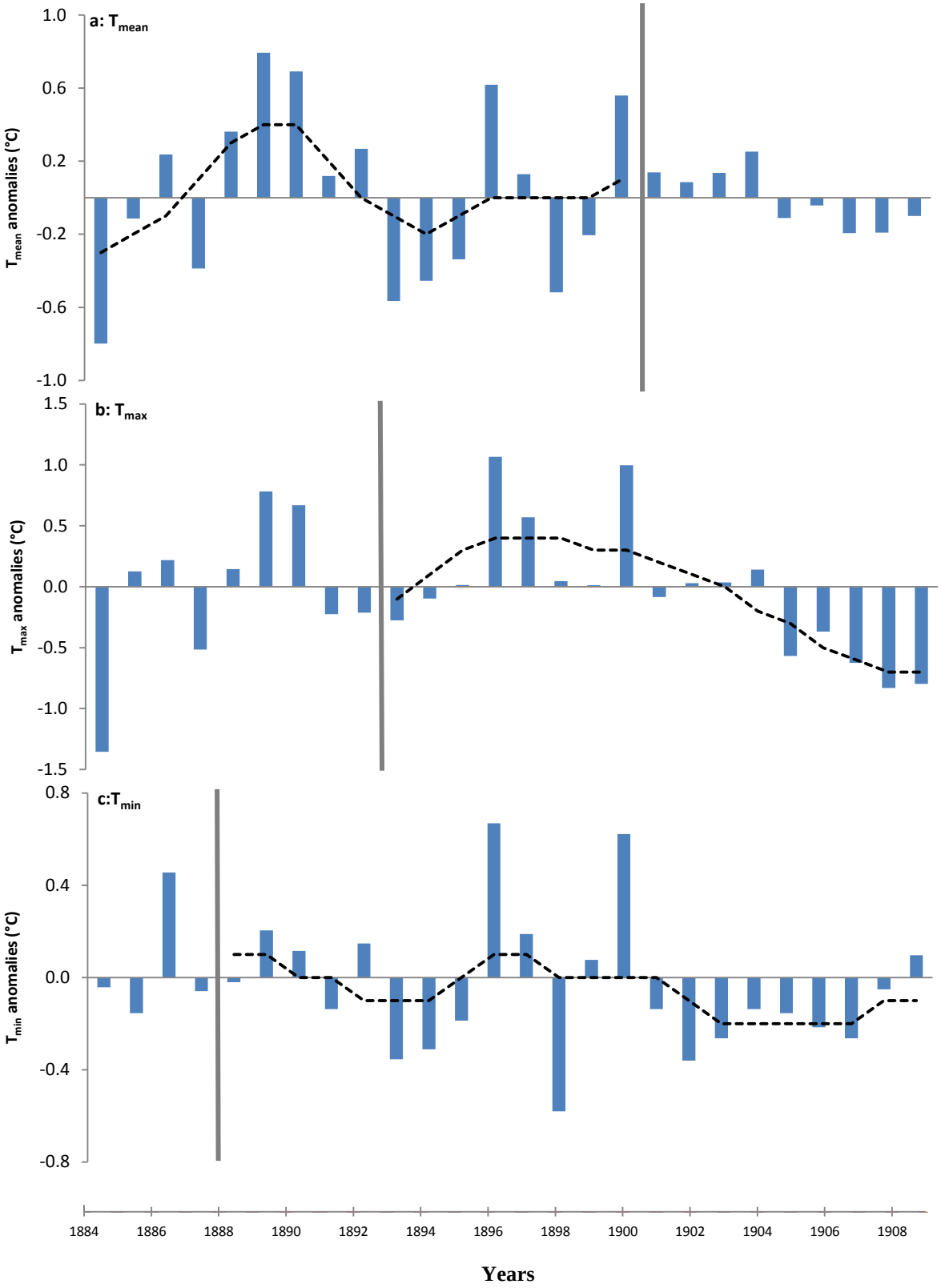

Figure 4.3: Mean annual (a) T_{mean}, (b) T_{max} and (c) T_{min} anomalies for the "Natal Observatory" (53 m a.s.l.) in Durban: 1884-1909, with 10-year Gaussian filter indicated by the black dotted line and the break indicated by the gray vertical line.

4.4.4. Temperature trends over the period 1985-2015

Temperature trends for the most recent decades (~30 years) are often determined for comparison with those for previous periods (e.g. Rebetez and Reinhard, 2008; Sonali and Kumar, 2013; Ageena *et al*., 2014), despite the short temporal scale of assessment. For the period 1985-2015, annual T_{mean} significantly increases by 0.20°C/decade at Mount Edgecombe, 0.23°C/decade at Cedara and 0.30°C/decade at Emerald Dale. This is largely owing to significant increases in annual T_{max} at all stations: by 0.32°C/decade at Mount Edgecombe; 0.32°C/decade at Cedara and 0.40°C/decade at Emerald Dale. Over the same period, annual T_{min} at Mount Edgecombe significantly increased by 0.14°C/decade, and at inland stations warmed by 0.19°C/decade at Cedara and 0.21°C/decade at Emerald Dale (Table 4.3).

4.4.5. Decadal temperature variability

A 10-year Gaussian filter was applied to the annual temperature, so as to establish whether decadal variability was different/similar at coastal and adjacent interior stations. For T_{mean} at Mount Edgecombe, the Gaussian filter displays cooler periods between 1930 and 1990, but subsequently positive departures (from the 1961-1990 mean) have been recorded. At inland stations, Cedara records mostly negative temperature departures over the period 1960-1981, and above mean conditions since 1981 (with few exceptions; Figure 4.5). The 10-year Gaussian filter for T_{max} indicates broadly warmer times between 1930 and 1963, cooler (below mean) conditions between 1964 and 1975, and a warming trend since 1977 at Mount Edgecombe. A broadly warmer period between 1930 and 1962 is observed at Cedara, followed by below mean conditions until 1981, and thereafter oscillates above average until the end of the record. At Emerald Dale, above mean conditions prevail between 1930 and 1950, with a cooler period until 1982. The most recent decades show smaller T_{max} oscillations for inland stations, with short cooler (below mean) periods between 1987-1991 and 1995-1998. Notably, such cooler episodes are manifested more weakly at the coastal station of Mount Edgecombe (Figure 4.5). While T_{max} at the coast remained above the long-term mean since ca 1977, this has been delayed at adjacent inland sites by ca 21 years (Cedara) to 33 years (at Emerald Dale).



Figure 4.4: T_{max}, T_{min} and T_{mean} for different stations in Pietermaritzburg: a) Mental hospital (1896-1953), b) Purification Works (1970-1992) and c) Pietermaritzburg CBD (1994-2015). The vertical gray lines represent the breaks in the time series.

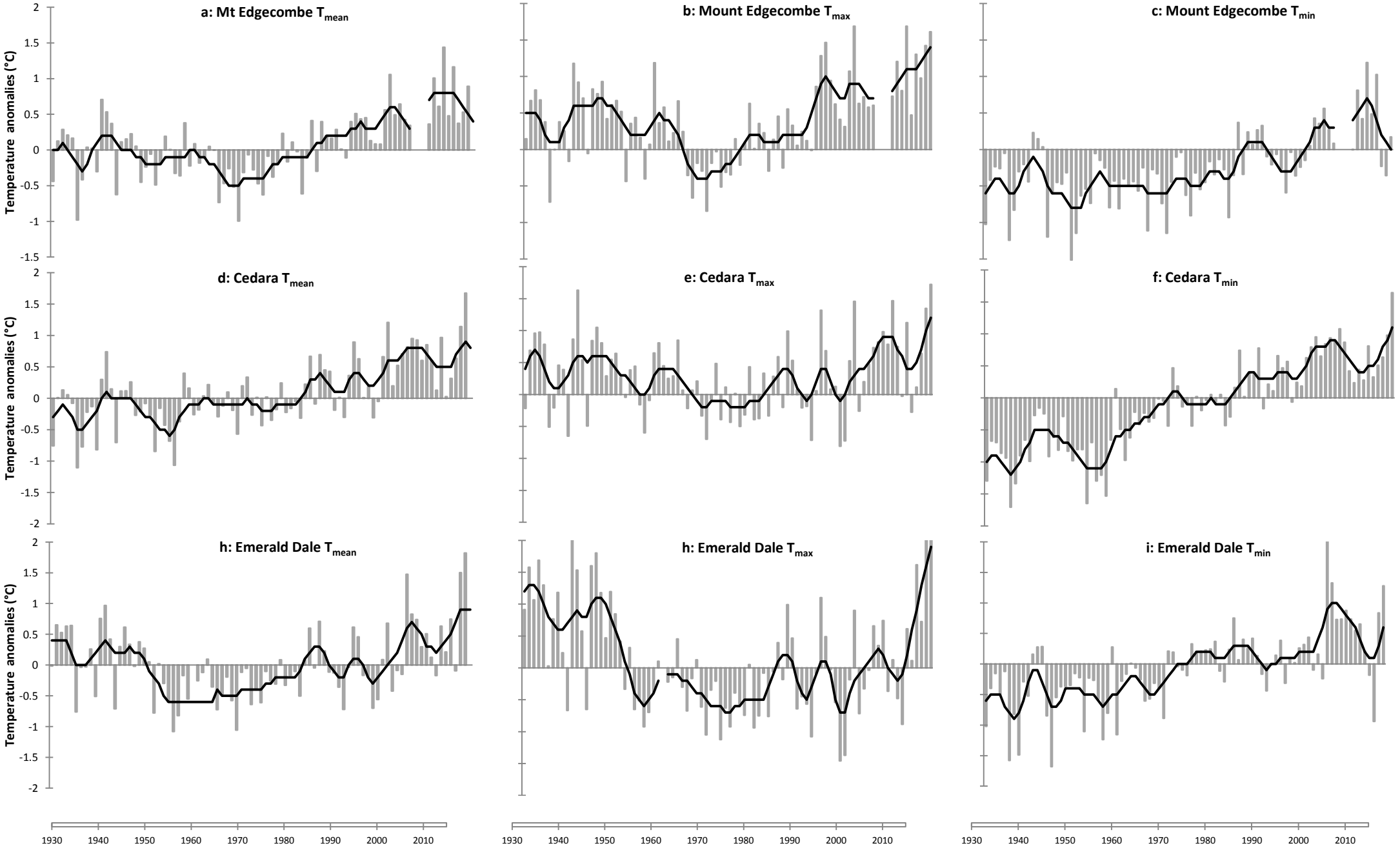

Figure 4.5: Annual T_{mean}, $T_{max,}$ and T_{min} anomalies, with respect to the long term mean (1961-1990) for KZN stations, with the 10 year Gaussian filter.

The Gaussian filters for T_{min}, indicate a broadly cooler period from 1930-1984 at Mount Edgecombe; 1930-1981 at Cedara and 1930-1973 at Emerald Dale. Thereafter, positive departures are recorded at Cedara (1982-2015) and at Emerald Dale (1974-2015). Mount Edgecombe experiences short periods of above (1985-1988) and below (1989-1997) mean departures, a warmer period from 1999-2012, and slight cooling toward the end of the record, possibly due to oceanic moderating effects that only influence the coastal belt (Figure 4.5).

4.5. DISCUSSION

Notwithstanding the challenges and limitations of early (i.e. 19th century) instrumental temperature recordings which likely influence results, this study provides the first, albeit tentative, observations on late 19th century temperatures for KZN, South Africa. A recent 19th century rainfall chronology for KZN identifies the 1850s as the wettest decade, 1851 as a particularly severe wet year, and the years 1865/1866 as a severe drought period (Nash *et al*., 2016). Coincidently, 1851 is the first complete year for which a full set of $T_{max, min}$ data are available for Durban, and notably stands out as the coldest year for which records are available (i.e. 1858, 1884-1906, 1994-2013), with a T_{mean} departure of -1.1°C from the combined average of these years (Table 4.2). While the idea of the Little Ice Age (LIA) being a globally synchronous cold period has been dismissed (Mann, 2002), this coldest year in KZN (i.e. 1851) might indicate considerably cooler conditions during the first half of the 19th C, than times since then. Such LIA cooling is also evident from proxy-based southern African palaeotemperature reconstructions (Nicholson *et al*., 2013). However, one cannot rule out that these early records contain inhomogeneities, which may result in the cooler condition recorded in 1851.

The earliest available temperature record for Pietermaritzburg is from 1858, which was a warm year compared to those for the period 1860-1865, but much colder than mean temperatures between 1994 and 2015 (Table 4.2). The mean temperature departure (from the 1951-1970 mean) for 1858 in the Southern Hemisphere was -0.25°C, while negative departures for 1860-1865 varied between -0.04°C (1865) and -0.47°C (1865) (Jones *et al*., 1986a). The 1860-1865 data available for Pietermaritzburg also record cool temperatures, but 1865 stands out as a particularly warm year (Table 4.2). Given that 1865 was classified as a moderate El Niño year, the particularly warm temperatures may be due to strong and

coherent teleconnections between El Niño and temperature patterns globally and regionally (cf. Gergis and Fowler, 2008). Hence, past broad-scaled Southern Hemisphere temperature chronologies are not necessarily compatible with those in parts of southern Africa. Mean temperatures during the early 1860s were colder than any periods since and could tentatively indicate a terminal LIA stage before the onset of warming to the present day. In contrast, the period 1994-2015 stands out as substantially warmer than any previous period tested in this study.

In the Northern Hemisphere, warming occurred from ~1910 to the mid-1940s, followed by gradual cooling from the mid-1940s to mid-1970s, and rapid warming is reported thereafter (Jones *et al*., 1986b). In contrast, Southern Hemisphere warming was less pronounced between ~1910-1930, but rapid (lagged) warming occurred from 1930 to the mid-1940s, succeeded by an abrupt shift to cooler temperatures after 1945, variable temperatures until the mid-1970s, and gradually increasing temperatures since then (Jones *et al*., 2016). For southern Africa, Kruger and Shongwe (2004) report that mean annual temperatures start increasing during the early 1980s. While the current study records the start of T_{mean} warming at a similar time over the interior (1981 at Cedara), warming at the coast was delayed by a decade (1991 at Mount Edgecombe).

Globally, studies portray inconsistent temperature trends between coastal and adjacent inland stations. Several studies report coastal cooling and strong interior warming over North and South America (Morgan *et al*., 1993; Falvey and Garreaud, 2009; Lebassi *et al*., 2009). Lebassi *et al*. (2009) suggest coastal cooling may be due to greenhouse gas induced global warming over the interior which results in increased sea breeze flow, thus overwhelming warming along the coast. Elsewhere, such as along the Canadian east coast and Mediterranean south coast, coastal warming has generally been slower than over the adjacent interior (Kafle and Bruins, 2009; Tyler *et al*., 2015). The current study finds only marginally faster warming (by 0.01°C) over parts of the KZN interior compared to the coast during the past 85 years. However, more noteworthy is that annual T_{max} and T_{min} have increased at considerably faster rates (by 0.04°C/decade and 0.06°C/decade faster, respectively) over the interior compared to the coast during the most recent 30 years.

The oscillatory temperature characteristics of the current study indicate above average T_{max} for the period 1930-1962/1963 at the coast and at one inland station (Cedara), with transition to below average conditions occurring much sooner (1952) at Emerald Dale. The inconsistency between stations clearly indicates that periods of cooler and warmer conditions are controlled by the geography of place, which may differ considerably over relatively short spatial scales. Such inconsistencies are also noted in the seasonal trends at all stations, for the period 1930-2015. Similarly, Kruger and Shongwe (2004) recorded locational and seasonal variations in South African temperature trends for the period 1960-2003. A previous study reported increasing annual T_{mean}, T_{max} and T_{min} trends at coastal and adjacent interior stations in KZN for the period 1960-2003, with the exception of decreasing T_{mean} and T_{max} trends at Emerald Dale (Kruger and Shongwe, 2004). $T_{mean,}$ T_{max} and T_{min} record increasing trends during all seasons at the coast. However, over the interior of KZN, variable seasonal trends are recorded between stations, with no T_{mean} trends during winter and decreasing T_{max} trends during spring. Notably, significant T_{min} warming trends are recorded at all stations during all seasons, with rates of warming being 1.31 (summer), 2.75 (autumn), 3.33 (winter) and 1.25 (spring) times faster over the interior compared to the coast. Faster warming rates have been reported for the more recent decades over the Northern Hemisphere, Southern Hemisphere as well as globally (Rebetez and Reinhard, 2008). Similarly, this study also records faster warming trends for the most recent decades compared to previous periods over KwaZulu-Natal, South Africa.

Finally, high positive T_{max} departures are noted at Cedara for the years 1985 (mean departure = 1.0°C); 1992 (mean departure = 1.3°C); 1999 (mean departure = 1.5°C) and 2015 (mean departure = 1.7°C), coincidently at 7 year intervals for the first two periods and at 8 year intervals for the following two periods. While 1992 and 2015 coincide with El Niño years, 1985 and 1999 are La Niña years and thus extreme departures are not only associated with a particular phase of ENSO. However, such successive (near perfect 7/8 year cyclic) pulses of record breaking annual T_{max} may be due to a combination of factors operating synergistically (i.e. anthropogenically induced global warming + maximum phases of ENSO). The highest recorded annual T_{max} departures at Mount Edgecombe (mean departure = 1.6°C), Cedara (mean departure = 1.7°C) and Emerald Dale (mean departure = 2°C) also reflect amplified warming/departures over the interior compared to the coast.

4.6. **CONCLUSION**

This paper compares changes in coastal and adjacent (within ~100 km) higher lying interior temperatures over KZN for the period 1851-2015. The most striking characteristic of the results is the considerably faster annual and seasonal warming for higher lying interior regions compared to the adjacent coastal areas over the last 30 years in particular, mainly due to strong T_{min} warming trends over the interior. The recent occurrence of regularly-intervalled high record-breaking positive temperature departures with maximum ENSO phases, is likely associated with the complexities of synergistically operating climate mechanisms (i.e. anthropogenically-induced CO_2 warming or ENSO itself). Yet, the interplay of these mechanisms and how they may collectively influence one another, and ultimately the spatio-temporal differences in regional warming, remains to be fully investigated and understood. Nonetheless, it seems that climate warming trends over relatively small sub-regional scales may continue at disproportionate rates in some global regions, such as coastal and adjacent hinterland regions, especially where these patterns of warming might reinforce or alter local airflow dynamics. Determining the nature of such warming trends at a fine–scale is thus important for appropriate future preparedness and planning, particularly for the agricultural and human/livestock health sectors.

4.7. **ACKNOWLEDGEMENTS**

Thanks to the SAWS for providing temperature data. RL-G appreciates the Research Development Grant provided by the Tshwane University of Technology (TUT), South Africa, the Department of Higher Education and Training and the National Research Foundation (NRF) of South Africa (98258).

4.8. **REFERENCES**

Ageena I, Macdonald N, Morse AP. 2014. Variability of maximum and mean average temperature across Libya (1945–2009). *Theoretical and Applied Climatology* **117**: 549-563.

Aguilar E, Auer I, Brunet M, Peterson TC, Wieringa J. 2003. Guidelines on Climate Metadata and Homogenisation. WCDMP-No. 53, WMO-TD No. 1186, World Meteorological Organization, Geneva, Switzerland.

Ashcroft L, Gergis J, Karoly DJ. 2014. A historical climate dataset for southeastern Australia, 1788–1859. *Geoscience Data Journal* **1**: 158-178.

Baumann H, Doherty O. 2013. Decadal changes in the world's coastal latitudinal temperature gradients. *PlosOne* **8**: e67596. doi:10.1371/journal.pone.0067596

Department of Transport Reports on Meteorological data (1920-1977) The Government Printer, Pretoria. Available online NOAA Central Library http://www.lib.noaa.gov/collections/foreign_climate_data_pages/foreign_climate_data_south_africa.html (Accessed 22 July 2016).

Dube LT, Jury MR. 2000. The nature of climate variability and impacts of drought over Kwazulu-Natal, South Africa. *South African Geographical Journal* **82**: 44-53.

Eeley H A C, Lawes MJ, Piper SE. 1999. The influence of climate change on the distribution of indigenous forest in KwaZulu-Natal, South Africa. *Journal of Biogeography* **26**: 595–617.

Falvey M, Garreaud RD. 2009. Regional cooling in a warming world: Recent temperature trends in the southeast Pacific and along the west coast of subtropical South America (1979–2006*). Journal of Geophysical Research* **114**: 1-16. doi:10.1029/2008JD010519.

Gergis JL, Fowler AM. 2008. A history of ENSO events since A.D. 1525: implications for future climate change. *Climatic Change* **92**: 343-387.

Green AN, Ovechkina MN, Mostovski MB. 2012. Late Holocene shore face evolution of the wave dominated Durban Bight, KwaZulu-Natal, South Africa: A mixed storm and current driven system. *Continental Shelf Research* **49**: 56–64.

Gocic M, Trajkovic S. 2013. Analysis of changes in meteorological variables using Mann-Kendall and Sen's slope estimator statistical tests in Serbia. *Global Planetary Change* **100**: 172–182.

Hanna E, Mernild SH, Cappelen J, Steffen K. 2012. Recent warming in Greenland in a long-term instrumental (1881–2012) climatic context: I. Evaluation of surface air temperature records. *Environmental Research Letters* **7**: 1-16. doi:10.1088/1748-9326/7/4/045404

Hannaford MJ, Nash DJ. 2016. Climate, history, society over the last millennium in southeast Africa. *Wiley Interdisciplinary Reviews: Climate Change* **7**: 370-393.

Holden WC. 1855. History of the Colony of Natal. Heylin, A. London. 10-32. Available online at https://books.google.co.za/books?hl=en&lr=&id=SRRDAAAAcAAJ&oi=fnd&pg=PR1&dq=Holden,+W.C.+1855.+History+of+the+Colony+of+Natal.+Published+by+Heylin,+A.,+London.&ots=Rs3AP3XEPB&sig=JYR5Eu6YRGRS-P7Dyr1ydI5Yofs#v=onepage&q&f=false (Accessed 17 April 2016).

IPCC. 2013. Summary for Policymakers. In: Climate Change 2013: The Physical Science Basis. Contribution of Working Group I to the Fifth Assessment Report of the Intergovernmental Panel on Climate Change (Stocker, TF, Qin D, Plattner G-K, Tignor M, Allen SK, Boschung J, Nauels A, Xia Y, Bex V, Midgley PM (eds.)). Cambridge University Press, Cambridge, United Kingdom and New York, NY, USA. pp. 29.

Jones PD, Raper SCB, Wigley TML. 1986a. Southern Hemisphere surface air temperature variations: 1851-1984. *Journal of Climate and Applied Meteorology* **25**:1213-1230.

Jones PD, Raper SCB, Wigley TML, Diaz HF, Kelly PM Wigley TML. 1986b. Northern Hemisphere surface air temperature varations: 1851-1984. *Journal of Climate and Applied Meteorology* **25**: 161-179.

Jones PD, Moberg A. 2003. Hemispheric and Large-Scale Surface Air Temperature Variations: An Extensive Revision and an Update to 2001. *Journal of Climate* **16**: 206-223.

Jones PD, Parker DE, Osborn TJ, Briffa KR. 2016. Global and hemispheric temperature anomalies—land and marine instrumental records. In *Trends: A Compendium of Data on Global Change*. Carbon Dioxide Information Analysis Center, Oak Ridge National Laboratory, U.S. Department of Energy, Oak Ridge, Tenn., U.S.A. doi: 10.3334/CDIAC/cli.002.

Jury MR. 1998. Statistical analysis and prediction of KwaZulu-Natal climate. *Theoretical and Applied Climatology* **60**: 1-10.

Kafle HK, Bruins HJ. 2009. Climatic trends in Israel 1970-2002: warmer and increasing aridity inland. *Climatic Change* **96**: 63-77.

King'uyu SM, Ogallo LA, Anyamba EK. 2000. Recent trends of minimum and maximum over Eastern Africa. *Journal of Climate* **13**:2876-2886.

Kruger AC, Shongwe S. 2004. Temperature trends in South Africa: 1960–2003. *International Journal of Climatology* **24**: 1929–1945.

Kruger AC, Nxumalo M. 2017. Surface temperature trends from homogenized time series in South Africa: 1931-2015. *International Journal of Climatology* **37:** 2364-2377.

Lakhraj-Govender R, Grab S, Ndebele NE. 2017. A homogenized long-term record for the Western Cape Province in South Africa:1916-2013. *International Journal of Climatology* **37**: 2337-2357.

Landman WA, Kgatuke MJ, Mbedzi M, Beraki A, Bartman A, du Piesanie A. 2009. Performance comparison of some dynamical and empirical downscaling methods for South Africa from a seasonal climate modelling perspective. *International Journal of Climatology* **29**:1535-1549.

Lebassi B, Gonzalez J, Fabris D, Maurer E, Miller N, Milesi, C, Bornstein R. 2009. Observed 1970-2005 cooling of summer daytime temperatures in coastal California. *Journal of Climate* **22**: 3558-3573.

MacKellar N, New M, Jack C. 2014. Observed and modelled trends in rainfall and temperature for South Africa: 1960–2010. *South African Journal of Science* **110**:1-13. http://dx.doi.org/10.1590/sajs.2014/20130353.

McGranahan G, Balk D, Anderson B. 2007. The rising tide: assessing the risks of climate change and human settlements in low elevation coastal zones. *Environment and Urbanization* **19**: 17–37.

Mann RJ. 1859. The Colony of Natal. Jarrod & Sons. pp.47-69. Available online *https://babel.hathitrust.org/cgi/pt?id=uc1.b3983713;view=1up;seq=5*. (Accessed 16 April 2016).

Mann RJ. 1878. Contributions to the meteorology of Natal-Observations taken at Maritzburg. *Quarterly Journal of the Royal Meteorological Society* **4**:173-185.

Mann ME. 2002. Little Ice Age. In MacCraken MC, Perry JS (ed.) The Earth system: physical and chemical dimensions of global environmental change. *Encyclopaedia of Global Environmental Change*. John Wiley & Sons, Chichester, pp. 504-509.

Morgan MR, Drinkwater KF, Pocklington R. 1993. Temperature trends at coastal stations in Eastern Canada. *Climatological Bulletin* **27**: 135-153.

Nash DJ, Pribyl K, Klein J, Neukom R, Endfield, GH, Adamson GCD, Kniveton DR. 2016. Seasonal rainfall variability in southeast Africa during the nineteenth century reconstructed from documentary sources. *Climatic Change* **134**: 605-619.

Nicholson SE, Nash DJ, Chase BM, Grab SW, Shanahan TM, Verschuren D, Asrat A, Lezine AM, Umer M. 2013. Temperature variability over Africa during the last 2000 years. *The Holocene* **23**: 1085–1094.

NOAA National Centers for Environmental Information, State of the Climate: Global Analysis for Annual 2015, published online January 2016, http://www.ncdc.noaa.gov/sotc/global/201513. (Accessed 1 September 2016).

Rabalais NN, Turner RE, Diaz RJ, Justic D. 2009. Global change and eutrophication of coastal waters. *ICES Journal of Marine Science* **66**: 1528–1537.

Reason CJC. 2001. Evidence for the influence of the Agulhas Current on regional atmospheric circulation patterns. *Journal of Climate* **14**: 2769-2778.

Rebetez M, Reinhard M. 2008. Monthly air temperature trends in Switzerland 1901-2000 and 1975-2004. *Theoretical and Applied Climatology* **91**: 27-34.

Rohde R, Muller RA, Jacobsen R, Muller E, Perlmutter S, Rosenfeld A, Wurtele J, Groom D, Wickham C. 2013. A new estimate of the average earth surface land temperature spanning 1753 to 2011. *Geoinformatics and Geostatistics: An overview.* **1:**1-7.

Santos F, Gomez-Gesteira M, Maite deCastro1, Alvarez I. 2012. Variability of Coastal and Ocean Water Temperature in the Upper 700 m along the Western Iberian Peninsula from 1975 to 2006. *PlosOne* **7:** 1-7. doi:10.1371/journal.pone.0050666.

Shahid S, Harun SB, Katimon A. 2013. Changes in diurnal temperature range in Bangladesh during the time period 1961–2008. *Atmospheric Research* **118**: 260-270.

Štěpánek P. 2008. AnClim - software for time series analysis. Dept. of Geography, Faculty of Natural Sciences, MU, Brno. http://www.climahom.eu/AnClim.html. (Accessed 25 June 2015).

Sen PK. 1968. Estimates of the regression coefficient based on Kendall's Tau. *Journal of the American Statistical Association* **63**: 1379–1389.

Tularam GA, Ilahee M. 2010. Time series analysis of rainfall and temperature interactions in coastal catchments. *Journal of Mathematics and Statistics* **6**: 372-380.

Tyler K, White T, Anslow F. 2015. Indicators of Climate Change for British Columbia 2015 Update. Ministry of Environment, Victoria, Canada. pp. 50.

Tyson PD, Preston-Whyte RA. 2000. *The Weather and Climate of Southern Africa*. Oxford University Press Southern Africa, Cape Town.

Venema VKC, Mestre O, Aguilar E, Auer I, Guijarro JA, Domonkos P, Vertacnik G, Szentimrey T, Štěpánek P, Zahradnicek P, Viarre J, Muller-Westermeier G, Lakatos M, Williams CN, Menne MJ, Lindau R, Rasol D, Rustemeier E, Kolokythas K, Marinova T, Andresen L, Acquaotta F, Fratianni S, Cheval S, Klancar M, Brunetti M, Gruber C, Prohom Duran M, Likso T, Esteban P, Brandsma T. 2012. Benchmarking monthly homogenisation algorithms. *Climate of the Past Discussions* **7**: 2655–2718.

Wang XL, Chen H, Wu Y, Feng Y, Pu Q. 2010. New techniques for detection and adjustment of shifts in daily precipitation data series. *Journal of Applied Meteorology and Climatology* **49**: 2416-2436.

XLSTAT. 2015. Available online: https://www.xlstat.com/en/ (Accessed 2 January 2014).

Yue S, Wang C. 2004. The Mann-Kendall Test Modified by Effective Sample Size to Detect Trend in Serially Correlated Hydrological Series. *Water Resources Management* **18**: 201–218.

CHAPTER FIVE

ASSESSING THE IMPACT OF ENSO ON SOUTH AFRICAN TEMPERATURES: 1884-2016

5.1. ABSTRACT

Using composite and Fourier analysis, the timing and extent of El Niño-Southern Oscillation (ENSO) impacts on maximum temperature (T_{max}) and minimum temperature (T_{min}) is investigated for South Africa over the period 1940-2016. Monthly composites of stations with the longest records (1884-2016) cover up to 23 El Niño and 15 La Niña events, while the Index Time Series (ITS) (1940-2016) cover 16 El Niño and 9 La Niña events. Spatial coherence for T_{max}/T_{min} over the different regions of South Africa varies between 0.99 - 1.00 during both ENSO phases. T_{max}/T_{min} responses to El Niño over the northern interior region record above median temperature for the period October (0) - March (+), while that for the remaining regions are delayed by one or two months. Higher temporal consistency rates (38%-82%) are noted for T_{max}/T_{min} for El Niño events compared to that for La Niña events, which are lower (33%-56%). The probability of a random occurrence of the signal period during El Niño/La Niña phases, based on the hypergeometric distribution, indicate a statistically significant relationship with high significance levels (99.7% - 99.99%) for all regions. This is based on a very low chance of random occurrence of the ITS value above/below the median. Strong coherent relationships exist between ENSO events and T_{max}/T_{min} over South Africa. To further investigate the impact of ENSO events on South African temperature, contingency tables were constructed for each station during the austral summer season (December, January and February) and analysed using the Chi-squared statistic. The most notable finding of this study is that El Niño events have had a stronger warming effect over many regions in South Africa after the late 1970s. The most prominent regions are the northern interior and southeast coast, where associated T_{max} record an average of 0.41°C and 0.45°C, respectively, higher values for the period 1979-2016 compared to the earlier period (1940-1978). The Chi-squared statistic results reflect the findings of the composite analysis, indicating that ENSO phases exert a stronger influence over the interior of South Africa compared to that over the coast.

Keywords: El Niño, La Niña, teleconnections, surface air temperature, South Africa.

5.2. INTRODUCTION

The El Niño-Southern Oscillation (ENSO) is now widely known for its strong and globally distributed climatic influence. This phenomenon occurs as a product of fluctuating equatorial Pacific Ocean temperatures (extending from the coast of Peru to the International Date Line) and large-scale air pressure changes known as the Southern Oscillation (Bartholomew and Jin, 2013; WMO, 2014). ENSO consists of two components - El Niño (warm phase) and La Niña (cold phase), which occur approximately every 2 to 7 years (McPhaden *et al*., 2006). Although ENSO phases display an irregular periodicity, the El Niño phase typically lasts a shorter duration (9-12 months) compared to La Niña phases, which may last 1-2 years (Warner and Oberheide, 2014). However, El Niño phases occur more frequently (31% of the time) than La Niña (23% of the time), while neutral conditions account for the remaining 56% of time over the period 1950-1997 (Trenberth, 1997; Welhouse *et al*., 2016). El Niño is generally associated with higher than usual temperature globally while La Niña is often (but not always) linked to below normal temperature on land (Davey *et al*., 2014). These phases disturb global atmospheric circulation, thereby affecting weather variability patterns and the probability of floods, drought, heat waves and other extreme events. In addition, ENSO influences global mean surface air temperature changes due to heat exchanges across and between the atmosphere, oceans and land (Trenberth *et al*., 2002; McPhaden *et al*., 2015).

Previous studies have reported strong and coherent teleconnections between ENSO and temperature patterns, both globally (Cai *et al*., 2014; WMO, 2014; Banholzer and Donner, 2014) and regionally (e.g. Jones and Trewin, 2000; Barros *et al*., 2002; Soltani and Gholipoor, 2006; Chowdary *et al*., 2014). The impact of different ENSO events on regional and global temperature is not always the same because the intensity and timing of each event as well as the interaction with other climatic factors varies with each event (WMO, 2014). For instance, the 1982-1983 and 1997-1998 El Niño events severely disrupted global weather, leading to major natural disasters (e.g. floods in the eastern equatorial region of Ecuador and northern Peru) (Cai *et al*., 2014). In addition, the strong El Niño events in 1997-1998 and 2009-2010 resulted in the years 1998 and 2010 recording global temperature departures of ~0.52°C and 0.55°C above the 1961-1990 long-term average, respectively (WMO, 2014). The 2015-2016 El Niño event is comparable in strength to the previous 1982-1983 and 1997-1998 strong events (WMO, 2016). This recent event resulted in the year 2016

being reported as the hottest year (globally) since 1880, with globally averaged temperatures being 0.99°C above the 1951-1980 average (Potter *et al*., 2017).

ENSO is well-known for its significant impacts over southern Africa, with regional and inter-event variations. For instance, the 1991-1992 and 2002-2003 El Niño events were associated with severe drought whereas dry conditions were less intense during the 1997-1998 El Niño (Reason and Jagadheesha, 2005). However, southern African ENSO studies have placed greater emphasis on the relationship between ENSO and rainfall, rather than temperatures (Schulze, 1986; Lindesay, 1988; Van Heerden *et al*., 1988; Kruger, 1999; Reason and Rouault, 2002; Landman and Beraki, 2012; Philippon *et al*., 2012; Weldon and Reason, 2014).

Halpert and Ropelewski (1992) first reported teleconnections between ENSO events and southeast African temperature. Although, more recently, Kruger and Shongwe (2004) examined the correlation between average late summer NINO3 sea surface temperatures (SSTs) and late summer temperatures (January - March), the study only investigated eight stations in the central part of South Africa (i.e. Upington, Vanwyksvlei, Armoedsvlakte, Glen College, Bloemfontein, Addo, Cedara and Emerald Dale), and for a relatively short period (1960-2003). Using regression analysis, Kruger and Shongwe (2004) report that El Niño and La Niña do not play a significant role in late summer temperature increases. Yet, Manatsa and Reason (2017) report a strong ENSO influence on maximum surface air temperature (SAT_{max}) over southern Africa during late austral summer.

Despite some past investigations on the impacts of ENSO on southern African temperatures, no previous study has investigated the impact of such phases on both maximum (T_{max}) and minimum (T_{min}) temperatures using long-term quality controlled and homogenized data over the broader South African region. To this end, the aim of this study is to determine the impact (i.e. timing and amplitude) of El Niño/La Niña phases on T_{max}/T_{min} at various localities in South Africa for a longer period (1884-2016) compared to previous studies, using composite and Fourier analysis. In addition, the impact of El Niño/ La Niña phases on temperature variables for the periods 1940-1978 and 1979-2016 is compared to determine possible changes in the strength of influence over time.

5.3. METHODS

5.3.1. Study area and data

The climate over southern Africa is influenced by major atmospheric operating systems such as the Intertropical Convergence Zone (ITCZ), subtropical cyclones, jet streams and teleconnections with regional and large scale quasi-periodic climate systems (e.g. Quasi-Biennial Oscillation (QBO), intraseasonal waves and ENSO) (Tyson and Preston-Whyte, 2000). The warm southerly moving Mozambique and Agulhas currents play a strong role in moderating temperatures along the east coast of southern Africa, while the cold northerly moving Benguela current has a cooling effect along the west coast of the subcontinent. South Africa's climate ranges from Mediterranean in the southwest, to temperate over the interior plateau, and subtropical in the northwest and along the northeast coast (Tyson and Preston-Whyte, 2000). In this study, the Skukuza, Warmbad and Messina stations represent the northern interior region of South Africa, while Vryburg, Marico, Kimberely, Glen College and Zuurbekom stations represent the central interior (Figure 5.1). Pofadder and Vanwysksvlei stations represent the western interior region, while the eastern summer rainfall region is divided into the northeast coast (i.e. Mount Edgecombe) and the northeastern interior (i.e. Cedara), each only represented by one station given the absence of reliable long-term datasets. The southeast coastal region which receives year-round rainfall is represented by East London and Port Elisabeth (hereafter referred to as the southeast coast). The South African Astronomical Observatory, Cape Agulhas and Cape Columbine stations were selected to represent the winter rainfall region in the Western Cape Province (hereafter referred to as the southwest coast) (Table 5.1 and Figure 5.1). These stations were selected based on availability of long-term surface temperature data with minimal gaps and with suitable spatial coverage across South Africa.

Monthly T_{max} and T_{min} for South Africa were obtained from the South African Weather Services (SAWS). Temperature data were quality controlled and homogenized using ProClimDB and AnClim (see Lakhraj-Govender *et al*., 2017). Standardized monthly T_{max}/T_{min} are statistically analyzed for various sub-regions, specifically in the context of El Niño and La Niña phases for the period 1884- June 2016 (Table 5.2). The longest record (Cape Agulhas: 1884-2016) captures 23 El Niño and 15 La Niña phases, while the majority of other stations capture 16 El Niño and 9 La Niña phases between 1940 and 2016. According to Halpert and Ropelewski (1992), for a station to be included in composite

analysis, the period of analysis must cover a minimum of five warm phases or five cold phases.

Several indices have previously been used to measure ENSO, including the normalized Tahiti minus Darwin pressure difference, also called the 'Troup' Southern Oscillation Index (SOI) (Jones and Trewin, 2000), Multivariate ENSO Index (Hänsel *et al*., 2016) and the Oceanic Niño Index (ONI) (Warner and Oberheide, 2014), to name a few. The SOI is used in this study to select El Niño and La Niña phases, since the index covers a longer period (Table 5.2). The SOI, calculated as the difference in standardized pressure between Tahiti and Darwin, is derived from the Climate Research Unit (CRU) at the University of East Anglia in England (http://www.cru.uea.ac.uk/cru/data/soi.htm - based on Allan *et al*., 1991) for the period 1866-2015, while values for 2016 were obtained from the National Oceanic and Atmospheric Administration (NOAA) website: (http://www.esrl.noaa.gov/psd/gcos_wgsp/Timeseries/Data/tni.long.data).

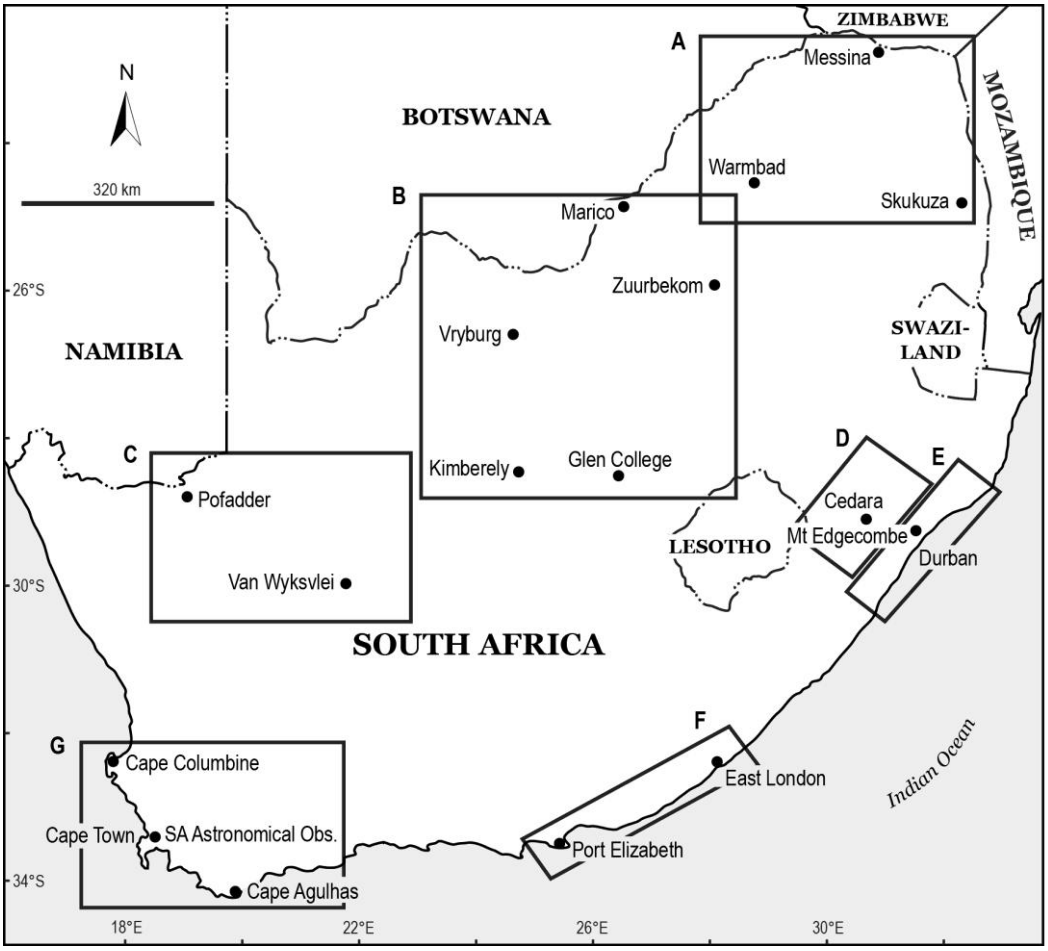

Figure 5.1: Map showing location of South African temperature stations used in this study. The boxes labeled A-G represent the different regions in South Africa.

Table 5.1: South African stations, detailing GPS coordinates and start/end dates for each station.

Province	Station	Start year	End year	Latitude (deg. S)	Longitude (deg. E)	Altitude (m. a.s.l.)
Northern interior						
Mpumalanga	Skukuza	1941	2016	-24.99	31.59	263
Limpopo	Warmbad	1937	2016	-24.90	28.33	1143
Limpopo	Messina	1934	2016	-22.27	29.90	538
Central interior						
North West	Vryburg	1920	2016	-26.95	24.65	1234
North West	Marico	1934	2016	-25.50	26.35	1078
Northern Cape	Kimberley	1940	2016	-28.80	24.80	1196
Free State	Glen College	1915	2016	-28.95	26.33	1303
Gauteng	Zuurbekom	1910	2016	-26.30	27.80	1578
Western interior						
Northern Cape	Vanwyksvlei	1926	2016	-30.35	21.80	962
Northern Cape	Pofadder	1940	2016	-29.12	19.39	982
Northeastern interior						
KwaZulu-Natal	Cedara	1930	2016	-29.54	30.27	1071
Northeast coast						
KwaZulu-Natal	Mount Edgecombe	1930	2016	-29.70	31.05	103
Southeast coast						
Eastern Cape	East London	1940	2016	-33.03	27.83	116
Eastern Cape	Port Elizabeth	1940	2016	-33.98	25.60	63
Southwest coast						
Western Cape	SA Astronom.	1933	2016	-33.56	18.28	15
Western Cape	Cape Agulhas	1884	2016	−34.49	20.01	11
Western Cape	Cape Columbine	1937	2016	−32.49	17.51	62

Table 5.2: List of ENSO episode years (Year 1) included in this study.

El Niño			La Niña	
1888	1951	1987	1889	1973
1896	1953	1991	1893	1975
1905	1957	1993	1910	1988
1911	1963	1997	1917	1998
1914	1965	2002	1928	2000
1919	1972	2009	1938	2008
1923	1977	2015	1964	2010
1941	1982		1971	

5.3.2. Composite and Fourier analysis

Regions with consistent SO-temperature relationships are identified using composite and Fourier analysis. Recent studies (e.g. Fogt *et al*., 2011; McAfee and Wise, 2016) have analyzed composites of El Niño and La Niña phases separately, which is valuable for determining distinct features of each ENSO phase (Welhouse *et al*., 2016). Composite analysis is considered a superior method compared to correlating ENSO teleconnections (Fogt *et al*., 2011). Correlation does not offer insight into the magnitude of each event and is also influenced by outliers (Fogt *et al*., 2011). For instance, colder/warmer winters over northern Europe are associated with El Niño/La Niña phases (Scaife, 2010). However, interannual correlation coefficients between Europe/Atlantic climate and ENSO seem small (Scaife, 2010). This is possibly due to other influences on seasonal climate for the highly variable climate over this region. However, Scaife (2010) cautions against confining composites for ENSO to the definition of a season (e.g. austral summer is defined DJF). Therefore, 24-month standardized temperature ENSO composites were produced for a 2-year period starting in July preceding the episode (denoted July (-)) and follow through to June (+) the year after the event (Mohsenipour *et al*., 2013; Lee and Julien, 2016a, b). Composites of temperatures are computed independently when the warm/cold phase of ENSO occurred in consecutive years (e.g. 1997 and 1998) (Banholzer and Donner, 2014).

Based on the Standardized Precipitation Index (SPI) calculation by McKee *et al.* (1993), monthly temperature data are transformed into a Standardized Temperature Index (STI), whereby T_{max} and T_{min} are fitted to a normal distribution and transformed into a cumulative density function, with a mean of zero and a standard deviation of one. The resulting standard deviates are used to create composites (Lee and Julien, 2016a).

ENSO composites were subjected to Fourier analysis using XLSTAT 2015, to extract harmonic information such as amplitudes and phase angles of the first harmonic of the ENSO cycle. Fourier analysis decomposes time series into time-frequency space and extracts information about the persistent oscillations or recurrent temperature variations (Humlum *et al*., 2012). Amplitude represents the magnitude of the temperature response and the phase indicates the time when a maximum departure from the mean occurs (Mohsenipour *et al*., 2013; Lee and Julien, 2016a). The coherence is estimated with the average vector ([V]) and the average of the individual vector magnitudes (S).

Coherence is calculated as:

$$C = \frac{[V]}{S}, \quad (1)$$

where,

$$[V] = \frac{[(\sum V \cos\theta)^2 + (\sum V \sin\theta)^2]^{1/2}}{L} \quad (2)$$

and S is the scalar mean (i.e. scalar sum divided by the total number of vectors (L)).

$$S = \frac{\sum V}{L} \quad (3)$$

V is the magnitude of the vector and θ is the direction measured clockwise from north. A coherence value equal to or greater than 0.80 is chosen to eliminate inconsistent amplitudes and phases to identify a candidate region (Ropelewski and Halpert, 1986; Kahya and Dracup, 1993). A coherence of zero denotes a group of vectors with the same magnitude but different directions, while a value of one indicates all vectors have the same direction (Lee and Julien, 2016a). Coherence rates could not be calculated for regions represented by individual stations.

5.3.3. Season selection

All ENSO composites in a candidate region are averaged to create aggregate composite series (Figure 5.2 to Figure 5.7). The phase angle of Fourier analysis determines the time of maximum response (Mohsenipour *et al*., 2013) and the signal period is selected from the aggregate composite, where a group of temperature departures have the same sign for more than four consecutive months (Lee and Julien, 2016a; 2016b). Overlapping El Niño and La Niña phases must be taken into account when selecting the signal period (Dracup and Kahya, 1994). The length of the composite is chosen as a 24-month rather than 36-month composite, so as to reduce the risk of El Niño and La Niña event overlap and incorrect signal detection (Kahya and Dracup, 1993; Mohsenipour *et al*., 2013).

5.3.4. Index Time Series and core regions

Index Time Series (ITS) are created using the signal period selected from the aggregate composite for 1940-2016. Given that the selected period for the El Niño-temperature response spans the years (0) and (+), the year (+) is marked for the ITS. The statistical

significance of the ENSO-temperature relationship is determined using a hypergeometric distribution, which determines the cumulative probability (P_h) that there are at least *m* successes in *n* trials from a finite population of size *N* containing *k* successes (Haan, 1977; Grimm and Tedeschi, 2009; Tedeschi *et al*., 2015). This test calculates the probability of random occurrence of the signal period during an ENSO event, and has been used to calculate the significance of the composites in several previous studies (Halpert and Ropelewski, 1992; Grimm and Tedeschi, 2009; Tedeschi *et al*., 2013, 2015). "N" is the total number of ITS values (N = 76 in this study), "n" is the number of warm or cold events (n = 11 for La Niña and 16 for El Niño events), "m" is the number of years when the ITS value associated with an El Niño or La Niña event is greater (lower) than the median for a signal season. A success (*k*) is defined as the occurrence of an ITS value either above or below the median (Ropelewski and Halpert, 1986; Dracup and Kahya, 1994; Tedeschi *et al*., 2015; Lee and Julien, 2016a). Core regions are determined using the rate of temporal consistency.

5.3.5. Assessing temperature response to El Niño and La Niña phases through time

The selection of the two epochs (1940-1978 and 1979-2016) is based on the midpoint of the complete dataset (1940-2016) for majority of stations, which coincides with the increased frequency of El Niño phases and decreased frequency of La Niña phases since the late 1970s (Kane, 2009). Warming/cooling rates were determined using Mann Kendall statistics for all years and for specific El Niño and La Niña phases for the detected signal period. The difference between the average warming/cooling for ENSO phases and the general warming for all years provides an estimate of the relative impact ENSO has for each period (i.e. 1940-1978 and 1979-2016). A comparison of the relative impacts between the two periods is then made to determine possible changes in the strength of ENSO influence (positive or negative) through time over various sub-regions of South Africa. The final strengthening/weakening value is only deemed to be significant if the average warming/cooling for all years and ENSO years in both epochs are significant.

5.3.6. Contingency table and Chi-square test

The austral summer (December, January and February) is used for this part of the analyses as this is a common period identified during the season selection of the composite analysis. The temperature data were detrended using differencing, to remove the long-term trend. Twenty five percent and seventy five percent are selected as thresholds for SOI data; therefore the number of El Niño phases is the same as that for La Niña phases, which is 19. The T_{max}/T_{min}

data for the 76 year period (1940-2016) are divided into terciles where the number of high and low years is the same (i.e. 25 years). To analyse the degree of independance of two variables (i.e. El Niño/La Niña/neutral vs. T_{max}/T_{min} anomalies) 3X3 contingency tables were constructed by counting the number of high/low years corresponding to El Niño/La Niña/neutral years. This method does not have assumptions about the distribution or climate averaging periods (Davey *et al*., 2014). The chi-square test is a nonparametric statistical analysis used to assess the probability of association or the independence of ENSO phases and temperature. The chi-square statistic, quantified from the contingency table, is calculated as follows:

$$X^2 = \sum_{i=1}^{3} \sum_{j=1}^{3} \cdot \frac{(O_{ij} - E_{ij})^2}{E_{ij}},$$

where *i* is the row indicator, *j* is the column indicator and O_{ij} and *Eij* are the observed and expected counts, respectively. When any cell deviates substantially from the expected count resulting in a large chi-squared value, there is a lower probability that the null hypothesis of independant (Fogt *et al*., 2011). For the Chi-squared test to be used with confidence, the theoretical count must be greater than 5. The Fisher's exact test is normally employed for data sets that are not large, therefore this study presents the results of both these tests. The strengthening/weakening influence of El Niño phase was also investigated for the austral summer season using the two epochs (1940-1978 and 1979-2016) as previously selected.

5.4. RESULTS

The South African stations in this study are divided into regions (i.e. northern interior, central interior, western interior, northeastern interior, northeast coast, southeast coast and southwest coast) based on location (see Table 5.1 for the stations included in each region). The sections below present the El Niño-T_{max}/T_{min} response over the different regions, and finally the La Niña - T_{max}/T_{min} response over the aforementioned regions (see Tables 5.3 and 5.4). Following the establishment of an ENSO-temperature related response, the strength of El Niño/La Niña temperature response over time is presented.

5.4.1. Northern interior region

For El Niño, the spatial coherence rates are 1.00 and 0.99 for T_{max} and T_{min} over the northern interior region, respectively. The aggregate composite series indicate above median T_{max} for October (0) to March (+), denoted by the dashed box in Figure 5.2(a). The period September (0) to March (+) for T_{max} has a lower temporal consistency rate compared to the period October (0) to March (+). The months marginally above/below normal ($<\pm 0.40$°C) were thus not included in the subsequent selection of a signal period. The signal period is a combination of months from consecutive years (i.e. the (0) and (+) years); therefore the year after the selected El Niño event is shown in the ITS. The ITS for the T_{max} signal period displays 11 (out of 16) El Niño phases associated with positive departures, resulting in a 69% rate of temporal consistency (Figure 5.2(b), Table 5.3).

For the T_{min} aggregate El Niño composite over the northern interior region, October (0) - March (+) was identified as the period of El Niño-temperature response (Figure 5.2(c)). The detected signal period identified by composite analysis illustrates that nature does not comply with human definition of seasons. The ITS for T_{min} also indicate above median temperatures for 13 of 16 El Niño phases, also resulting in the highest temporal consistency rate of 82% in South Africa (Figure 5.2(d), Table 5.3). The El Niño-T_{max}/T_{min} relationships over the northern interior are highly significant at 99.96% and 99.99%, respectively, based on a low chance of random occurrence of the selected period (Table 5.4). The northern interior region thus has a strong and consistent teleconnection between El Niño and T_{max}/ T_{min}.

The La Niña spatial coherence rates over the northern interior region are 1.0 for both T_{max} and T_{min}. The aggregate ENSO composite indicate below median T_{max} and T_{min} for the period May (0) - August (0) (Figures 2e and g). ITS for the signal period record 5 out of 9 below median La Niña years for both T_{max} and T_{min}, indicating a consistency rate of 56% (Figures 5.2(f) and (h); Table 5.3). One of the 9 La Niña phases for T_{min} is, however, only marginally above median (i.e., 1998 (0.03°C)) (Figure 5.2(h)). The relationships between La Niña phases and T_{max}/T_{min} are highly significant at 99.78% and 99.76%, respectively (Table 5.4).

Table 5.3: Temporal consistency rates and coherence rates for each region.

Event	Region	T_{max}/ T_{min}	Season	Total episodes	Coherence rates	Number of phases	Consistency
El Niño							
	Northern interior	T_{max}	October (0)-March (+)	16	1.00	11	69%
	Northern interior	T_{min}	October (0)-March (+)	16	0.99	13	82%
	Central interior	T_{max}	October (0)-March (+)	16	1.00	11	69%
	Central interior	T_{min}	November (0)-March (+)	16	0.99	10	63%
	Western interior	T_{max}	December (0)-March(+)	16	1.00	8	50%
	Western interior	T_{min}	December (0)-April (+)	16	0.99	6	38%
	Northeastern interior	T_{max}	December (0)-March(+)	16	-	11	69%
	Northeastern interior	T_{min}	November (0)-March(+)	16	-	10	63%
	Northeast coast	T_{max}	December (0)-April (+)	16	-	11	69%
	Northeast coast	T_{min}	December (0)-April (+)	16	-	13	82%
	Southeast coast	T_{max}	December (0)-April (+)	16	1.00	9	56%
	Southeast coast	T_{min}	December (0)-March(+)	16	0.99	9	56%
	Southwest coast	T_{max}	December (0)-April (+)	16	0.99	9	57%
	Southwest coast	T_{min}	December (0)-March(+)	16	0.99	10	63%
La Niña							
	Northern interior	T_{max}	May (0)-August (0)	9	1.00	5	56%
	Northern interior	T_{min}	May (0)-August (0)	9	1.00	5	56%
	Central interior	T_{max}	May (0)-August (0)	9	1.00	3	33%
	Central interior	T_{min}	May (0)-August (0)	9	1.00	4	44%
	Western interior	T_{max}	May (0)-September (0)	9	1.00	5	55%
	Western interior	T_{min}	June (0)-September (0)	9	1.00	5	55%
	Northeastern interior	T_{max}	May (0)-August (0)	9	-	5	55%
	Northeastern interior	T_{min}	May (0)-August (0)	9	-	4	44%
	Northeast coast	T_{max}	June (0)-October (0)	9	-	4	44%
	Northeast coast	T_{min}	May (0)-September (0)	9	-	4	44%
	Southeast coast	T_{max}	June (0)-October (0)	9	1.00	4	44%
	Southeast coast	T_{min}	May (0)-September (0)	9	1.00	5	56%
	Southwest coast	T_{max}	June (0) - September (0)	9	0.99	3	33%
	Southwest coast	T_{min}	June (0) - September (0)	9	1.00	4	44%

5.4.2. Central interior

For El Niño, the central interior region has spatial coherence rates of 1.00 and 0.99 for T_{max} and T_{min}, respectively. The aggregate T_{max} and T_{min} composite series for the central interior region display above median temperatures for the periods October (0) to March (+) and November (0) to March (+), respectively (Figures 5.3(a) and 5.3(c)). The ITS indicate above median T_{max} for 11 (out of 16) El Niño phases, resulting in a temporal consistency rate of

69% (Figure 5.3(b) and 5.3(d)). The ITS indicate above median T_{min} for 10 (out of 16) El Niño phases resulting in a temporal consistency rate of 63%. The central interior is a region with strong and consistent teleconnection between El Niño and T_{max}/T_{min}.

For La Niña phases, the spatial coherence rates over the central interior are 1.00 for both T_{max} and $T_{min.}$ The aggregate La Niña composite indicate below median T_{max} and T_{min} for the period May (0) - August (0) (Figures 5.3(e) and 5.3(g)). The ITS for this signal period record below median T_{max} for 3 (out of 9) La Niña phases, resulting in a low temporal consistency rate of 33%. The temporal consistency rate is slightly higher for T_{min} (44%) (Figures 5.3(f) and 5.3(h); Table 5.3). The relationships between La Niña phases and T_{max}/T_{min} are highly significant at 99.8% and 99.7%, respectively, even though the temporal consistency rates are low (Table 5.4).

5.4.3. Western interior

For El Niño, the western interior has spatial coherence rates of 1.00 and 0.99 for T_{max} and T_{min}. The aggregate T_{max} and T_{min} composite series display above median temperature for the period December (0) - March (+) and December (0) - April (+), respectively (Figure 5.4(a) and 4c). The ITS indicate above median T_{max} for 8 (out of 16) El Niño phases while that for T_{min} is 6 (out of 16) phases (Figure 5.4(b) and 5.4(d)). The lowest temporal consistency rates in South Africa are noted over the western interior for T_{max}/T_{min} at 50% and 38%, respectively (Table 5.3).

The spatial coherence rates over the western interior are 1.00 for both T_{max} and $T_{min.}$ The aggregate La Niña composite indicate below median T_{max} and T_{min} for the period May (0) - August (0) and June (0) - September (0), respectively (Figures 5.4(e) and 5.4(g)). The ITS for this signal period record below median T_{max} and T_{min} for 5 (out of 9) La Niña phases, with a temporal consistency rate of 55% (Figures 5.4(f) and 5.4(g); Table 5.3). The hypergeometric test indicates significant relationships at 99.74% between La Niña phases and both T_{max}/T_{min} (Table 5.4).

Table 5.4: Probability of random occurrence based on the hypergeometric distribution for El Niño and La Niña phases.

Event	**Region**	**T_{max}/ T_{min}**	**N**	**k**	**n**	**m**	**P_h**
El Niño	Northern interior	T_{max}	76	36	16	11	0.04
El Niño	Northern interior	T_{min}	76	38	16	13	0.004
El Niño	Central interior	T_{max}	76	38	16	11	0.06
El Niño	Central interior	T_{min}	76	38	16	10	0.12
El Niño	Western interior	T_{max}	76	38	16	8	0.22
El Niño	Western interior	T_{min}	76	35	16	6	0.17
El Niño	Northeastern interior	T_{max}	76	37	16	11	0.05
El Niño	Northeastern interior	T_{min}	76	37	16	10	0.10
El Niño	Northeast coast	T_{max}	76	39	16	11	0.007
El Niño	Northeast coast	T_{min}	76	38	16	13	0.004
El Niño	Southeast coast	T_{max}	76	38	16	11	0.12
El Niño	Southeast coast	T_{min}	76	38	16	12	0.02
El Niño	Southwest coast	T_{max}	76	36	16	9	0.16
El Niño	Southwest coast	T_{min}	76	36	16	10	0.09
La Niña	Northern interior	T_{max}	76	38	9	5	0.26
La Niña	Northern interior	T_{min}	76	38	9	5	0.26
La Niña	Central interior	T_{max}	76	37	9	3	0.18
La Niña	Central interior	T_{min}	76	38	9	4	0.27
La Niña	Western interior	T_{max}	76	38	9	5	0.26
La Niña	Western interior	T_{min}	76	38	9	4	0.26
La Niña	Northeastern interior	T_{max}	76	38	9	5	0.26
La Niña	Northeastern interior	T_{min}	76	36	9	3	0.19
La Niña	Northeast coast	T_{max}	76	43	9	4	0.21
La Niña	Northeast coast	T_{min}	76	41	9	4	0.23
La Niña	Southeast coast	T_{max}	76	37	9	4	0.27
La Niña	Southeast coast	T_{min}	76	38	9	5	0.26
La Niña	Southwest coast	T_{max}	76	38	9	3	0.16
La Niña	Southwest coast	T_{min}	76	37	9	4	0.26

5.4.4. Northeastern interior

For El Niño, the spatial coherence rates over the Northeastern interior could not be calculated because only one station was available for the region. The aggregate T_{max} and T_{min} composite series display above median temperature for the period December (0) - March (+) and November (0) - March (+), respectively (Figures 5.5(a) and 5.5(c)). The ITS indicate above median T_{max} for 11 (out of 16) El Niño phases resulting in a temporal consistency rate of 69%

(Figures 5.5(b) and 5.5(d)). Above median T_{min} were recorded for 10 (out of 16) El Niño phases, resulting in a 63% temporal consistency rate.

The aggregate La Niña composites indicate below median T_{max} and T_{min} for the period May (0) - August (0) (Figures 5.5(e) and 5.5(g)). The ITS for this signal period record below median T_{max} for 5 (out of 9) La Niña phases, with a temporal consistency rate of 55% (Table 5.3). The temporal consistency rate is slightly lower for T_{min} at 44%, with 5 La Niña phases being below median (Figures 5.5(f) and 5.5(h)). The hypergeometric distributions indicate that relationships between La Niña phases and T_{max}/T_{min} are significant at 99.7% and 99.8%, respectively (Table 5.4).

5.4.5. Northeast coast

For El Niño, the spatial coherence rates over the northeast coast could not be calculated because only one station was available for the region. The aggregate T_{max} and T_{min} composite series display above median temperature for the period December (0) to April (+) for both variables (Figures 5.6(a) and 5.6(c)). The ITS indicate above median T_{max} for 11 (out of 16) El Niño phases resulting in a temporal consistency rate of 69% (Figure 5.6(b)). The ITS for T_{min} show above median T_{min} for 13 (out of 16) El Niño phases at a temporal consistency rate of 82% (Figure 5.6(d); Table 5.3). Notably, together with the T_{min} response over the northern interior, 82% is the highest regional temporal consistency rate measured in South Africa. The relationships between El Niño phases and T_{max}/T_{min} are both highly significant at 99.9%, based on a low probability of random occurrence (Table 5.4). The northeast coastal region thus has a strong and consistent teleconnection between El Niño and T_{max}/ T_{min}.

The aggregate La Niña composite indicates below median T_{max} and T_{min} for June (0) - October (0) and May (0) - September (0), respectively (Figures 5.6(e) and 5.6(g)). The ITS for this signal period record below median for 4 (out of 9) La Niña phases, indicating a temporal consistency rate of 44% for T_{max} and $T_{min,}$(Figures 5.6(f) and 5.6(h)). The relationships between La Niña phases and T_{max}/T_{min} are significant at 99.79% and 99.77% (Table 5.4).

5.4.6. Southeast coast

For El Niño, the spatial coherence rates over the southeast coast are 1.00 and 0.99 for T_{max} and T_{min}. The aggregate T_{max} and T_{min} composite series display above median temperature for

the period December (0) to April (+) and December (0) to March (+), respectively (Figures 5.7(a) and 5.7(c)). The ITS indicate above median T_{max} and T_{min} for 9 (out of 16) El Niño phases resulting in a temporal consistency rate of 56% for both variables (Figure 5.7(b) and 5.7(d)). The relationships between El Niño phases and T_{max} /T_{min} are highly significant at 99.88% and 99.98%, respectively, based on a low probability of random occurrence (Table 5.4).

The spatial coherence rates for La Niña phases over the southeast coast are 1.00 for both T_{max} and T_{min}. The aggregate T_{max} and T_{min} composite series display below median temperature for the period June (0) - October (0) and May (0) - September (0), respectively (Figures 5.7(e) and 5.7(g)). The ITS indicate below median T_{max} for 4 (out of 9) La Niña phases resulting in a temporal consistency rate of 44% (Figure 5.7(f)). The temporal consistency rate is slightly higher for T_{min} at 56%, recording 5 La Niña phases below median (Figure 5.7(h)). The relationships between La Niña phases and T_{max} /T_{min} are highly significant at 99.7% for both variables, based on a low probability of random occurrence (Table 5.4).

5.4.7. Southwest coast

For El Niño, the spatial coherence rates over the southwest coast are 0.99 for both T_{max} and T_{min}. The aggregate T_{max} and T_{min} composite series display above median temperature for the period December (0) to April (+) and December (0) to March (+), respectively (Figures 5.8(a) and 5.8(c)). The ITS indicate above median T_{max} for 9 (out of 16) El Niño phases resulting in a temporal consistency rate of 57% (Figure 5.8(b)). The temporal consistency is slightly higher for T_{min} (63%), with 10 (out of 16) phases being above median (Figure 5.8(d)). The relationships between El Niño phases and T_{max}/T_{min} are highly significant at 99.84% and 99.91%, respectively, based on a low probability of random occurrence (Table 5.4).

For La Niña, the spatial coherence rates over the southwest coast region are 0.99 and 1.00 for T_{max} and T_{min}. The aggregate series indicate below median T_{max} and T_{min} for the period June (0) - September (0) (Figures 5.8(e) and 5.8(g)). The ITS for T_{max} indicate below median temperatures for only 3 (out of 9) La Niña phases, resulting in a consistency rate of 33% (Figures 5.8(f) and 5.8(h); Table 5.3). The ITS for T_{min} indicate below median temperatures for 4 (out of 9) La Niña phases, resulting in a consistency rate of 44%. The relationships are significant at 99.8% and 99.74% for T_{max} and T_{min}, respectively, based on a low chance of random occurrence of the selected period (Table 5.4).

5.4.8. ENSO influence on temperature through time

A strengthening (positive) influence of El Niño phases on T_{max} through time is observed for the northern interior, and southeast and southwest coasts of South Africa. A strengthening (positive) influence is also measured for T_{min} over the northern interior, western interior, northeast coast, southeast and southwest coasts through time. For the northern interior region, El Niño associated T_{max} departures for the signal period October (0) - March (+) increased by 0.41°C in recent years (1979-2016) compared to the earlier period (1940-1978), while associated T_{min} departures increased to a lesser extent (0.02°C) (Table 5.5). Similarly, over the southeast coast, El Niño influence on T_{max} for the signal period December (0) - April (+) in recent years (1979-2016) increased by 0.45°C compared to the earlier period (1940-1978), while associated T_{min} departures increased to a lesser extent (0.15°C) for its signal period (December (0) - March (+)). In addition, a greater strengthening influence of El Niño phases on T_{max} (by 0.16°C) is recorded for the signal period December (0) - April (+) compared to T_{min} (0.15°C) for the signal period December (0) - March (+) through time over the southwest coast (Table 5.5). The strongest El Niño related T_{max} warming occurred over the southeast coast (0.45°C) when comparing the more recent period to the earlier period. El Niño phases influence T_{max} to a lesser extent for the more recent period compared to earlier times over the central interior, western interior, northeastern interior and northeast coast. El Niño phases also influence T_{min} to a lesser extent for the more recent period compared to earlier times over the central interior and northeastern interior for the respective signal periods through time (Tables 5.3 and 5.5).

The earlier epoch (1940-1978) records positive La Niña - T_{max} departures for the respective signal periods over all regions, while that for the more recent epoch varies between regions. For the signal period May (0) - August (0) detected over the northern interior, associated with La Niña, T_{max} increased by 0.11°C when comparing the periods 1940-1978 with 1979-2016. The largest T_{max} decreases occurred over the northeastern interior (-1.10°C) and northeast coast (1.09°C) when comparing the earlier with later epochs for the signal periods May (0) - August (0) and June (0) - October (0), respectively. For the signal period June (0) - September (0), T_{max} over the southwest coast also records a decrease of -0.2°C when comparing the periods 1940-1978 with 1979-2016. For La Niña, T_{min} positive departures increased in magnitude over the central interior (by 0.16°C), northeast (0.01°C), southeast

(0.07°C) and southwest (0.05°C) coasts through time (Table 5.5). However, the remaining regions (northern interior, western interior, and northeastern interior) record decreasing T_{min} departures (-0.17°C, -0.04 and -0.4, respectively) through time for their respective signal periods (May (0) - August (0), June (0)-September (0) and June (0)-September (0)) during La Niña (Tables 5.3 and 5.5).

5.4.9. Chi-square test results

The results associated with the Chi-square test for the austral summer (December, January and February) display p-values lower than the significance level of 0.05 for all stations in the northern and central interior of South Africa. This indicates that El Niño/La Niña and T_{max}/T_{min} are not independant (i.e., null hypothesis is rejected), again emphasizing the influence of these ENSO phases on temperature over the interior (Table 5.6). However, at Messina, Glen College and Skukuza, the p-values are higher than 0.05 for T_{min}, indicating that El Niño/La Niña phases do not influence T_{min}. Signifiant ENSO associations are also recorded at Vanwyksvlei, Cedara and Cape Columbine for T_{max} and Mt. Edgecombe for T_{min}. Although T_{max} at Marico and T_{min} at Zuurbekom and Messina recorded counts below 5, the Fisher's exact test corresponded to the p-value for Chi-square test in all instances (Table 5.6). A strengthening El Niño influence on T_{max} is also recorded for majority of the stations across South Africa, with the exception of the SA Astronomical Observatory and Pofadder stations. A larger proportion of stations record a weakening influence of El Niño phase on T_{min} (namely Cedara, Zuurbekom, Vryburg, Marico Kimberely and Warmbad) with time.

Table 5.5: Strengthening/weakening of the ENSO influence on temperature through time, determined by calculating the difference between T_{max}/T_{min} for all years and that for ENSO years only.

	T_{max}/T_{min}	Average warming/cooling for all years during the signal period (°C)		Average warming/cooling during the signal period for ENSO phases (°C)		Strengthening/ Weakening of ENSO influence
		1940-1978	1979-2016	1940-1978	1979-2016	
El Niño						
Northern interior	T_{max}	-0.21*	0.49*	-0.34	0.77*	0.41
Northern interior	T_{min}	0.01	0.11*	-0.08	0.006	0.02
Central interior	T_{max}	-0.04	0.27*	0.12	0.03	-0.40
Central interior	T_{min}	0.08*	0.02	0.09	-0.12	-0.19
Western interior	T_{max}	-0.27*	0.19*	0.17	0.23*	-0.40*
Western interior	T_{min}	0.04	0.19*	0.19*	0.40*	0.06
Northeastern interior	T_{max}	-0.04	0.19*	0.18	0.37*	-0.04
Northeastern interior	T_{min}	0.08*	0.15*	0.07	0.05	-0.09
Northeast coast	T_{max}	-0.61*	0.72*	0.02	1.19*	-0.16
Northeast coast	T_{min}	0.15*	0.53*	-0.01	0.67*	0.30
Southeast coast	T_{max}	0.15*	0.08*	0.18*	0.55*	0.45*
Southeast coast	T_{min}	0.27*	-0.11*	0.19	-0.03	0.15
Southwest coast	T_{max}	0.19*	0.27*	0.21*	0.44*	0.16*
Southwest coast	T_{min}	0.19*	0.23*	0.28*	0.47*	0.15*
La Niña						
Northern interior	T_{max}	-0.03	0.68*	0.16	0.99*	0.11
Northern interior	T_{min}	-0.08	0.11*	0.36*	0.38*	-0.17
Central interior	T_{max}	-0.04*	0.32*	0.30	0.19	-0.46
Central interior	T_{min}	-0.03	0.08	0.03	0.30*	0.16
Western interior	T_{max}	-0.02	0.15*	0.06	0.23	-0.01
Western interior	T_{min}	0.02	0.08*	-0.05	-0.02	-0.04
Northeastern interior	T_{max}	-0.43*	0.65*	0.08	0.80*	-1.10
Northeastern interior	T_{min}	0.31*	0.34*	0.80*	0.44*	-0.40
Northeast coast	T_{max}	-0.57*	0.76*	0.55*	0.79*	-1.09*
Northeast coast	T_{min}	-0.08	0.27*	0.31*	0.66*	0.01
Southeast coast	T_{max}	-0.11	0.30*	0.12	0.10	-0.44
Southeast coast	T_{min}	0.27*	-0.23*	0.35*	-0.08	0.07
Southwest coast	T_{max}	0.08	0.23*	0.26*	0.21*	-0.20
Southwest coast	T_{min}	0.23*	0.03	0.12	-0.03	0.05

*= significant

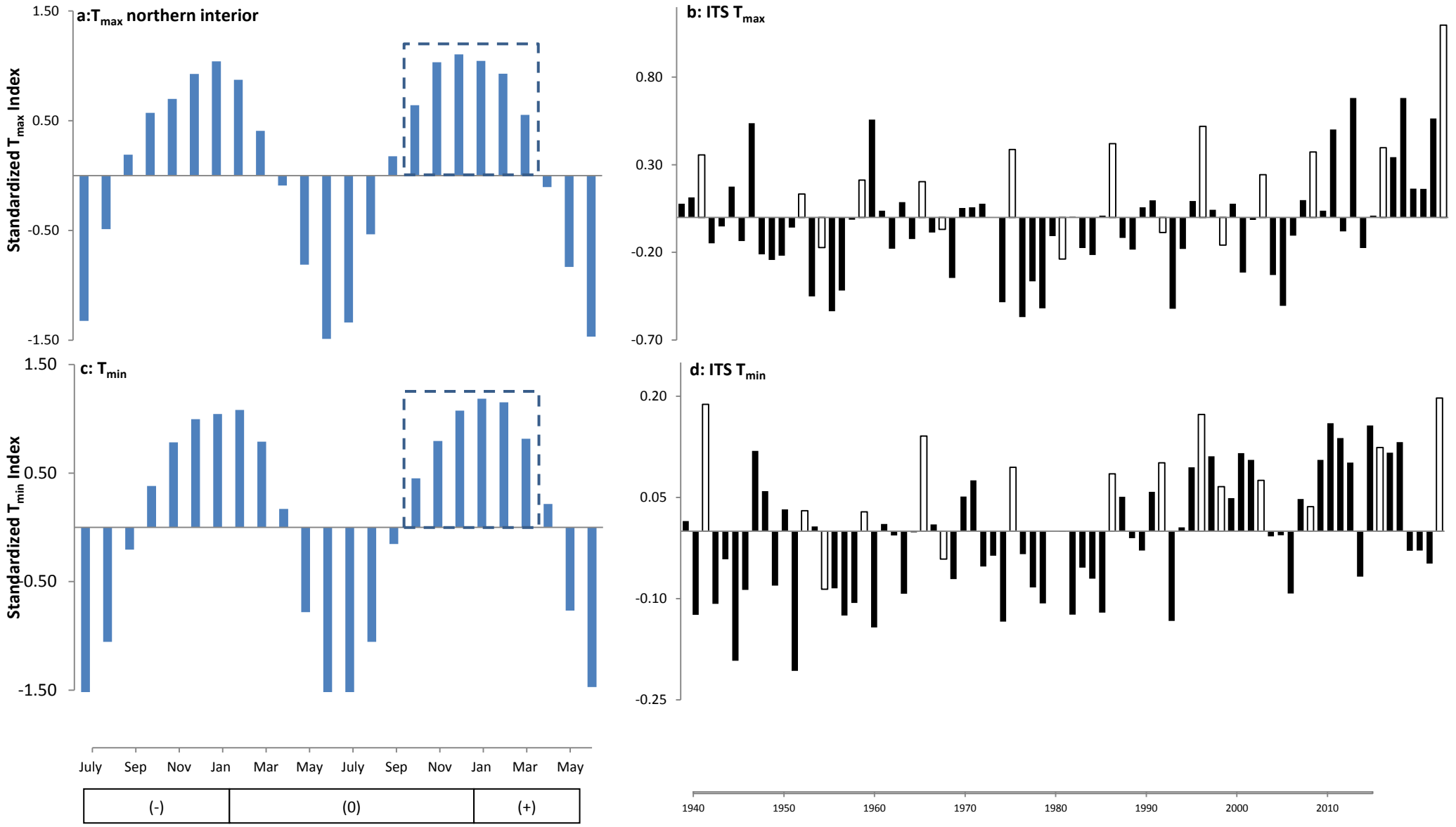
a:T$_{max}$ northern interior
Standardized T$_{max}$ Index
1.50
0.50
-0.50
-1.50
b: ITS T$_{max}$
0.80
0.30
-0.20
-0.70
c: T$_{min}$
Standardized T$_{min}$ Index
1.50
0.50
-0.50
-1.50
d: ITS T$_{min}$
0.20
0.05
-0.10
-0.25
July Sep Nov Jan Mar May July Sep Nov Jan Mar May
(-)
(0)
(+)
1940 1950 1960 1970 1980 1990 2000 2010

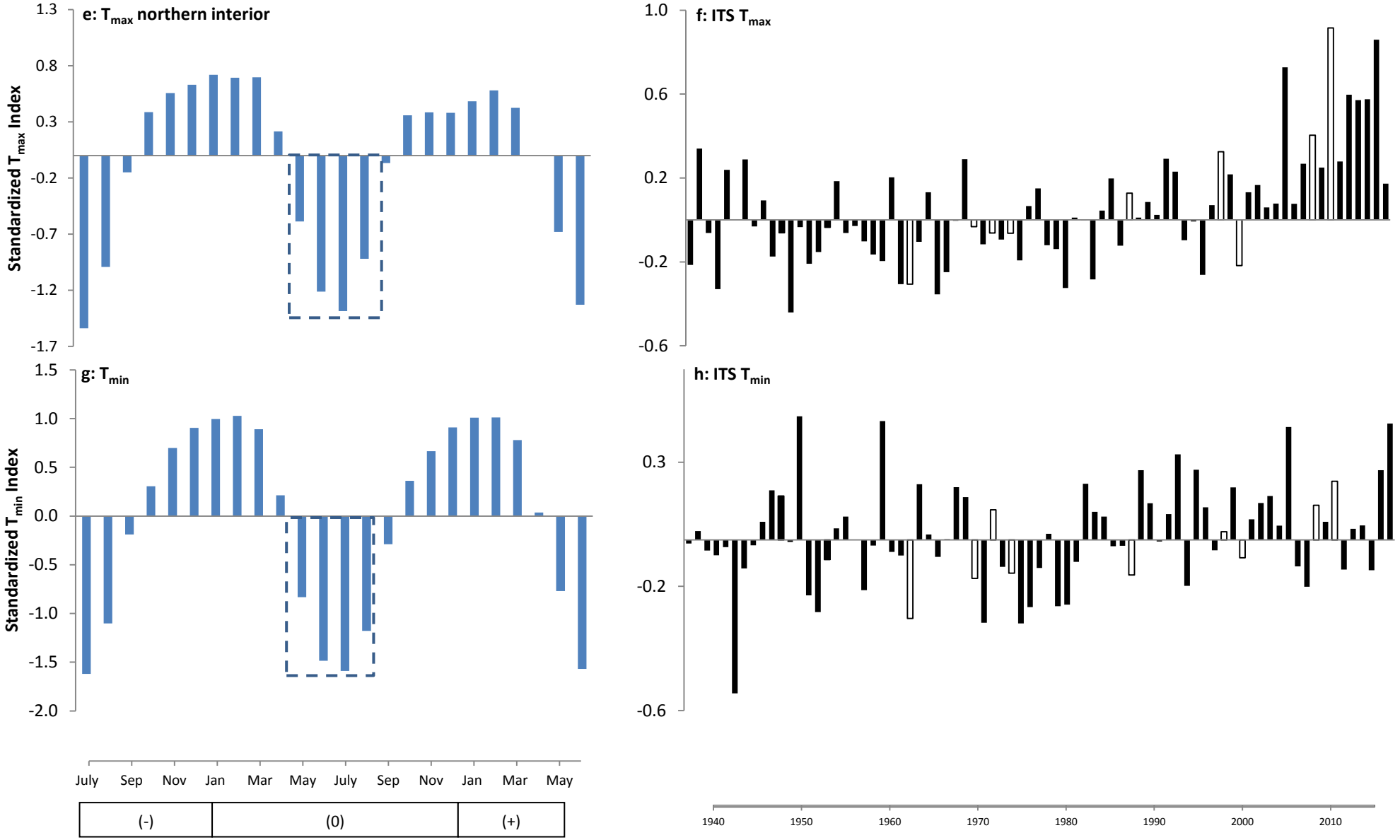

Figure 5.2: El Niño T_{max} (a) and T_{min} (c) and La Niña T_{max} (e) and T_{min} (g) aggregate composite, with the dashed box denoting the possible signal period. The index time series for El Niño T_{max} (b); El Niño T_{min} (d); La Niña T_{max} (f) and La Niña T_{min} (h) for the signal season detected from the aggregate composite over the northern interior region. White bars indicate ENSO years, black bars are the neutral years and and the boxes represent the months of the year before the ENSO event (-), the year of the ENSO event (0) and the months of the year after the ENSO event (+), respectively.

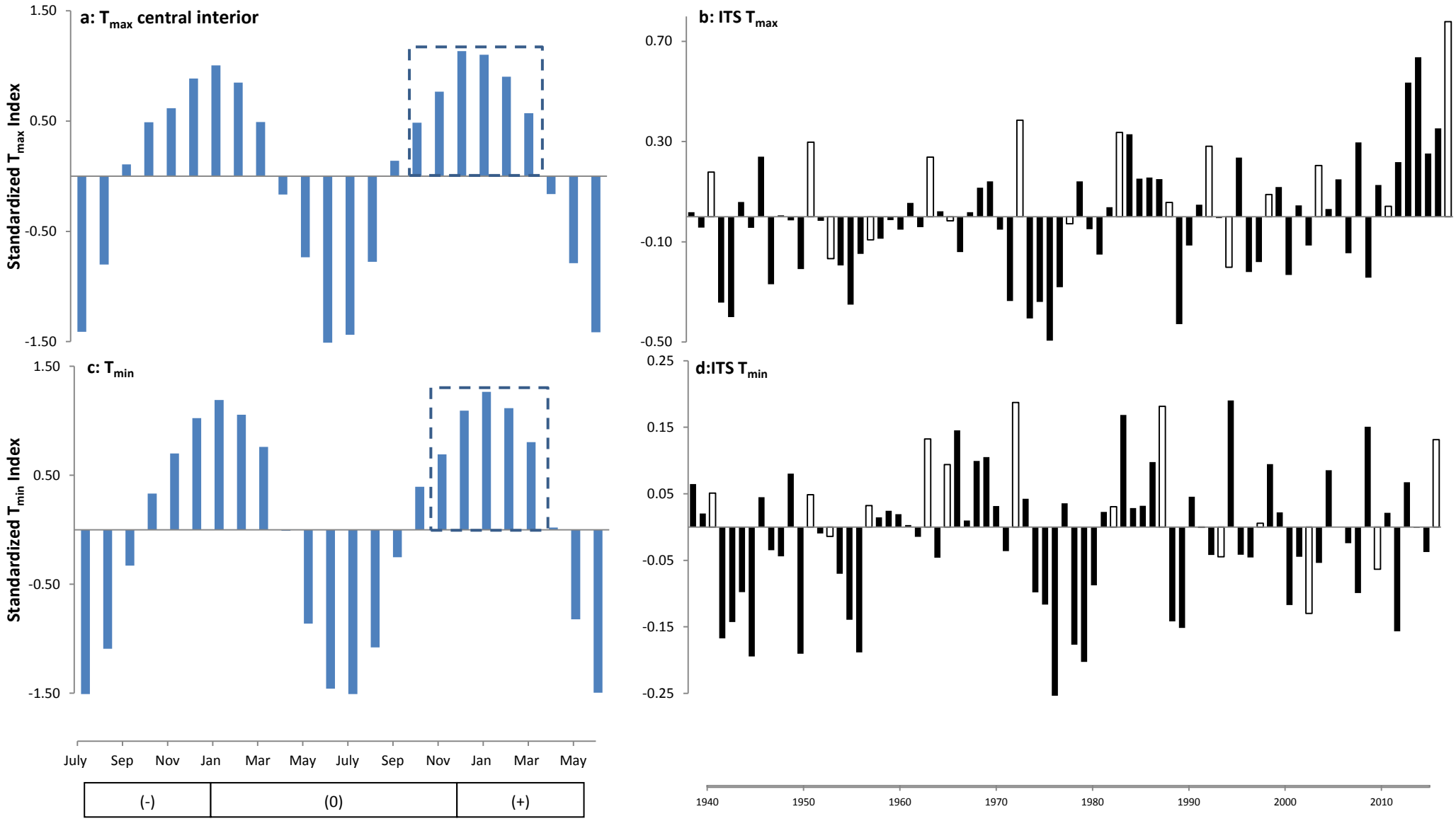
a: T_{max} central interior
Standardized T_{max} Index
1.50
0.50
-0.50
-1.50
b: ITS T_{max}
0.70
0.30
-0.10
-0.50
c: T_{min}
Standardized T_{min} Index
1.50
0.50
-0.50
-1.50
d:ITS T_{min}
0.25
0.15
0.05
-0.05
-0.15
-0.25
July
Sep
Nov
Jan
Mar
May
July
Sep
Nov
Jan
Mar
May
(-)
(0)
(+)
1940
1950
1960
1970
1980
1990
2000
2010

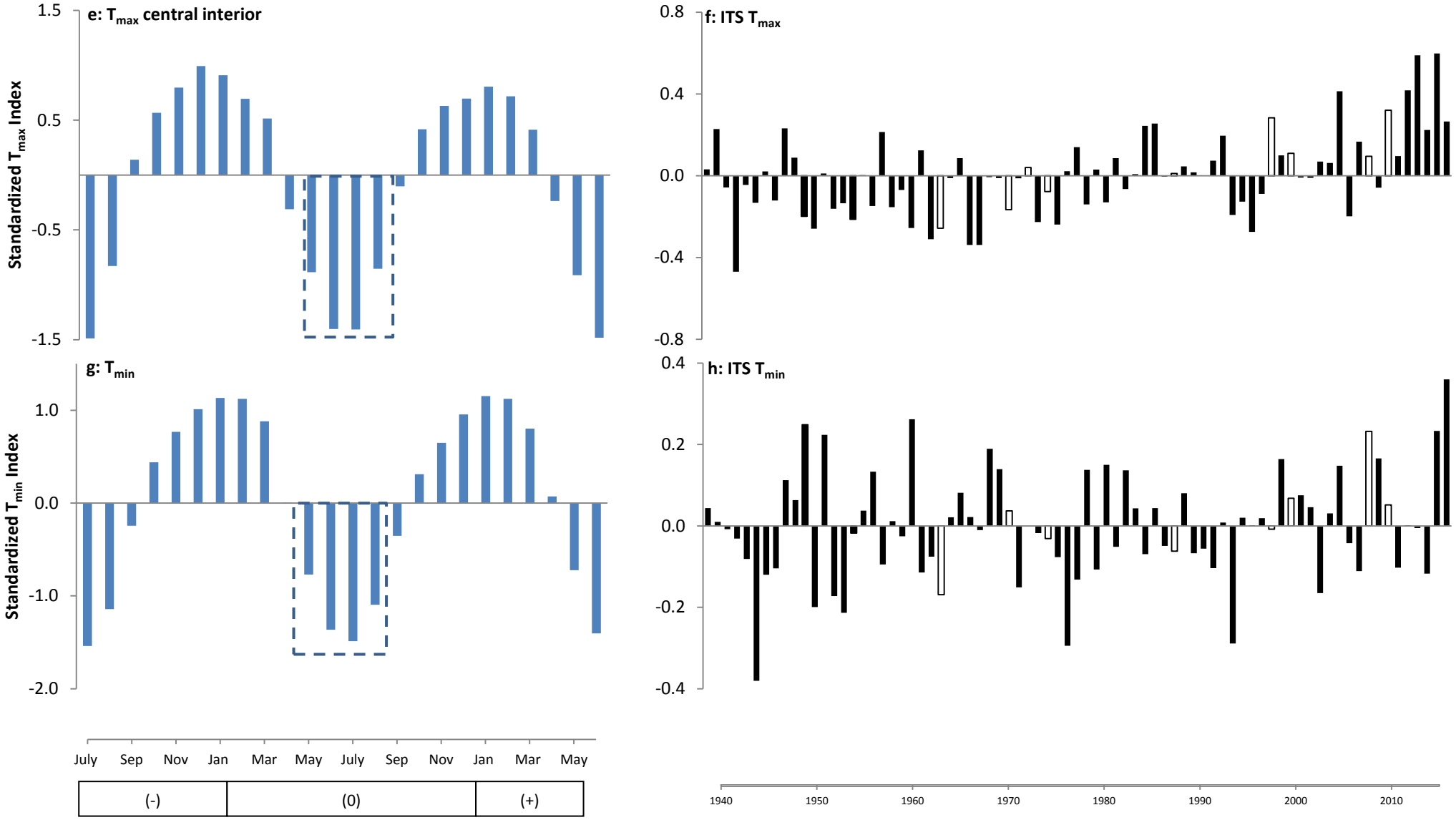

Figure 5.3: El Niño T_{max} (a) and T_{min} (c) and La Niña T_{max} (e) and T_{min} (g) aggregate composite, with the dashed box denoting the possible signal period. The index time series for El Niño T_{max} (b); El Niño T_{min} (d); La Niña T_{max} (f) and La Niña T_{min} (h) for the signal season detected from the aggregate composite over the central interior region. White bars indicate ENSO years, black bars are the neutral years and the boxes represent the months of the year before the ENSO event (-), the year of the ENSO event (0) and the months of the year after the ENSO event (+), respectively.

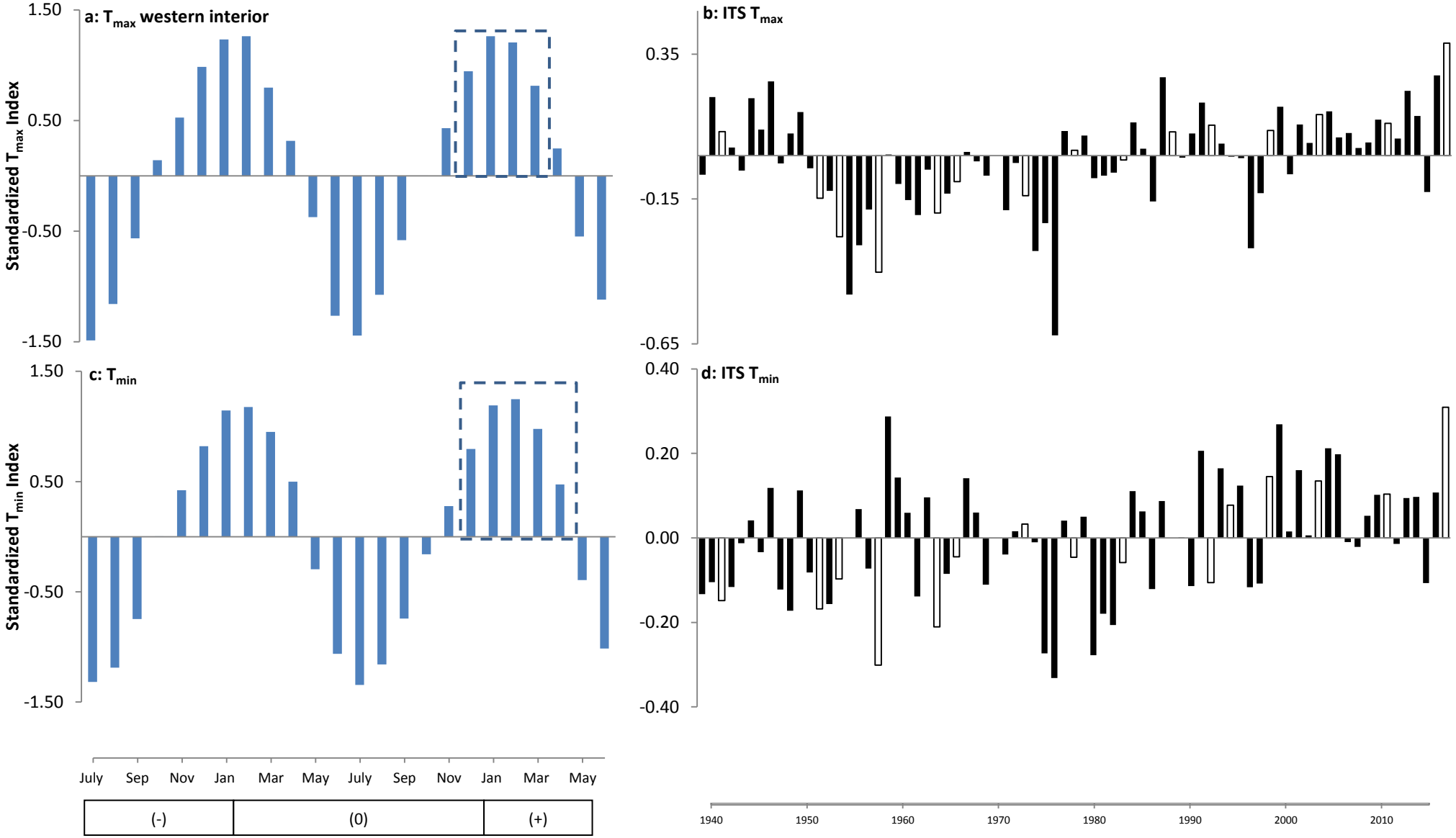
a: T_{max} western interior
Standardized T_{max} Index
1.50
0.50
-0.50
-1.50
b: ITS T_{max}
0.35
-0.15
-0.65
c: T_{min}
Standardized T_{min} Index
1.50
0.50
-0.50
-1.50
d: ITS T_{min}
0.40
0.20
0.00
-0.20
-0.40
July
Sep
Nov
Jan
Mar
May
July
Sep
Nov
Jan
Mar
May
(-)
(0)
(+)
1940
1950
1960
1970
1980
1990
2000
2010

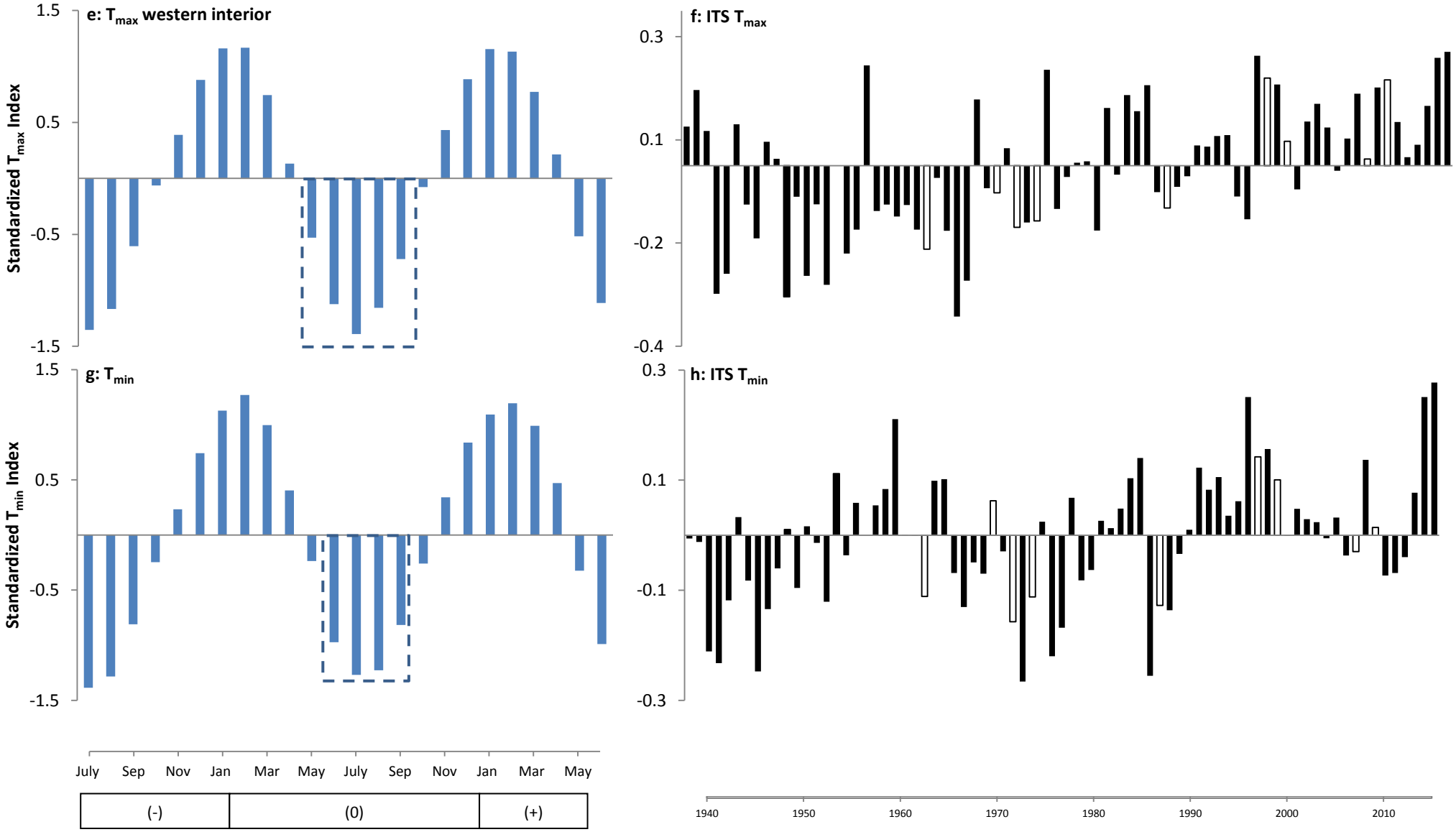

Figure 5.4: El Niño T_{max} (a) and T_{min} (c) and La Niña T_{max} (e) and T_{min} (g) aggregate composite, with the dashed box denoting the possible signal period. The index time series for El Niño T_{max} (b); El Niño T_{min} (d); La Niña T_{max} (f) and La Niña T_{min} (h) for the signal season detected from the aggregate composite for the western interior region. White bars indicate ENSO years, black bars are the neutral years and the boxes represent the months of the year before the ENSO event (-), the year of the ENSO event (0) and the months of the year after the ENSO event (+), respectively.

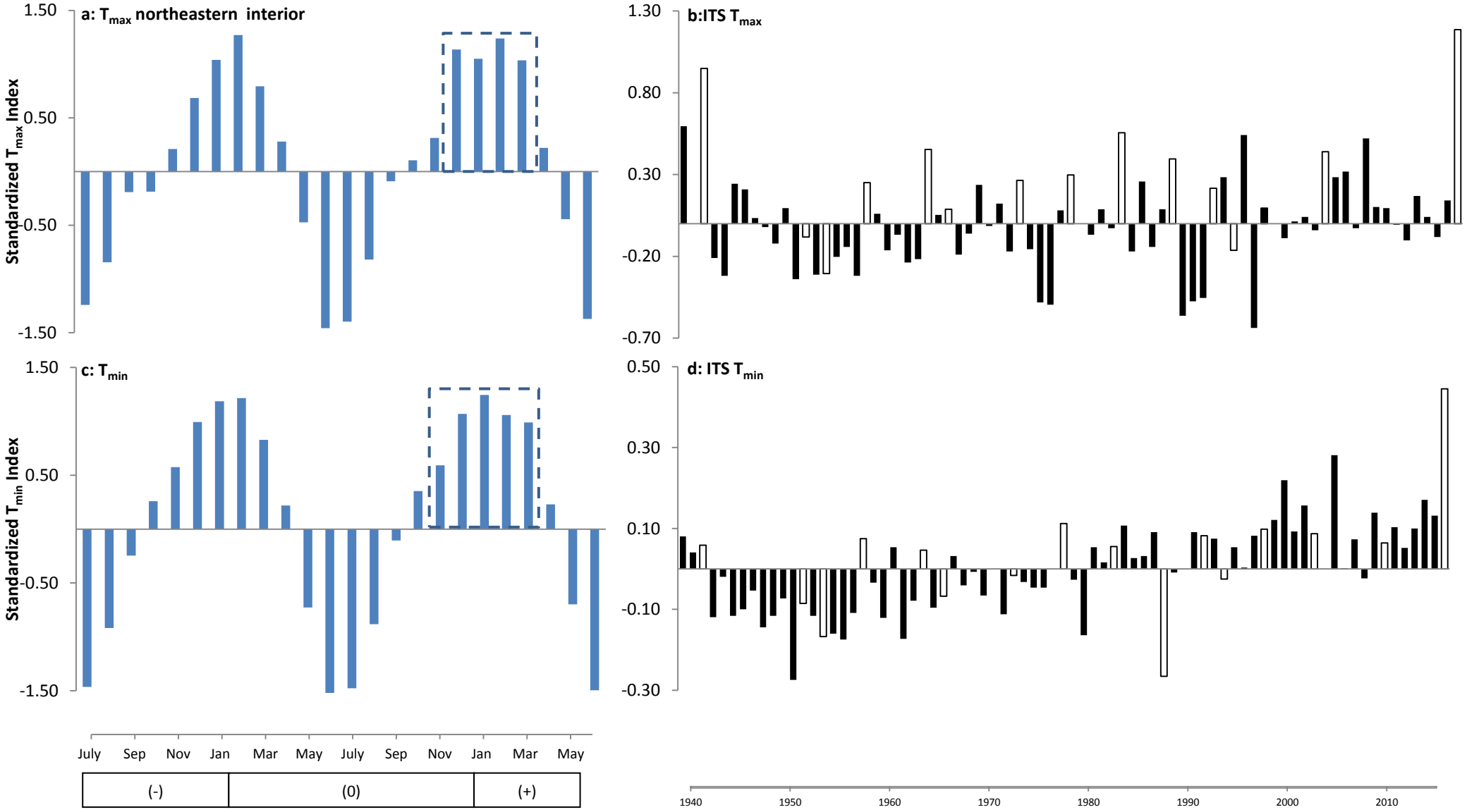
a: T_{max} northeastern interior
Standardized T_{max} Index
1.50
0.50
-0.50
-1.50
b:ITS T_{max}
1.30
0.80
0.30
-0.20
-0.70
c: T_{min}
Standardized T_{min} Index
1.50
0.50
-0.50
-1.50
d: ITS T_{min}
0.50
0.30
0.10
-0.10
-0.30
July Sep Nov Jan Mar May July Sep Nov Jan Mar May
(-)
(0)
(+)
1940 1950 1960 1970 1980 1990 2000 2010

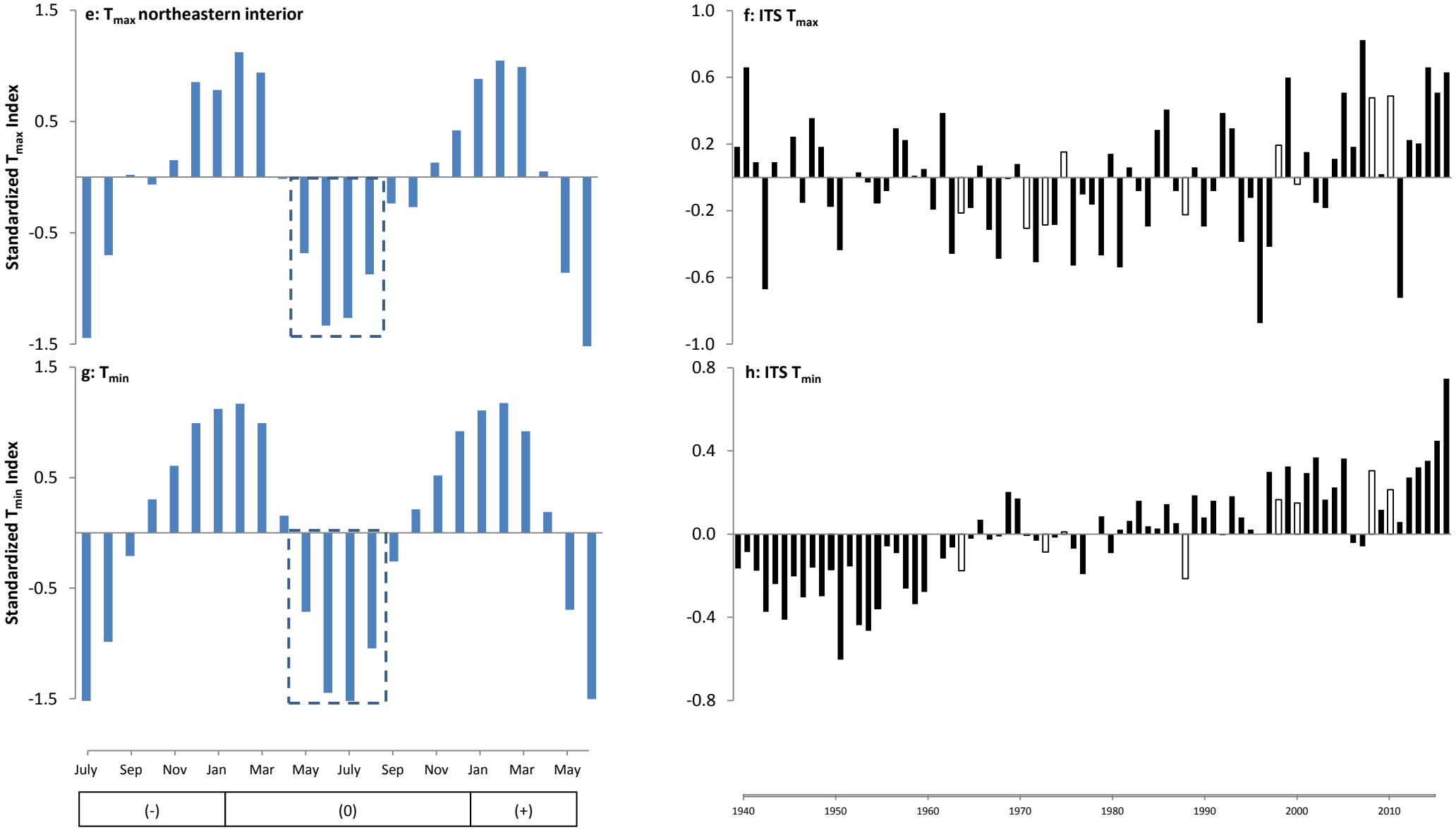

Figure 5.5: El Niño T_{max} (a) and T_{min} (c) and La Niña T_{max} (e) and T_{min} (g) aggregate composite, with the dashed box denoting the possible signal period. The index time series for El Niño T_{max} (b); El Niño T_{min} (d); La Niña T_{max} (f) and La Niña T_{min} (h) for the signal season detected from the aggregate composite over the northeastern interior region. White bars indicate ENSO years and black bars are the neutral years and the boxes represent the months of the year before the ENSO event (-), the year of the ENSO event (0) and the months of the year after the ENSO event (+), respectively..

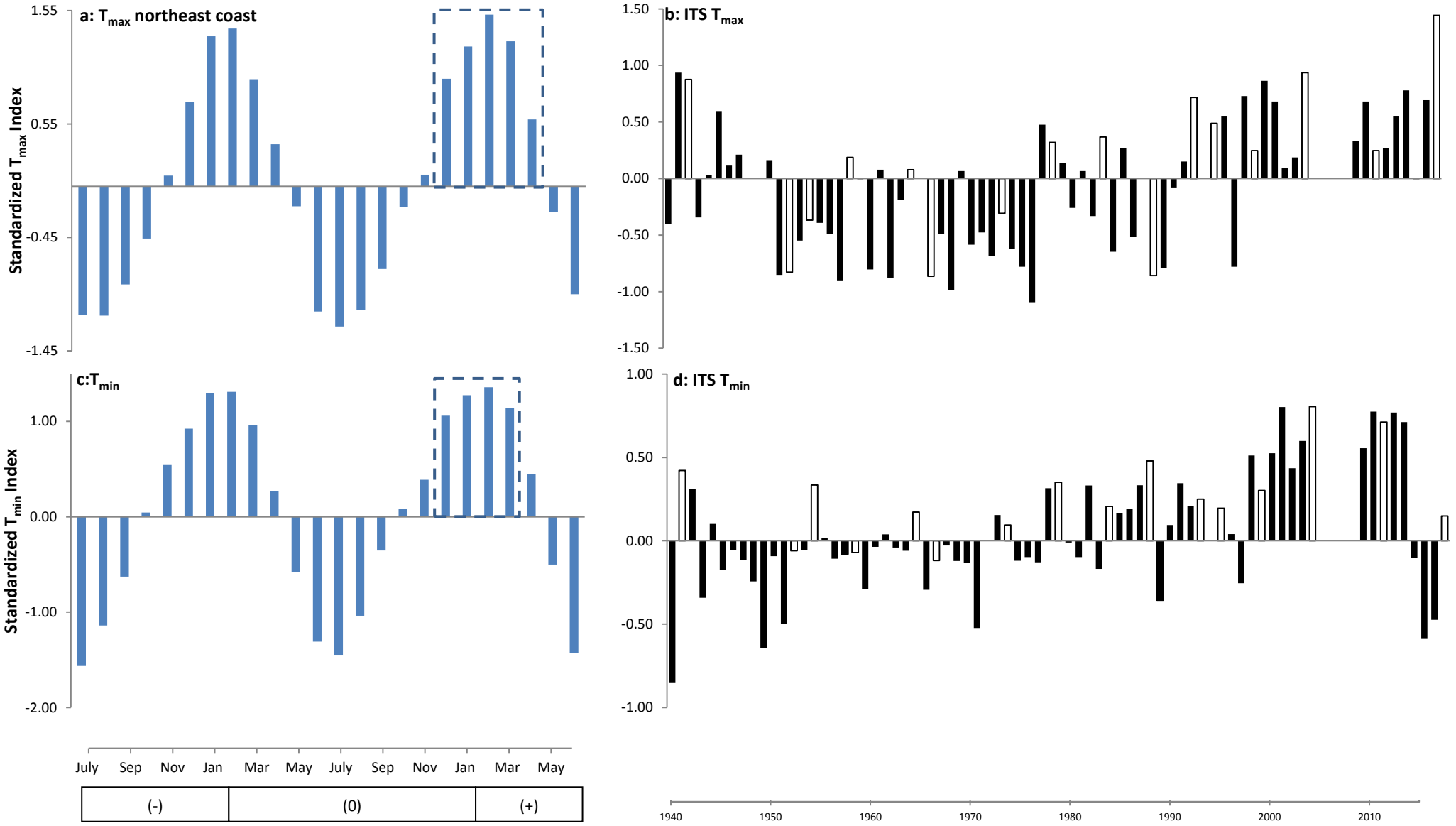
a: T_{max} northeast coast
Standardized T_{max} Index
1.55
0.55
-0.45
-1.45
b: ITS T_{max}
1.50
1.00
0.50
0.00
-0.50
-1.00
-1.50
c:T_{min}
Standardized T_{min} Index
1.00
0.00
-1.00
-2.00
d: ITS T_{min}
1.00
0.50
0.00
-0.50
-1.00
July Sep Nov Jan Mar May July Sep Nov Jan Mar May
(-)
(0)
(+)
1940 1950 1960 1970 1980 1990 2000 2010

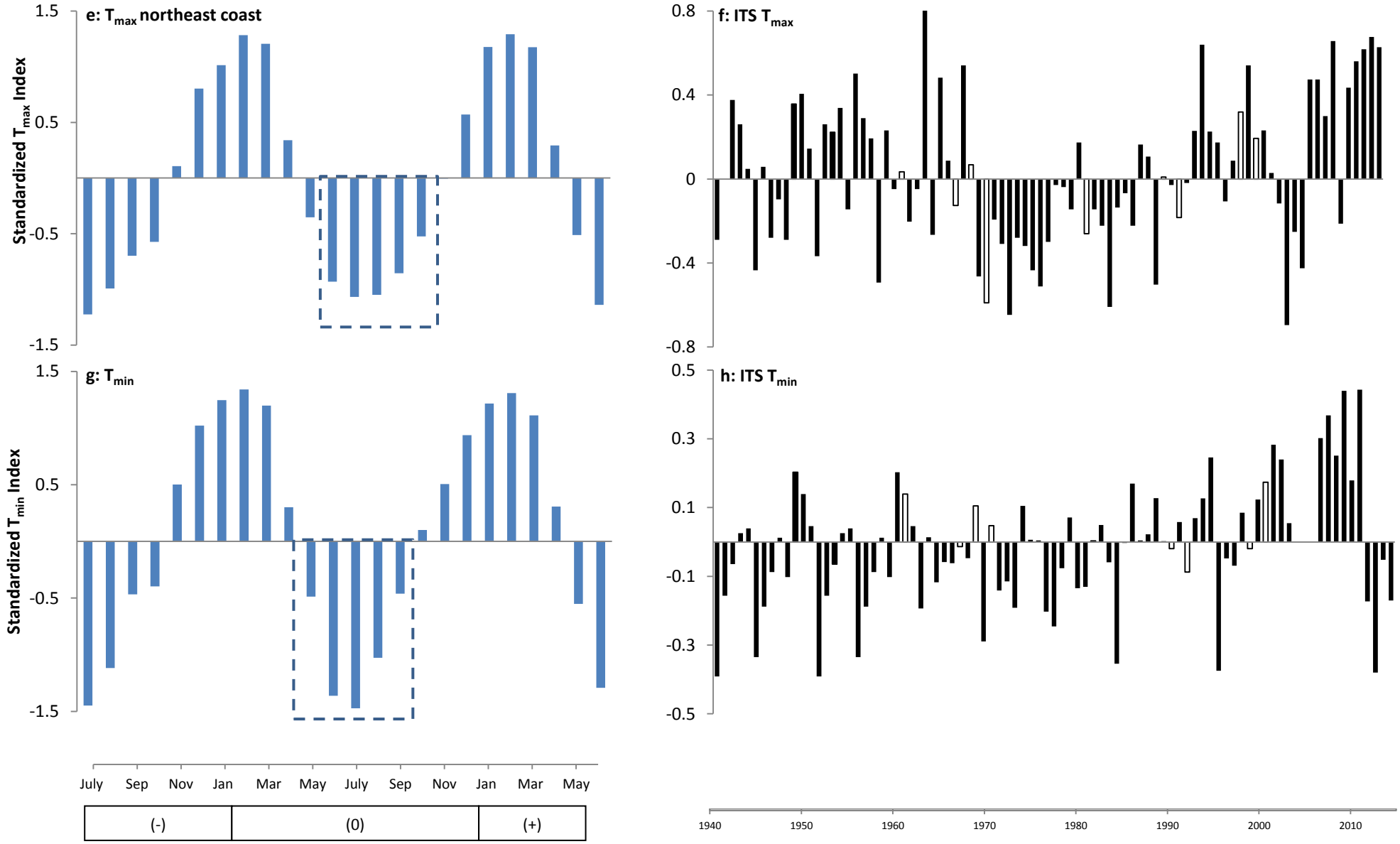

Figure 5.6: El Niño T_{max} (a) and T_{min} (c) and La Niña T_{max} (e) and T_{min} (g) aggregate composite, with the dashed box denoting the possible signal period. The index time series El Niño T_{max} (b); El Niño T_{min} (d); La Niña T_{max} (f) and La Niña T_{min} (h) for the signal season detected from the aggregate composite over the northeast coast region. White bars indicate ENSO years and black bars are the neutral years and the boxes represent the months of the year before the ENSO event (-), the year of the ENSO event (0) and the months of the year after the ENSO event (+), respectively.

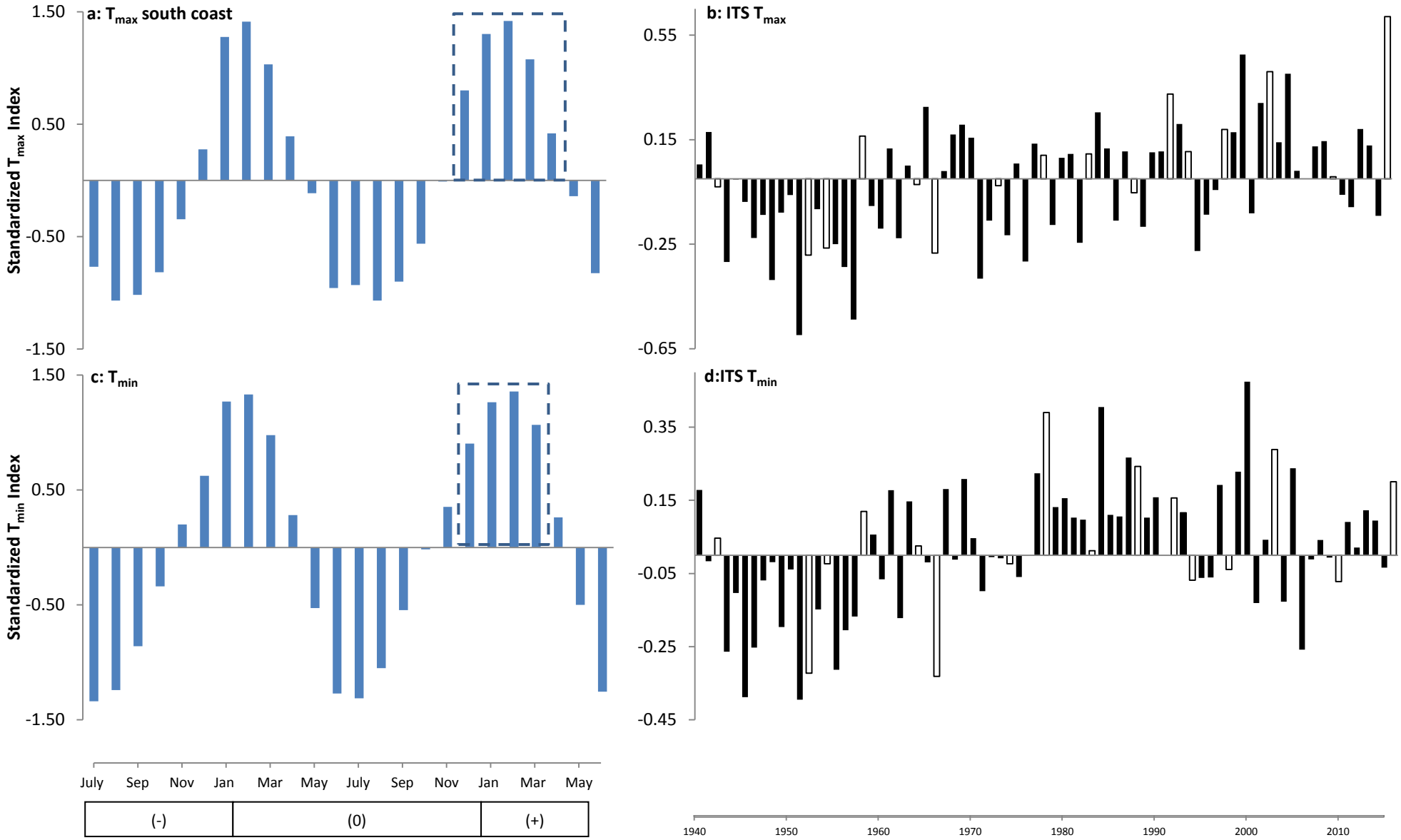
a: T_{max} south coast
Standardized T_{max} Index
1.50
0.50
-0.50
-1.50
b: ITS T_{max}
0.55
0.15
-0.25
-0.65
c: T_{min}
Standardized T_{min} Index
1.50
0.50
-0.50
-1.50
d:ITS T_{min}
0.35
0.15
-0.05
-0.25
-0.45
July Sep Nov Jan Mar May July Sep Nov Jan Mar May
(-)
(0)
(+)
1940 1950 1960 1970 1980 1990 2000 2010

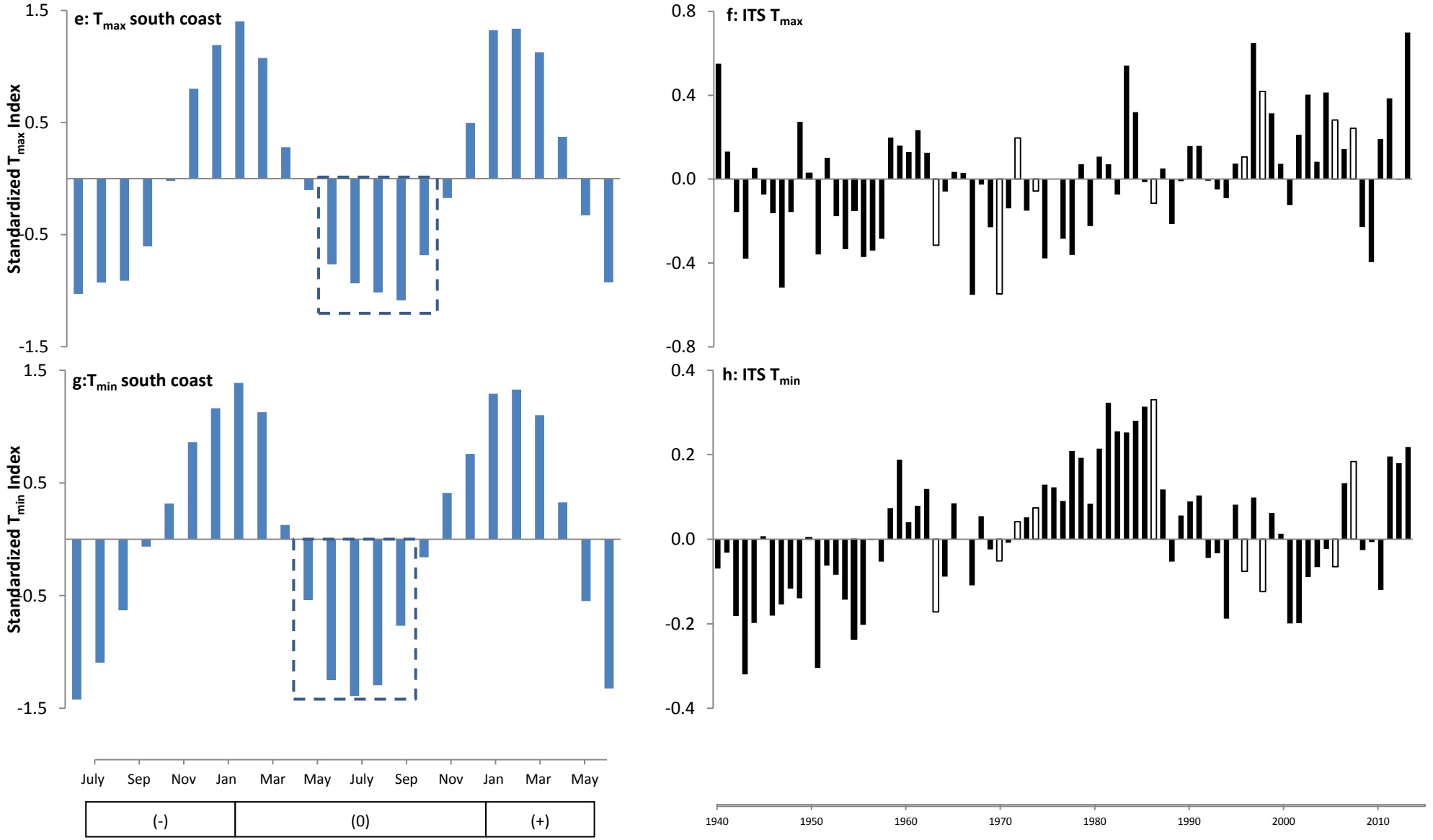

Figure 5.7: El Niño T_{max} (a) and T_{min} (c) and La Niña T_{max} (e) and T_{min} (g) aggregate composite, with the dashed box denoting the possible signal period. The index time series El Niño T_{max} (b); El Niño T_{min} (d); La Niña T_{max} (f) and La Niña T_{min} (h) for the signal season detected from the aggregate composite over the southeast coast region. White bars indicate ENSO years, black bars are the neutral years and the boxes represent the months of the year before the ENSO event (-), the year of the ENSO event (0) and the months of the year after the ENSO event (+), respectively.

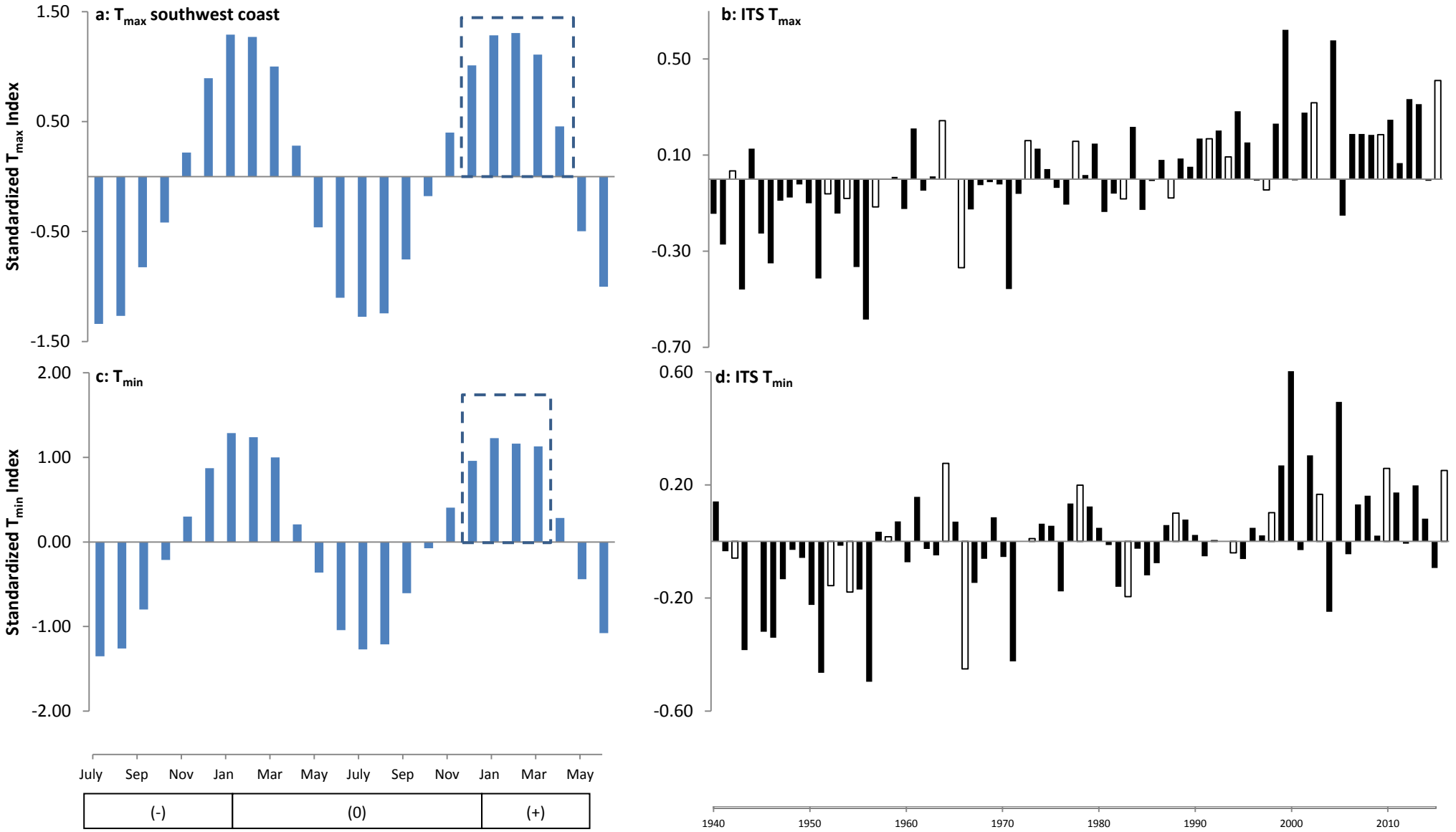
a: T_{max} southwest coast
Standardized T_{max} Index
1.50
0.50
-0.50
-1.50
b: ITS T_{max}
0.50
0.10
-0.30
-0.70
c: T_{min}
Standardized T_{min} Index
2.00
1.00
0.00
-1.00
-2.00
d: ITS T_{min}
0.60
0.20
-0.20
-0.60
July Sep Nov Jan Mar May July Sep Nov Jan Mar May
(-)
(0)
(+)
1940 1950 1960 1970 1980 1990 2000 2010

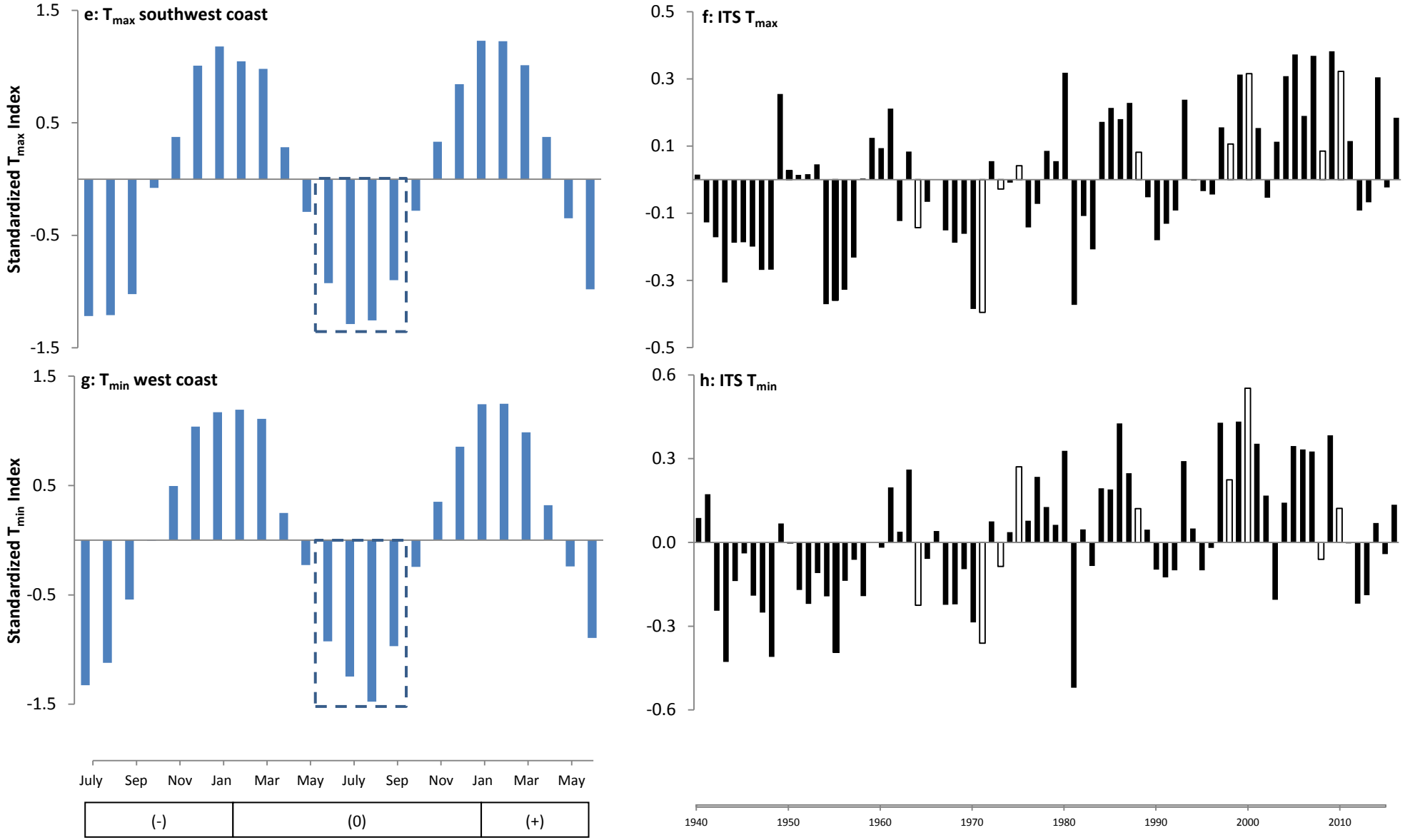

Figure 5.8: El Niño T_{max} (a) and T_{min} (c) and La Niña T_{max} (e) and T_{min} (g) aggregate composite, with the dashed box denoting the possible signal period. The index time series El Niño T_{max} (b); El Niño T_{min} (d); La Niña T_{max} (f) and La Niña T_{min} (h) for the signal season detected from the aggregate composite over the southwest coast. White bars indicate ENSO years, black bars are the neutral years and the boxes represent the months of the year before the ENSO event (-), the year of the ENSO event (0) and the months of the year after the ENSO event (+), respectively.

Table 5.6: Regional chi-square statistics for traditional summer T_{max}/T_{min} anomalies (average of December, January and February), rate of occurrence and strengthening/ weakening influence of El Niño phases on T_{max}/T_{min}. Chi-square critical value = 9.48 degree of freedom = 4 and p-values in bold are significant.

Region	Station/ T_{max}/T_{min}	Chi-square (Observed value)	p-value	Fisher's exact	Rates of high T_{max}/T_{min} occurrence for El Niño years	Rates of low T_{max}/T_{min} occurrence for La Niña years	Strengthening/ Weakening influence of El Niño on T_{max}/T_{min}[a]		Contingency table: High T_{max}	Medium T_{max}	Low T_{max}		Contingency table: High T_{min}	Medium T_{min}	Low T_{min}
North - eastern interior	**Cedara**							El Niño	11	6	1	El Niño	10	5	3
	T_{max}	13.286	**0.010**	0.011	0.61	0.50	0.43	La Niña	3	6	9	La Niña	4	8	6
	T_{min}	6.836	0.145	0.079	0.56	0.44	-0.39	Neutral	10	17	14	Neutral	10	16	15
Southeast coast	**East London**							El Niño	7	5	6	El Niño	8	7	3
	T_{max}	5.238	0.264	0.28	0.39	0.50	0.50	La Niña	4	5	9	La Niña	4	5	9
	T_{min}	5.336	0.255	0.29	0.44	0.50	0.37	Neutral	13	18	9	Neutral	12	16	12
	Port Elisabeth							El Niño	2	9	7	El Niño	4	8	6
	T_{max}	7.002	0.136	0.129	0.22	0.22	0.41	La Niña	9	6	3	La Niña	7	7	4
	T_{min}	2.051	0.726	0.722	0.11	0.17	0.11	Neutral	13	14	14	Neutral	14	13	14
Central interior	**Zuurbekom**							El Niño	9	6	3	El Niño	11	5	2
	T_{max}	10.012	**0.040**	0.048	0.50	0.33	1.03	La Niña	1	11	6	La Niña	5	6	7
	T_{min}	11.035	**0.026**	0.032	0.61	0.39	-0.77	Neutral	9	22	10	Neutral	8	17	16
	Vryburg							El Niño	10	6	2	El Niño	11	4	3
	T_{max}	11.947	**0.018**	0.022	0.56	0.56	0.03	La Niña	10	6	10	El Niño	1	9	8
	T_{min}	13.137	**0.011**	0.011	0.61	0.44	-0.22	Neutral	12	17	12	Neutral	12	16	13
	Glen College							El Niño	11	6	1	El Niño	9	6	3
	T_{max}	15.992	**0.003**	0.002	0.61	0.61	0.86	La Niña	2	5	11	La Niña	5	5	8
	T_{min}	5.935	0.204	0.231	0.5	0.44	0.25	Neutral	10	12	18	Neutral	10	18	13
Central interior	**Marico**							El Niño	10	7	1	El Niño	11	5	2
	T_{max}	12.048	**0.017**	0.016	0.56	0.50	0.96	La Niña	2	7	9	La Niña	3	9	6
	T_{min}	10.641	**0.031**	0.043	0.61	0.33	-0.21	Neutral	13	17	11	Neutral	10	17	14

	Kimberley							El Niño	12	6	0	El Niño	10	7	1
	T_{max}	25.229	**< 0.0001**	< 0.0001	0.67	0.67	0.64	La Niña	1	5	12	La Niña	5	5	8
	T_{min}	10.442	**0.034**	0.027	0.56	0.44	-0.12	Neutral	11	18	12	Neutral	9	17	15
Western interior	**Vanwyksvlei**							El Niño	8	7	3	El Niño	8	6	4
	T_{max}	9.163	**0.057**	0.067	0.44	0.63	0.63	La Niña	5	3	10	La Niña	5	6	7
	T_{min}	2.479	0.648	0.672	0.44	0.41	0.41	Neutral	11	19	11	Neutral	11	17	13
	Pofadder							El Niño	8	2	8	El Niño	6	6	6
	T_{max}	3.326	0.505	0.512	0.44	0.44	-0.02	La Niña	4	6	8	La Niña	4	6	8
	T_{min}	2.403	0.662	0.665	0.33	0.44	0.33	Neutral	13	10	18	Neutral	14	16	10
North-east coast	**Mt Edgecombe**							El Niño	7	9	2	El Niño	10	7	1
	T_{max}	5.907	0.206	0.180	0.39	0.44	0.29	La Niña	6	4	8	La Niña	7	5	6
	T_{min}	12.233	**0.016**	0.011	0.56	0.33	0.26	Neutral	11	15	14	Neutral	7	17	17
Northern interior	**Warmbad**							El Niño	12	4	2	El Niño	9	9	0
	T_{max}	16.289	**0.003**	0.005	0.67	0.5	0.61	La Niña	2	8	8	La Niña	3	9	6
	T_{min}	13.504	**0.009**	0.003	0.44	0.33	-0.63	Neutral	9	18	14	Neutral	11	12	18
	Skukuza							El Niño	11	6	1	El Niño	6	6	6
	T_{max}	9.777	**0.044**	0.040	0.61	0.39	1.24	La Niña	4	7	7	La Niña	6	4	8
	T_{min}	3.800	0.434	0.426	0.33	0.44	0.04	Neutral	10	15	16	Neutral	12	19	10
	Messina							El Niño	11	3	4	El Niño	9	8	1
	T_{max}	13.440	**0.009**	0.013	0.61	0.5	1.11	La Niña	2	7	9	La Niña	9	7	2
	T_{min}	8.224	0.084	0.089	0.50	0.5	0.54	Neutral	11	19	11	Neutral	12	15	14
Southwest coast	**SA Astronom.**							El Niño	7	8	3	El Niño	7	6	5
	T_{max}	2.518	0.641	0.627	0.39	0.39	-0.15	La Niña	5	6	7	La Niña	5	4	9
	T_{min}	5.226	0.265	0.291	0.39	0.5	0.15	Neutral	12	14	14	Neutral	12	19	10
	Cape Columbine							El Niño	7	9	2	El Niño	10	5	3
	T_{max}	10.211	**0.037**	0.056	0.50	0.56	0.22	La Niña	2	7	9	La Niña	1	8	9
	T_{min}	3.880	0.422	0.437	0.44	0.44	0.40	Neutral	15	13	13	Neutral	13	15	12
	Cape Agulhas							El Niño	9	5	4	El Niño	8	6	4

T_{max}	3.956	0.412	0.437	0.50	0.56	0.44	La Niña	4	4	10	La Niña	3	7	8
T_{min}	6.880	0.142	0.056	0.44	0.44	0.06	Neutral	11	20	10	Neutral	13	16	12

a:The difference between the T_{max}/T_{min} anomalies for El Niño phases for the periods 1940-1978 and 1979-2016.

5.5. DISCUSSION

South African surface air temperatures are influenced by both phases of ENSO. The earliest and longest response to El Niño phases occurred over the northern interior region for the period October (0) - March (+) for both T_{max} and T_{min} (Table 5.3). The region of the globe most directly affected by the Southern Oscillation is the global tropics (i.e., including all areas within 20°N/S of the equator) (Halpert and Ropelewski, 1992). In addition, the lag surface air temperature response to El Niño phases is slightly less in the tropics compared to other regions of the world (Trenberth *et al*., 2002). It is therefore expected that the stations in closest proximity (such as northern interior region of South Africa) to the tropics will experience an earlier and longer (six months compared to four/five months) response compared to regions further south. In addition, the interior is more likely to show a stronger ENSO/temperature response because it is less influenced by coastal climatic moderating effects. The central interior region records above median T_{max} for El Niño phases during October (0) - March (+), while that for T_{min} is from November (0) - March (+). The observed lag response (by 1 month) for T_{min} is possibly due to the influence of T_{max} on T_{min}, particularly during the warmer months when T_{min} are more strongly influenced by T_{max} from the previous day (Jones and Trewin, 2000; Ashcroft *et al*., 2014).

With the exception of the northern interior and central interior, the T_{max}/T_{min} signal period for El Niño phases occur between December (0) - March (+)/April (+) (Table 5.3). The signal period is influenced by the distance between the Pacific Ocean and South Africa, as also the various stages of an ENSO event in the Pacific Ocean. A typical El Niño event in the Pacific Ocean undergoes antecedent conditions in September (-), an early stage of warming (onset phase) during December (-1) and the peak phase during April (0) (i.e., just before the maximum temperature occurs near the Equador-Peru coast) (Rasmusson and Carpenter, 1982). This is followed by the transition phase in September (0), which is the end of the first sharp decrease of Sea Surface Temperatures (SSTs) and finally the mature stage, during January (+1), when composite SSTs decrease along the coast and approach normal (Rasmusson and Carpenter, 1982). However, the weather/climatic consequences of each El Niño event are not identical given that these depend on the intensity of the event, the time of year when the event develops and the interaction with other climate dynamics (WMO, 2014).

Previous studies over southeastern Africa noted above median T_{mean} for El Niño phases starting in October (0), with the detected signal period extending to June (+) following El Niño phases for the period 1880-1988 (Halpert and Ropelewski, 1992). The differences in the signal periods selected by this study and that of Halpert and Ropelewski (1992) may arise from the different periods of observation, temperature variables used, and stations used. In addition, Jones and Trewin (2000) note a greater impact of ENSO on Australian T_{mean} compared to other temperature variables, such as diurnal temperature range, suggesting that the influence of ENSO phases on temperature reported by previous investigations (i.e., Halpert and Ropelewski, 1992) may be stronger compared to the current study.

Different ENSO responses are noted for the various regions (northern interior, central interior, western interior, northeastern interior, northeast coast, southeast coast and southwest coast), different periods (1940-1978; 1979-2016) as well as different temperature variables (T_{max}/T_{min}). Similarly, Ashcroft *et al*. (2016) note that different regions in Australia may experience various climatic responses to ENSO phases. For instance, in Australia the relationship between ENSO phases and rainfall is strongest over the inland eastern region while a more complex relationship exists between ENSO and south eastern Australian rainfall due to topography and other remote large scale atmospheric circulation features (Ashcroft *et al*., 2016). In the South African context, positive correlations (+0.45) are observed for SOI and rainfall during December, January and February over central South Africa, while negative correlations (-0.10) occur over the southwestern Cape Province (Lindesay, 1988).

For La Niña events, earlier studies report below normal T_{mean} for the period August (0) - June (+) over southeastern Africa for the period 1880-1988 (Halpert and Ropelewski, 1992). This study demonstrates below normal T_{max}/T_{min} for May (0) - August (0) over the northern and central interior regions, while that for the remaining regions is below the median T_{max}/T_{min} during May (0)/June - September (0)/October (see Table 5.3). Temporal consistency rates are low, varying between 33%-56% for T_{max}/T_{min} during La Niña phases (Table 5.4). Previous studies also noted the difficulty in determining La Niña related responses due to the occurrence of El Niño and La Niña in subsequent years (Dracup and Kahya, 1994). For instance, the year 1998, categorised as a La Niña event in this study, is preceded by an El Niño event, resulting in above median T_{max}/T_{min} over various regions (northern interior, central interior, western interior, northeastern interior, southeast coast and southwest coast). It is possible that the strong El Niño event affected the subsequent La Niña temperature

influence over this region. Notably, La Niña phases resulting in above median temperatures mostly occur after 1973, which perhaps reflects the combined effect of regional warming and the response to El Niño phases. Previous studies record increased magnitudes of El Niño phases since the mid-1970s (Haines *et al*., 2000), which possibly overwhelmed the La Niña-temperature response. Also noteworthy is that climate change may alter the frequency and magnitude of the ENSO cycle (Haines *et al*., 2000).

The destructive environmental and socio-economic impacts of ENSO demand an improved understanding of how ENSO and its influence on temperature will change under greenhouse warming conditions (Kim *et al*., 2014). Therefore, the relative strength of ENSO's influence on T_{max} and T_{min} through time was investigated, taking into account regional warming. The 1976/1977 climatic shift of ENSO activity resulted in more frequent El Niño phases after 1976 (Trenberth *et al*., 2002). The influence of El Niño phases on T_{max} and T_{min} strengthens when comparing the periods 1940-1978 with 1979-2016 over the northern interior region, southeast and southwest coasts of South Africa (see Table 5.5). The strengthening influence of El Niño phases on T_{max} over the southwest coast (0.16°C) is less than that for the southeast coast (0.15°C), possibly due to the cold Benguela upwelling system along the southwest coast (Philippon *et al*., 2012). In addition, a previous investigation of ENSO impacts on the Western Cape summer climate and SSTs, where prevailing southeasterly winds drive a coastal upwelling, found that wind speed is weaker (stronger) than normal during El Niño (La Niña) phases leading to changes in SSTs (Rouault *et al*., 2010). A strengthening influence of El Niño phases on T_{min} over the northeast coast is observed when comparing the earlier and later epochs. Notably, the strengthening influence of El Niño phases on T_{max} through time over the northern interior and southeast coast are significantly the strongest (0.45°C) compared to all other regions tested in this study (see Table 5.5). A similar strengthening of the ENSO association with summer rainfall has been reported over the northern and eastern regions of South Africa since the mid 1970s (Richard *et al*., 2000). For the winter rainfall region of South Africa, Philippon *et al*. (2012) also report a significant correlation between ENSO and winter rainfall after the 1976/1977 climatic shift, indicating a strengthened association with time. Using a simple dynamical model, it has been shown that the ENSO related signal emerging from the tropics was three times stronger in amplitude over the period 1978-1997 compared with 1958-1977 (Greatbatch *et al*., 2004). Sun *et al*. (2015) also observe a stronger influence of ENSO on summer surface temperature over western Russia

and suggest that the enhancement of ENSO teleconnection may be attributed to a change in the ENSO-related tropical thermal forcing after 1980.

In contrast to the El Niño-temperature response recording a strengthening influence of positive temperature departures over the majority of regions, La Niña phases record a weakening influence on T_{max}/T_{min} through time, which reflect the asymmetric impacts of the two ENSO phases. With the exception of the northern interior, all other regions record a weakening influence of La Niña phases on T_{max} when comparing the periods 1940-1978 with 1979-2016, indicating that the cooling influence of La Niña phases on T_{max} for the later epoch is no longer as strong as the earlier epoch during the relevant signal periods. The greatest weakening influence of La Niña occurs over the northeastern interior and northeast coast when comparing the earlier epoch with later epoch. This is due to the stronger warming trends observed for the more recent epoch, which may also be influenced by the intensification of the warm Agulhas current along the east of the country (Rouault *et al*., 2010). The influence of La Niña phases on T_{min} also weakens through time over the northern interior, western interior and northeastern interior, while a weak strengthening influence is recorded over the central interior and northeast, southeast and southwest coasts (Table 5.5). The weak strengthening influence of La Niña phases over the northeast and southeast coasts are a result of stronger warming in the later epoch while that over the south west coast is due to a weakened cooling effect (Table 5.5). This may, in part, be due to a reduced frequency of La Niña phases since the late 1970s (Kane, 2009).

The rates of occurrence of the various temperature categories when ENSO phases occur provide relevant information for risk assessment and management (Davey *et al*., 2014). However, counts of a specific temperature category can easily vary by 1 or 2 yielding inaccurate rates of occurrence (Davey *et al*., 2014), thereby presenting some limitations for the contingency table and Chi-Square test results. In addition, the rates of occurrence are lower than the consistency rates obtained by composite analysis. This is possibly due to the selection of ENSO years from the average of SOI data for the specific months of December, January and February. However, the Chi-Square test results reflect the findings of the composite analysis, indicating that ENSO phases exert a stronger influence over the interior of South Africa compared to its influence over coastal regions, possibly due to substantially reduced oceanic influences over these regions.

The aforementioned results have important implications for use in future research of ENSO-temperature relationships over South Africa, given that little is known about the physical processes responsible for surface temperature signals, such as the role of water vapour, clouds and land surface properties (Zhang *et al.*, 2011). ENSO phases result in global mean surface air temperature because of heat exchanges across ocean-atmosphere-land boundaries (Trenberth *et al.*, 2002). The physical mechanism responsible for ENSO's influence on climate over South Africa is still largely unknown (Boulard *et al.*, 2013). A possible mechanism may be through the loss of heat from the ocean to the atmosphere via evaporation which results in latent heat responsible for teleconnections (Trenberth *et al.*, 2002). Power *et al*. (1998) suggest that surface temperature changes (associated with rainfall) are forced by surface short wave radiation and latent heating, with the latter being a greater source of heating compared to the former in low latitude regions of deep convection. Decreased temperature is associated with cloudy conditions and a decrease of incoming short-wave radiation while increased temperature is linked to decreased cloudy conditions (Jones and Trewin, 2000). In addition, recent studies indicate that the response of ENSO is dependent on the phase of the Madden Julian Oscillation (MJO) over the Northern Hemisphere (Shimizu *et al*., 2016). However, the combined effects of ENSO and MJO over the Southern Hemisphere are not well understood (Shimizu *et al*., 2016). In addition, quasi-biennial oscillations (QBO) and quasi-triennial oscillations (QTO) may also influence the impact of ENSO phases on temperature and need to be further investigated (Kane, 2009). Further investigations are also required to understand the influence of the Southern Annular Mode on ENSO teleconnections (Fogt *et al*., 2011).

5.6. CONCLUSION

The results of this study demonstrate the importance of assessing the impacts of El Niño and La Niña phases on T_{max}/T_{min} independently for different climatic regions of South Africa. The variety of T_{max}/T_{min} responses to El Niño/La Niña phases (magnitude and timing) for the different climate regions have important implications for regional disaster planning, given the destructive environmental consequences of ENSO events. Most notable is the strengthening/weakening influence of El Niño/La Niña phases on T_{max} and T_{min} when comparing the periods 1940-1978 with 1979-2016. The strengthening influence of El Niño on both T_{max} and T_{min} through time occurs over the northern interior region, southeast and southwest coasts. This strengthening influence of El Niño phases on T_{max} is also evident over

the northeast coast. Further studies are required to help improve the understanding of ENSO teleconnections in the Southern Hemisphere and determine whether the changes in these teleconnections are a result of global warming or internal decadal climate variability (Sun *et al*., 2016).

5.7. ACKNOWLEDGEMENTS

Thanks to the SAWS for providing temperature data. RL-G appreciates the Research Development Grant provided by the Tshwane University of Technology (TUT), South Africa, the Department of Higher Education and Training and the National Research Foundation of South Africa (98258).

5.8. REFERENCES

Allan RJ, Nicholls N, Jones PD, Butterworth IJ. 1991. A further extension of the Tahiti-Darwin SOI, early SOI results and Darwin pressure. *Journal of Climate* **4**: 743-749.

Ashcroft L, Karoly DJ, Gergis J. 2014. Southeastern Australian climate variability 1860-2009: A multivariate analysis. *International Journal of Climatology* **34**: 1928-1944.

Ashcroft L, Gergis J, Karoly DJ. 2016. Long-term stationarity of El Niño–Southern Oscillation teleconnections in southeastern Australia. *Climate Dynamics* **46**: 2991-3006.

Banholzer S. Donner S. 2014. The influence of different El Niño types on global average temperature. *Geophysical Research Letters* **41**: 2093-2099.

Barros VR, Grimm AM, Doyle ME. 2002. Relationship between temperature and circulation in southeastern South American and its influence from El Niño and La Niña events. *Journal of the Meteorological Society of Japan* **80**: 21-32.

Bartholomew H, Jin S. 2013. ENSO effect on land skin temperature variations: a global study from satellite remote sensing and NCEP/NCAR reanalysis. *Climate* **1**:53-73.

Boulard D, Pohl B, Cretat J, Vigaud N, Pham-XuanT. 2013. Downscaling large-scale climate variability using a regional climate model: the case of ENSO over Southern Africa. *Climate Dynamics* **40**:1141–1168.

Cai W, Borlace S, Lengaigne M, van Rensch P, Collins M, Vecchi G, Timmermann A, Santoso A, McPhaden MJ, Wu L, England MH, Wang G, Guilyardi E, Jin F. 2014. Increasing frequency of extreme El Niño events due to greenhouse warming. *Nature Climate Change* **4**: 111–116.

Chowdary JS, John N, Gnanaseelan C. 2014. Interannual variability of surface sir-temperature over India: impact of ENSO and Indian Ocean Sea surface temperature. *International Journal of Climatology* **34**: 416-429.

Davey MK, Brookshaw A, Ineson S. 2014. The probability of the impact of ENSO on precipitation and near-surface temperature. *Climate Risk Management* **1**:5-24.

Dracup JA, Kahya E. 1994. The relationships between US streamflow and La Niña events. *Water Resources Research* **30**: 2133-2141.

Fogt RL, Bromwich DH, Hines KM. 2011. Understanding the SAM influences on the South Pacific ENSO teleconnection. *Climate Dynamics* **36**: 1555-1576.

Greatbatch RJ, Lu J, Peterson KA. 2004. Nonstationary impact of ENSO on Euro-Atlantic winter climate. *Geophysical Research Letters* **31**: L02208, doi:10.1029/2003GL018542.

Grimm AM, Tedeschi RG. 2009. ENSO and extreme rainfall events on South America. *Journal of Climate* **22**: 1589-1609.

Haan CT. 1977. *Statistical Methods in Hydrology*. Iowa State University Press: Ames, IA.

Haines A, McMichael AJ, Epstein PR. 2000. Environment and health: Global climate change and health *Canadian Medical Association Journal* **163**:729-34.

Halpert MS, Ropelewski CF. 1992. Surface temperature pattern associated with Southern Oscillation. *Journal of Climate* **5**: 577-593.

Hänsel S, Medeiros DM, Matschullat J, Petta RA, de Mendonça Silva I. 2016. Assessing homogeneity and climate variability of temperature and precipitation series in the capitals of North-Eastern Brazil. *Frontiers Earth Science* **4**: 1-21. doi: 10.3389/feart.2016.00029.

Humlum O, Solheim J-E, Stordahl K. 2012. Spectral analysis of the Svalbard temperature record: 1912-2010. *Advances in Meteorology* 2012, Article ID 175296, 1-14. doi:10.1155/2012/175296.

Jones DA, Trewin BC. 2000. On the relationship between the El Niño-Southern Oscillation and Australian land surface temperature. *International Journal of Climatology* **20**: 697-719.

Jin YH, Kawamura A, Jinno K, Berndtsson R. 2005. Detection of ENSO-influence on the monthly precipitation in South Korea. *Hydrological Processes* **19**: 4081-4092.

Kahya E, Dracup JA. 1993. US streamflow patterns in relation to El Niño-Southern Oscillation. *Water Resources Research* **29**: 2491-2503.

Kane RP. 2009. Periodicities, ENSO effects and trends of some South African rainfall series: an update. *South African Journal of Science* **105**: 199-207.

Kiladis GN, Diaz HF. 1989. Global climatic anomalies associated with extremes in the Southern Oscillation. *Journal of Climate* **2**: 1069-1090.

Kim ST, Cai W, Jin F, Santoso A, Wu L, Guilyardi E, An S. 2014. Response of El Niño sea surface temperature variability to greenhouse warming. *Nature Climate Change* **4**: 786-790.

King'uyu SM, Ogallo LA, Anyamba EK. 2000. Recent trends of minimum and maximum over Eastern Africa. *Journal of Climate* **13**: 2876-2886.

Kruger AC. 1999. The influence of the decadal-scale variability of summer rainfall on the impact of El Niño phase and La Niña events in South Africa. *International Journal of Climatology* **19***:* 59–68.

Kruger AC, Shongwe S. 2004. Temperature trends in South Africa: 1960–2003. *International Journal of Climatology* **24**: 1929–1945.

Kumar P, Kumar KR, Rajeevan M, Shai AK. 2007. On the recent strengthening of the relationship between ENSO and northeast monsoon rainfall over South Asia. *Climate Dynamics* **28**: 649-660.

Lakhraj-Govender R, Grab S, Ndbele NE. 2016. A homogenized long-term temperature record for the Western Cape Province in South Africa: 1916-2013. *International Journal of Climatology* **37**: 2337-2353.

Landman WA, Beraki A. 2012. Multi-model forecast skill for mid-summer rainfall over southern Africa. *International Journal of Climatology* **32**: 303–314.

Lee JH, Julien PY. 2016a. ENSO impacts on temperature over South Korea. *International Journal of Climatology* **36**: 3651-3663.

Lee JH, Julien PY. 2016b. Teleconnections of the ENSO and South Korean precipitation patterns. *Journal of Hydrology* **534**: 273-250.

Lindesay JA. 1988. South African rainfall, the Southern Oscillation and a Southern Hemisphere semi-annual cycle. *Journal of Climatology* **8**: 17–30.

Manatsa D, Reason C. 2017. ENSO–Kalahari Desert linkages on southern Africa summer surface air temperature variability. *International Journal of Climatology* **37**: 1728-1745.

McAfee SA, Wise EK. 2016. Intra-seasonal and inter-decadal variability in ENSO impacts on the Pacific Northwest. *International Journal of Climatology* **36**: 508-516.

McKee TB, Doesken NJ, Kleist J. 1993. The relationship of drought frequency and duration to time series. In *Proceedings of the 8th Conference on Applied Climatology*, Anaheim, California, 179–187.

McPhaden MJ, Zebiak SE, Glantz MH. 2006. ENSO as an integrating concept in Earth Science. *Science* **314**: 1740-1745.

McPhaden MJ, Timmermann A, Widlansky MJ, Balmaseda MA, Stockdale TN. 2015. The curious case of the El Niño that never happened: A perspective from 40 years of progress in climate research and forecasting. *Bulletin of the American Meteorological Society* **96**: 1647-1665.

Mohsenipour M, Shahid S, Nazemosadat MJ. 2013. Effects of El Niño Southern Oscillation on the discharge of Kor River in Iran. *Advances in Meteorology*. doi 10.1155/2013/846397.

Philippon N, Rouault M, Richard Y, Favre A. 2012. The influence of ENSO on winter rainfall in South Africa. *International Journal of Climatology* **32**: 2333-2347.

Potter S, Cabbage M, McCarthy L. 2017. NASA, NOAA Data Show 2016 Warmest Year on Record Globally. Available online: https://www.nasa.gov/press-release/nasa-noaa-data-show-2016-warmest-year-on-record-globally (Accessed 22 January 2017).

Power S, Tseitkin F, Torok S, Lavery B, Dahni R, McAvaney B. 1998. Australian temperature, Australian rainfall and the Southern Oscillation, 1910-1992: coherent variability and recent changes. *Australian Meteorological Magazine* **47**: 85-101.

Rasmusson EM, Carpenter TH. 1982. Variations in Tropical Sea Surface temperature and surface wind fields associated with the Southern Oscillation/El Niño. *Monthly Weather Review* **110**: 354-384.

Reason CJC, Rouault M. 2002. ENSO-like decadal variability and South African rainfall. *Geophysical Research Letters* **29**: 1638-1641.

Reason CJC, Jagadheesha D. 2005. A model investigation of recent ENSO impacts over southern Africa. *Meteorology and Atmospheric Physics* **89**: 181–205.

Richard Y, Trzaska S, Roucou P, Rouault M. 2000. Modification of the southern African rainfall variability /ENSO relationship since the late 1960s. *Climate Dynamics* **16**: 883-895.

Ropelewski CF, Halpert MS. 1986. North American Precipitation and temperature pattern associated with El Niño/Southern oscillation (ENSO). *Monthly Weather Review* **114**: 2352-2362.

Rouault M, Pohl B, Penven P. 2010. Coastal oceanic climate change and variability from 1982 to 2009 around South Africa. *African Journal of Marine Science* **32**: 237-246.

Scaife AA. 2010. Impact of ENSO on European climate. ECMWF Seminar on Predictability in the European and Atlantic regions, 6 to 9 September 2010. Met. Office Hadley Centre. Available at http://www.ecmwf.int/sites/default/files/elibrary/2012/12119-impact-enso-european-climate.pdf.

Schulze GC. 1986. South African Rainfall Related to Warm and Cold Events, Second International Conference on Southern Hemisphere Meteorology (Wellington, New Zealand) 1–5 December 1986, American Meteorological Society, pp. 465–467.

Shimizu MH, Ambrizzi T, Liebmann B. 2016. Extreme precipitation events and their relationship with ENSO and MJO phases over northern South America. *International Journal of Climatology* **37**: 2977-2989.

Sun C, Li J, Ding R. 2015. Strengthening relationship between ENSO and western Russian summer surface temperature. *Geophysical Research Letters* **43**: 843-851.

Soltani A, Gholipoor M. 2006. Teleconnections between El Niño/Southern Oscillation and rainfall and temperature in Iran. *International Journal of Agricultural Research* **1**: 603-608.

Tedeschi RG, Grimm AM, Cavalcanti IFA. 2015. Influence of central and east ENSO on extreme events of precipitation in South America during austral spring and summer. *International Journal of Climatology* **35**: 2045-2064.

Tedeschi RG, Cavalcanti IFA, Grimm AM. 2013. Influences of two types of ENSO on South American precipitation. *International Journal of Climatology* **33**: 1382-1400.

Trenberth K. 1997. The definition of El Niño. *Bulletin of the American Meteorological Society* **78**: 2771-2777.

Trenberth KE, Caron JM, Stepaniak DP, Worley S. 2002. Evolution of El Niño-Southern-oscillation and global atmospheric surface temperature. *Journal of Geophysical Research* **107**: 5-12.

Tyson PD, Preston-Whyte RA. 2000. *The Weather and Climate of Southern Africa*. Oxford University Press Southern Africa, Cape Town.

Van Heerden J, Terblanche, DE, Schulze GC. 1988. The Southern Oscillation and South African summer rainfall. *Journal of Climatology* **8**: 577–597.

Warner K, Oberheide J. 2014. Nonmigrating tidal heating and MLT tidal wind variability due to the El Niño-Southern Oscillation. *Journal of Geophysical Research: Atmospheres* **119**: 1249-1265.

Weldon D, Reason CJC. 2014. Variability of rainfall characteristics over the South Coast region of South Africa. *Theoretical and Applied Climatology* **115**: 177-185.

Welhouse LJ, Lazzara MA, Keller LM, Tripoli GJ, Hitchman MH. 2016. Composite analysis of the effects of ENSO on Antarctica. *Journal of Climate* **29**: 1797-1808.

WMO. 2014. El Niño/Southern Oscillation. WMO No. 1145, Geneva, Switzerland, 2–4. Available online http://www.wmo.int/pages/prog/wcp/wcasp/documents/JN142122_WMO1145_EN_web.pdf (Accessed 27 June 2016).

WMO. 2016. El Niño/La Niña May 2016 Update. Available online http://www.wmo.int/pages/prog/wcp/wcasp/enso_update_latest.html (Accessed 20 April 2016).

Zhang T, Hoerling MP, Perlwitz, Sun D, Murray D. 2011. Physics of U.S. surface temperature response to ENSO forcing. *Journal of Climate* **24**: 4874-4887.

CHAPTER SIX

SYNTHESIS

6.1. INTRODUCTION

The significant unprecedented warming of the earth's surface over the past century as well as the observed spatial and temporal non-uniform warming (Ji *et al*., 2014), emphasizes the need for research at regional and sub-regional levels, as carried out in this PhD study. The increased interest in temperature variability is related to global warming as a result of anthropogenic enhancement of the greenhouse effect (Bradzil *et al*., 2005). The Intergovernmental Panel on Climate Change (IPCC) reports indicate that there is strong scientific evidence to support that climate change is attributed to human activities (IPCC, 2013). In addition, these reports have highlighted the comprehensive assessment of temperature changes at the global scale but emphasize the need for long-term trends at regional and local scales due to knowledge gaps that remain at this level (Niang *et al*., 2014). To this end, regional efforts in southern Africa to further understand surface temperature changes under current global warming scenarios will speak to this call.

South Africa has been identified as highly vulnerable to climate change and climate variability (Akoon *et al*., 2010). South Africa consists of vastly different climatological regions, with the plateau experiencing hot summers and cold winters, while oceans moderate coastal climates, providing milder winters (Akoon *et al*., 2010). This spatial variability presents challenges for weather prediction, seasonal forecasting and projection of climate change (Akoon *et al*., 2010). An advanced understanding of temperature variability through time is also of extreme importance to South Africa, given the many sectors (e.g. agricultural, water resources, energy, biodiversity and health) affected by the pronounced temperature changes through time (Niang *et al*., 2014).

Previous temperature trend analyses for South Africa have covered relatively short periods (i.e. 35-43 years) extending back to 1960 (Kruger and Shongwe, 2004; MacKellar *et al*., 2014). Kruger and Shongwe (2004) used stations that had not moved and had no changes to exposure of instrumentation, to ensure homogeneity did not influence the accuracy of temperature trends. Research using long-term temperature data for South Africa has been limited to the recent study by Kruger and Nxumalo (2017) who use absolute homogenization methods to detect change points and adjust temperature time series. This absolute homogenization method, without the use of a reference series, has been deemed potentially

problematic due to the separation of the climate signal which decreases the homogeneity of the data for monthly and annual means (Venema *et al*., 2012). To address these limitations and challenges of previous studies, the main aim of this PhD study was to use accurate relatively long-term data sets (spanning 1851-2016) to establish a deeper understanding of temporal and spatial temperature variability over South Africa. This is achieved through robust methodology, such as data quality control and relative homogenization (with a reference series) to produce high quality temperature datasets, spatial analyses (continental vs coastal temperature trends) and an assessment of the impact of El Niño-Southern Oscillation (ENSO) events on temperature. This chapter synthesizes the research presented in previous chapters, reflecting on the objectives and how these were achieved. In addition, the key findings are placed in the broad context of existing literature. Finally, the limitations of this study, potential future research, and a final synopsis are presented.

6.2. ACHIEVEMENT OF STUDY OBJECTIVES

This PhD study has advanced our understanding of South African temporal temperature variability by providing temperature trends of long-term quality controlled and homogenized (with a composite reference series) temperature records for specific regions, with an assessment of the extent and timing of the impact of ENSO events on temperature. The specific objectives of this study are presented in bold below and how these objectives are met is then reflected upon.

- **Objective 1: To provide a homogeneous dataset for the Western Cape region in South Africa and establish the first long-term (97 years) annual and seasonal instrumental temperature trends for this region.**

This objective is achieved through robust quality control (Chapter three, sections 3.3.2 and 3.4.1), relative homogenization procedures (Chapter three, sections 3.3.3; 3.3.4 and 3.4.2) and nonparametric statistics (i.e. Mann Kendall and Sen's slope) (Chapter three, sections 3.3.5 and 3.4.3). The quality control of temperature data was conducted using RClimDex software and station history. The detection of change points and the adjustment of temperature time series datasets were conducted utilizing ProClimDB and AnClim software.

The temperature trend analysis results discussed in Chapter three, section 3.4.3 and presented in Figure 3.4 and Tables 3.6 and 3.7, report increasing mean annual T_{max}/T_{min} trends of 0.13°C/decade and 0.12°C/decade respectively over the Western Cape region for the common period 1937-2001. Similarly, mean seasonal T_{max} and $T_{min,}$ record statistically significant increasing trends over the Western Cape, with the exception of decreasing T_{max} trends during summer and autumn at Kirstenbosch (see Table 3.8). In addition, the results discussed in Chapter three, section 3.4.3., indicate that mean annual T_{max} and T_{min} data for the Western Cape region of South Africa maintain the same direction before and after homogenization over their respective recording periods (1916 to 2013). An exception to this is T_{min} at Jonkershoek, which changed from a decreasing trend before homogenization to an increasing trend after homogenization (see Figure 3.4h). The quality control, homogenization and trend analysis methods established in the achievement of the first objective were further applied to the KwaZulu-Natal (KZN) region (in Chapter four), hence determining precise temperature trends which address objective two for this PhD.

- **Objective 2: To extend past work by examining temperature trends for KZN over a considerably long period, with a specific focus on contrasting coastal and adjacent higher lying interior regions (see Chapter four).**

This objective is achieved through analyzing instrumental temperature records from the coastal stations of Durban and Mount Edgecombe, and interior stations of Pietermaritzburg, Cedara and Emerald Dale. The second half of the 19th century (i.e. 1851, 1858, 1860-1864) record cooler conditions compared to more recent times in KZN. Mann Kendall trend analyses indicate that annual T_{max} record a weak significant increasing trend at the coast and no trend over the interior for 1930-2015. Annual T_{min} record significant warming at all stations, with warming rates over the interior being double that for the coast over the period 1930-2015 (Chapter four, Figure 4.5). Annual T_{mean} warming over the interior started during the early 1980s while warming at the coast was delayed by a decade. Notably, annual T_{max} and T_{min} increased at considerably faster rates (0.04°C/decade and 0.06°C/decade faster, respectively) over the interior compared to the coast during the most recent 30 years. Rates of T_{min} warming are 1.31 (summer), 2.75 (autumn), 3.33 (winter) and 1.25 (spring) times faster over the interior compared to the coast for the period 1930-2015. (Chapter four, Table 4.3).

- **Objective 3: To assess the extent and timing of El Niño/La Niña impacts on T_{max} and T_{min} over selected South African stations for the period 1884-2016, and to establish any possible change in such temperature responses to ENSO over time (see Chapter five).**

The detailed T_{max}/T_{min} response to El Niño/La Niña events for the northern interior, central interior, western interior, northeastern interior, northeast, southeast and southwest coasts of South Africa are presented in Chapter five (see Figures 5.2 to 5.8) and discussed in sections 5.4.1 and 5.4.7. The detailed results for the investigation of the change in temperature response to ENSO events through time are presented in Table 5.5. The most important finding is that El Niño events have had a stronger warming effect over many regions in South Africa for the more recent period (1979-2016) compared to the earlier epoch (1940-1978).

Collectively, the successful recovery, digitisation, robust quality control and homogenization of long-term temperature data sets in this PhD have led to the precise determination of temperature trends. Therefore, the main aim to use high quality, relatively long-temperature data sets to determine temperature trends and deepen our understanding of spatial distribution and temporal temperature variability over South Africa, has been achieved. The warming trends observed for South Africa's west and east coasts at annual and seasonal scales is consistent with global warming trends, as well as previous South African studies (such as Kruger and Shongwe, 2004). This differential warming across South Africa has been attributed to atmospheric circulation changes (Kruger and Sekele, 2013). The complexity of studying the temporal and spatial distribution of temperature variations of specific areas is further illustrated by ENSO's influence on temperature over various regions of South Africa, which is known to result in decadal and multi-decadal climate variability. The physical mechanisms responsible for the role of oceanic and atmospheric drivers of regional climate are briefly explored.

6.3. KEY FINDINGS

The purpose of this section is to place the key findings of this PhD research in context with the current theoretical knowledge in this field and integrate the three different research papers

(Chapters three-five). The global average land and ocean surface temperature linear trend has increased by 0.85°C over the period 1880-2012 (IPCC, 2013). Global surface temperatures continue to increase, with the years 2014, 2015 and 2016 setting new record-breaking highs since the beginning of instrumental records (Rahmstorf *et al*., 2017). There have been publications stating a slowing-down/hiatus in the observed warming, however, Rahmstorf *et al*. (2017) indicate that these are merely short-term fluctuations. In addition, Karl *et al*. (2015) report warming trends of 0.113°C/decade over the period 1950-1999 and 0.116°C/decade for the period 2000-2014, indicating that the linear global temperature trend is not slowing down. Global temperature changes are a subject of discussion not only within the scientific community but also amongst the public as the rising temperatures directly affect people at all levels as well as various sectors of multiple countries. Combined with the consequences (such as the natural disasters across the globe) and anthropogenic causes of climate change, the importance of temperature trend studies is revealed and emphasized. Whilst the IPCC reports and the literature review (in Chapter two of this PhD thesis) highlight the overwhelming scientific studies conducted across the globe on temperature trend investigations, such studies have been more limited for the southern African region. This emphasizes the importance of the current PhD work. The findings of this PhD study represent a significant step forward to expand on the foundational work of Kruger and Shongwe (2004), MacKellar *et al*. (2014) and Kruger and Nxumalo (2017).

While Kruger and Nxumalo (2017) homogenize temperature records for South Africa, without a reference series, the absolute methods used have been severely criticized by COST (European Cooperation in Science and Technology) Action ES0601 project: *advances in homogenization methods of climate series: an integrated approach* (HOME). This PhD study has therefore laid the foundation for research focused on long-term temperature change in South Africa, based on high quality relatively homogenized records. This research has shown that different rates of warming are obtained before and after homogenization procedures are applied to time series (see Chapter three), thereby demonstrating the importance of critically assessing and preparing temperature datasets when establishing temperature trends in South Africa or elsewhere.

The key findings are as follows (graphically represented in Figure 6.1):

- Statistically significant increasing annual temperature trends were observed for adjusted (homogenized) T_{max} and T_{min} data over the Western Cape region over the period 1916-2013, with the exception of an insignificant decreasing T_{max} trend at Cape St Blaize. For the common period (1937-2001), a statistically significant increasing trend (0.13°C/decade) is recorded for all stations in the Western Cape Province, with a 0.04°C/decade stronger warming signal than before homogenization was applied.

- Mean seasonal T_{max} and $T_{min,}$ record statistically significant increasing trends over the Western Cape, with the exception of decreasing T_{max} trends during summer and autumn at Kirstenbosch.

- Considerably faster annual and seasonal warming were reported for higher lying interior regions compared to the adjacent coastal areas over the most recent 30 years in particular, mainly due to strong T_{min} warming trends over the interior.

- Coherent relationships exist between El Niño/La Niña events and T_{max}/T_{min} over various regions of South Africa (northern interior, central interior, northeastern interior, western interior, northeast, southeast and southwest coasts), with the northern interior region displaying an earlier and longer response to El Niño events compared other regions.

- El Niño events have had a stronger warming effect over many regions in South Africa after the late 1970s (1979-2016) compared to the previous period (1940-1978). The most prominent regions being the northern interior and southeast coast, where associated T_{max} record an average of 0.41°C and 0.45°C, respectively, higher values for the period 1979-2016 compared to the earlier period (1940-1978).

Collectively, the recovery of historical temperature data for South Africa is essential for a complete understanding of temporal and spatial temperature variability. Without such data, it would be impossible to determine precise long-term temperature changes and make important associations with temperature control mechanisms. In determining these changes, quality control and homogenization procedures are emphasized. It is clear from the findings of this

PhD study that warming has occurred over various regions of South Africa for the period 1851-2015. To place the homogenized records in the context of existing literature, temperature trends over the Western Cape Province were analysed for the period 1960-2003. For this period, Kruger and Shongwe (2004) report greater warming trends compared to the homogenized data for five stations (Cape Agulhas, Cape Columbine, Cape Point, Jonkershoek and Langgewens) in the Western Cape Province (this PhD thesis).

The extent of warming, however, is affected by various spatial factors such as altitude, distance from the coast (i.e., interior vs coastal temperature trends) and topography. For instance, this study has shown that annual T_{min} warming rates over the interior were double that over the coast for the period 1930-2015. Seasonal T_{min} warming rates were also faster over the interior compared to the coast. Kruger and Shongwe (2004) also report higher warming rates for central stations compared to the coastal stations in South Africa over the period 1960-2003. In addition, the extent of warming is dependent on temporal factors such as the length of the time series. For instance, Chapter four reflects faster warming rates for the most recent 30-year period compared to the full 85-year period. This has not been demonstrated for any previous temperature trend analyses for South Africa.

The findings of Chapter four (such as the lagged warming at the coast) are also expected to increase the understanding of oceanic influence on temperature, which is important given previous efforts to improve the representation of oceanic influence in modeling approaches (DEA, 2013). While Kruger and Shongwe (2004) report higher temperature trends over the interior compared to the coastal regions of South Africa, for the period 1960-2003, Kruger and Nxumalo (2017) record strong decreasing trends at the coast over the period 1931-2015. These studies do not provide detailed comparisons of coastal vs. interior temperature trends. In addition, the interplay of synergistic operating climate mechanisms, such as anthropogenically-induced CO_2 warming, the Madden-Julian Oscillation, Quasi Biennial Oscillation and ENSO are not completely understood, therefore the findings in Chapter five are expected to contribute to further understanding the influence of mechanisms on temperature variability over South Africa. El Niño events have also strengthened its warming influence through time, however the extent of this strengthening varies between regions of South Africa. For instance, the strengthening influence of El Niño events on T_{max} through time over the northern interior and southeast coast are significantly the strongest compared to

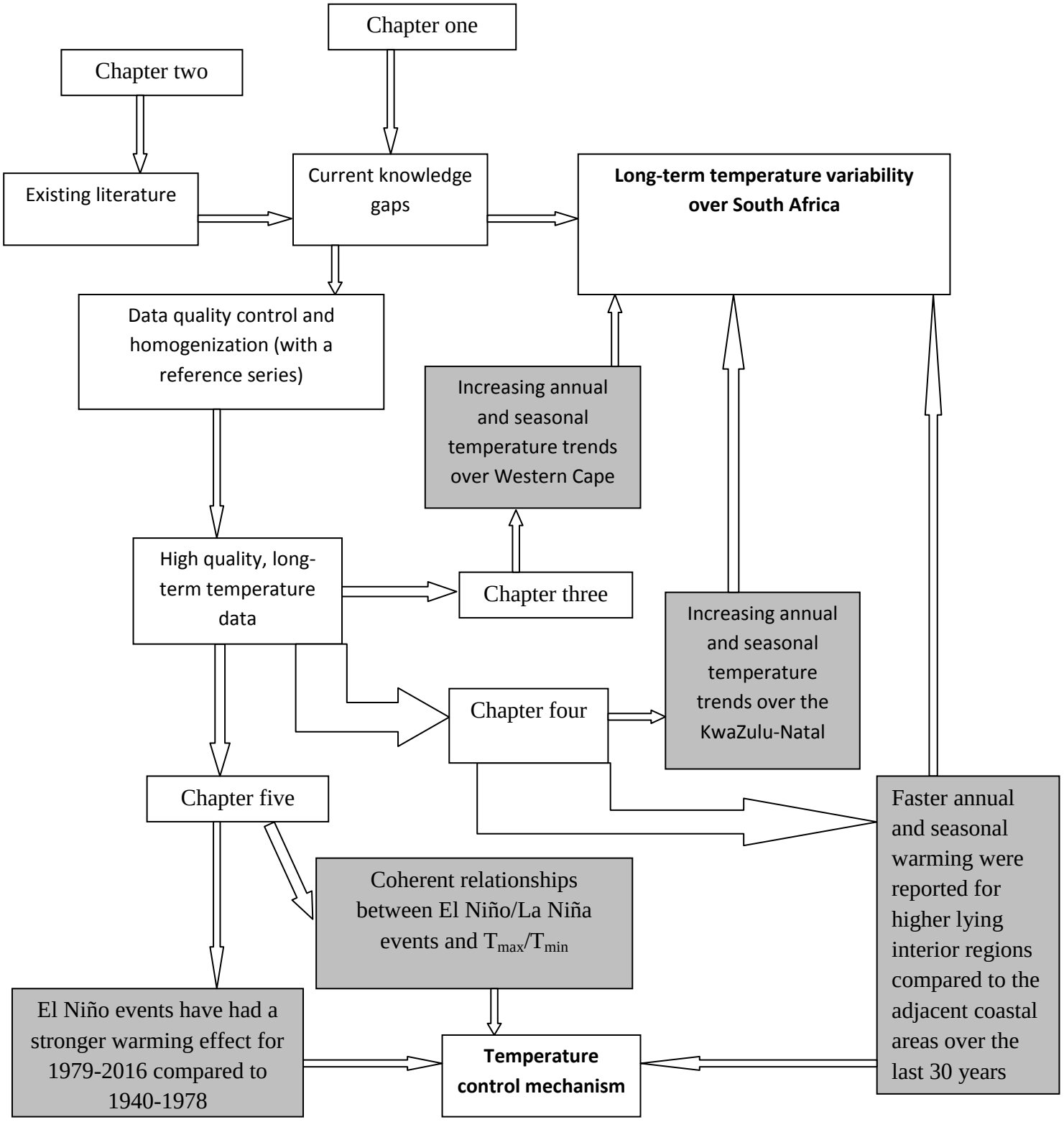

Figure 6.1: Graphical summary of major findings (gray shaded boxes), chapter numbers and major themes (bold).

all other regions tested in this study. In addition, the strengthening influence of El Niño events on T_{max} over the southwest coast is less than that of the southeast coast, possibly due to the cold Benguela upwelling system along the southwest coast (Philippon *et al*., 2012). Previous studies conducted for the effect of ENSO events on South African temperature have been limited to the global analyses (by Halpert and Ropelewski, 1992), while majority of the investigations have determined ENSO's effect on rainfall. The findings of this ENSO study contribute to the originality of the work conducted by this PhD. Notably, the increased temperature response to ENSO phases over the interior, compared to the coast of South Africa, have been reported in studies on Australia, indicating that this is the case because the interior regions are not subjected to oceanic influences (Ashcroft *et al*., 2016). Collectively, the comprehensive temperature trend analyses through time, the role of oceanic and continental influence on sub-regional temperature changes, and the various temperature responses to El Niño/La Niña events, provide valuable insight into temporal and spatial temperature variability across South Africa.

6.4. ADVANTAGES AND LIMITATIONS OF THIS STUDY

The scope of this PhD study has been limited to the availability of long-term temperature datasets with minimal gaps and missing data. Scientific methods are laden with uncertainties and limitations, during the development of models, whilst taking measurements, during the analyses and interpretation of assumptions (Cubasch *et al.*, 2013). The most important limitation of historical temperature trend studies is the unavailability of long-term data to adequately represent a region's climate. Therefore, intensifying data recovery and digitization efforts will increase the data available for use in temperature trend studies, provided that such historic data exist. The homogenization of early temperature records (pre-20th century) is particularly challenging due to the lack of documentation detailing with historical instrument exposure and instrument changes (Trewin, 2010). In addition, pre-20th century data were measured in exposures that are not consistent with recent methods (Trewin, 2010). Nineteenth century data sets are also short and there is a lack of available neighbour stations for use in the creation of reference series (Ashcroft *et al*., 2014). According to an IPCC technical paper, advancing the understanding of ongoing temperature changes is dependent on increased data access and availability (Bates *et al*., 2008). In addition, the recovery of data records (to extend existing data) is essential because short-term records may

not reflect the full extent of natural variability (Bates *et al*., 2008). There are still many regions of South Africa where historical temperature data need to be recovered and digitised, such as those conducted for KZN in this PhD project.

The limitations of this PhD study included data gaps that prevented analyses of long-term data (such as those presented in Chapter four), the lack of access to detailed metadata to statistically verify detected change points, and most importantly the inherent limitations of the homogenization process. Despite the advantage of homogenization techniques, which remove non-climatic biases in climate time series, these methods are not perfect and thus leave several uncertainties and limitations (Trewin, 2010). For instance, statisical homogeneity testing produces results with a degree of uncertainty because of the noise in time series (Štěpánek *et al*., 2009). Homogeneity is assessed more reliably by using multiple statistical tests (SNHT and Bivariate tests) available in ProClimDB and AnClim software (Štěpánek *et al.,* 2009). Even so, the most effective homogenization techniques may produce false detections and detect only some of the inhomogeneities (Venema *et al*., 2012). Significant effort has been made to develop and improve these techniques in order to address these uncertainties (Hartmann *et al*., 2013). However, substantial uncertainty also remains in global homogenized data products as a result of the restricted access to metadata and the lack of a dense station network for use in the development of reference series (Trewin, 2010).

A considerable amount of work has been conducted to develop techniques for the detection of inhomogeneities and the adjustment of climate time series to produce homogeneous climate time series. Two broad methods of detecting inhomogeneities are the use of metadata or the statistical tests, which identify significant change points (Trewin, 2010). The problems associated with metadata include incomplete or inaccurate records. Although relative homogenization (detecting change points and adjusting time with the use of a reference series) is a preferred method compared to absolute homogenization, the former methods rely on the assumption that the reference series is homogeneous (Trewin, 2010). This presents challenges when parallel adjustments affecting the whole network are made simultaneously. These include observation techniques, such as changes in observation time or the method of calculating the T_{mean} (Trewin, 2010). This means that data from neighbour stations used as reference series will also have the change/bias due to non-climatic conditions.

A major limitation of relative homogenization is the creation of a homogeneous reference series using data with unknown inhomogeneities (Peterson *et al*., 1998). The construction of a homogeneous reference series that represents same climatic variation is often difficult. Finding suitable reference series is particularly challenging in data-sparse regions (Trewin, 2010). As a result of the limited number of neighbour stations, the Pearson Correlation Coefficient used in this PhD study is 0.6. A higher correlation coefficient would have produced a more reliable reference series, however, this resulted in the elimination of many of the neighbour stations (Štěpánek *et al*., 2009). Peterson and Easterling (1994) point out that using correlation coefficients can also be problematic because two stations with a few years of overlap may have high correlations due to chance. This PhD work used various other techniques to minimize inhomogeneities in the reference series (such as selecting stations which did not exceed a distance of 300km and altitudinal range of 500m; and a minimum overlap of 10 years is required between stations) (Peterson *et al*., 1998). The statistical detection of change points without metadata is based on subjective decisions as to which change points should be adjusted in the time series, which can lead to inaccuracies.

Although some South African stations changed to automatic weather stations toward the end of the period of record, inhomogeneities detected within 4 years of the end of the time series were not adjusted (Štěpánek and Mikulová, 2008). A widely used homogenization method is to retain the most recent homogeneous portion of the time series and adjust the portion prior to this section (Domonkos, 2013). This method works on the assumption that data were collected under good technical and environmental conditions and the last section of the time series is of a high quality (Domonkos, 2013). However, if this homogeneous section is influenced by urbanization, the entire homogenized time series will be affected (Domonkos, 2013).

Many weather stations began temperature recordings in small towns which developed into major cities, resulting in urban growth affecting long-term temperature records (Jones and Wigley, 2010). Urbanisation has been associated with an increase in temperature as a result of "heat islands" and other local anthropogenic effects (Giugni *et al*., 2015). Assessing the effects of urbanization is particularly challenging because stations are not necessarily located in the central part of the city and the effect will differ from city to city (Jones 2016). Nevertheless, the urban heat island effect has apparently only had a minor impact on global land surface air temperatures over the period 1906-2005 (Parker, 2010). According to Jones

(2016), numerous studies have found large differences between temperature differences at urban and rural stations, but the results do not affect long-term averages. Similarly, Jones and Wigley (2010) indicate that the effect of urbanization on temperature may be large locally, especially where urban development is rapid, but the magnitude of the differences between rural and urban regions is small compared to long-term increases. Although Hughes and Balling (1996) displayed that warming over South Africa for the period 1960-1990 is inflated by urban effects, Kruger and Shongwe (2004) indicate that urban stations in South Africa (located on the outskirts of cities) are not substantially influenced by the urban heat island effect over the period 1960-2003. This PhD study did not account for the effect of urbanization on temperature records, given the sparse station network and the difficulty in finding matching urban and rural counterparts.

6.5. FUTURE WORK

Findings from this study and literature cited in this PhD suggest knowledge gaps with regard to long-term temperature variability over South Africa still remain. This study focussed on specific regions in South Africa and therefore future work is required to expand the availability of high quality temperature data sets across all regions. Future work includes subjecting temperature data for the remaining stations (not used in this PhD study) in regions of South Africa to quality control and homogenization procedures (with reference series) in order to increase the availability of high quality data. The increased availability of high quality datasets across the various climatological regions of South Africa is expected to increase the accuracy of temperature trend analysis and advance our understanding of how temperature has changed through time, under various influencing factors (such as altitude, latitudinal position, effect of the interior plateau or oceanic influence). While Chapter four has contributed to our understanding of oceanic influence on temperature changes along the east coast, similar fine scale comparisons, at the west coast or south coast of South Africa, where different currents (i.e. Benguela and Agulhas currents) influence temperature trends, remains a knowledge gap. In addition, these high quality datasets can be used to determine trends in extreme temperature indices, such as conducted by Kruger and Sekele (2013), however, they only used stations that did not undergo major moves and had limited gaps to ensure inhomogeneities did not affect the time series. Such studies would increase the

accuracy of outcomes and the results will contribute to improved planning strategies for extreme weather events, which are indicative of the serious disruptions of the world's climate patterns as a result of global warming.

Based on the research findings, the following future work has been identified:

- Increasing the number of high quality data sets for each region is important as the regional inferences based on individual stations are dependent on how well a station or group of stations represents a particular region (MacKellar *et al*., 2014). In addition, future work must use detailed metadata to confirm change points to obtain more accurate long-term trends and scientific outcomes.

- Data recovery, quality control and homogenization efforts will lead to more accurate temperature trends analyses. This will increase the understanding of temperature variability across South Africa through time. In addition, these efforts will advance our understanding of spatial temperature changes across the various climate zones in South Africa. The insufficient information with regard to the impacts of temperature changes at fine spatial scales calls for future work relating to, but not limited to, the differences/similarities of temperature variability between coastal and adjacent higher lying interior regions, at different altitudes or within various topographical settings.

- The aforementioned data recovery, quality controlled and homogenized time series (i.e. high quality data sets) can lead to in-depth analyses of precise temperature trends as well as establish important associations with various temperature control mechanisms such as Madden Julian Oscillation (MJO), Southern Annular Mode (SAM), quasi-biennial oscillations (QBO) and quasi-triennial oscillations (QTO) (Kane 2009; Shimizu *et al*., 2016). An increased understanding of these important drivers of climate variability over Africa is not well represented in GCMs (Hulme *et al*., 2000).

- An assessment of the impact of major volcanic eruptions, such as El Chichón (April 1982) and Pinatubo (June 1991) on South African temperature is a knowledge gap. It is important to determine whether these eruptions have impacted temperatures over certain or all regions of South Africa because El Chichón and Pinatubo resulted in a global

cooling of 0.2°C and 0.5°C, respectively, approximately 13 months after the eruption (Trenberth *et al*., 2002). This is important for future planning and disaster risk management strategies.

- The inconsistencies between observed and General Circulation Model (GCM) simulations reported by previous studies (e.g. DEA, 2013; Jury, 2013) as discussed in Chapters one and two, warrant the need for further research. Future studies should determine whether these discrepancies still exist, with the use of the homogenized records for observed temperature trend analyses. The temperature trend results from this PhD may be used together with GCMs to produce more reliable projections of temperature changes across South Africa.

- The attribution of regional warming temperatures to natural or anthropogenic processes, such as increasing greenhouse gas concentrations and land use changes will increase the understanding of the factors that play a role in climate change. Insufficient information is available at this fine spatial scale, therefore future work involving correlation of air pollution levels with that of temperature will provide valuable information to establish effective adaptation and mitigation strategies.

- In an agriculturally intensive country such as South Africa, future work on spatial and temporal temperature trends is vital for food security to feed the exponentially growing population, given that temperature changes have ecological impacts on fauna, flora and ecosystems. The outcomes of such studies would aid managers and decision makers when planning agricultural activities (Kousari *et al*., 2013).

- Observational records and climate projections provide ample evidence that water resources are vulnerable to climate change (Bates *et al*., 2008). However, the IPCC AR5 report has identified important knowledge gaps related to the uncertainty of the impact of climate change on water quality in Africa and limitations of climate models to capture rainfall projections (Niang *et al*., 2014). Surface and groundwater are controlled by multiple interacting factors such as land use change, water usage and natural climate variability (Niang *et al*., 2014). Surface air temperature changes have been identified as a major factor controlling water resources, through evapotranspiration regulation (Manatsa

and Reason, 2016). Therefore, in a water scarce, semi-arid country such as South Africa, research related to the impact of future temperature changes on water supply is essential for decision making and policy planning.

- An assessment of temporal and spatial temperature variability is not complete without examining the impact climatic drivers on temperature variables, given the role of ENSO in inter-annual variability. A previous study of ENSO influence on European climate demonstrated discrepancies in the strength of results when using different methods of analysis (Scaife, 2010). Whilst this PhD study examined composite analysis and contingency tables future studies should use correlation coefficient to compare the results obtained in this PhD project.

6.6. SYNOPSIS

It is particularly difficult for climate models to replicate all the physical processes and complexity of their feedback across the various temporal and spatial scales over the heterogeneous continent of Africa (Dosio *et al*., 2015). The outcomes of this PhD study, in combination with existing publications and continued research, are extremely important to climate modellers because these may help improve the resolution and accuracy of temperature projections. Continued efforts in historical data recovery, data quality control and homogenization procedures will increase the accuracy of temperature trends, which may be used to improve Regional Climate Models (RCMs) (Dosio *et al*., 2015). This is extremely important given the observed impacts of climate change (such as the increasing natural disasters as a result of global temperature increases). The major aim of this study was to use high quality, relatively long-term temperature data to advance the understanding of spatial and temporal temperature variability over South Africa. Despite the uncertainties associated with homogenization techniques, this PhD study successfully applied data quality control and relative homogenization (with a reference series) procedures to produce high quality datasets (using RClimDex, ProClimDB and Anclim software), thereby improving the accuracy of long-term trends. Increasing temperature trends are recorded at annual and seasonal scales across various regions in South Africa. The majority of warming trends recorded in this PhD are in line with recent global and regional warming trends. In addition, comparisons of

coastal and higher lying adjacent interior temperature trends, revealed faster warming rates over the interior compared to that for the coast, possibly due to oceanic influences on coastal temperatures. Annual T_{min} record warming rates over the interior being double that for the coast for the period 1930-2015. In addition, faster warming rates are recorded for the most recent decades, compared to the full 85-year period. The assessment of climatic control mechanisms (ENSO) showed that various regions (northern interior, central interior, western interior, northeastern interior, southeast coast and southwest coast) across South Africa exhibit different T_{max}/T_{min} responses to El Niño/La Niña events. El Niño events have also had a stronger warming effect over many regions (northern interior region, southeast and southwest coasts) in South Africa for more recent times, compared to an earlier period. This strengthening influence of El Niño events on T_{max}, is significantly stronger over the northern interior and southeast coast, compared to all other regions tested in this study. The warming temperature trends recorded (following homogenization), along both South Africa's east and west coasts, are of global significance because these regional temperature trends are expected to contribute toward a more accurate calculation of global warming trends. The successful application of relative homogenization techniques on South African data, strengthens the call for further temperature trend studies.

6.7. REFERENCES

Akoon I, Archer E, Engelbrecht F, Landman W, Le Roux A, Van Huyssteen E, Fatti C, Vogel C, Maserumule R, Colvin C, Le Maitre D, Lotter D, Olwoch J, Wright C, Meyer AA, Theron A, Diedericks G, Maherry A, Rossouw M, Midgley G, Davis C, Stevens N, Sinden LA, Warburton M, Nkambule C. 2010. South African risk and vulnerability atlas. Department of Science and Technology, Pretoria. pp. 62.

Ashcroft L, Gergis J, Karoly DJ. 2014. A historical climate dataset for southeastern Australia, 1788–1859. *Geoscience Data Journal* **1**: 158-178.

Ashcroft L, Gergis J, Karoly DJ. 2016. Long-term stationarity of El Niño–Southern Oscillation teleconnections in southeastern Australia. *Climate Dynamics* **46**: 2991-3006.

Bates BC, Kundzewicz ZW, Wu S, Palutikof JP. 2008. Climate Change and Water. Technical Paper of the Intergovernmental Panel on Climate Change, IPCC Secretariat, Geneva, pp. 210.

Bradzil R, Pfister C, Wanner H, von Storch H, Luterbacheer J. 2005. Historical Climatology In Europe – The State Of The Art. *Climatic Change* **70**: 363-430.

Collins JM. 2011. Temperature Variability over Africa. *Journal of Climate* **24**: 3649-3666.

Department of Environmental Affairs (DEA). 2013. Long-Term Adaptation Scenarios Flagship Research Programme (LTAS) for South Africa. Climate Trends and Scenarios for South Africa. Pretoria, South Africa. pp. 132.

Domonkos P. 2013. Measuring performances of homogenization methods. *Quarterly Journal of the Hungarian Meteorological Service* **117**: 91-112.

Dosio A, Panitz J, Schubert-Frisius, Luthi D. 2015. Dynamical downscaling of CMIP5 global circulation models over CORDEX-Africa with COSMO-CLM: evalustion over the present climate and analysis of the added value. *Climate Dynamics* **44**: 2637-2661.

Giugni M, Simonis I, Bucchignani E, Capuano P, de Paolo F, Engelbrecht F, Mercogliano P, Topa ME. 2015. The Impacts of Climate Change on African Cities. In: Pauleit S. Coly A, Fohlmeister S, Gasparinin P, Jorgensen G, Kabisch S, Kombe WJ, Lindley S, Simonis I, Yeshitela K. (eds.) *Urban Vulnerability and Climate Change in Africa.* Springer International Publishing, Switzerland. pp. 37-75.

Halpert MS, Ropelewski CF. 1992. Surface temperature pattern associated with Southern Oscillation. *Journal of Climate* **5**: 577-593.

Hartmann DL, Klein Tank AMG, Rusticucci M, Alexander LV, Brönnimann S, Charabi Y, Dentener F, Dlugokencky EJ, Easterling DR, Kaplan A, Soden BJ, Thorne PW, Wild M, Zhai PM. 2013: Observations: Atmosphere and Surface. In: Climate Change 2013: The Physical Science Basis. Contribution of Working Group I to the Fifth Assessment Report of the Intergovernmental Panel on Climate Change (Stocker TF, Qin D, Plattner G-K, Tignor M, Allen SK, Boschung J, Nauels A, Xia Y, Bex V, Midgley PM (eds.)). Cambridge University Press, Cambridge, United Kingdom and New York, NY, USA. pp. 159-254.

Hulme M, Doherty R, Ngara T, New M, Lister D. 2001. African climate change: 1900-2100. *Climate Research* **17**: 145-168.

IPCC. 2013. Summary for Policymakers. In: Climate Change 2013: The Physical Science Basis. Contribution of Working Group I to the Fifth Assessment Report of the

Intergovernmental Panel on Climate Change (Stocker, TF, Qin D, Plattner G-K, Tignor M, Allen SK, Boschung J, Nauels A, Xia Y, Bex V, Midgley PM (eds.)). Cambridge University Press, Cambridge, United Kingdom and New York, NY, USA. pp. 29.

Ji F, Huang ZW Chassignet EP. 2014. Evolution of land surface air temperature trend. *Nature Climate Change* **4**: 462-466.

Jones PD, Wigley TML. 2010. Estimation of global temperatures: what's important and what isn't. *Climatic Change* **100**: 59-69.

Jones P. 2016. The reliability of global and hemispheric surface temperature records. *Advances in Atmospheric Sciences* **33**: 1-14, doi: 10.1007/s00376-015-5194-4.

Jury MR. 2013. Climate trends in southern Africa. *South African Journal of Science* **109**: 1-11.

Karl TR, Arguez A, Huang B, Lawrimore JH, McMahon JR, Menne MJ, Peterson TC, Vose RS, Zhang HM. 2015. Possible artifacts of data biases in the recent global surface warming hiatus. *Science* **348**: 1469-1472.

Kruger AC, Shongwe, S. 2004. Temperature trends in South Africa: 1960–2003. *International Journal of Climatology* **24**: 1929–1945.

Kruger AC, Sekele SS. 2013. Trends in extreme temperature indices in South Africa: 1962-2009. *International Journal of Climatology* **33**: 661-676.

Kruger AC, Nxumalo M. 2017. Surface temperature trends from homogenized time series in South Africa: 1931-2015. *International Journal of Climatology* **37**: 2364-2377.

Kousari MR, Ahani H, Hendi-zadeh R. 2013. Temporal and spatial trend detection of maximum air temperature in Iran during 1960–2005. *Global and Planetary Change* **111**: 97–110.

MacKellar N, New M, Jack C. 2014. Observed and modeled trends in rainfall and temperature for South Africa: 1960–2010. *South African Journal of Science* **110:** 1-13. http://dx.doi.org/10.1590/sajs.2014/20130353

Manatsa D, Reason C. 2016. ENSO-Kalahari Desert linkages on southern Africa summer surface air temperature. *International Journal of Climatology* 37: 1728-1745.

Niang I, Ruppel OC, Abdrabo MA, Essel A, Lennard C, Padgham J, Urquhart P. 2014. Africa. In: *Climate Change 2014: Impacts, Adaptation, and Vulnerability. Part B: Regional Aspects. Contribution of Working Group II to the Fifth Assessment Report of the Intergovernmental Panel on Climate Change* (Barros VR, Field CB, Dokken DJ, Mastrandrea, MD, Mach, KJ, Bilir TE, Chatterjee M, Ebi KL, Estrada YO, Genova, RC, Girma B, Kissel ES, Levy AN, MacCracken S, Mastrandrea PR, White LL (eds.)). Cambridge University Press, Cambridge, United Kingdom and New York, NY, USA, pp. 1199-1265.

Parker DE. 2010. Urban heat island effects on estimates of observed climate change. *WIREs Climate Change* **1**: 123-133. doi: 10.1002/wcc.21.

Philippon N, Rouault M, Richard Y, Favre A. 2012. The influence of ENSO on winter rainfall in South Africa. *International Journal of Climatology* **32**: 2333-2347.

Rahmstorf S, Foster G, Cahill N. 2017. Global temperature evolution: recent trends and some pitfalls. *Environmental Research Letters* **12**: doi.org/10.1088/1748-9326/aa6825.

Scaife AA. 2010. Impact of ENSO on European climate. ECMWF Seminar on Predictability in the European and Atlantic regions, 6 to 9 September 2010. Met. Office Hadley Centre.

Štěpánek P, Mikulová K. 2008. Homogenization of air temperature and relative humidity monthly means of individual observation hours in the area of the Czech and Slovak Republic. In *5th Seminar for Homogenization and Quality Control in Climatological Databases*. Hungarian Met. Service: Budapest, Hungary.

Štěpánek P, Zahradníček P, Skalák P. 2009. Data quality control and homogenization of air temperature and precipitation in the area of the Czech Republic in the period 1961-2007. *Advances in Science and Research* **3**: 23-26.

Trewin B. 2010. Exposure, instrumentation, and observing practice effects on land temperature measurements. *Wiley Interdisciplinary Reviews - Climate Change.* John Wiley & Sons, Inc. 1: 490-506, doi: 10.1002/wcc.46.

Venema VKC, Mestre O, Aguilar E, Auer I, Guijarro JA, Domonkos P, Vertacnik G, Szentimrey T, Štěpánek P, Zahradnicek P, Viarre J, Muller-Westermeier G, Lakatos M, Williams CN, Menne MJ, Lindau R, Rasol D, Rustemeier E, Kolokythas K, Marinova T, Andresen L, Acquaotta F, Fratianni S, Cheval S, Klancar M, Brunetti M, Gruber C, Prohom

Duran M, Likso T, Esteban P, Brandsma T. 2012. Benchmarking monthly homogenisation algorithms. *Climate of the Past Discussions* **7**: 2655–2718.

APPENDICES

Table A1: Mean temperature (°C) values for observations taken at sunrise, noon and night at Briercliffe near Durban for the period Nov 1850 to Feb 1852 (data calculated from Holden, 1855).

	Monthly/Seasonal Averages		
Time	**T_{mean}**	**T_{max}**	**T_{min}**
November 1850	20.6	25.4	13.7
December 1850	22.2	26.3	19.3
January 1851	23.9	27.2	19.3
February 1851	23.3	26.7	18.5
March 1851	21.7	25.9	17.8
April 1851	20.6	24.8	17.4
May 1851	18.3	23.1	11.1
June 1851	17.2	21.3	11.1
July 1851	14.4	21.7	9.6
August 1851	16.1	21.9	8.5
September 1851	17.2	23.1	11.3
October 1851	19.4	26.3	13.9
November 1851	22.2	25.7	18.7
December 1851	22.8	26.3	17.4
January 1852	24.4	28.3	19.6
February 1852	22.8	28.3	19.3
Summer 1851 (DJF)	23.1	26.7	19
Autumn 1851 (MAM)	20.2	24.6	15.4
Winter 1851 (JJA)	15.9	21.6	9.8
Spring 1851 (SON)	19.6	25.1	14.6
Summer 1852 (DJF)	23.3	27.7	18.8
Annual 1851	19.8	24.5	14.6

Table A2: Mean temperature (°C) values for Pietermaritzburg (657m a.s.l) and Durban (27m a.s.l.) in 1858 (data calculated from Mann, 1859). Only T_{mean} available for Durban.

Months	Durban	Pietermaritzburg		
	T_{mean}	T_{mean}	T_{max}	T_{min}
January	23.4	20.4	24.5	15.7
February	25.0	22.9	27.9	17.4
March	25.9	20.8	25.9	16.0
April	21.6	18.7	24.2	13.4
May	17.8	15.3	21.9	8.6
June	17.6	14.8	25.7	4.1
July	16.9	14.5	20.9	8.3
August	18.4	16.3	21.4	11.1
September	19.5	18.1	23.8	12.3
October	18.8	17.7	21.6	13.8
November	22.2	20.1	24.4	15.9
December	23.3	20.7	24.8	16.7
Summer (DJF)	24.2	21.7		
Autumn (MAM)	21.8	18.2		
Winter (JJA)	17.6	15.2		
Spring (SON)	20.2	18.6		
Annual	20.9	18.4		

Table A3: T_{max} and T_{min} correlation coefficients and distances between neighbour stations, KZN.

Candidate station	**Neighbour station**	**Start year**	**End year**	**Dist. (km)**	**Alt (m a.s.l.)**	**Correl. T_{max}**	**Correl. T_{min}**
Cedara		1919	2013		1071		
	Emerald Dale	1930	2013	53.67	1189	0.86	0.76
	Mt Edgecombe	1928	2013	77.55	103	0.72	0.67
	Cape St Lucia	1920	2005	237.46	107	0.64	0.65
Emerald Dale		1930	2013		1189		
	Cedara	1919	2013	53.67	1071	0.86	0.76
	Mt Edgecombe	1928	2013	108.61	103	0.69	0.68
	Cape St Lucia	1920	2005	286.15	107	0.60	0.67
Mt Edgecombe		1928	2013		103		
	Cedara	1919	2013	77.55	1071	0.72	0.67
	Emerald Dale	1930	2013	108.61	1189	0.69	0.68
	Cape St Lucia	1920	2005	187.31	107	0.65	0.71

Alt =altitude of the station (meters above sea level (m a.s.l.)); Dist=Distance; Correl.=Pearson correlation coefficient.

Table A4: Change points selected for adjustment, detected using the Standard Normal Homogeneity Test (SNHT) and Bivariate tests at a monthly scale for stations in KZN.

Name of station	**Climate variable**	**Year of change point**	**Average change (°C)[a]**
Cedara	T_{max}	1938	0.9
		1950	0.8
		1955	0.7
		1977	1.0
Cedara	T_{min}	1939	0.9
		1950	-1.1
		1997	0.9
		2005	-0.8
Emerald Dale	T_{max}	1943	1.0
		1956	0.8
		1978	1.0
Emerald Dale	T_{min}	1957	-1.0
		2007	-1.5
Mt Edgecombe	T_{max}	No change points	
Mt Edgecombe	T_{min}	No change points	

a: The average temperature adjustment per month in the given year.

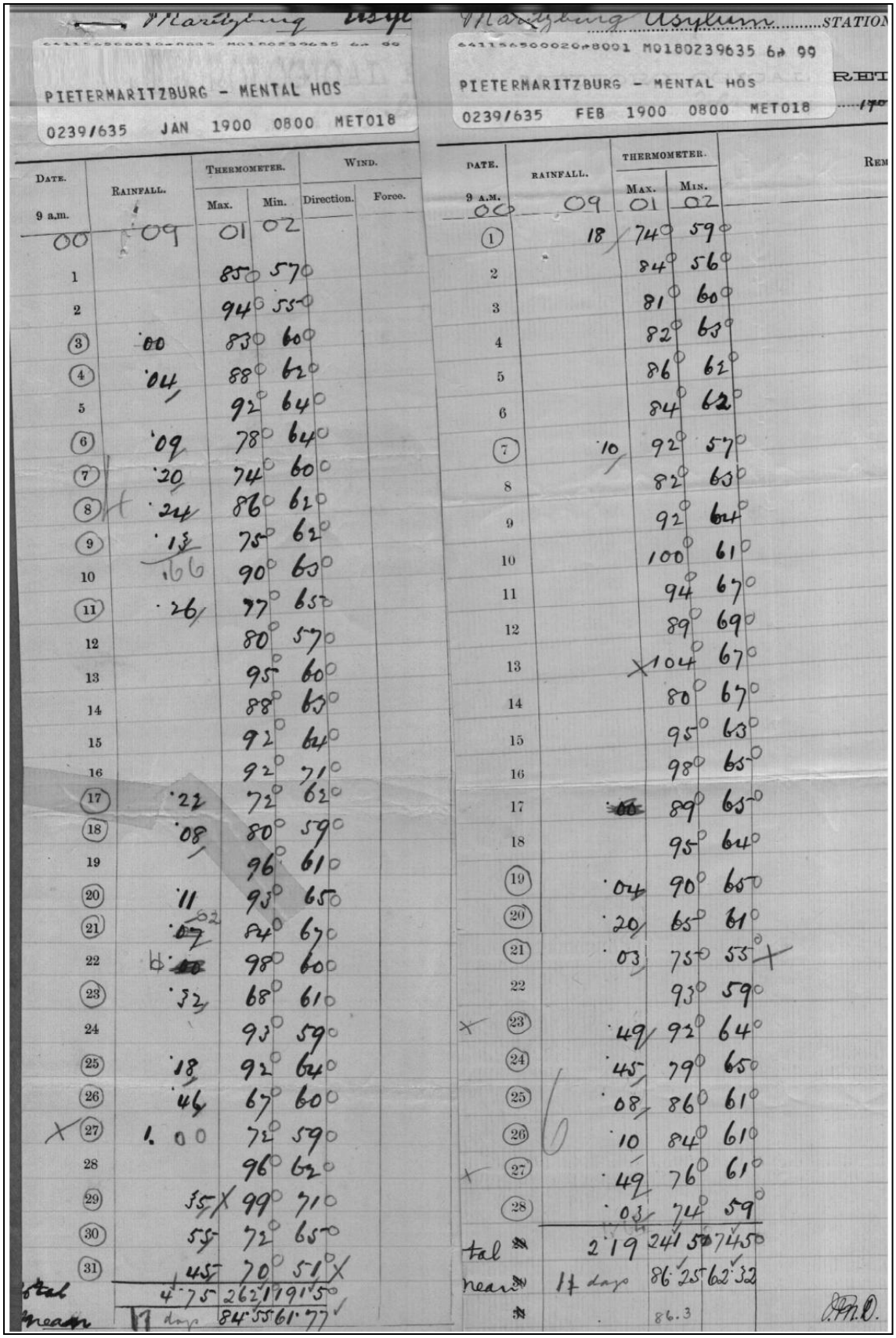

Figure A1: Photograph of the hard copy for Pietermaritzburg data record at South African Weather Service.